Master's thesis

NTNU
Norwegian University of Science and Technology
Faculty of Natural Sciences
Department of Chemistry

Haakon Kristvik Bye

Synthesis of 4-Amine Substituted Thieno[2,3-*d*]pyrimidines for Breast Cancer and HER2 Activity Testing

Master's thesis in Chemical Engineering and Biotechnology

Supervisor: Bård Helge Hoff
Co-supervisor: Fredrik Heen Blindheim

June 2021

NTNU
Norwegian University of
Science and Technology

Haakon Kristvik Bye

Synthesis of 4-Amine Substituted Thieno[2,3-*d*]pyrimidines for Breast Cancer and HER2 Activity Testing

Master's thesis in Chemical Engineering and Biotechnology
Supervisor: Bård Helge Hoff
Co-supervisor: Fredrik Heen Blindheim
June 2021

Norwegian University of Science and Technology
Faculty of Natural Sciences
Department of Chemistry

NTNU
Kunnskap for en bedre verden

I hereby declare that this Master thesis is an independent work according to the exam regulations of the Norwegian University of Science and Technology.

Trondheim, June 2021

Haakon K Bye

Haakon Kristvik Bye

Preface

The work presented in this Master thesis has been carried out at the Department of Chemistry at the Norwegian University of Science and Technology, during the spring of 2021. It has been supervised by Professor Bård Helge Hoff and PhD candidate Fredrik Heen Blindheim.

First, I would like to thank my supervisor Bård for always finding time throughout the work on my Master thesis and pre-Master project, for the invaluable help with the lab work, analysis and writing. I would also like to thank my co-supervisor Fredrik for always finding time to help when i had challenges in the lab and for the guidance on various new methods.

Thank you to my lab partners at the D2-102 for the unforgettable fun times and the countless hours of talking about training, sports and other nonsense. Thank you to the rest of the Hoff/Sundby family for a good year together.

A special thanks to Roger Aarvik for supplying chemicals, Susanna Villa Gonzales for running the MS experiments, Julie Asmunsen for guidance on the HPLC lab and Torun Margareta Melø for guidance regarding NMR.

Lastly I would like to thank my friends, family and fellow students for all the support throughout my study.

Abstract

The objective of this Master thesis was to synthesize 4-amine substituted thienopyrimidines, and study their breast cancer activity and their effect as human epidermal growth factor receptor 2, HER2, inhibitors. Abnormal HER2 signaling has been detected in 15-25% of breast cancers. Amplified HER2 signaling in breast cancers is an indicator for poor prognosis. The HER2 receptor is therefore an important target for the treatment of breast cancer.

The thienopyrimidines where prepared by amination, through nuceophilic aromatic substitution, of 4-chloro-6-bromo-thieno[2,3-*d*]pyrimidine and subsequently Suzuki-Miyaura cross-coupling. The 4-alkoxy aniline substrates were formed by ether synthesis, through either Williamson ether synthesis or nucleophilic aromatic substitution, followed by selective reduction.

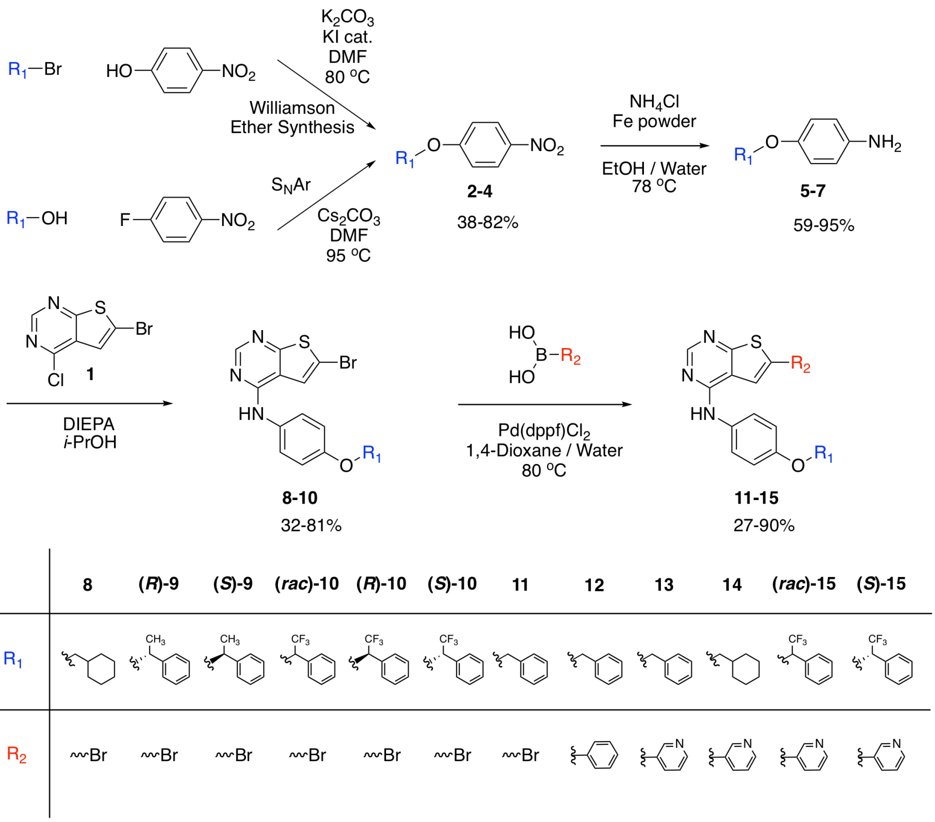

The Williamson ether synthesis proceeded in moderate yield. A series of S_NAr test reactions was performed between 1-fluoro-4-nitrobenzyl and phenylethan-1-ol. By changing the base from NaH to Cs_2CO_3 and increasing the temperature the reaction proceeded with faster reaction rates. The ether syntheses through nuclophilic aromatic substitution proceeded with varying yields. The selective reduction of the nitro arenes were performed using Fe powder and NH_4Cl. The reductions proceeded with full conversion and the products were isolated in mostly high yields.

The aminations were performed between substrate amines and 4-chloro-6-bromo-thieno[2,3-*d*]pyrimidine. The reactions proceeded with full conversion towards the products, and were isolated in moderate yields. A test reaction and assay NMR revealed that the loss of product occurred during the work up of the reaction. Suzuki cross-couplings were performed between numerous 4-amine substituted thienopyrimidines and boronic acids. The cross-couplings were carried out mostly with full conversion and high yields.

A selection of six of the target compounds were tested for their HER2 inhibitory activity. The compounds exhibited moderate to low percentage HER2 inhibition. The biological study revealed that including a stereocenter at the benzylic position reduced the inhibitor activity. It also showed that including 3-pyridine at C-6 increased the affinity towards the HER2 receptor.

Sammendrag

Målet med denne masteroppgaven var å syntetisere 4-aminsubstituerte tienopyrimidiner, og studere deres brystkreftaktivitet og deres aktivitet som human epidermal vekstfaktor reseptor 2, HER2, hemmere. Unormal HER2-signalisering har blitt påvist i 15-25% av brystkreft tilfeller. Økt HER2-signalering i brystkreft er en indikator for dårlig prognose. HER2-reseptoren er derfor et viktig mål for behandling av brystkreft.

De substituerte tienopyrimidinene ble fremstilt ved aminering, gjennom nukleofil aromatisk substitusjon av 4-klor-6-brom-tieno[2,3-*d*]pyrimidin, og deretter Suzuki-Miyaura kryss-kobling. 4-alkoxyanilin substratene ble dannet ved etersyntese, enten gjennom Williamson etersyntese eller nukleofil aromatisk substitusjon, etterfulgt av selektiv reduksjon.

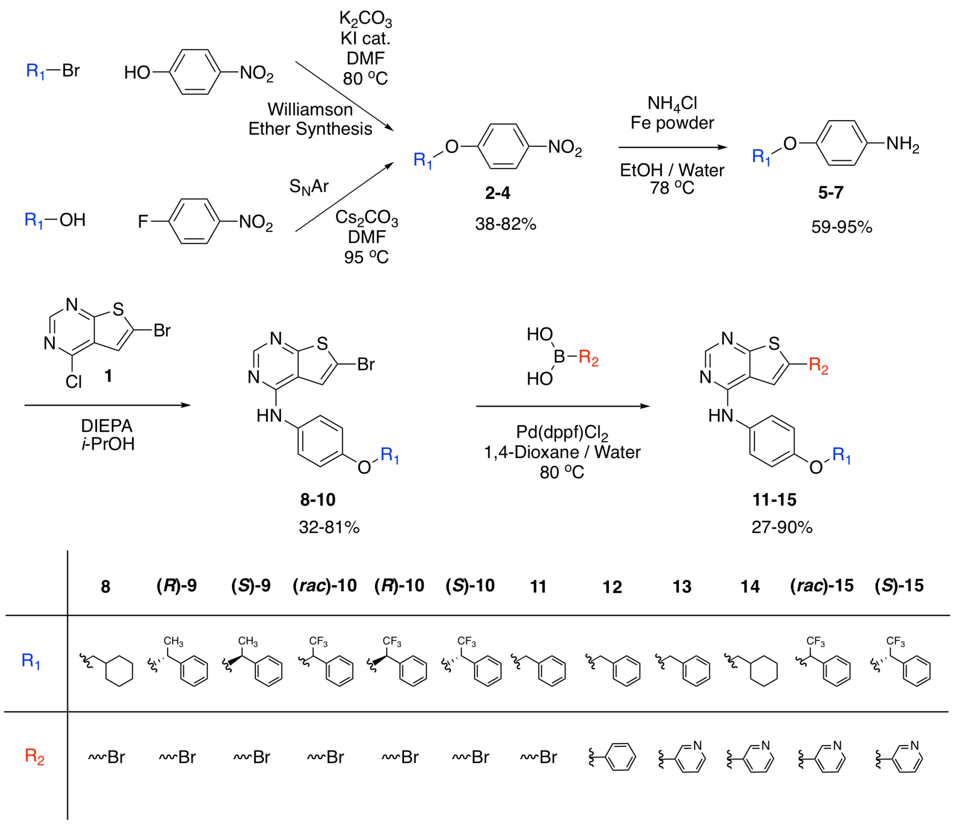

Williamson etersyntese ble gjennomført med moderat utbytte. En serie S_NArtestreaksjoner ble utført mellom 1-fluor-4-nitrobenzyl og fenyletan-1-ol. Ved å endre basen fra NaH til Cs_2CO_3 og øke temperaturen, økte reaksjonshastigheten. Etersyntese gjennom nuklofil aromatisk substitusjon ble isolert med varierende utbytter. Selektiv reduksjon av nitroarenene, ble utført ved bruk av Fe-pulver og NH_4Cl. Reduksjonene ble gjennomført med fullstendig omsetting og produktet ble isolert med stort sett høye utbytter.

Amineringsreaksjonene ble utført mellom substrat anilinene og 4-klor-6-bromtieno[2,3-*d*]pyrimidin. Reaksjonene ble gjenomført med fullstendig omsetting, mot ønsket produkt, og ble isolert med moderate utbytter. En testreaksjon og assay NMR avslørte at tap av produkt oppstår under opparbeidelsen av reaksjonen. Suzuki kryss-koblingene ble utført mellom en rekke 4-aminsubstituerte tienopyrimidiner og borsyrer. Kryss-koblingene ble utført hovedsakelig med fullstendig omsetting og høye utbytter.

Et utvalg på seks av sluttproduktene ble testet for deres HER2-hemmende aktivitet. Forbindelsene oppnådde moderat til lav prosent HER2-inhibering. Den biologiske studien avslørte at inkludering av et stereosenter i benzylisk posisjon reduserte hemmeraktiviteten. Studien viste også at å inkludere 3-pyridin ved C-6 økte affiniteten til HER2 reseptoren.

Table of Contents

Abbreviations and Symbols

δ	Chemical shift [ppm]
^{13}C-NMR	Carbon Nuclear Magnetic Resonance
1D-NMR	One Dimensional Nuclear Magnetic Resonance
2D-NMR	Two Dimensional Nuclear Magnetic Resonance
^{19}F-NMR	Fluorine Nuclear Magnetic Resonance
^{1}H-NMR	Proton Nuclear Magnetic Resonance
ASAP+	Atmospheric Solid Analysis Probe
ACN	Acetonitrile
ATP	Adenosine Triphosphate
BINAP	(2,2-bis(diphenylphosphino)-1,1-binaphthyl)
c-Met	Mesenchymal-Epithelial Transition Factor
Conv.	Conversion
COSY	Correlation Spectroscopy
CYP	Cytochromes P450
d	doublet
DCM	Dichloromethane
DIPEA	N,N-Diisopropylethylamine
DMF	Dimethylformamide
DMSO	Dimethyl Sulfoxide
DNA	Deoxyribonucleic acid
EE(%)	Enantiomeric Excess
EGFR	Epidermal Growth Factor Receptor
eq.	Equivalents
ER	Estrogen receptor
ERBb2	Human Epidermal Growth Factor receptor 2
ES+	Electronespray
FGFR1	Fibroblast Growth Factor Receptor 1
FGI	Functional Group Interchange
HER	Human Epidermal Growth Factor receptor
HER2	Human Epidermal Growth Factor receptor 2
HER3	Human Epidermal Growth Factor Receptor 3
HER4	Human Epidermal Growth Factor Receptor 4
HIV	Human Immunodeficiency Virus
HMBC	Heteronuclear Multiple Bond Correlation
HSQC	Heteronuclear Single Bond Correlation
HPLC	High Performance Liquid Chromatography
HRMS	High Resolution Mass Spectroscopy
IC_{50}	Half Maximum Inhibitory Concentration
IgE	Immunoglobulin E

IR	Infrared
J	Coupling Constant [Hz]
K_M	Michaelis Constant
LG	Leaving group
m	Mulitiplet
MFC-7	Michigan Cancer Foundation-7
mmol	millimole
Mp	Melting Point
MS	Mass Spectroscopy
nM	Nanomolar
NMR	Nuclear Magnetic Resonance
Nu	Nucleophile
NRTK	Non-Receptor Tyrosine Kinase
$Pd_2(dba)_3$	Tris(dibenzylideneacetone)dipalladium(0)
$Pd(dppf)Cl_2$	[1,1'-Bis(diphenylphosphino)ferrocene]dichloropalladium(II)
$Pd(PPh_3)_4$	Tetrakis(triphenylphosphine)palladium(0)
PI3K	Phosphoinositide 3-kinase
ppm	Parts Per Million
PR	Progesterone Receptor
PTC	Phase-Transfer Catalyst
rac	Racemate
R_f	Retention Factor
Rs	Resolution Factor
RT	Room Temperature
RTK	Reseptor Tyrosine Kinase
s	Singlet
SAR	Structure Activity Relationship
S_NAr	Nuclear aromatic substitution
Sphos	2-Dicyclohexylphosphino-2', 6'-dimethoxybiphenyl
t	Triplet
TK	Tyrosine Kinase
TLC	Thin Layer Chromatography
t_R	Retention time
UV	Ultraviolet
VEGFR2	Vascular Endothelial Growth Factor Receptor 2
Xphos	2-Dicyclohexylphosphino-2',4',6'-triisopropylbiphenyl
Å	Ångström

Compound numbering

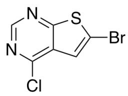

1

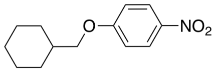

2

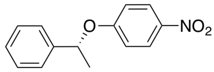

(*R*)-3

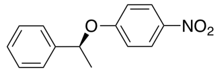

(*S*)-3

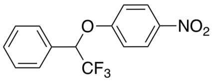

(*rac*)-4

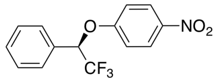

(*R*)-4

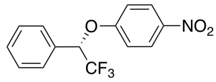

(*S*)-4

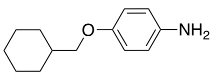

5

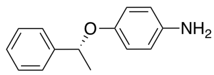

(*R*)-6

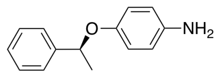

(*S*)-6

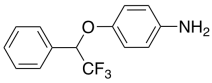

(*rac*)-7

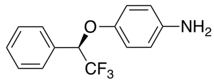

(*R*)-7

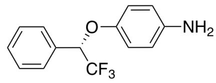

(*S*)-7

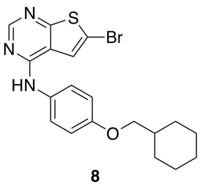

8

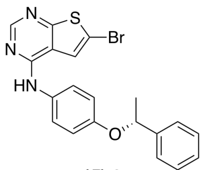

(*R*)-9

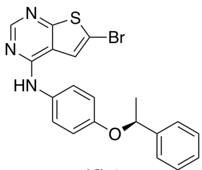

(*S*)-9

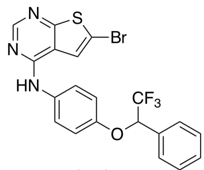

(*rac*)-10

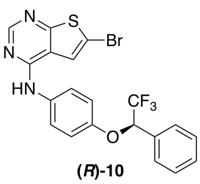

(*R*)-10

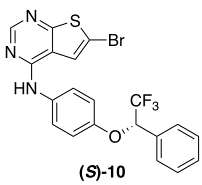

(*S*)-10

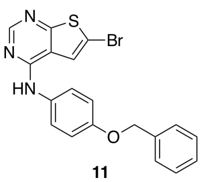

11

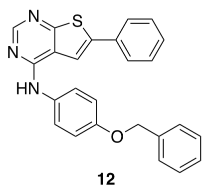

12

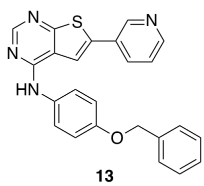

13

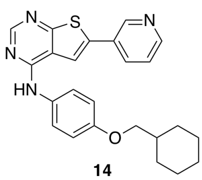

14

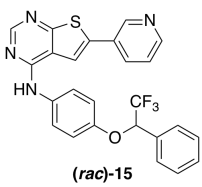

(*rac*)-15

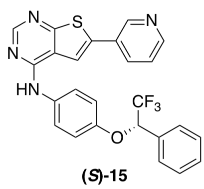

(*S*)-15

Chapter 1

Introduction and Theory

In recent times small molecule drug agents have emerged as an extensive field of research.[1] Receptor tyrosine kinases (RTK) are regulators of crucial cell mechanisms, such as cell growth and survival.[2] The mutation or abnormal activity of tyrosine kinases have been linked with the development of cancers and several other diseases. Small molecule drug agents have become an effective method to inhibit RTKs, and treat diseases that stem from abnormal activity of RTKs.

The second leading cause of cancer related deaths in woman are breast cancers.[3] [4] The abnormal activity of the RTK, Human epidermal growth factor 2 (HER2/ERBb2) are found in 15-25% of breast cancers. HER2 positive breast cancers are associated with poor prognosis. Patients with HER2 positive breast cancer have twice the mortality rate of patients with HER2 negative breast cancer.[5]

Previous work by the research group has found two hit compounds that are biological active towards a breast cancer cell line. The objective of this Master thesis was to prepare a series of compounds, investigate their cellular activity and HER2 inhibitor activity. The biological activity was investigated through a structure activity relationship (SAR) study. The hit compounds have shown cytotoxicity towards cancer cell lines, however the mechanism of cytotoxicity is unknown. The project aims to confirm whether or not the target molecules have activity towards HER2. In addition, an aim was to investigate the effect of various substituents in position R_1, R_2 and R_3 on biological activity. The structure of the hit compounds and the target compounds of this thesis are illustrated in Figure 1.1.

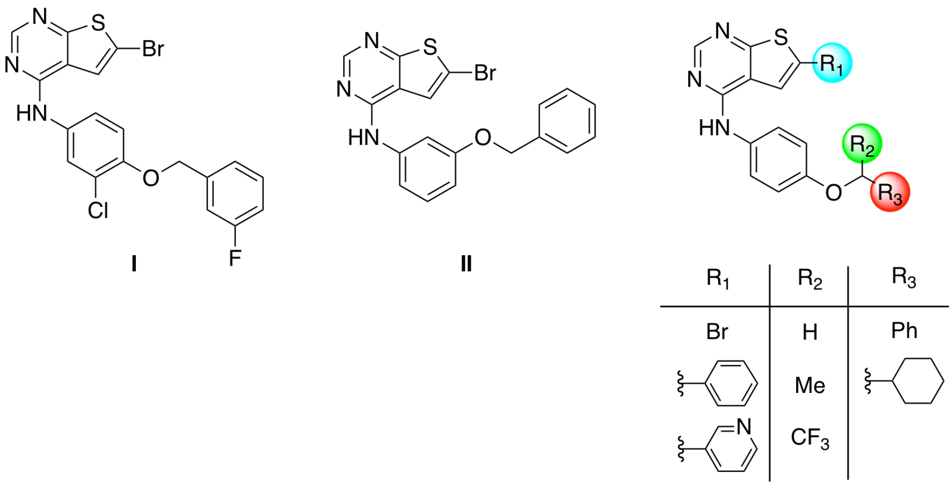

Figure 1.1: The structure of the two hit compounds and scaffold structure of target compounds in the thesis.

1.1 Breast cancer

Breast Cancer is the second leading cause of cancer-related death in woman.[3] Breast cancer is a genetic disease caused by inherited mutant genes and/or acquired molecular alterations over an individual's lifetime. The development of breast cancer is also affected by hormonal factors through breast proliferative activity.[6]

Breast cancer is categorized into different major molecular subtypes based on their gene expression profiling. The key factors determining the subtypes are estrogen receptor (ER) and progesterone receptor (PR), as well as Human epidermal growth factor 2 (HER2) gene amplification. The molecular subtypes of breast cancer is; luminal A, luminal B, HER2 enriched and basal-like breast cancer. Luminal A breast cancer is ER and/or PR positive and HER2 negative. Luminal B breast cancer is both ER and/or PR positive and HER2 positive. HER2 enriched cancer is HER2 positive and ER/PR negative. Basal-like breast cancer is both ER/PR negative and HER2 negative.[7] [8] The treatment of breast cancer is determined by the molecular subtypes of breast cancer. Whereas Luminal types cancer are treated with endocrine agents to down regulate ER signaling, HER2 enriched cancers is treated with small molecule tyrosine kinase inhibitors.

In the search for anti-cancer drugs, one widely used method is testing towards cancer cell lines. A suitable and frequently used breast cancer cell line is the Michigan Cancer Foundation-7 (MCF-7) cell line. The parental MCF-7 cell line was isolated from luminal A molecular subtype metastatic breast cancer in 1973. The MCF-7 cell line is ER, PR, HER2 and Epidermal growth factor receptor (EGFR) positive.[9]

1.2 Tyrosine Kinase

Tyrosine kinases are a group of enzymes which catalyze the phosphorylation of tyrosine amino acid residues on target proteins. The phosphorylation of tyrosine in proteins plays a key role in regulating processes such as, cell growth/proliferation, differentiation and survival. The regulating effect of tyrosine phosphorylation is caused by specialized binding domains on other proteins that recognize phosphorylated tyrosines, and these interactions initiate intracellular signaling pathways. [10] [11] Tyrosine kinases catalyze the transferring of the y-phosphate of an adenosine triphosphate (ATP) to the hydroxyl group of the tyrosine units in the target proteins. Through the phosphorylation reaction, tyrosine kinase functions as a switch for signaling of different cellular functions. [12]

Tyrosine kinases are classified into receptor type and non-receptor type kinases. Receptor tyrosine kinases (RTKs) consists of an extracelular binding site, a transmembrane domain and an intracellular tyrosine kinase domain. [13] [2] [14] Non-receptor tyrosine kinases (NRTKs) are intracellular cytoplasmic proteins without receptor-like functions and rely on intracellular signals. [15] Extracellular ligand binding to RTKs causes receptor dimerization and autophosphorylation in the intracellular tyrosine kinase domain. This leads to the activation of the signaling cascade, where NRTKs have a significant role. [15]

Normally the cellular tyrosine kinase phosphorylation levels are highly regulated by the antagonizing effects of tyrosine kinases. The TKs signaling can become continuously activated, independent of ligands, by over-expression or mutations. The continuous activation causes uncontrolled cell proliferation as well as other unregulated mechanisms. The unregulated cell responses cause inflammatory responses and diseases such as cancers. [16] [17]

Inhibitors which inhibit the activity of tyrosine kinases and the signaling pathways they activate, can function as anti-cancer agents. [16] TKs inhibitors are divided into small molecule inhibitors and monoclonal antibodies. [17] [18] Small molecule inhibitors binds to the ATP binding site, of their target kinase, to function as competitive inhibitors within the catalytic domain. Monoclonal antibodies binds to the extracellular domain of the target RTKs.

1.3 Human Epidermal Growth Factor Receptor 2

Human epidermal growth factor receptor 2 (HER2) is one of four members in the human epidermal growth factor RTK family, which also includes EGFR, HER3 and HER4. The HER family is responsible for oncogenic processes such as proliferation, survival, motility and angiogenesis. [19] [3] EGFR, HER3 and HER4 have cognate ligands binding to their extracellular domains, whereas HER2 is an non-autonomous orphan receptor with no assigned ligands. Ligand binding to the extracellular domains induces conformational changes in the receptor that promotes homo- or hetrodimerization and activation as RTKs. [20] [21] The different dimerizations can trigger diverse intracellular signaling pathways. Despite being non-autonomous and with the lack of a known ligand, HER2 participates in an extensive network of ligand induced formation of heterodimeric complexes, with other HER receptors, that are capable of generating potent cellular signals.[19][21] The dimerization activation is illustrated in Figure 1.2

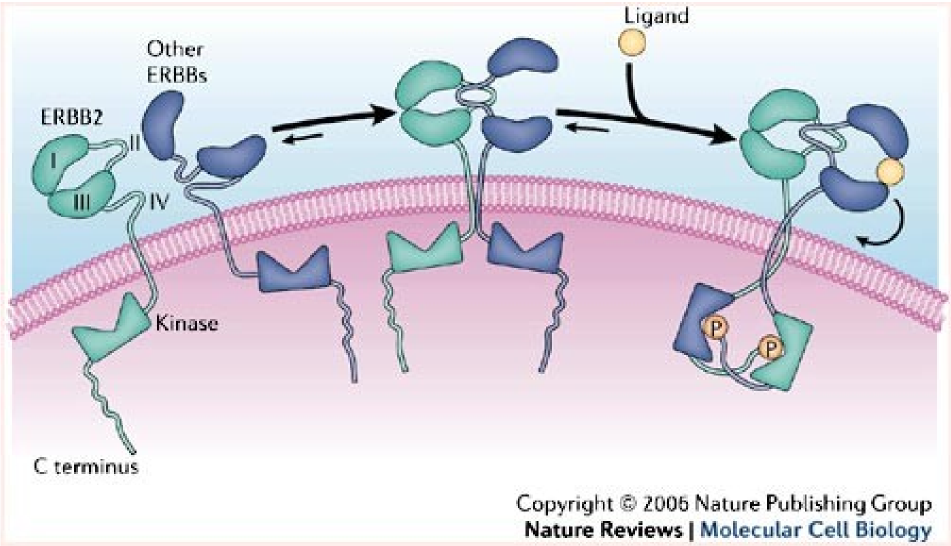

Figure 1.2: The structural basis for HER-receptor dimerization and activation.[21]

The HER heterodimeric complexes that contains HER2 are more stable and their signaling is more potent. HER2 is regarded as a non-autonomous amplifier of the network. HER2 is favoured as the heterodimerization partner by the other HER receptors. Since HER2 is incapable of binding with ligands, it is constantly primed for heterodimerization with ligand-bound HER receptors.[21]

1.3.1 HER2 and Breast Cancer

Amplification of the HER2 gene and over-expression of the corresponding protein has been detected in 15-25% of breast cancers.[22][23] Cancers with genomic alteration of HER2 are associated with poor prognosis and aggressive behavior. The HER2 gene amplification has been found to be a significant predictor for both overall survival and time before relapse.[24]

The mechanisms of how HER2 amplification and over-expression contribute to breast cancer are still unknown.[23] HER2 breast cancer can have up to 25-50 copies of the the gene, and subsequently 40-100 fold increase of the corresponding protein, resulting in 2 million receptors expressed at the tumor cell surface. In addition, a constitutively active aberrant form of HER2, which lack the extracellular domain, is found in some breast cancers.[24]

Inhibition of HER2 can be done by either monoclonal antibodies binding to the extracellular domain, or by small molecule tyrosine kinase inhibition targeting the intracellular kinase domain of HER2.[25]

Currently there are some clinical approved HER2-targeted agents for treatment of HER2 positive metastatic breast cancer. These include the monoclonal antibodies Trastuzumab and Pertuzumab and the small molecule HER2/EGFR kinase inhibitors Lapatinib and Neratinib.[25][26] The molecular structure of Lapatinib and Neratinib is presented in Figure 1.3

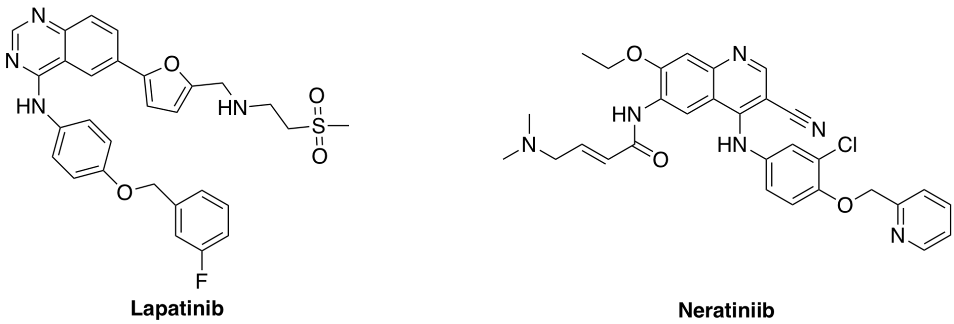

Figure 1.3: The structure of Lapatinib[27][28] and Neratinib[26].

1.4 Thieno[2,3-*d*]pyrimidine

Thienopyrimidines are a group of fused heterocyclic compounds, which contains an electron rich thiophene moiety and an electron deficient pyrimidine moiety. There are three forms of thienopyrimidine, based on thiophenes annelation to the pyrimidine: thieno[2,3-*d*]pyrimidine, thieno[3,2-*d*]pyrimidine and thieno[3,4-*d*]pyrimidine, see Figure 1.4.[29] Thienopyrimidine can be formed through two main methods. The first route is by forming the pyrimidine moiety by intramolecular cyclization of appropriately substituted aminothiopene derivatives.[29] The other synthesis route is thiophene ring closure for appropriately substituted pyrimidine derivatives.[29] The three isomeric thienopyrimidine systems and their conventional numbering systems are illustrated in Figure 1.4

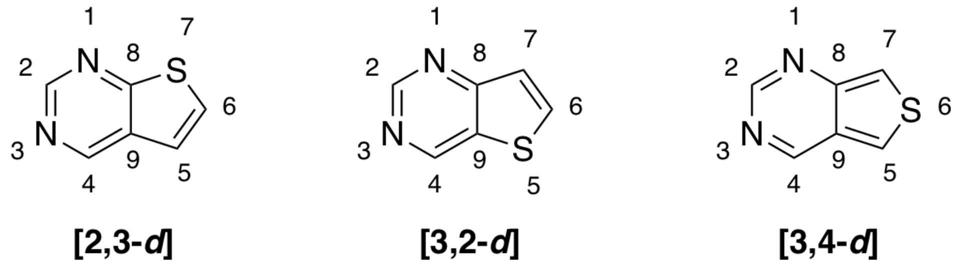

Figure 1.4: The structure and conventional numbering system of thieno[2,3-*d*]pyrimidines , thieno[3,2-*d*]pyrimidine and thieno[3,4-*d*]pyrimidine.

Both the [2,3-*d*] and [3,2-*d*] isomers of thienopyrimidine can be synthesized from amine and methyl ester substituted thiophene. Chloro substituted thienopyrimidines is formed by the substituted thiophene reacting with formamide, in an pyrimidone formation reaction followed by chlorination with $POCl_2$.[30] [31]

The synthesis pathway of formation of 6-bromo-4-chlorothieno[2,3-*d*]pyrimidine performed by Bugge *et al.*[30] is presented in Scheme 1.4.1

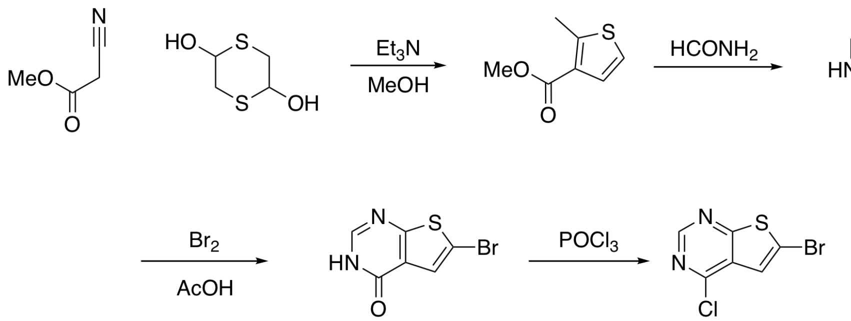

Scheme 1.4.1: The synthesis route to prepare 6-bromo-4-chlorothieno[2,3-*d*]pyrimidine.[30]

Thienopyrimidines possess a variety of biological applications, which depends on their detailed substitution patterns, for instance anti-microbial[32] [33], anti-tumor[32] and immunosuppressive agents[34]. The pharmacological potential of thienopyrimidines has been evaluated through numerous biological studies. As mentioned, thienopyrimidine derivatives have displayed a number of pharmacological applications. Thienopyrimidines have been identified as inhibitors of Human IgE synthesis, as histone deacylase inhibitors and as inhibitors of signaling pathways contributing to cancer activity.[35] [36] [37] [38] Specifically thieno[2,3-*d*]pyrimidine derivatives have been identified as inhibitors of signaling pathways, such as EGFR[39] [40], mesenchymal-ephitheial transition factor (c-Met)[41], phosphatidylinostol-3-kinase (PI3K)[37], fibroblast growth factor receptor 1 (FGFR1)[42], vascular endothelial growth factor receptor 2 (VEGFR2) and HER2.[43]

Thienopyrimidine derivatives, with an aromatic aniline moiety, have been identified as potent EGFR and HER2 inhibitors.[43] The structures of known HER2 inhibitors are presented in Figure 1.5.

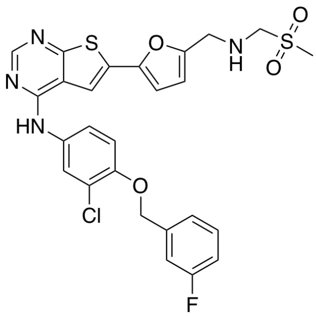

IC_{50} = 6 nM
16

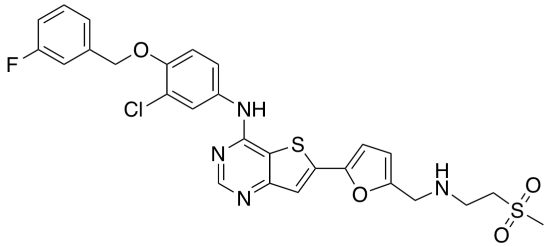

IC_{50} = 71 nM
17

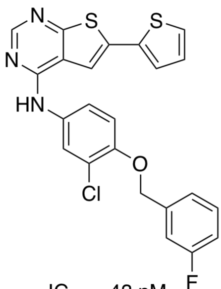

IC_{50} = 43 nM
18

Figure 1.5: Structures of known HER2 and EGFR inhibitors.[43]

In the study by Rheault *et al.* thieno[2,3-*d*]pyrimidine derivatives with the C-4, C-6 substitution pattern, were identified as dual EGFR and HER2 inhibitors. The C-4 substituent in the inhibitors is an aniline, while the C-6 substituent is a heteroaromatic group.[43] Compounds **16** and **18** have an IC_{50} value towards HER2 of 6 and 43 nM, respectively. Thieno[2,3-*d*]pyrimidines with similar substitution patterns, with C-4 aniline moiety, have shown anticancer effect towards MCF-7 breast cancer cell lines and inhibition of VEGFR2 with IC_{50} of 200 nM, as well as inhibition of FGFR1 with IC_{50} of 160 nM.[42] [44] [45] The structure of known VEGFR2 and FGFR1 inhibitors is illustrated in Figure 1.6

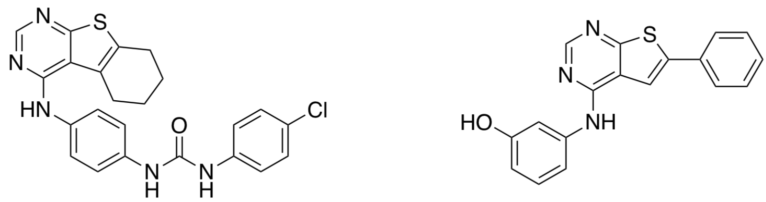

VEGFR2
IC_{50}=200 nM

FGFR1
IC_{50}=160 nM

Figure 1.6: Structure of known VEGFR2 and FGFR1 inhibitors.[44] [42].

1.5 Previous work by the research group

In previous work by the research group thieno[2,3-*d*]pyrimidines with C-4 and C-6 substitution pattern have been identified as potent EGFR inhibitors.[39] [40] In addition, a series of 6-bromothieno[2,3-*d*]pyrimidines were synthesized as precursors for EGFR inhibitors.[46] In unpublished work by the research group, two of the 6-bromothieno[2,3-*d*]pyrimidine compounds have shown promising cytotoxcicty towards two cancer cell lines , HeLa and MCF-7. The structures of the hit compounds are presented in Figure 1.7.

I

II

Figure 1.7: The structure of the two biologically active thienopyrimidines.

The mechanism, by which the compounds triggers cytotoxcicty towards the two cancer cell lines, is unknown. Structural related compounds such as Lapatinib and compound **18** have been identified as HER2 inhibitors. Hit compound (**I**) has the exact same aniline part as Lapatinib and compound **18**. Hit compound (**II**) has a closely related aniline substitute to that to pyrrolopyrimidine HER2 inhibitors, see Figure 1.8, found in a study by Caravatti *et al.*.[47] The hit compounds could be HER2 inhibitors, however, the biologically active molecules could antagonize other biological targets as well.

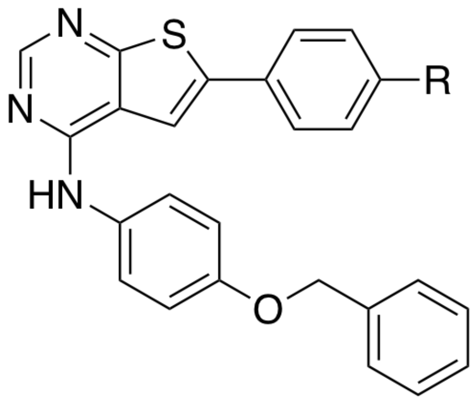

Figure 1.8: The structure of pyrrolopyrimidine HER2 inhibitor.[47]

1.6 Fluoride in Pharmaceuticals

The addition of fluorine to medicinal chemistry is relatively recent. Fluorine is frequently introduced to be applied in a couple of strategies. The metabolic stability of a compound is a crucial factor of bioavailability of the specific compound.[48] A recurring problem in drug discovery is low metabolic stability. Lipophilic drug-targets have disposition to be oxidised, by the cytochrome P450 (CYP) enzymes, in the liver, which is a frequent limiting factor for bioavailability. A strategy to circumvent the issue of oxidation is to add a fluorine substituent, which blocks the reactive site of the liver enzymes, hoping that it does not impair the binding to the drug target.[48]

The addition of fluoride substituents to a compound affects the physiochemical properties greatly.[48][49][50] In pharmacological chemistry the need for highly basic functional groups is often required to bind to specific receptors. However, highly basic groups are also found to lower the bioavailabilty of certain compounds, due to reduced membrane permeability. Addition of fluoride in close proximity of functional groups, has great effect on pK_a.[48][49][50] The basicity of the highly basic compounds, will be reduced and the membrane permeability and bioavailability will increase. The change in pK_a may also negatively effect the compounds binding affinity towards the target.[48][51]

Fluorine substituents are also introduced to increase the binding affinity of a drug.[48][52] The fluorine substituents may affect binding affinity in a several of ways. The fluorine substituents may be used to affect the binding affinity through direct interaction between fluorine and the target protein. The fluorine substitutes can also affect the binding affinity through conformational changes in the molecule and through the formation of Van der Waal bonds. Fluorine derivatives of compounds have also increased lipophilicity, which increases the overall molecule nonspecific affinity towards proteins.[52]

In conclusion, fluoride subtituents are used to block metabolic labile sites, to modulate the physiochemical properties and to increase the binding affinty and potency of the compound.[48] [52]

Some examples of fluorinated compounds, illustrated in Figure 1.9, used in pharmaceuticals are: Lapatinib which is a HER2 inhibitor used in treatment of breast cancer, Clofarabine which inhibits DNA polymerase in the treatment of leukemia, Emitricitabine which is a nucleoside reverse transcriptase inhibitor used in treatment of HIV and hepatitis B.[27] [28] [53]

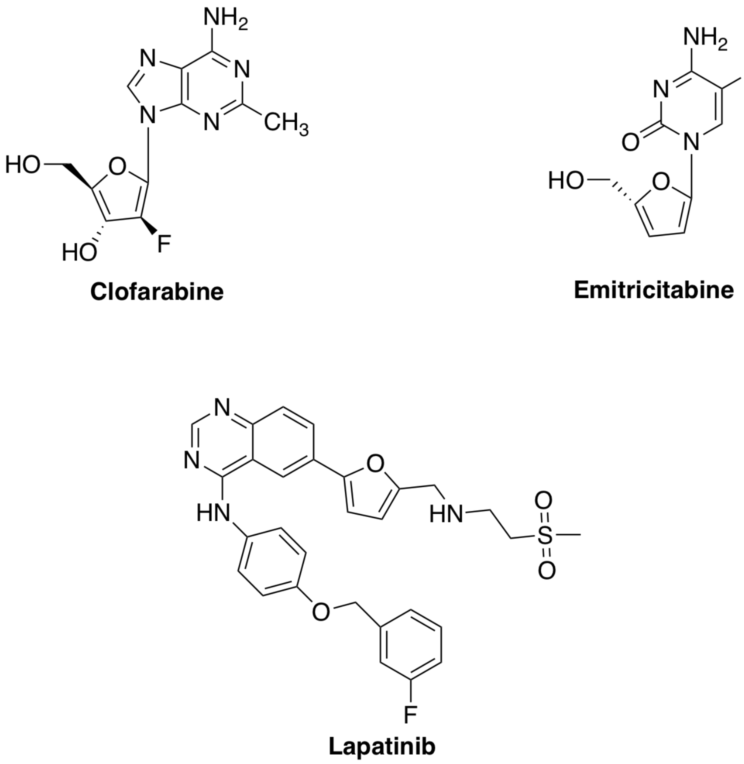

Figure 1.9: The structure of Clofarabine, Emitricitabine and Lapatinib.[27] [28] [53]

1.7 Synthesis of Aniline

Anilines as mentioned are an important intermediate, used in a variety of pharmaceuticals. Alkoxy substituted anilines are present in known HER2 inhibitors. Alkoxy substituted anilines can be formed through various methods. Anilines with an alkoxy substituent are formed through two part syntheses where the ether moiety is formed first, then the amine functionality is formed through functional group interchange, FGI. Two widely used methods to form aromatic ethers are Williamson ether synthesis and nucleophilic aromatic substitution. The FGI to form the amine functionality in the aniline, is often formed through either specific reduction of a nitro group or hydrolysis of acetamide.[54] [55] [56] A retrosynthetic approach to synthesize 4-alkoxy substituted anilines is illustrated in Scheme 1.7.1

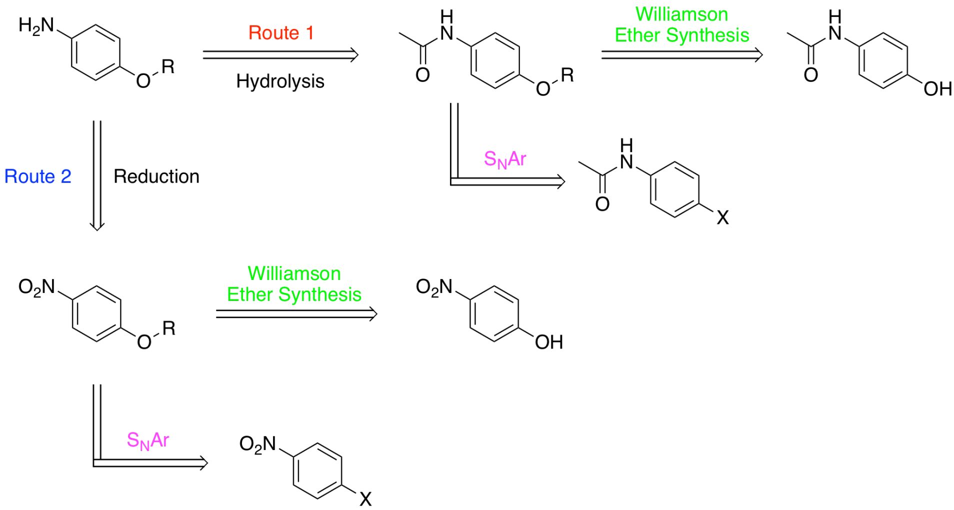

Scheme 1.7.1: Retro synthetic approach of formation of aniline ethers. X= Halide.

Route 1 utilizes the hydrolysis of acetamide to form the aniline, where the ether part could either be formed through Williamson ether synthesis or through nucleophilic aromatic substitution. Yang *et al.* have previously synthesized 4-alkoxy anilines through Williamson ether synthesis followed by hydrolysis of acetamide, starting out with N-(4-hydroxyphenyl)acetamide.[57]

Route 2 employs the reduction of the nitro group to form the aniline, the second route can also employ both Williamson ether synthesis and nucleophilic aromatic substitution to form the ether moiety. Bugge *et al.* synthesized 4-alkoxy substituted anilines, starting from 4-nitrophenol, by Williamson reaction followed by selective reduction of the nitro group.[46] Yang *et al.* also synthesized alokoxy substituted anilines through nucleophilic aromatic substitution followed by reduction.[57]

1.7.1 Williamson Ether Synthesis

The most utilized and versatile method to prepare ethers, which allows for forming both symmetric and assymetric ethers, is the Williamson ether synthesis. The Williamson reaction was developed in the 1800s by the English chemist Alexander Williamson. The synthesis consists of the coupling between alkoxides and alkyl-/benzyl- halides, or alkyl-/benzyl compounds with other good leaving groups. The reaction mechanism proceeds through an S_N2 type mechanism, in which alkoxide acts a nucleophile, to displace halide from the alkyl-/ benzyl- halide to form the ether. The Williamson reaction proceed best with primary alkyl, benzylic and alyllic halides.[58] The reactivity of alkyl halides is affected by the alkyl group and the leaving group. The reactivity of alkyl follows the trend methyl > allylic, benzylic > primary alkyl > secondary alkyl. The order of reactivity based on the leaving group is OTs, I > OMs > Br > Cl. Williamson ether synthesis face some limitations; tertiary and sterical hindred primary and secondary alkyl halides will undergo E2 eliminations, when reacting with alkoxide, rather than S_N2 type mechanism. The Williamson reaction mechanism is illustrated in Scheme 1.7.2

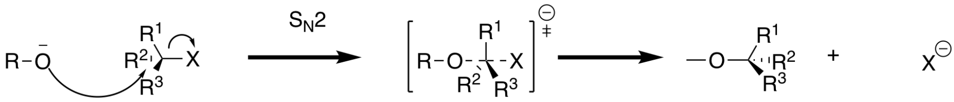

Scheme 1.7.2: The mechanism of Williamson ether synthesis.[58] [59]

The Williamson ether synthesis is usually carried out by reacting an alkyl halide and the alkali-metal salt of the hydroxy compound as well as an inorganic base in an organic solvent.[60] The formation of alkali-metal salt from phenols is usually obtained by treating phenols with weak bases, e.g potassium or sodium hydroxide or by reacting them with alkali metal carbonates.[61] To minimize the by-products formed in the reaction, from dehydrohalogenation, the reaction is generally performed in an aprotic dipolar solvent. Phase-transfer catalyst, PTC, may also be employed during Williamson reaction.[62] The function of phase-transfer catalysts are to facilitate the reaction between hydrophobic and hydrophilic compounds. The use of PTCs allows the reaction to be carried out at milder reaction conditions. The use of PTC during Williamson ether synthesis has shown significant advances in convenience, reaction rate and yield.[62]

Another way to perform the Williamson reaction, without organic auxiliary substances like phase-transfer catalysts, is the use of combined microwave and ultra sonication.[63]

1.8 Reduction of Nitro Aromatics

The reduction of nitro aromatics is the most widely utilized and facile method to prepare functionalized anilines.[55] There are numerous methods and reaction conditions to achieve reduction of aromatic nitro groups reported in the literature, such as $FeCl_3 \cdot 6H_{20}$[64], Pt (nanoparticles)/C[65] and $NiCl_2$-$NaBH_4$.[66]

The first method of reducing nitro compounds to anilines was the Zinin reduction developed in 1842. This reaction is carried out in basic media employing divalent sulfur, such as sulfides, hydrosulfides and polysulfides, as reducing agents.[67] The Zinin reduction was soon replaced by the oldest commercial process for preparing anilines, which was the Béchamp process. The Béchamp process reduces nitro compounds in good yields with iron and diluted HCl acid.[67]

Today most large scale anilines are prepared through continuous high pressure catalytic hydrogenation of nitro aromatics with various heterogeneous catalysts.[67]

The hydrogenation of nitro compounds can be performed in gas or liquid phase, by employing supported metal catalysts and organic solvents such as alcohols, acetone, benzene, ethyl acetate or aqueous acidic solutions.[68]

In the reduction of complex nitro aromatic compounds, containing other reducible substituents or acid labile functional groups, the reaction conditions during hydrogenation employing heterogenous catalysts are to harsh. When reducing complex nitro aromatic compounds, the most important factor for forming functionalized anilines is the specificity of the reduction. The need to find reduction conditions which are chemoselective towards the nitro group and leaves the substituents intact, is important.

The use of hydrogen gas in the presence of either metal or metal oxide, is one method for reduction of nitro groups to anilines.[69] The general reaction is illustrated in Scheme 1.8.1

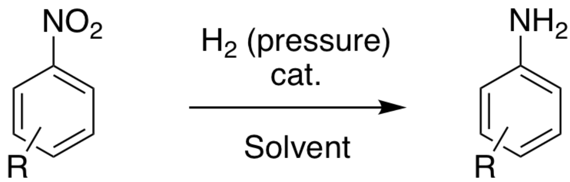

Scheme 1.8.1: Reduction of nitro aromatic compounds employing molecular hydrogen.[69]

The use of metal-bound catalysts brings issues with metal leaching, low catalyst loading, higher turnover cycle, recovery of catalyst and chemioselectivity. Platinum (Pt) oxide with methanol as solvent has previously been used for the chemoselectiv reduction of nitro aromatic compounds, with an ether functionality, without effecting the ether moiety.[70]

Another method of reduction, employing H_2-gass, is the use of polysiloxane gels with Pt species [Pt]@Si_{C6} as recyclable heterogeneous catalyst. This system has been used to reduce various nitro aromatics, such as benzyl, alcohol, ketone, ester and ether, in excellent yields.[71]

The catalytic system Pt/SiO_2 has been used to selectively reduce ester and alkene substituted nitro compounds in a hydrogen atmosphere at room temperature.[72] The main problem with Pt catalysts is their reduction selectivity when there are other functional groups present.[65] Pt catalysts tend to reduce other functional groups, in addition to the nitro group, when used on complex nitro aromatics.

The use of colloidal nickel(0) on carboxymethylcellulose in methanol is an effective method to selectively reduce nitro aromatic compounds. The catalyst system has been used to selectively reduce nitro arenes with ester, alcohol and amine substituents, in high yields.[73]

A disadvantage of molecular hydrogen in the presence of metal or metal oxide is the need for high pressure conditions. By generating hydrogen *in situ* under the reduction, the need for sophisticated equipment for handling hydrogen gas can be avoided.[69] Sodium borohydrid has been used as an *in situ* source for generation of hydrogen in fuel cells, in which various metal bound catalysts can be employed, for the reduction of nitro aromatic compounds. The reduction can be performed with catalyst systems, such as PdCu/graphene and ethanol, Co_3S_4 and $CuBr_2$ in ethanol.[74] [75] [76]The general sodium borohydrid mediate reaction is illustrated in Scheme 1.8.2

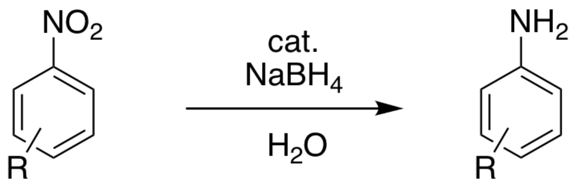

Scheme 1.8.2: Reduction of nitro aromatic compounds mediated by sodium borohydrid.[69]

Reductions mediated by sodium borohydride are safer than the use of H_2-gass, however, the reactions have issues during workup with extraction of the product. In addition functional groups which are reduced by sodium borohydride are not tolerated during this reaction.[69]

Hydrazine hydrate decomposes into nitrogen and hydrogen gas when exposed to transition metals. Hydrazine hydrate is therefore used as an *in situ* hydrogen donor, which facilitates reduction reactions.[69] The general hydrazine hydrate facilitated reaction is illustrated in Scheme 1.8.3

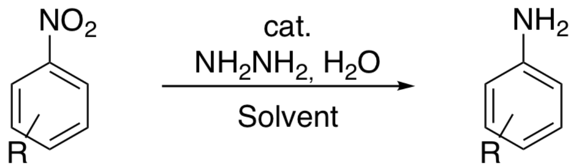

Scheme 1.8.3: Reduction of nitro aromatic compounds with Hydrazine hydrate as reducing agent.[69]

Hydrazine hydrate has been used as reducing agent in combination with Pd/C in methanol or ethanol. This reducing system has shown selective reduction of halogenated nitro compounds, when refluxed in an open system. If performed in a sealed environment, dehalogenation occurs.[77] *In situ* generation of iron oxide nanocrystals (Fe_3O_4) in ethanol is a reduction system which is used in combination with Hydrazin hydrate to selectivly reduce nitro compounds with; halogen, ester, amide, nitrile or ether substituents in high yields.[78] A drawback with the use of Hydrazine as reducing agent is toxicity in addition to risk of combustion.

A method for selective reduction of nitroarenes to anilines is the use of a metal catalyst. Active metal can react with water and generate hydrogen, which can reduce nitro groups in the presence of metal. Metal can directly reduce nitroarenes through electron-transfer reaction, where water functions as a proton donor.[69] Iron nanoparticles in water, in an inert atmosphere, at room temperature have been used to selectivly reduce nitroarenes, with a widespread of substituents.[79] Iron nanoparticles have chemoselectivly reduced nitro compounds with ether, halide, aldehyde and carboxyl acid functional groups, in excellent yields.

Iron powder has also been employed in combination with ammonium chloride in aqueous ethanol, to obtain chemoselctive reduction to anilines when refluxed. In this case, the iron powder function as reducing agent and the ammonium chloride serves as proton donor.[46] [80] [81]

A powerful acidic reduction system is the use of stannous chloride ($SnCl_2$) in combination with hydrochloric acid (HCl).[82] This method has been developed from only reducing water soluble nitro aromatics to a chemioselective reduction system by introducing ionic-liquids, different solvents and sonication.[83] [84] [85]

An illustration of a proposed reaction pathway for the formation of anilines from reduction of functionalized aromatic nitro compounds, is presented in Scheme 1.8.4.[72]

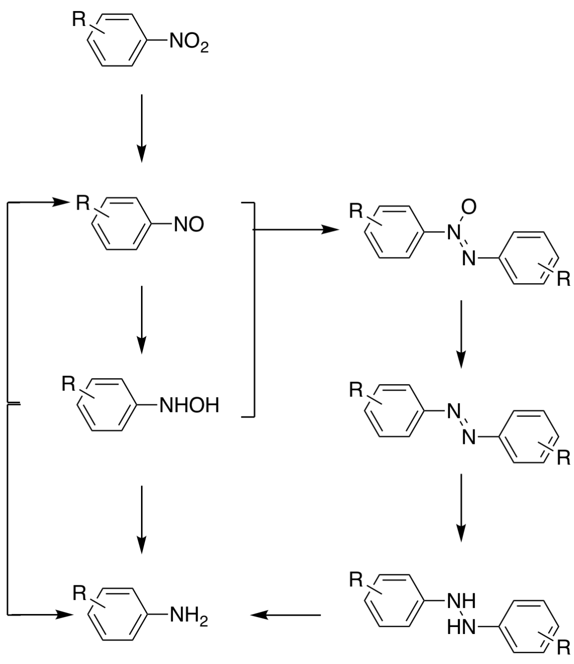

Scheme 1.8.4: Proposed reaction pathway for the reduction of nitroaromatics.[72]

1.9 Amination

1.9.1 Nucleophilic Aromatic Substitution

Nucleophilic aromatic substitution is considered as one of the most common methods of amination.[55] Nucleophilic aromatic substitution is the reaction where a neutral or charged nucleophilic species replaces an atom or functional group, in an aromatic substrate.[86] The electrophilic character of the aromatic ring is caused by electron deficiencies, which can be caused by electron withdrawing groups or by the specific structure of some aromatic heterocycles.[87] Numerous of substrate-nucleophile couples are known. Typically, reactions with nucleophiles, which are weak basic, only occurs if an electron withdrawing group is present in either para or ortho position of the leaving group in the aromatic compound.[88]

In contrast to nucleophilic substitution of aliphatic compounds, neither S_N2 or S_N1 nucleophilic substitution mechanisms occur on aromatic compounds. Nucleophilic aromatic substitutions occur via three main mechanisms; addition-elimination, elimination-addition and unimolecular mechanism.[86] [89]

The addition-elimination mechanism is the most common of the nucleophilic aromatic substitutions. The reaction follows a two step mechanism where addition occurs through nucleophilic attack on the carbon position occupied by halogene or other nucleofugal groups in an electron deficient aromatic ring.[90] The addition step occurs through nucleophilic attack on the aromatic ring, which uses a vacant π-orbital to form a bond with the nucleophile, without expelling any existing substituents.[91] The nucleophilic attack causes the development of a negative charge in the arene, known as the Meisenheimer complex. The general formation of the Meisenheimer complex is illustrated in Scheme 1.9.1

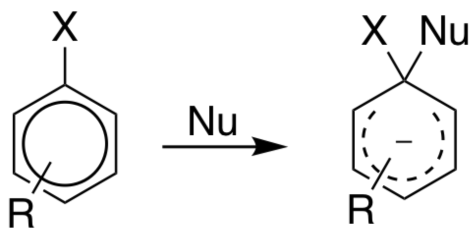

Scheme 1.9.1: The general Meisenheimer complex, where X is a leaving group.[90] [92] [93]

The addition step is the rate determining step, and is greatly affect by electron withdrawing groups, such as the nitro group. The disruption of the aromatic π system in the addition step is a great energy cost, which only transpires with an electron withdrawing group present, with heteroatoms in annular sites, or under extreme reaction conditions. Such groups or atoms stabilize the Meisenheimer intermediate and associated transition states. The addition step is subsequently followed by the departure of the leaving group from the anionic Meisenheimer complex intermediate, which is energetically favorable due to the rearomatization.[94] [91]

The reaction rate of the addition-elimination mechanism, is influenced by multiple factors, such as the stability of the Meisenheimer complex, the reactivity of the electrophile, the nucleophile, the nucleofugal leaving group and the solvent.

The use of polar aprotic solvents rather than protic solvents, often accelerates the rates of substitution. This is a consequence of poor solvation of centers of negative charge in aprotic solvents, which increases the reactivity of nucleophile.[95] Protic solvents can also accelerate the reaction rate, by contrast to polar aprotic solvents, negatively charged centers is easily solved in protic media, stabilizing the transition state and therefore lowering the energy to obtain the transitions state.[95] However, protic media also stabilizes the negatively charged nucleophile, decreasing the reactivity of the nucleophile. To increase the rate of substitution it is important to obtain a net decrease in activiation energy. In finding the best solvent for nucleophilic aromatic substitution, the increase in reactivity, of the nucleophile, must be weighed up against the stabilization of the transition state.

The reaction rate is also affected by the strength of the nucleophile, since the nucleophilic attack and the formation of the Meisenheimer complex is the rate determining step of the addition-elimination nucleophilic aromatic substitution. The nucleophilic strength is based on three factors, which are their basicity, polarizability and the presence of unshared electron pairs in adjacent atom of the nucleophile, the alpha effect.[96]

The nucleofugality of the leaving group will also affect the reaction rate of the substitution. Since the rate determining step, RDS, is the formation of the Meisenheimer intermediate and not the bond breaking, the reaction rate is more affected by the leaving groups ability to stabilize the complex, than the bond strength of the leaving group. The Meisenheimer complex is stabilized by the electronegativity/ electron withdrawing effect of the leaving group, therefore in contrast to normal substitution, the nucleofugality of halogenes in nucleophilic aromatic substitutions follows as $F \gg Cl > Br > I$.[90]

The reactivity of the electrophile affects the reaction rate. As mentioned the electrophilic character of the aromatic ring is caused by electron deficency. In the case of the hetroaromatic pyrimidine rings, the nitrogen atoms in the aromatic ring makes the electrophile more electron deficient. Pyrimidines are activated towards nucleophilic aromatic substitution at C-2 and C-4 due the heteroaromatic ring's ability to stabilize the addition intermediate through resonance structures.[97] This is illustrated in Scheme 1.9.2

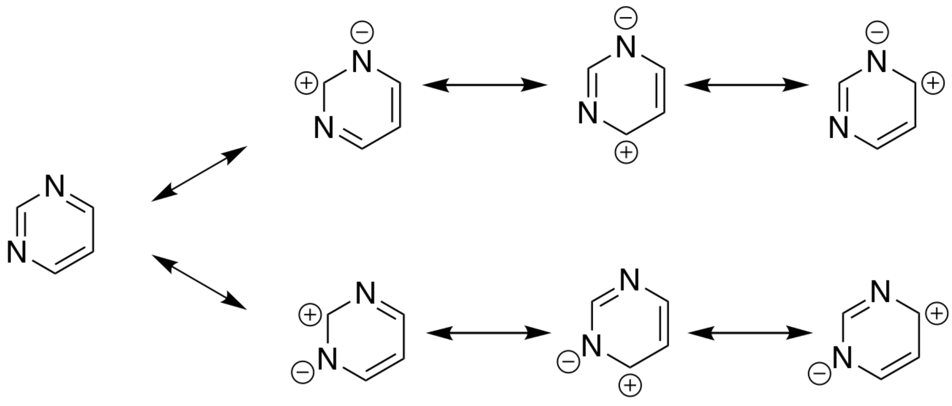

Scheme 1.9.2: The pyrimidines ability to stabilize negative charge through resonance.[97]

In the particular case of amination of pyrimidines, the reaction proceeds through a nucleophilic attack by aniline, on the halogenated pyrimidine. After the formation of the Meisenheimer intermediate, removal of the excess proton in the amine is needed. Deprotonation can occur by another aniline molecule acting as base or by adding a co-base to the reaction mixture. Subsequently the nucleofugal halide anion is expelled. In this project amination will be carried out by 6-bromo-4-chloro-thieno[2,3-*d*]pyrimidine reacting with aniline as nucleophile. This will expel the chlorine atom at C-4 in the electron deficient pyrimidine ring, while the bromine atom at C-6 in the electron rich thiophene, will be unaffected. A proposed mechanism of S_NAr amination of thieno[2,3-*d*]pyrimidine with anilines, in basic conditions, is presented in Scheme 1.9.3.

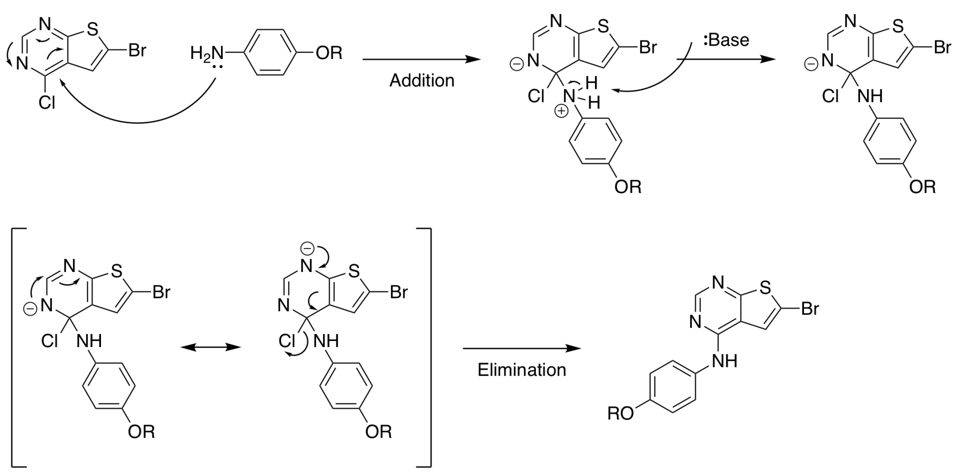

Scheme 1.9.3: A proposed mechanism of S_NAr amination of thieno[2,3-*d*]pyrimidine.[90] [98] [97]

Introduction of substituents at C-4 in thienopyrimidnines can be carried out through various methods. Previously Han *et al.* have introduced alkoxy subtituents at C-4 by nucleophilic aromatic substitution in basic conditions.[99] The research group has previously introduced anilines at C-4 in thienopyrimidines through different methods. The research group have performed amination through S_NAr in thermal and in slightly basic conditions.[46] Kurup *et al.* have reported amination of thienopyrimidines with acidic reaction conditions.[100] All the different detailed reaction conditions to perform nucleophilic aromatic substitution, at C-4 in thienopyrimidines, are reported in excellent yields.

1.9.2 Buchwald-Hartwig Amination

Another popular method of amination is the Buchwald-Hartwig cross-coupling.[55] Buchwald-Hartwig cross-coupling is a palladium (Pd) catalyzed process between aryl halides and amines with stoichiometric amounts of base present for the formation of C-N bonds.[101]

The Buchwald-Hartwig mechanism goes through a catalytic cycle which is similar to other cross couplings.[102] [103] [104] The catalytic cycle for the Buchwald-Hartwig cross-coupling is illustrated in Scheme 1.9.4. The first step is oxidative addition between palladium, Pd(0), and the aryl halide. The next step in the cycle is amine binding to form the Pd(II)-aryl amine complex which can occur in two possible ways, as illustrated in the two different routes in Scheme 1.9.4. The two ways are from the direct displacement of halide from the Pd(II)-complex by the amine or from amine reacting with an Pd(II)-alkoxide intermediate complex. In both routes deprotonation of the amine moiety of the complex occurs by the alkoxide base. The final step of the catalytic cycle is reductive elimination, which forms the desired C-N coupled aryl amine and regenerates the catalyst.[105]

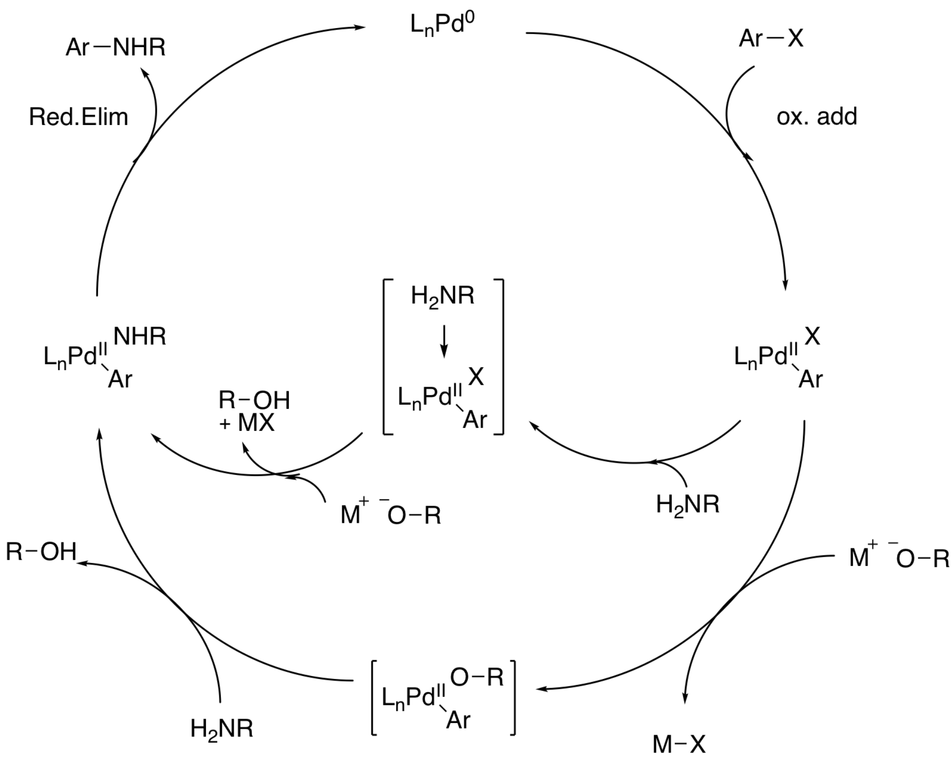

Scheme 1.9.4: The catalytic cycle for the Buchwald-Hartwig cross-coupling.[106] [103] [105] [107]

A possible issue with the Buchwald-Hartwig cross-coupling is that it is not controlled by the electron deficiency of the aryl halide. In the case of amination of 6-bromo-4-chloro-thieno[2,3-*d*]pyrimidine in this project, it is possible to form unwanted by-products through amination at both C-4 and C-6. Buchwald-Hartwig cross-coupling has previously been performed by Gonzalez *et al.* to add amine groups to thienopyrimidnes.[108] However, the amination was carried out in relative low yields.

1.10 Suzuki-Miyaura Cross-Coupling

Reactions in which formation of carbon-carbon bonds occur, are important, since they provide essential steps in the development of complex molecules from simple substrates. The palladium catalyzed reaction between organoboron compounds and organic halides is an effective method for the formation of carbon-carbon bonds, known as Suzuki-Miyaura cross-coupling. The Suzuki-Miyaura cross-coupling is frequently referred to as the Suzuki reaction. Only catalytic amounts of palladium catalyst and a suitable base is necessary for the reaction to take place.[109] A general Suzuki reaction is given in Scheme 1.10.1.

The Suzuki reaction is the most versatile and widely used method for forming sp^2-sp^2 bonds.[110] [111] The Suzuki-Miyaura cross-coupling is one of the easiest and effective methods to form biaryls through aryl-aryl cross-couplings.[112] The broad application of the Suzuki reaction is due to the many commercial available organoboron reagents, mild reaction conditions and toleration of a broad span of functional groups.[113] The reaction also tolerates water, which allows for efficient and facile removal of inorganic by-products. In addition, the reaction is generally stereo- and regioselective. The use of non-toxic environmentally friendly organoborons in the Suzuki reaction, compared to the toxic organostannanes used in alternative cross-couplings, makes the Suzuki cross-coupling a green option as well.[104]

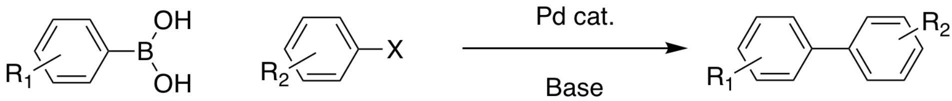

Scheme 1.10.1: A general Suzuki-Miyaura cross-coupling[114]

The mechanism, of the Suzuki cross-coupling, follows the general catalytic circle for cross-coupling reactions. The catalytic cycle consists of four mechanistic stages; Oxidative addition, metathesis, transmetalation and reductive elimination.[104] [115] The Suzuki reaction is initiated by oxidative addition, which alters the oxidation state from Pd(0) to Pd(II). This occurs from the addition of the organo halide to the Pd(0) complex catalyst, to form a Pd(II) organo halide complex. The initiation of the Suzuki reaction requires anionic Pd(0) intermediate, which is important for the rate of the oxidative step.[116]

The next step in the catalytic cycle, which differentiate the Suzuki reaction from general catalytic cycles, is metathesis.[104] During metathesis, the halide anion attached to the Pd complex, is displaced and exchanged with the anion from the base. This forms a more reactive organopalladium alkoxide or hydroxide complex, based on the base utilized in the reaction.[117] Metathesis is followed by transmetallation between Pd(II) and the organoboron compound, where the organo moiety of the organoboron compound is transferred to the Pd(II)-complex.[118] There has been some discussion about the reaction pathway, whether or not the transmetallation step occurs between trihydroxyborate and the organopalladium halide species[119] or with the organopalladium hydroxo complex and boronic acid. Recent studies have provided evidence which concluded that the transmetallation occurs between the boronic acid and the organopalladium hydroxo species.[118] [112] The biorgano palladium complex, from the transmetallation step, can finally undergo reductive elimination, as the final step of the catalytic cycle, to form the carbon-carbon bond, as well as regenerate the Pd(0) catalyst.[118] [112] The general Suzuki-Miyaura cross-coupling catalytic cycle is illustrated in Scheme 1.10.2

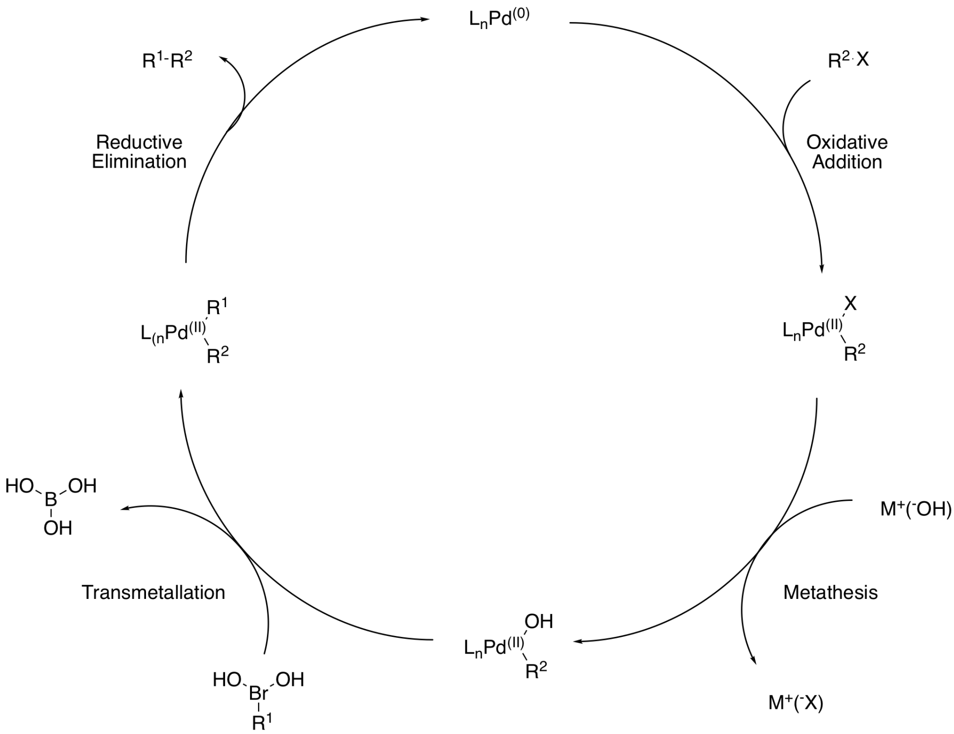

Scheme 1.10.2: The general catalytic cycle of Suzuki-Miyaura cross-coupling.[104] [115]

The rate determining step of the catalytic cycle depends on the identity of the organohalide, as well as the base used in the reaction. The rate determining step can either be the oxidative addition or the transmetallation. The rate determining factor of oxidative addition is the bond dissociation energies of the carbon-halide bond. The bond dissosciation energy of carbon-halide bonds follows as Ar-I > Ar-Br > Ar-Cl > Ar-F.[120] [121] The dissociation energy trend can change due to electron density. In cases where multiple halides are present, intrinsic electrophilicty of ring positions affect the electron density. The bond strength of aryl halides is also lowered by the addition of electron withdrawing groups to the aromatic compound.[121]

The choice of palladium catalyst greatly affect the Suzuki reaction. The catalyst's nature and amount, as well as ligands utilized, influence the reaction rate and the formation of by-products. The electronic and steric properties of ligands have effect on the reaction rate of the cross-coupling.[122] Catalysts with phosphine ligands, which are electron rich and bulky, can improve stability, hence enhance the selectivity and rate of the reaction.[123] By stabilizing the Pd(II)-complex formed in the oxidative addition step, electron rich ligands will increase the reaction rate.

The first catalyst reported utilized in Suzuki-Miyaura cross-coupling was $Pd(PPh_3)_4$.[124]

The traditional palladium catalysts were improved to widen the application of the reaction, by addition of bulky, electron-rich ligands.[123] With the addition of new ligands, new cross-couplings, such as biaryl formation from aryl chloride and aryl boron compounds, were feasible. Illustration of widely used palladium catalysts and ligands is presented in Figure 1.10.3.

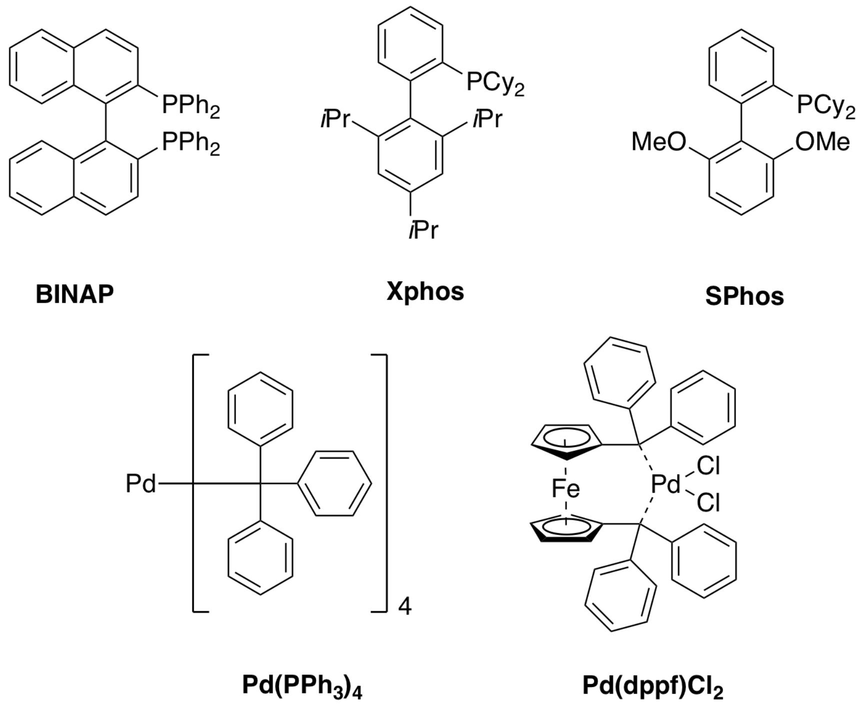

Scheme 1.10.3: Ligands and palladium catalysts used in Suzuki-Miyaura cross-coupling.[123] [125]

The use of the $Pd(Ph_3)_4$ catalyst in Suzuki cross-couplings on 4-amine-substituted thienopyrimidines has been reported in excellent yields.[39] The $Pd_2(dba)_3$ catalyst also was reported used in Suzuki reactions with thienopyrimidines, however problems with purification were reported along with the use of the catalyst.[126]

Chapter 2

Results and Discussion

In previous work, the research group has found thieno[2,3-*d*]pyrimidnes with aniline ether substituents at C-4 to have cytotoxicity towards HeLa and MCF-7 cancer cell lines. The aim of this project was to synthesise a library of thieno[2,3-*d*]pyrimidnes, with C-4 and C-6 substituents, to perform a structure activity relationship (SAR) study towards HER2 and to investigate their cellular activity. The aim of the SAR study was to investigate the importance of C-4 and C-6 substituents for the biological activity. The structures of the target compounds are given in Figure 2.1.

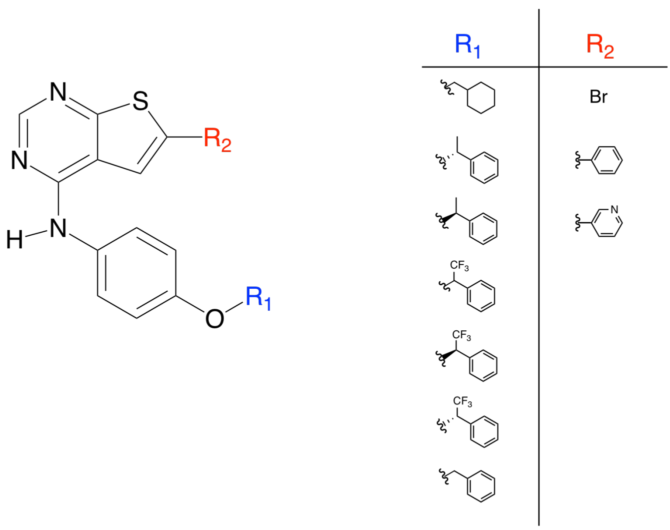

Figure 2.1: Structure of target molecules

The thieno[2,3-*d*]pyrimidine **1** was prepared previously by the research group and compound **11** was synthesized in the pre-Master project.[127] These compounds were used as building blocks in this thesis. This project introduced aniline substituents at C-4 and aromatic ring moieties at C-6. The first steps of the synthesis were preparing the aniline substrates, through either Williamson ether synthesis or S_NAr with a nitroarene reagent, followed by reduction of the nitro group, to form the anilines. The next step was amination of the thienopyrimidine at C-4 through S_NAr. The final step towards the target molecules was Suzuki-Miyaura cross-coupling to add the arene substitute at C-6. The synthesis route is presented in Scheme 2.0.1.

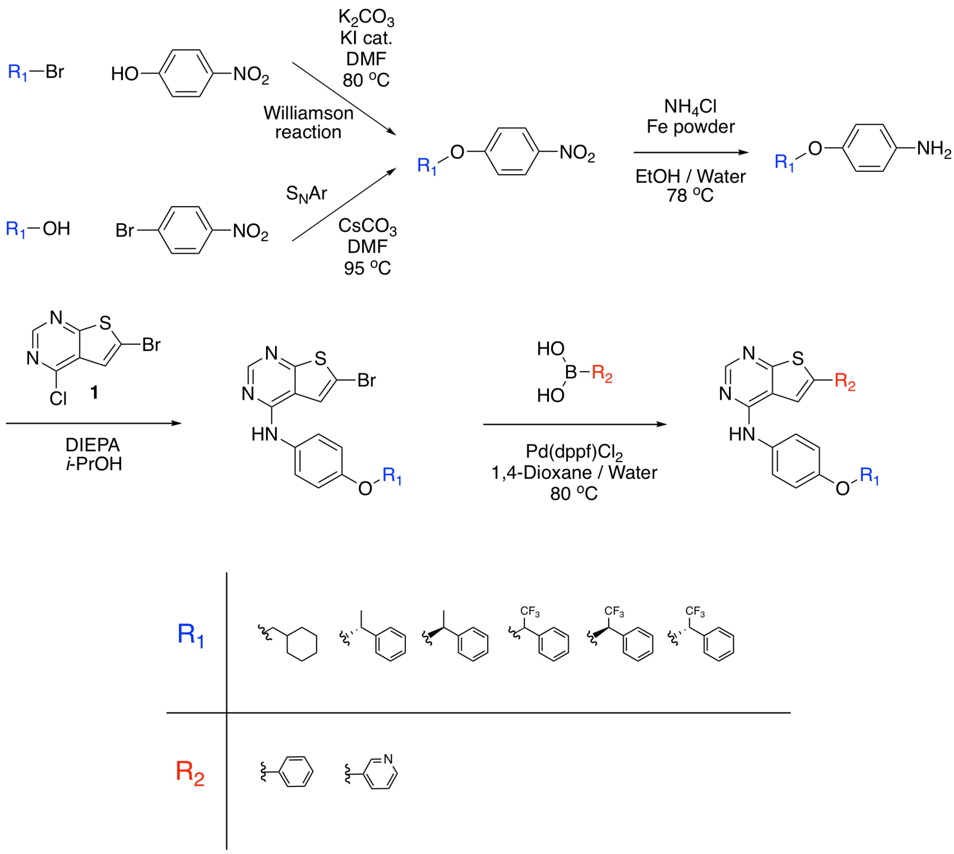

Scheme 2.0.1: The synthesis route to prepare the C-4 and C-6 substituted thieno[2,3-*d*]pyrimidine target molecules.

This chapter is divided into seven sections. The four first sections discuss the different synthetic steps: ether synthesis, reduction, amination and Suzuki cross-coupling. The last sections covers chromatography, structure elucidation of the synthesized compounds and biological testing.

2.1 Ether Synthesis

The first step, in preparation of the aniline substrates, used in C-4 amination of the thieno[2,3-*d*]pyrimidine, was ether synthesis. The ether synthesis was carried out either by Williamson ether synthesis or nucleophilic aromatic substitution. The Williamson reaction was performed between alkylbromide and 4-nitrophenol. The S_NAr reaction was carried out with benzylic alcohols and 1-fluoro-4-nitrobenzene.

2.1.1 Synthesis of Compound 2

Compound **2** was synthesized by Williamson ether synthesis between 4-nitrophenol and (bromomethyl)cyclohexane. The reaction was carried out with K_2CO_3 as the base. The reaction conditions are presented in Scheme 2.1.1

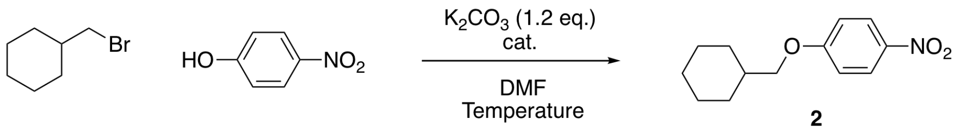

Scheme 2.1.1: Williamson ether synthesis between 4-nitrophenol and (bromomethyl)-cyclohexane.

A series of test reactions was carried out in a 100 mg scale. The reaction conditions for the first test reaction was taken from the pre-Master project.[127] Test reaction one was carried out for 24 hours at 22 ℃ with 1.2 equivalents of K_2CO_3 as the base. This reaction had 25% conversion. The conversion was determined by ^{1}H-NMR using the integral of the protons in the ortho-position to the nitro group in the starting material and the product. After extraction, a yellow solid was obtained. The crude yield was 15%. Due to the low conversion rate and yield, another test reaction was performed. The reaction was carried out with the same reaction conditions, with the addition of 0.1 equivalents of KI as nucleophilic catalyst. The reaction had 42% conversion after 24 hours and crude yield of 25%.

Based on the significant increase in both conversion and crude yield with the addition of KI, further test reactions with KI were carried out. The test reactions were performed at 60, 80 and 100 ℃. The conversion at 24 hours and crude yields are reported in Table 2.1.

Table 2.1: Conversion after 24 hours and crude yield of test reactions.

Temperature [℃]	Conversion [%]	Crude Yield [%]
60	89	58
80	>95	78
100	>95	64

When a satisfactory conversion rate and crude yield was obtained, a scale up reaction was performed. It was carried out at 80 °C, since the test reaction at 80 °C had full conversion and the highest crude yield. The reaction was carried out in a 2.77 g scale and was stopped after 24 hours with >95% conversion. A off-white were obtained in a 43% yield. A similar reaction, between (bromomethyl)cyclohexane and *N*-(4-hydroxyphenyl)acetamide with the same equivalents of base and nucleophilic catalyst at room temperature, has previously been performed by Yang *et al.* in 26% yield.[57]

2.1.2 Synthesis of Compounds (*R*)-3 and (*S*)-3

Compounds **(*R*)-3** and **(*S*)-3** were synthesized by nucleophilic aromatic substitution between 1-fluoro-4-nitrobenzyl and (*R*)-1-phenylethan-1-ol and (*S*)-1-phenylethan-1-ol, respectively. The reaction was carried out with Cs_2CO_3 as the base in DMF. The reaction conditions are presented in Scheme 2.1.2

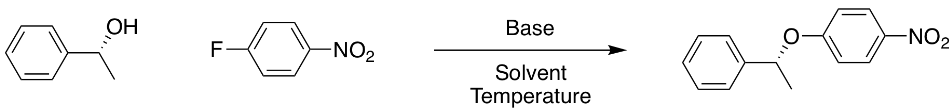

(*R*)-3

Scheme 2.1.2: Nucleophilic aromatic substitution between (*R*)-1-phenylethan-1-ol and 1-fluoro-4-nitrobenzyl

To investigate how different temperatures, solvents and bases affected the reaction rate, a series of test reactions were conducted with 1-fluoro-4-nitrobenzyl and (*R*)-1-phenylethan-1-ol. The reaction conditions and results from the test reactions are presented in Table 2.2.

Table 2.2: Reaction conditions and results from the test reactions.

Entry	Scale [mg]	Temperature [°C] [°C]	Solvent	Base	Conversion [a] [%] 2.5 h	24 h
1	100	22	DMF	1.3 eq. NaH	27	-
2	500	65	DMF	1.3 eq. NaH	25	40
3	100	95	ACN	1.2 eq. Cs_2CO_3	33	53
4	100	95	DMF	2.5 eq. Cs_2CO_3	55	>95

[a] The conversion was determined by ^{1}H-NMR using the integral of the protons in the benzylic position in the starting material and in the product.

The test reactions with NaH / DMF (Entry 1, Entry 2) were slower than that of reactions employing Cs_2CO_3 as base. The reactions with NaH / DMF, showed that higher temperature had no significant impact on the conversion. The increase of reactivity of Cs_2CO_3 / ACN (Entry 3) as compared to NaH / DMF (Entry

1, Entry 2), may be due to the base's, Cs_2CO_3, high degree of solubility, and Cs-alkoxide's low degree of solvation.[99] The use of Cs_2CO_3 / DMF (Entry 4), instead of Cs_2CO_3 / ACN (Entry 3) showed a major increase in conversion rate. The use of polar aprotic solvents is known to accelerate the rate of substitution in nucleophilic aromatic substitutions.[95]

Compound ***(R)*-3** was then synthesized with the reaction conditions of Entry 4 in Table 2.2. The reaction was carried out in a 1 g scale and stopped after 24 hours with >95% conversion. After one round of silica-gel column chromatography, the product was isolated as a orange solid in 82% yield, with a specific rotation of $[\alpha]_D^{20}$ = + 63.70°.

Enantiomer ***(S)*-3** was synthesized with the same method in a 1 g scale. The reaction was stopped after 24 hours with >95% conversion. After one round of silica-gel column chromatography a orange solid were obtained. The product was isolated in 59% yield with specific rotation of $[\alpha]_D^{20}$ = - 52.95°.

Compounds ***(R)*-3** and ***(S)*-3** were unstable during mass-spectroscopy analysis. Both electronspray (ES+) and atmospheric solid analysis probe (ASAP+) high resolution mass-spectroscopy have been employed. The [M+H] peak was not detected, however the fragments, see Figure 2.2, of the compounds were observed during ASAP+ HRMS. The presence of the fragments in combination with NMR analysis, as well as further synthesis, confirms the formation of the compounds.

Figure 2.2: The structure of fragments observed during MS.

2.1.3 Synthesis of Compounds (*rac*)-, (*R*)- and (*S*)-4

Nucleophilic aromatic substitution was performed on 1-fluoro-4-nitrobenzene and rac-, (*R*)- and (*S*)-2,2,2-trifluroro-1-phenylethanol. The reaction conditions are presented in Scheme 2.1.3.

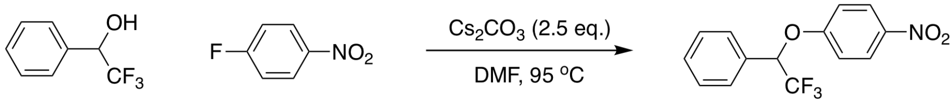

(*rac*)-4

Scheme 2.1.3: Nucleophilic aromatic substitution between 2,2,2-trifluroro-1phenylethanol and 1-fluoro-4-nitrobenzyl

A test reaction with the racemate was carried out in a 200 mg scale with the reaction conditions found in the optimization of the synthesis of compound ***(R)*-3**. ^{1}H-NMR analysis showed >95% conversion after 2.5 hours. The addition of the -CF_3 group, as compared to the methyl group in compound ***(R)*-3**, had a major increase in reactivity. This is probably due to the electron withdrawing effect of the -CF_3 group, which makes the adjacent proton substantially more acidic.

TLC of the test reaction showed that by-products were formed. The by-products made the purification and isolation of the desired product difficult. Extraction with EtOAc and saturated $NaHCO_3$ brine did not remove the formed by-products from the reaction mixture. The product was isolated by one round of silica-gel column chromatography. The column employed an eluent gradient that started at 98% *n*-pentane and 2% EtOAc composition, which was gradually increased to 90% *n*-pentane and 10% EtOAc. During the silica-gel column a lot of tailing and some overlapping between the desired product and by-products were observed. The product was isolated pure at the cost of the yield, as a colourless oil. The yield of the reaction was 38%. The by-products formed in the synthesis were not isolated or further investigated.

Compounds ***(rac)*-4**, ***(R)*-4**, ***(S)*-4** were synthesized in scale up reactions with (*R*)-, (*S*)-, and 2,2,2-trifluroro-1-phenylethanol, carried out with 2.5 eq. of Cs_2CO_3 and DMF at 96 °C. ^{1}H-NMR analysis showed that reactions achieved high to full, >95%, conversion after 2-3,5 hours. The products were isolated as pale yellow crystals. The scale, reaction time and results of the scale up reactions are presented in Table 2.14

Table 2.3: Results of the synthesis of compounds ***(rac)*-4** - ***(S)*-4** through S_NAr reactions. All reactions were carried out in DMF at 96 °C, with Cs_2CO_3 as base.

Product	Stereochem.	Scale [g]	RX time [h]	Conv.^{a} [%]	Yield [%]	Mp [°C]	$[\alpha]_D^{20}$ [°]
***(rac)*-4**	*rac*	2.0	2.5	>95	48	67.1-68.8	-
***(R)*-4**	(*R*)	0.78	2	>95	61	83.4-85.0	-39.57
***(S)*-4**	(*S*)	1.5	3.5	94	71	66.9-70.3	45.58

^{a} Conversion was determined by ^{1}H-NMR using the integral of the proton in the benzylic position in the starting material and in the product.

The issues with the work up were still apparent in the scale up reactions. However, there was less formation of by-products in the synthesis of the enantiomers, compared with the racemate.

In the ^{1}H-NMR-specter of the purified compound ***(S)*-4**, some impurities affiliated with the unreacted 2,2,2-trifluoro-1-phenylethanol were observed, equivalent to 6% of the product. Compound ***(S)*-4** was not further purified due the difficult silica-gel column chromatography. The further purification was not performed, since the remaining alcohol would not affect the subsequent synthetic steps, and the work up in latter synthetic steps were much simpler.

2.1.4 Summary of Ether Synthesis

Ether synthesis has been performed through Williamson ether synthesis and nucleophilic aromatic substitution. The Williamsons reaction was performed between 4-nitrophenol and (bromomethyl)cyclohexane. S_NAr reactions were performed between 1-fluoro-4-nitrobenzene and various benzylic alcohols. Table 2.4 gives a summary of the results from the ether syntheses.

Table 2.4: Summary of the results from the ether syntheses. The Williamson ether synthesis was carried out in DMF at 80 °C, with K_2CO_3 as base and catalytic amount of KI. All the S_NAr reactions were carried out in DMF at 95 °C, with Cs_2CO_3 as base.

Prod.	Scale [g]	Rx time [h]	Conv.[a] [%]	Yield [%]	State	Mp. [°C]
2	2.77	24	>95	43	Off-white solid	43.6-44.7
(*R*)-3	1.0	24	>95	82	Orange solid	45.6-47.8
(*S*)-3	1.0	24	>95	59	Orange solid	43.1-45.4
(*rac*)-4	0.20	2.5	>95	38	Colourless oil	-
	2.0	2.5	>95	48	Pale yellow crystals	67.1-68.8
(*R*)-4	0.78	2	>95	61	Pale yellow crystals	83.4-85.0
(*S*)-4	1.5	3.5	>95	71	Pale yellow crystals	66.9-70.3

[a] Conversion was determined by ^{1}H-NMR using the integral of the proton in the benzylic position in the starting material and the product.

The Williamson ether synthesis had a moderate yield, however higher than expected from previously reported yields.[57] Overall, the S_NAr reactions achieved varying yields. To improve S_NAr ether synthesis, the base and solvent system requires further development. Each substituent in the reagents affects the reactivity towards the reaction distinctly. More tailored reaction conditions may limit the formation of by-products. The general work up of the ether syntheses may also be improved.

2.2 Reduction of Nitro-aromatics

The anilines used in amination of C-4 carbon, in the target compounds, were finalized through the reduction of the nitro group. The reaction conditions for selective reduction of nitro arenes with an ether group present, were established in the pre-Master project.[127] These conditions resulted in high yields and fairly easy work up. The method utilized was 3 equivalents iron powder and 9 equivalents ammonium chloride in aqueous ethanol, illustrated in Scheme 2.2.1. The pre-master project showed that the presence of 30% water was crucial for the reaction to proceed with a decent rate.[127]

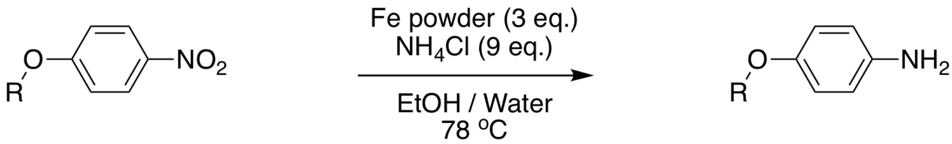

Scheme 2.2.1: General reaction conditions for the reduction of nitro arenes with an ether group present.

2.2.1 Synthesis of Compound 5

The cylohexyl derivative **5** was synthesized by reduction of compound **2**. The reaction was carried out with iron powder and NH_4Cl. The reaction conditions are presented in Scheme 2.2.2

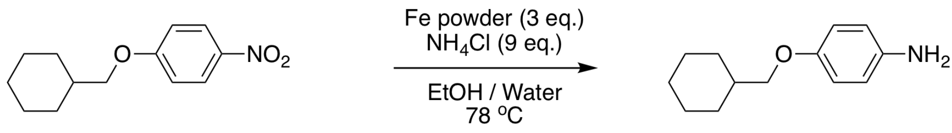

2 **5**

Scheme 2.2.2: Reaction conditions of the reduction of compound **2**

The reaction was carried out twice, in 500 mg and 1.5 g scale. Both reactions reached full conversion according to TLC, after 3 hours. The work up for the 500 mg scale reaction consisted of filtration through celite with 50/50 ethanol and water and extraction with EtOAc and water.

In the crude product of the 1.5 g scale reaction, by-products, not present in the crude product of the 500 mg scale, were observed on TLC and in crude ^{1}H-NMR analysis. The presence of by-products added additional steps to the purification. After filtration and extraction, the product was purified through one round of silica-gel column chromatography. The products from both reactions were isolated as brown solids. The product from the 500 mg scale parallel was isolated in 95% yield, while the product from the 1.5 g scale parallel was isolated in 62% yield.

The major difference in yield between the two different parallels is due to a combination of formation of by-products at the cost of the desired product and loss of product on the silica-gel column. The loss of product on the silica-gel column occurred through tailing due to crystallization of the product on the silica.

2.2.2 Synthesis of Compounds (*R*)-, (*S*)-6 and (*rac*)-, (*R*)-, (*S*)-7

Compounds **(*R*)-**, **(*S*)-6** and **(*rac*)-**, **(*R*)-**, **(*S*)-7** were synthesized through reduction of the nitro derivatives **(*R*)-**, **(*S*)-3** and **(*rac*)-**, **(*R*)-**, **(*S*)-4** respectively. The reductions were carried out applying the iron powder and NH_4Cl reducing system. The reactions are presented in Scheme 2.2.3.

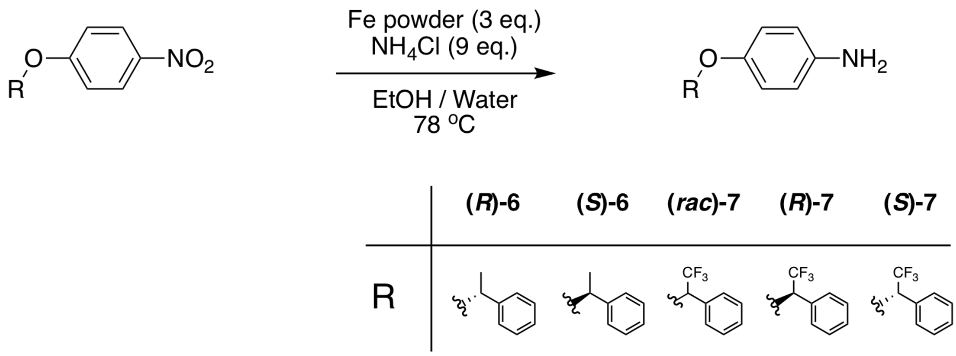

Scheme 2.2.3: Reduction reactions with the nitro arene substrates (**(*R*)-3**-**(*S*)-4**).

^{1}H-NMR analysis showed that all the reactions reached full conversion, >95%, after 1.5 - 3.5 hours. The conversion was calculated from the integral of protons in the benzylic position in both the product and the starting material. The work up of the reactions consisted, as in Section 2.2.1, by filtration through celite and extraction. The products were isolated as brown oils. The scales, results and reaction times of the reactions are presented in Table 2.5.

Table 2.5: Results from the synthesis of compounds ***(R)*-**, ***(S)*-6** and ***(rac)*-**, ***(R)*-**, ***(S)*-7** through selective reduction of nitro arenes. All reactions were carried out in EtOH / water with the reducing system of Fe powder/ NH_4Cl.

Substrate	Prod.	Stereochem.	Scale [g]	Rx time [h]	Conv.^{a} [%]	Yield [%]	$[\alpha]_D^{20}$ [°]
***(R)*-3**	***(R)*-6**	(*R*)	0.70	3.5	>95	62	52.80
***(S)*-3**	***(S)*-6**	(*S*)	0.80	3.5	>95	59	-60.57
***(rac)*-4**	***(rac)*-7**	(*rac*)	0.99	1.5	>95	79	-
***(R)*-4**	***(R)*-7**	(*R*)	0.50	2.0	>95	85	-72.71
***(S)*-4**	***(S)*-7**	(*S*)	1.03	2.5	>95	86	82.93

^{a} Conversion was determined by ^{1}H-NMR using the integral of the proton in the benzylic position in the starting material and in the product.

2.3 Amination

Nucleophilic aromatic substitution was used to add the anilines, formed in the previous synthetic steps, at the C-4 position in thienopyrimidine **1**. The synthesis was based on the work of Bugge *et al.* for similar compounds.[46] In the pre-Master project, the reaction conditions of C-4 amination of thieno[2,3-*d*]pyrimidines through nucleophilic aromatic substitution were evaluated.[127] The S_NAr reaction was performed with various substituted anilines and diverse substituted thieno[2,3-*d*]pyrimidines. The general reaction conditions employed with C-4 amination is given in Scheme 2.3.1.

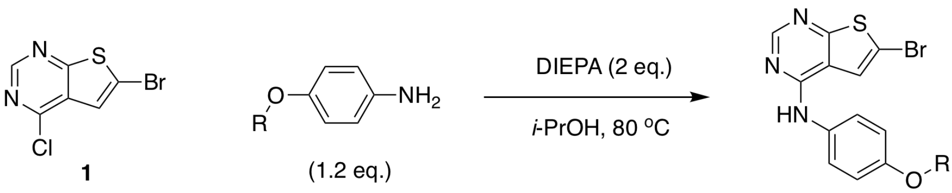

Scheme 2.3.1: The general reaction conditions for the amination of thienopyrimidine **1** with aniline substrates.

2.3.1 Synthesis of Compound 8

Compound **8** was synthesized through nucleophilic aromatic substitution of aniline **5** to thienopyrimidine **1**. The reaction was carried out in *i*-PrOH at 80 ℃ with DIEPA as co-base, see Scheme 2.3.2.

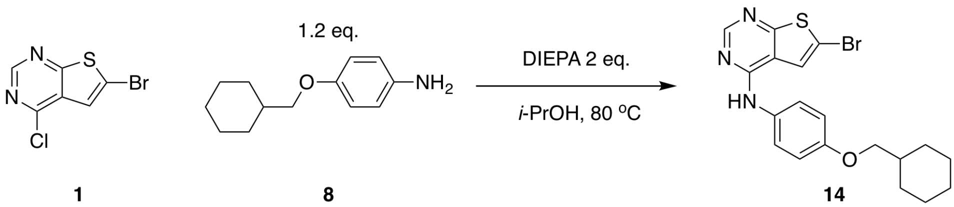

Scheme 2.3.2: Selective amination of thienopyrimidine **1** with aniline **5**.

The reaction, performed in a 346 mg scale, reached >95% conversion after 4 hours. The conversion was calculated from [1]H-NMR analysis by the integral of the proton at C-2 position in the product and in the starting material. The product was isolated through one round of silica-gel column, starting out with 9 : 1 /n]-pentane / EtOAc eluent composition. However, when crystallisation of the product on the silca was observed, the product was flushed out with 100% EtOAc. Compound **8** was isolated as an off-white solid, in a 48% yield, with HPLC purity of 99% and a melting point of 189.5 - 190.1 °C.

2.3.2 Synthesis of (*R*)-9 and (*S*)-9

The 1-phenylethylamine containing compounds **(*R*)-9** and **(*S*)-9** were synthesized through selective nucleophilic aromatic substitution using thienopyrimidine **1** and aniline **(*R*)-6** and **(*S*)-6** respectively, see Scheme 2.3.3. The reactions were carried out in 130 mg scale.

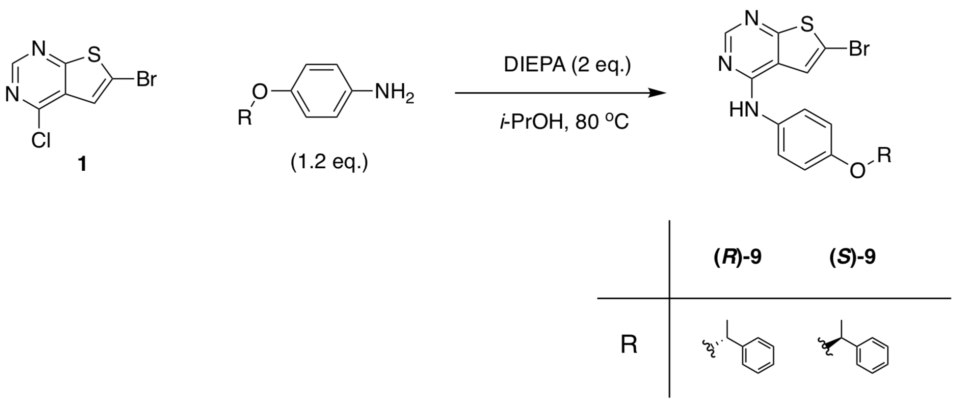

Scheme 2.3.3: The reaction conditions for the amination of thienopyrimidine **1** with aniline substrates **(*R*)-6** and **(*S*)-6**.

[1]H-NMR analysis showed that the reactions reached >95% conversion after 4 - 4.5 hours. The conversion was calculated from [1]H-NMR analysis by the integral of the proton at the C-2 position in the product and in the starting material. The

products were isolated as light brown solids, after two rounds of silica-gel column chromatography.

Purification of compound ***(R)*-9** consisted of two rounds of silica-gel column chromatography. The first silica-gel column employed 1:1 of *n*-pentane and EtOAc as the eluent giving good separation on TLC. The good separation on TLC did not transfer to the silica-gel column. To obtain better separation, the retention was increased by increasing the amount of non polar solvent in the eluent composition too 7 : 3 *n*-pentane / EtOAc. Compound ***(R)*-9** was isolated in a 32% yield, with HPLC purity of 99%, a melting point of 156.7-157.7 °C, $[\alpha]_D^{20}$ of 45.92° and EE(%) of 99.

To mitigate the need for two rounds of silica-gel column chromatography during purification of compound ***(S)*-9**, the amount of non polar solvent in the eluent composition was increased to 3 : 2 *n*-pentane / EtOAc for the first column. However, there were still some impurities in the product after the first silica-gel column. Another round of silica-gel column chromatography, with 4 : 1 *n*-pentane / EtOAc, was employed to ensure high purity of the product. Compound ***(S)*-9** was isolated in a 41% yield, with HPLC purity of 99%, a meltingin point of 157.9-158.6 °C, $[\alpha]_D^{20}$ of -37.85° and EE(%) of 99.

2.3.3 Synthesis of Compounds (*rac*)-, (*R*)- and (*S*)-10

Nucleophilic aromatic substitution was performed on thienopyrimidine **1** with the anilines ***(rac)*-7 - *(S)*-7**, to synthesize trifluoro derivatives ***(rac)*-10 - *(S)*-10**, see Scheme 2.3.4. The reactions were conducted in 100 mg and 200 mg scale.

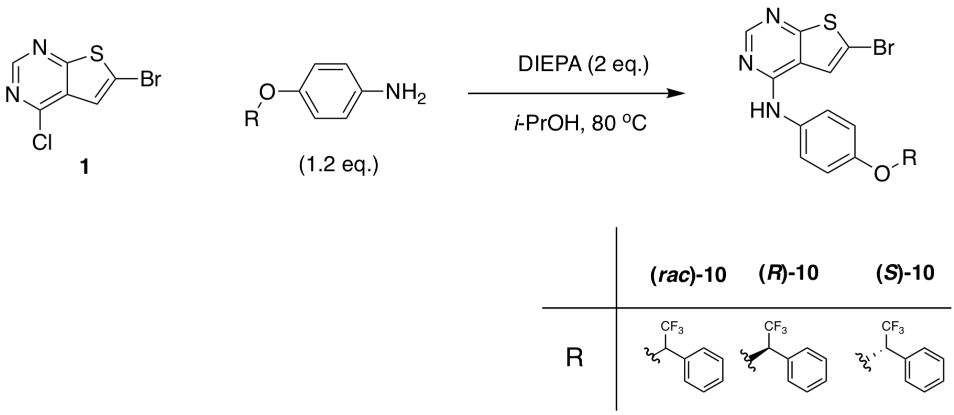

Scheme 2.3.4: The reaction conditions for the amination of thienopyrimidine **1** with aniline substrates ***(rac)*-10 - *(S)*-10**.

^{1}H-NMR analysis showed that the reactions reached full conversion, >95%, after 6 - 24 hours. All products were isolated, by one round of silica-gel column chromatography, as off-white solids. All the compounds had HPLC purity of >96%.

The scale and results from the reactions are presented in Table 2.6. The specific rotation, enantiomeric excess and melting point of the isolated compounds are given Table 2.7.

Table 2.6: Results from the synthesis of Compounds ***(rac)*-10-*(S)*-10** through amination of thienopyrimidine **1** with aniline substrates ***(rac)*-7 - *(S)*-7**. All reactions were carried out in *i*-PrOH 80 °C, with DIEPA as co-base.

Substrate	Prod.	Stereochem.	Scale [mg]	Rx time [h]	Conv.[a] [%]	Yield [%]	Purity[b] [%]
***(rac)*-7**	***(rac)*-10**	(*rac*)	200	6	>95	51	96
***(R)*-7**	***(R)*-10**	(*R*)	100	6.5	>95	56	99
***(S)*-7**	***(S)*-10**	(*S*)	200	24	>95	52	99

[a] Conversion was determined by ^{1}H-NMR analysis of the integral of the proton at C-2 position in the product and in the starting material.
[b] Purity was determined by the method described in Section 4.1.2.

Table 2.7: Melting point, specific rotation and enantiomeric excess of compounds ***(rac)*-10-*(S)*-10**.

Compound	Mp. [°C]	$[\alpha]_D^{20}$ [°]	EE(%)[a]
***(rac)*-10**	199.7 - 200.6	-	-
***(R)*-10**	174.9 - 176.5	-61.49	96
***(S)*-10**	173.8 - 175.8	61.82	97

[a] EE(%) were determined by method 1 described in Section 4.1.2.

The overall yield of the reactions were fairly similar, however the conversion time was a lot slower for compound ***(S)*-10**. This may be due to the presence of the impurity, from the synthesis of compound ***(S)*-4**, in the starting aniline ***(S)*-7**.

2.3.4 Loss of Product during Amination

The amination of thienopyrimidine **1** with various anilines (**5 - *(S)*-7**), achieved mediocre yields. The amination reaction of similar compounds has been performed by Bugge *et al.*, with slightly basic and thermal reaction conditions, in >80% yields.[46] The amination of similar compounds has also been done by Kurup *et al.*, in acidic conditions, in >80% yield.[100]. To investigate the loss of product during the amination, compound **11** from the pre-Master project was synthesized again, see Scheme 2.3.5. The reaction was carried out in a 1 gram scale.

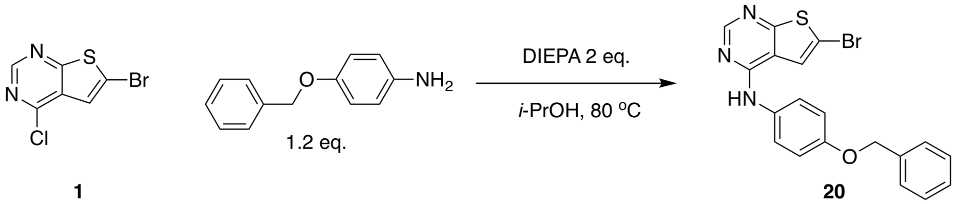

Scheme 2.3.5: The reaction condition for the amination of thienopyrimidine **1** with 4-(benzyloxy)aniline hydrochloride.

The reaction reached full conversion after 6.5 hours. After no further work up than concentration of the reaction mixture in *vacuo*, a ^{1}H-NMR assay was recorded. The assay ^{1}H-NMR was recorded with 4-chlorothieno[2,3-*d*]pyrimidine as standard, presented in Figure 2.3. The assay was used to determine whether or not the loss of product occurred during the reaction or in the work up.

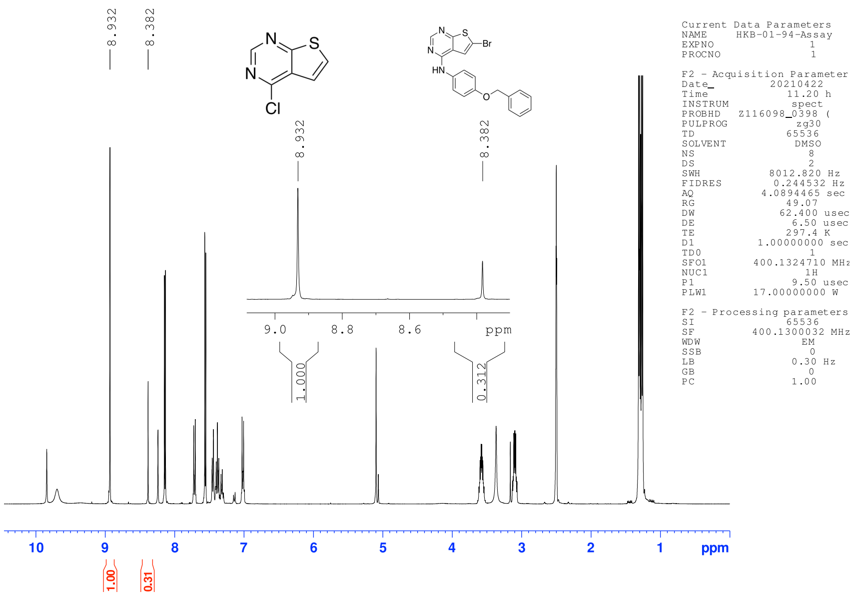

Figure 2.3: Assay NMR of the crude product of the reaction, with 4-chlorothieno[2,3-*d*]pyrimidine as standard.

^{1}H-NMR analysis of the integral of the proton at C-2 position in the product **11** and the standard, was used to determine the percentage of product in the crude mixture. The assay value obtained was 58 wt% of product in the crude, which correlates to 116% yield of compound **11**. The obvious deviation in yield from the theoretical value may be due to differences in the relaxation times for different protons during NMR analysis, which affect the intensities of the proton peaks. The ^{1}H-NMR assay strongly indicated that no product was lost during the reaction, therefore the loss of product is assumed to occur during the work up.

Each step of the work up was investigated to discover where the loss of product occurred. The silica-gel column chromatography step was performed on a part of the crude reaction mix. Extraction was not carried out prior to the silica-gel column chromatography, in contrast to the other amination reactions. The silica gel column removed all UV active impurities and the purification occurred without any substantial loss of product. However, the silica-gel column did not remove any of the HCl salt formed in the reaction. Since there was no significant loss of product, the silca-gel step was repeated on the rest of the crude product. The repeated step achieved the same outcome, which made the main suspect for the loss of product the extraction.

The final step to be investigated was extraction of HCl salt. The crude product was partitioned between EtOAc and (aq.) $NaHCO_3$. The organic phase was dried over Na_2SO_4 and filtrated. The product was isolated in a 81% yield. There was some loss of product during the final step of the work up, but less than expected. In the pre-Master project, compound **11** was synthesized in 37% yield.[127] Further investigation is needed to determine if it was the pH variation by the HCl salt, during silica gel column chromatography, that resulted in no loss on the column. Alternatively the investigation may confirm that the product was lost during the extraction.

2.3.5 Summary of Amination

Thienopyrimidine **1** has been selectively aminated in C-4 position with a number of anilines. A summary of the results is presented in Table 2.8

Table 2.8: Summary of the results achieved in the amination reactions. All reactions were performed in *i*-PrOH at 80 °C, with DIEPA as co-base.

Prod.	Scale [mg]	Rx time [h]	Conv.^{a} [%]	Yield [%]	State	Purity [%]	Mp. [°C]
8	350	4	>95	48	Off-white solid	99	189.5-190.1
(*R*)-9	130	4	>95	32	Light brown solid	99	156.7-157.7
(*S*)-9	130	4.5	>95	41	Light brown solid	99	157.9-158.6
(*rac*)-10	200	6	>95	51	Off-white solid	96	199.7-200.6
(*R*)-10	100	6.5	>95	56	Off-white solid	99	174.9-176.5
(*S*)-10	200	24	>95	52	Off-white solid	99	173.8-175.8
11	1000	6.5	>95	81	Off-white solid	99	174.9-177.6

^{a} Conversion was determined by ^{1}H-NMR analysis of the integral of the proton at C-2 position in the product and in the starting material.
^{b} Purity was determined by the method described in Section 4.1.2.

Overall, the products were isolated in mediocre yields. There was no formation of by-products or loss of product during the reaction itself. The loss of product during the S_NAr amination occurred during the work up. The yield was significantly increased by performing the silica-column chromatography first and then the extraction. To improve the amination reaction, the work up method needs further development.

2.4 Suzuki-Miyaura Cross-Coupling

The final step in the synthetic route towards the target compounds was Suzuki-Miyaura Cross-Coupling. The Suzuki reaction was performed to create Sp^2-Sp^2 couplings at C-6 in the target compounds. The reactions were carried out between boronic acids and a number of thienopyrimidines.

2.4.1 Synthesis of Compounds 12-15

The Suzuki reactions were performed with thienopyrimidines **8**, **(*rac*)-10**, **(*S*)-10** and **11** and phenyl- or 3-pyridinylboronic acid. The reactions were carried out in 1,4-dioxane and water at 80 °C, with K_2CO_3 as base. The catalyst employed during the reactions was $Pd(dppf)Cl_2$. All reactions achieved full conversion after 15 minutes - 2.5 hours. Conversion was determined from the ^{1}H-NMR integrals of the N-H protons of both products and starting materials. The compounds were isolated as off-white solids, after one round of silica-gel column chromatography. The scale, reaction time and results of the Suzuki cross-couplings are presented in Table 2.9

Table 2.9: The results of the Suzuki-Miyaura cross-couplings. All reactions were carried out in 1,4-dioxane / water at 80 °C, with K_2CO_3 as base and Pd(dppf)Cl_2 as catalyst.

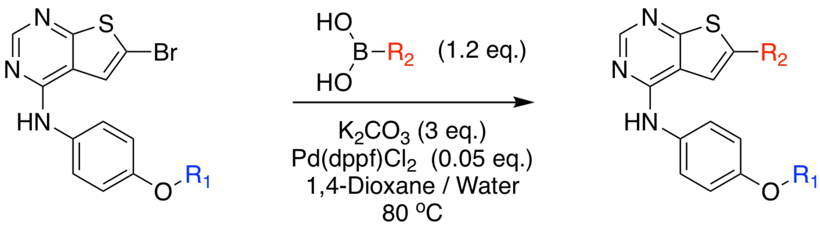

	12	**13**	**14**	***(rac)*-15**	***(S)*-15**
R_1	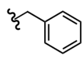	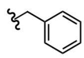	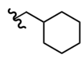	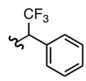	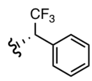

Substrate	Prod.	R_2	Scale [mg]	Rx time [min]	Yield [%]	Purity[a] [%]	Mp. [°C]
11	**12**	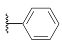	75	20	67	99	211.2-211.4
11	**13**	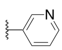	75	15	64	99	216.2-218.1
8	**14**	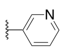	100	150	27	99	224.2-226.2
(*rac*)-10	**(*rac*)-15**	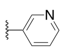	100	15	88	99	217.7-218.6
(*S*)-10	**(*S*)-15**	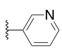	100	20	90	99	166.7-167.8

[a] Purity was determined by the method described in Section 4.1.2.

Compound **(*S*)-15** had a specific rotation, $[\alpha]_D^{20}$, of 53.30 ° and an enantiomeric excess, EE(%), of 99. The Suzuki reactions achieved overall high yields, except for compound **14**. The work up for the reactions was fairly facile. The cross-coupling with compound **8** was significantly slower compared to the other reactions. Compound **14** was also isolated in a considerably less yield. The presence of cyclohexane, in the molecule had major impact on the reactivity during the Suzuki reaction. The Suzuki cross-coupling may benefit from employing an alternative palladium-catalyst.

2.5 Determination of Enantiomeric Purity

Throughout the synthesis of enantioenriched compounds in this thesis, the specific rotation of enantiomeric pairs has had some deviation in absolute values. To ensure that racemization has not occurred during the synthetic steps, enantiomeric purity was determined using HPLC equipped with chiral stationary phases. The chiral analyses of C-6 bromide substituted target compounds were carried out with a ChiralCel OD column and *i*-PrOH:*n*-hexane (1:9) as mobile phase. This method had a relatively short rentention time and a resolution factor of Rs>3.5 for the racemic mixtures.

For the C-6 aryl substituted thienopyrimidines, the same method as for the bromide substituted substrates, did not give sufficient separation. To try to improve the separation, the ChiralCel OD column was exchanged with a LUX 5u Cellulose-1 column, without success. The retention time increased drastically and the enantiomers coeluted. Finally, sufficient separation was obtained by the eluent composition, EtOH (with 0.1% TFA):*n*-hexane (5:95) and with the ChiralCel OD column. This method of HPLC obtained Rs of 3.88, however the retention time was far from optimal. The enantiomeric excess for all the analyzed compounds was greater than 96%. EE(%)>96 confirms that the compounds are enantiomeric pure and that racemization did not occur, despite the reported specific rotations. The EE(%) of the compounds are specified in the sections discussing the synthesis of the specific compounds. The chromatograms for Compounds **(*R*)-**,**(*R*)-9**, **(*rac*)-**, **(*R*)-**, **(*S*)-10**, **(*rac*)-15** and **(*S*)-15** can be found in Appendix .2.

2.6 Structure Elucidation

To identify compounds which are not referenced in literature, structure elucidation was performed. Structure characterisation and assigning of shifts to the atoms in the compounds were assigned by 1D-NMR and 2D-NMR. The NMR-spectroscopy utilized to determine the chemical shifts was ^{1}H-, ^{13}C-,^{19}F-NMR, ^{1}H-^{1}H COSY, ^{1}H-^{13}C HSQC and ^{1}H-^{13}C HMBC. To validate the structures obtained from NMR analysis, high resolution mass spectroscopy (HRMS) was performed. Infrared (IR) spectroscopy was carried out to identify the common vibrational modes of the functionality in the different compounds. This section addresses the structure elucidation for each compound series. All spectra used in the structure elucidation can be found in Appendix .1.

The chemical shifts of solvents and some common impurities in DMSO-d_6 are given in Table 2.10

Table 2.10: ^{1}H-NMR and ^{13}C-NMR shifts of solvent and common impurities in DMSO-d_6.[128]

	^{1}H [ppm]	^{13}C [ppm]
DMSO-d_6	2.50	39.52
H_2O	3.33 (s)	-
Grease	0.82-0.88 (m), 1.24 (s)	-
EtOAc	1.17 (t), 1.99 (s), 4.03 (q)	14.5, 20.7, 59.7, 170.3

2.6.1 Nitro and Amine Compounds

Throughout the general synthesis series, there are changes in chemical shifts that are true for all target compounds series. During the synthesis of substrate anilines, the chemical shifts in position 3,4 and 5 decreased. The higher chemical shifts of the nitro compounds at position 3 and 5 are caused by the electron withdrawing nitro group. This reduces the electron density of the aromatic ring and causes deshielding. Reduction converts the electron withdrawing nitro group to the electron donating amine group. The atoms in position 3, 4 and 5 are now shielded. This also affects the carbon shifts in position 3 and 5.

Through reduction the ^{1}H-shift values in position 3 decreases from 8.12-8.20 ppm to 6.42-6.62 ppm. The ^{1}H-shifts in position 4 decreased from 7.11-7.27 ppm to 6.42-6.49 ppm. The ^{13}C-shifts in position 3 and 5 decreased from 125.8-125.9 and 160.6-164.2 ppm to 115.3-117.3 and 147.0-150.2 ppm respectively. In addition, by reducing the nitro groups to amine groups, a new ^{1}H-shift will be introduced in position 1. The chemical shifts in position 7 varies based on the chemical environment created by substituents.

2.6.2 Compound 2 and 5

The assigned ^{1}H and ^{13}C-NMR shifts for compound **2** and **5** are presented in Table 2.11. The spectroscopic data for the compounds are given in Appendix .1.1 and .1.7.

The chemical shifts of compounds **2** and **5** follows the change in chemical shifts described above, for nitro and amine compounds. The chemical shifts in position 7 are significant lower for the cyclohexyl derivatives compared to the benzylic derivatives. This is due to the aliphatic chemical environment of the cyclohexyl. The protons corresponding to the carbon shifts in the cyclohexane are split into two chemical shifts, due to the different chemical environments of axial and equatorial protons. The chemical shifts of the axial protons are significantly lower than for the equatorial protons.

Table 2.11: ^{1}H-NMR and ^{13}C-NMR shifts for compound **2** and **5** respectively, obtained at 600 MHz and 150 MHz. DMSO-d_6 was used as solvent for both compounds.

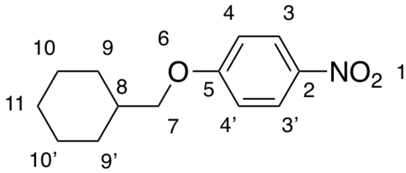

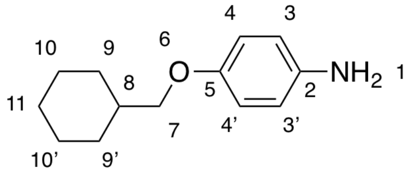

2 **5**

	^{1}H [ppm]		^{13}C [ppm]	
Pos.	**2**	**5**	**2**	**5**
1	-	4.56 (s, 2H)	-	-
2	-		140.6	142.2
3	8.19 (d, ^{3}J =9.3 Hz, 2H)	6.62 (d, ^{3}J =8.8 Hz, 2H)	125.9	115.3
4	7.14 (d, ^{3}J =9.3 Hz, 2H)	6.49 (d, ^{3}J =8.8 Hz, 2H)	115.0	114.9
5	-	-	164.2	150.2
6	-	-	-	-
7	3.93 (d, ^{3}J =6.3 Hz, 2H)	3.61 (d, ^{3}J =6.4 Hz, 2H)	73.6	73.4
8	1.76 (m, 1H)	1.65 (m, 1H)	36.9	37.2
9	1.79 (m, 2H) / 1.06 (m, 2H)	1.78 (m, 2H) / 0.99 (m, 2H)	29.0	29.4
10	1.71 (m, 2H) / 1.24 (m, 2H)	1.70 (m, 2H) / 1.21 (m, 2H)	25.2	25.3
11	1.64 (m, 1H) / 1.17 (m, 1H)	1.63 (m, 1H) / 1.16 (m, 1H)	25.9	26.1

2.6.3 Compounds (*R*)-, (*S*)-3 and (*R*)-, (*S*)-6

The assigned ^{1}H and ^{13}C-NMR shifts for the nitro substrates **(*R*)-3** are presented in Table 2.12, and the assigned ^{1}H and ^{13}C-NMR shifts for the aniline compound **(*R*)-6** are given in Table 2.13. The spectroscopic data for the compounds **(*R*)-**, **(*S*)-3**, **(*R*)-** and **(*S*)-6** is given in Appendix .1.2 - .1.3 and .1.8 - .1.9. All NMR-spectra are recorded using DMSO-d_6 as solvent.

Table 2.12: ^{1}H-NMR, ^{13}C-NMR shifts for compound ***(R)*-3** and ***(S)*-3** respectively, obtained at 600 MHz and 150 MHz. DMSO-d_6 was used as solvent.

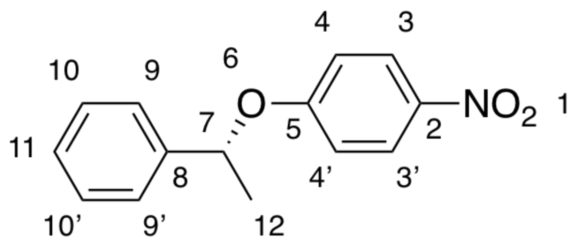

(*R*)-3

^{13}C [ppm] Pos.	^{1}H [ppm] (*R*)-3	(*R*)-3
1	-	-
2	-	140.7
3	8.12 (d, ^{3}J =9.3 Hz, 2H)	125.7
4	7.11 (d, ^{3}J =9.3 Hz, 2H)	116.1
5	-	162.8
6	-	-
7	5.71 (d, ^{3}J =6.4 Hz, 2H)	75.8
8	-	141.8
9	7.42 (d, ^{3}J =7.1 Hz, 2H)	125.7
10	7.36 (t, ^{3}J =7.5 Hz, 2H)	128.7
11	7.27 (t, ^{3}J =7.3 Hz, 1H)	127.8
12	1.59 (d, ^{3}J =6.4 Hz, 3H)	23.8

Table 2.13: ^{1}H-NMR and ^{13}C-NMR for compound ***(R)*-6**, obtained at 600 MHz and 150 MHz, respectively. DMSO-d_6 was used as solvent.

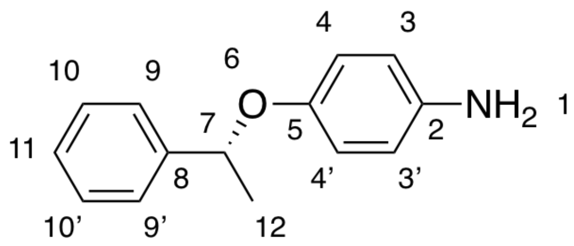

(*R*)-6

Pos.	^{1}H [ppm] **(*R*)-6**	^{13}C [ppm] **(*R*)-6**
1	4.55 (s, 1H)	-
2	-	142.5
3	6.61 (d, ^{3}J =8.6 Hz, 2H)	117.0
4	6.42 (d, ^{3}J =8.7 Hz, 2H)	114.7
5	-	148.6
6	-	-
7	5.23 (d, ^{3}J =6.3 Hz, 2H)	75.5
8	-	143.7
9	7.36 (d, ^{3}J =7.8 Hz, 2H)	125.8
10	7.31 (t, ^{3}J =7.5 Hz, 2H)	128.3
11	7.23 (t, ^{3}J =8.1 Hz, 1H)	127.1
12	1.48 (d, ^{3}J =6.4 Hz, 3H)	24.1

The chemical shifts of **(*R*)-3** and **(*S*)-3** are identical within 0.01 ppm for the ^{1}H-shifts and 0.1 ppm for the ^{13}C-shifts. Compounds **(*R*)-6** and **(*S*)-6** have identical chemical shifts within 0.02 ppm for the ^{1}H-shifts and 0.1 ppm for the ^{13}C-shifts. The ^{1}H- and ^{13}C-NMR shifts in position 7 varies with the chemical environment of the adjacent groups. The ^{1}H-shifts in benzylic position are significantly higher in compounds **(*R*)-3**/**(*S*)-3** and **(*R*)-6**/**(*S*)-6** compared to the ^{1}H-shifts of the cyclohexyl compounds. The chemical shifts in **(*R*)-3**, **(*S*)-3**, **(*R*)-6** and**(*S*)-6** experience the change described in Section 2.6.1, for reduction of nitro substrates to amine compounds.

2.6.4 Compounds (*rac*)-, (*R*)-, (*S*)-4 and (*rac*)-, (*R*)-, (*S*)-7

The assigned ^{1}H- and ^{13}C-NMR shifts for the nitro substrate **(*rac*)-4** are presented in Table 2.14, and the assigned ^{1}H- and ^{13}C-NMR shifts for the aniline compound **(*R*)-6** are given in Table 2.15. The spectroscopic data for the compounds **(*rac*)-**, **(*R*)-**, **(*S*)-4** and **(*rac*)-**, **(*R*)-**, **(*S*)-7** is given in Appendix .1.4 - .1.6 and .1.10 -

.1.12. All NMR-spectra are recorded using DMSO-d_6 as solvent.

Table 2.14: ^{1}H-NMR and ^{13}C-NMR shifts for compound ***(rac)*-4**, obtained at 600 MHz and 150 MHz respectively. DMSO-d_6 was used as solvent.

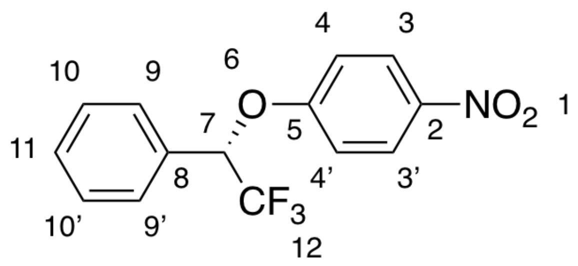

***(rac)*-4**

Pos.	^{1}H [ppm] ***(rac)*-4**	^{13}C [ppm] ***(rac)*-4**
1	-	-
2	-	142.1
3	8.19 (d, ^{3}J = 9.3 Hz, 2H)	125.9
4	7.26 (d, ^{3}J = 9.2 Hz, 2H)	116.4
5	-	160.6
6	-	-
7	6.58 (q, ^{3}J = 6.4 Hz, 1H)	75.6 (q, $^{2}J_{CF}$ = 31.9 Hz)
8	-	130.8
9	7.60 (d, ^{3}J = 6.5 Hz, 2H)	128.0
10	7.46 (m, 2H)	130.1
11	7.47 (m, 1H)	129.0
12	-	124.4 (q, $^{1}J_{CF}$ = 281.2 Hz)

The ^{19}F-NMR shifts of position 12 in compounds ***(rac)*-4**, ***(R)*-4** and ***(S)*-4** are all -77.80 ppm. The ^{19}F-NMR spectra are recorded at 565 MHz, with DMSO-d_6 as solvent and hexafluorbenzene as standard. The chemical shifts of the ***(rac)*-4**, ***(R)*-4** and ***(S)*-4** are identical, within 0.02 ppm for ^{1}H-shifts and 0.2 ppm for the ^{13}C-shifts.

Table 2.15: ^{1}H-NMR and ^{13}C-NMR shifts for compound ***(rac)*-7** obtained at 600 MHz and 150 MHz respectively. DMSO-d_6 was used as solvent.

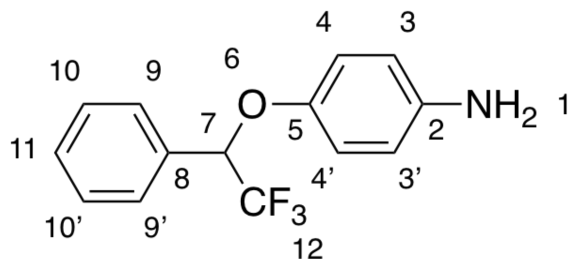

(*rac*)-7

Pos.	^{1}H [ppm] ***(rac)*-7**	^{13}C [ppm] ***(rac)*-7**
1	4.72 (s, 2H)	-
2	-	143.9
3	6.71 (d, ^{3}J =8.9 Hz, 2H)	117.3
4	6.44 (d, ^{3}J =8.9 Hz, 2H)	114.5
5	-	147.1
6	-	-
7	5.91 (q, ^{3}J =6.8 Hz, 1H)	76.9 (q, $^{2}J_{CF}$ = 30.8 Hz)
8	-	132.6
9	7.55 (d, ^{3}J =6.4 Hz, 2H)	128.1
10	7.41 (m, 2H)	129.4
11	7.42 (m, 1H)	128.5
12	-	124.9 (q, $^{1}J_{CF}$ = 282.2 Hz)

The ^{19}F-NMR shifts of position 12 in compounds ***(rac)*-7**, ***(R)*-7** and ***(S)*-7** are all -77.76 ppm. The chemical shifts of **(*rac*-, (*R*)** and **(*S*)-7** are identical within 0.03 ppm for the ^{1}H-shifts and 0.2 ppm for the ^{13}C-shifts.

The introduction of -CF_3 group in position 12 has major effect on the chemical shifts in position 7 and 12. Due to coupling to three fluoro atoms, the carbons in position 7 and 12 are observed as quartets in ^{13}C-NMR. The coupling constants of the ^{13}C-shifts in the 7th position is in the range 30.3 - 32.5 Hz. The coupling constants of the ^{13}C-shifts in the 12th position varies in the range 280.0 - 282.3 Hz, for compounds ***(rac)*-4** - ***(S)*-4** and ***(rac)*-7** - ***(S)*-7**. In addition to the splitting of the ^{13}C-shifts the introduction of CF_3 increased the ^{1}H-shifts in position 7 of the nitro substrates compared to that of the compounds with methyl group. This is caused by the electron withdrawing effect of CF_3 and the subsequent deshielding. The addition of CF_3 contributed to a small increase in the chemical shifts of the adjacent phenyl ring.

The change in chemical shifts between the nitro substrates and the amines follows the description in Section 2.6.1. In addition, the ^{1}H-shifts in 7th position of compounds ***(rac)*-4**, **(*R*)-4** and **(*S*)-4** decreases after reduction.

2.6.5 Amination

As for the reduction reaction, there are changes in chemical shifts that occur after amination, in all of the target compound series. The ^{1}H-shifts of the amine function increases drastically. The amine shifts jump form the range 4.55-4.72 to 9.46-9.54 ppm. This is caused by the coupling to the electron deficient pyrimidine group.

The shielding effect of secondary amines is weaker than for primary amines. The change from primary amine to secondary amine during amination, affects the chemical shifts in position 12, 13 and 14, which corresponds to position 3,4 and 5 in the aniline substrates. Less shielding by the amine group causes the observed increase in chemical shifts in position 12, 13 and 14.

In addition, the ^{13}C-shifts in position 11 decreases from the amination. The chemical shifts of the ether moiety of the compounds, remains mostly unaffected by the amination reaction. The addition of thienopyrimidine in the compounds introduces two new ^{1}H-shifts in position 2 and 5.

2.6.6 Compounds (*R*)- and (*S*)-9

The assigned ^{1}H and ^{13}C-NMR shifts for the compound **(*R*)-9** are presented in Table 2.16. The spectroscopic data for compounds **(*R*)-** and **(*S*)-9** is given in Appendix .1.14 and **??**. All NMR-spectra are recorded using DMSO-d_6 as solvent. The chemical shifts of the **(*R*)-9** and **(*S*)-9** are identical, within 0.02 ppm for the ^{1}H-shifts and 0.1 ppm for the ^{13}C-shifts. Compounds **(*R*)-9** and **(*S*)-9** follows the general transformation, described in Section 2.6.9, for aminated compounds.

Table 2.16: ^{1}H-NMR and ^{13}C-NMR shifts for compound ***(R)*-9**, obtained at 600 MHz and 150 MHz respectively. DMSO-d_6 was used as solvent.

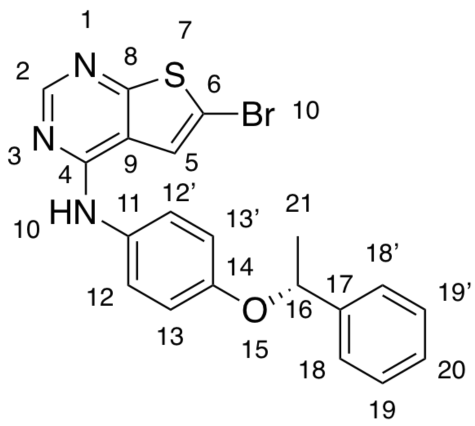

***(R)*-9**

Pos.	^{1}H [ppm] ***(R)*-9**	^{13}C [ppm] ***(R)*-9**
1	-	-
2	8.37 (s, 1H),	153.7
3	-	-
4	-	153.6
5	7.96 (s, 1H)	122.6
6	-	110.5
7	-	-
8	-	167.0
9	-	117.3
10	9.46 (s, 1H)	-
11	-	131.6
12	7.53 (d, ^{3}J =9.0 Hz, 2H)	123.4
13	6.92 (d, ^{3}J =9.0 Hz, 2H)	115.8
14	-	153.9
15	-	-
16	5.49 (q, ^{3}J =6.1 Hz, 2H)	74.9
17	-	143.0
18	7.42 (d, ^{3}J =7.7 Hz, 2H)	125.7
19	7.34 (t, ^{3}J =7.8 Hz, 2H)	128.5
20	7.25 (t, ^{3}J =7.3 Hz, 1H)	127.4
21	1.56 (d, ^{3}J =6.4 Hz, 3H)	24.2

2.6.7 Compounds 11, 12 and 13

The assigned ^{1}H- and ^{13}C-NMR shifts for the compounds **11** and **12** are presented in Table 2.17. The assigned ^{1}H- and ^{13}C-NMR shifts for compound **13** are given in Table 2.18 The spectroscopic data for the compounds is given in Appendix .1.19 - .1.21. All NMR-spectra are recorded using DMSO-d_6 as solvent. The chemical shifts of compound **11** follows as describe in Section .

Table 2.17: ^{1}H-NMR and ^{13}C-NMR shifts for compounds **11** and **12** respectively, obtained at 600 MHz and 150 MHz. DMSO-d_6 was used as solvent for both compounds.

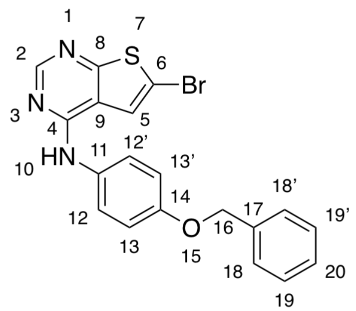

11

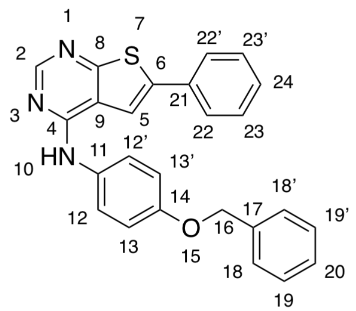

12

Pos.	^{1}H [ppm] **11**	^{1}H [ppm] **12**	^{13}C [ppm] **11**	^{13}C [ppm] **12**
1	-	-	-	-
2	8.41	8.43	153.8	153.5
3	-	-	-	-
4	-	-	153.7	154.6
5	8.01	8.23	122.7	115.3
6	-	-	110.5	138.9
7	-	-	-	-
8	-	-	167.0	165.8
9	-	-	117.4	118.0
10	9.53	9.58	-	-
11	-	-	131.9	132.2
12	7.63	7.71	123.5	123.2
13	7.05	7.07	114.8	114.8
14	-	-	154.8	154.7
15	-	-	-	-
16	5.11	5.12	69.4	69.4
17	-	-	137.2	137.2
18	7.46	7.48	127.7	127.7
19	7.40	7.40	128.5	128.4
20	7.33	7.34	127.8	127.8
21	-	-	-	133.1
21	-	7.73	-	125.8
23	-	7.53	-	129.5
24	-	7.43	-	128.8

Table 2.18: ^{1}H-NMR and ^{13}C-NMR shifts for compound **13**, obtained at 600 MHz and 150 MHz respectively. DMSO-d_6 was used as solvent.

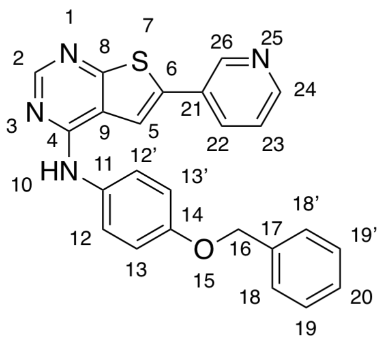

13

Pos.	^{1}H [ppm]	^{13}C [ppm]
1	-	-
2	8.45 (s, 1H)	153.9
3	-	-
4	-	154.72
5	8.31 (s, 1H),	116.9
6	-	134.1
7	-	-
8	-	166.2
9	-	117.9
10	9.64 (s, 1H)	-
11	-	132.0
12	7.70 (d, ^3J =9.0 Hz, 2H)	123.3
13	7.07 (d, ^3J =9.0 Hz, 2H)	114.8
14	-	154.74
15	-	-
16	5.12 (s, 1H)	69.4
17	-	137.2
18	7.48 (d, ^3J =7.1 Hz, 2H)	127.7
19	7.41 (t, ^3J =7.4 Hz, 2H)	127.8
20	7.34 (t, ^3J =7.3 Hz, 1H)	128.4
21	-	129.2
22	8.10 (s, 1H),	133.2
23	7.57 (q, ^3J =4.8 Hz, 1H)	124.3
24	8.62 (m, 1H)	149.5
25	-	-
26	8.96 (s, 1H)	146.4

After cross-coupling, the exchange of bromide with either phenyl or 3-pyridyl added

4-6 new chemical shifts to the compounds. The addition of an aromatic group affected the chemical shifts in position 5 and 6 in the thienopyrimidine ring. The nature of the 6-aryl group affected the chemical shifts differently, due to the electron poor nature of 3-pyridyl. In both cases the ^{1}H-shifts increased and the ^{13}C-shifts decreased in position 5. Exchanging bromide with phenyl increased the ^{13}C-shift in position 6 significantly. A modest increase in ^{13}C-shift in position 6 was also observed with addition of 3-pryidyl, in comparison to phenyl.

In the case of 3-pyridyl, the chemical shifts of the heterocycle have significantly higher chemical shifts for the atoms adjacent to the nitrogen, compared to the chemical shifts of the phenyl ring. The significant difference is caused by the electron poor nitrogen.

2.6.8 Compounds 8 and 14

The assigned ^{1}H- and ^{13}C-NMR shifts for compounds **8** and **14** are presented in Table 2.19. The spectroscopic data for the compounds is given in Appendix .1.13 and .1.22. All NMR-spectra are recorded using DMSO-d_6 as solvent. The chemical shifts of compound **8** follows the change by amination as described in Section . Compound **14** shows the same changes from cross-coupling with 3-pyridyl that are described for compound **13** in Section 2.6.7. The $^{2}J_{CH}$- $^{3}J_{CH}$-coupling in the cyclohexane moiety of compound 14 were not portrayed in the ^{1}H-^{13}C HMBC specter. The proton and carbon shifts of the cyclohexane were assigned by the ^{1}H-^{1}H COSY and ^{1}H-^{13}C HSQC interactions.

Table 2.19: ^{1}H-NMR and ^{13}C-NMR shifts for compound **8** and **14**, obtained at 600 MHz and 150 MHz respectively. DMSO-d_6 was used as solvent for both compounds.

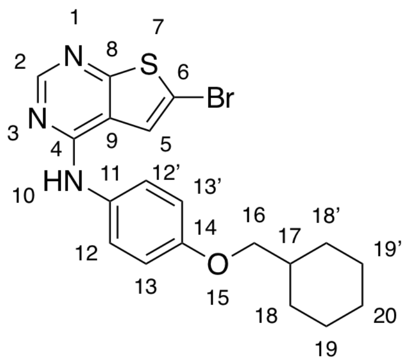

8

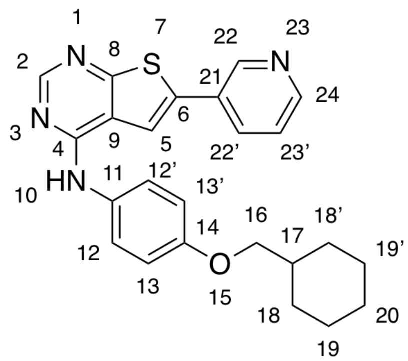

14

	^{1}H [ppm]		^{13}C [ppm]	
Pos.	**8**	**14**	**8**	**14**
1	-	-	-	-
2	8.40	8.46	153.8	153.9
3	-	-	-	-
4	8.00	8.32	153.6	154.7
5	-	-	122.7	116.9
6	-	-	110.8	135.1
7	-	-	-	-
8	-	-	166.9	166.1
9	-	-	117.4	117.8
10	9.50	9.63	-	-
11	-	-	131.6	131.7
12	7.62	7.69	123.4	123.3
13	6.93	6.98	114.4	114.4
14	-	-	155.4	155.3
15	-	-	-	-
16	3.76	3.80	72.9	72.9
17	1.73	1.74	37.1	37.1
18	1.81 / 1.04	1.81/1.05	29.3	29.3
19	1.72 / 1.25	1.72/1.26	25.3	25.3
20	1.65 / 1.16	1.67 /1.19	26.0	26.1
21	-	-	-	129.2
22	-	8.10	-	133.2
23	-	7.58	-	124.4
24	-	8.62	-	149.5
25	-	-	-	-
26	-	8.97	-	146.4

2.6.9 Compounds (*rac*)-,(*R*)-,(*S*)-10 and (*rac*)-,(*S*)-15

The assigned ^{1}H- and ^{13}C-NMR shifts for the compound **(*rac*)-10** are presented in Table 2.20. The assigned chemical shifts of compound **(*rac*)-15** are given in Table 2.21 The spectroscopic data for the compounds **(*rac*)-**, **(*R*)-**, **(*S*)-10** and **(*rac*)-**, **(*S*)-15** is given in Appendix .1.16 - **??**, .1.23 and .1.24. All NMR-spectra are recorded using DMSO-d_6 as solvent. The chemical shifts of **(*rac*)-**, **(*R*)-**, **(*S*)-10** are identical within 0.02 ppm for the ^{1}H-shifts and 0.1 ppm the ^{13}C-shifts. The chemical shifts of the aminated compounds **10** follow the change by amination as described in Section .

The chemical shifts of **(*rac*)-15** and **(*S*)-15** are identical within 0.01 ppm for ^{1}H-shifts and 0.3 ppm for ^{13}C-shifts. Compounds **(*rac*)-15** and **(*S*)-15** show the same changes from cross-coupling with 3-pyridyl that are described for compound **13** in Section 2.6.7.

Table 2.20: ^{1}H-NMR and ^{13}C-NMR shifts for compound ***(rac)*-10**, obtained at 600 MHz and 150 MHz respectively. DMSO-d_6 was used as solvent.

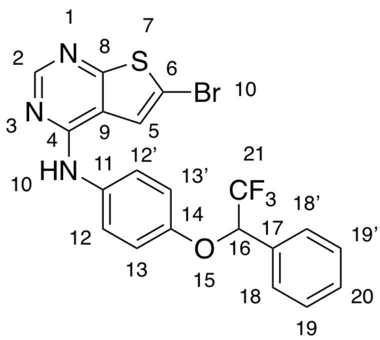

***(rac)*-10**

Pos.	^{1}H [ppm] ***(rac)*-10**	^{13}C [ppm] ***(rac)*-10**
1	-	-
2	8.39 (s, 1H)	153.7
3	-	-
4	-	153.5
5	7.98 (s, 1H)	122.6
6	-	110.7
7	-	-
8	-	167.1
9	-	117.4
10	9.52 (s, 1H)	-
11	-	133.2
12	7.62 (m, 2H)	123.2
13	7.06 (d, ^3J =8.9 Hz, 2H)	116.1
14	-	152.1
15	-	-
16	6.26 (q, ^3J =8.8 Hz, 1H)	76.0 (q, $^2J_{CF}$ = 31.3 Hz)
17	-	131.9
18	7.60 (m, 2H)	128.0
19	7.45 (m, 2H)	129.7
20	7.46 (m, 1H)	128.7
21	-	124.8 (q, $^1J_{CF}$ = 281.2 Hz)

Table 2.21: ^{1}H-NMR and ^{13}C-NMR shifts for compound **(*rac*)-15**, obtained at 600 MHz and 150 MHz respectively. DMSO-d_6 was used as solvent.

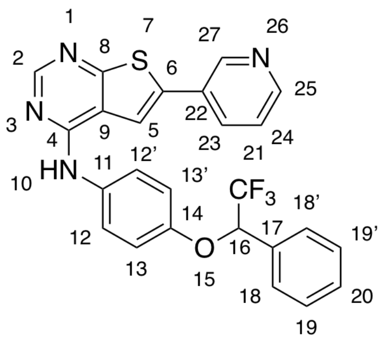

(*rac*)-15

Pos.	^{1}H [ppm] (*rac*)-15	^{13}C [ppm] (*rac*)-15
1	-	-
2	8.43 (s, 1H)	153.7
3	-	-
4	-	154.5
5	8.27 (s, 1H)	116.8
6	-	135.2
7	-	-
8	-	166.2
9	-	117.9
10	9.64 (s, 1H)	-
11	-	133.4
12	7.67 (d, ^{3}J =7.7 Hz, 2H)	123.2
13	7.08 (d, ^{3}J =7.8 Hz, 2H)	116.1
14	-	152.1
15	-	-
16	6.26 (q, ^{3}J =6.2 Hz, 2H)	76.0 (q, ^{3}J =31.5 Hz)
17	-	131.9
18	7.62 (d, ^{3}J =7.6 Hz, 2H)	128.1
19	7.45 (m, 2H)	129.7
20	7.47 (m, 1H)	128.8
21	-	124.8 (q)
22	-	129.2
23	8.08 (d, ^{3}J =8.0 Hz, 1H)	133.2
24	7.55 (m, 1H)	124.4 (q, ^{3}J =282.0 Hz)
25	8.61	149.5
26	-	-
27	8.94 (s, 1H)	146.5

The ^{19}F-NMR shifts of position 12 in compounds **(*rac*)-10**, **(*R*)-10** and **(*S*)-10** are all -77.75 ppm. The ^{19}F-NMR spectra are recorded at 565 MHz, using DMSO-d_6 as solvent and utilizing hexafluorbenzene as standard. The ^{19}F-NMR shifts of compounds **(*rac*)-15** and **(*S*)-15** are both -77.74 ppm.

To showcase how structure elucidation was performed, a detailed description of the structure elucidation of target compounds **(*rac*)-10** and **(*rac*)-15** is presented.

The chemical shifts were assigned through 1D- and 2D-NMR analysis. The chemical shifts of neighboring protons were assigned from their multiplicity, coupling-constants and integrals, as well as their ^{1}H-^{1}H COSY interactions. The ^{13}C-shifts of carbons with directly attached protons, were assigned based on their ^{1}H-^{13}C HSQC correlation via the $^1J_{CH}$ coupling. The ^{1}H-^{13}C HMBC spectra were used to validate the findings from the ^{1}H-^{1}H COSY correlations. The ^{1}H-^{13}C HMBC interactions were also used to position protons based on their $^2J_{CH}$- $^3J_{CH}$-coupling, where the ^{1}H-^{1}H COSY interactions were insufficient. The ^{1}H-^{13}C HMBC correlations used to determine the position of protons in compounds **(*rac*)-10** and **(*rac*)-15** are illustrated in Figure 2.4

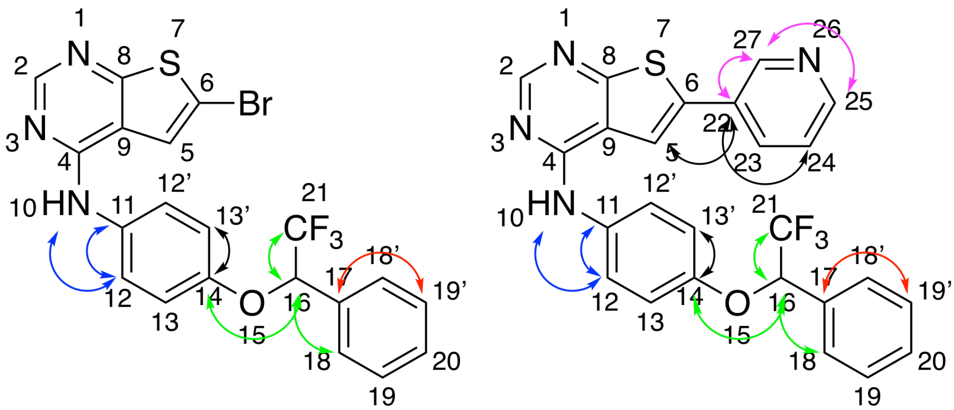

(*rac*)-10 **(*rac*)-15**

Figure 2.4: ^{1}H - ^{13}C HMBC correlations used to assign the position of protons in compounds **(*rac*)-10** and **(*rac*)-15** respectively.

The chemical shifts of carbons, with no directly coupled protons, were assigned by their ^{1}H-^{13}C HMBC correlations. The ^{1}H-^{13}C HMBC correlations used to assign ^{13}C-shifts in compounds **(*rac*)-10** and **(*rac*)-15** are showcased in Figure 2.5.

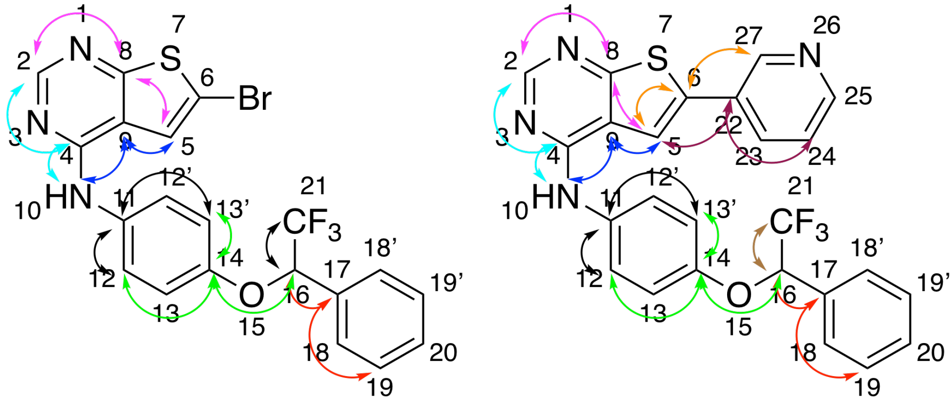

(rac)-10 **(rac)-15**

Figure 2.5: The HMBC correlations used to assign the position of carbons in compounds **(*rac*)-10** and **(*rac*)-15** respectively.

Along with the ^{1}H-^{1}H COSY, ^{1}H-^{13}C HSQC and ^{1}H-^{13}C HMBC spectra, numerous of the ^{1}H- and ^{13}C-shifts are in characteristic ranges, based on their chemical environment. The chemical shifts in position 2, 4 and 9 correlate with the typical shift ranges for pyrimidines. The amine group in position 10 in compounds **(*rac*)-10** and **(*rac*)-15** has the highest ^{1}H-shifts. The carbons in position 8 are between a nitrogen and a sulfur atom and have the highest ^{13}C-shift in substituted thieno[2,3-*d*]pyrimidines. The chemical shifts of both protons and carbons in position 16 are in the typical range of a -CH- group adjacent to an oxygen atom. In addition, the ^{13}C-shifts in position 16 and 21 experience the characteristic splitting of CF_3-coupling. The splitting pattern corresponds to characteristic coupling constants for both direct C-F coupling and for the adjacent carbon.

The chemical shifts in the phenyl ring are in the characteristic aromatic signature range. Carbons without directly coupled protons exhibits chemical shifts in the higher part of the range. The 3-pyridyl ring exhibits chemical shifts characteristic for heterocycles, where the chemical shifts are higher for the protons and carbons adjacent to the heteroatom.

2.6.10 Infrared Spectroscopy

The compounds were analyzed with IR-spectroscopy. The structural similarities of the analyzed compounds cause, the spectra to consist of almost identical absorption bands. The most important vibration modes, found in the spectra given in Appendix .1, are presented and discussed in this section.

All analyzed compounds exhibit weak broad peaks between 3200-2900 cm^{-1} which corresponds to aromatic C-H stretching.[129] Most of the compounds contains absorption bands between 3000-2840 cm^{-1}, corresponding to aliphatic C-H stretching. All the IR-spectra contain absorption bands corresponding to out-of plane aromatic C-H bending between 900-650 cm^{-1}. The compounds also exhibit absorption bands between 1600-1450 cm^{-1}, which equates to skeletal aromatic C-C and N-C stretching.

The nitro compounds exhibit an additional strong absorption peak within 1600-1580 cm^{-1}. The additional strong absorption band corresponds to N-O stretching. A medium absorption band in the region 1650-1580 cm^{-1} is present in all spectra, except for the nitro compounds, equating to N-H bending. All the spectra contain a strong peak between 1260-1220 cm^{-1}, correlating to the C-O stretching of the ether group.

The spectra of the thienopyrimidine compounds contain an absorption band in the region 1275-1030 cm^{-1}, corresponding to aromatic C-S stretching. The compounds containing bromine, **8 - 10**, exhibit absorption peaks in the region 850-515 cm^{-1} which correlates to C-Br stretching. The IR-spectra of the CF_3 compound series have an additional strong absorption band in the region 1400-1000 cm^{-1}, corresponding to C-F stretching.

2.7 Biological Activity

Based on the assumption that the synthesized compounds could be inhibitors of HER2 kinase, the HER2 inhibitory effect was evaluated by *in vitro* enzymatic assay. A selection of six of the synthesized thienopyrimidines was assayed for their inhibition at 500 nM test concentration. The ATP level was equal to K_M. Each of the compounds was assayed twice. The results of the assays are presented in Table 2.22.

Table 2.22: The percent inhibition of HER2 at 500 nM test concentration, of the six selected 4-amine substituted thieno[2,3-*d*]pyrimidines

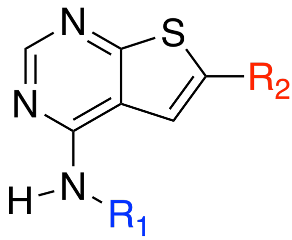

	Compound Identity			Inhibition (%)		
Compound	NTNU code	R_1	R_2	Assay 1	Assay 2	Average
11	HKB-01-20	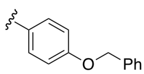	Br	26	20	23
(*R*)-9	HKB-01-71	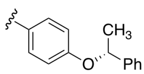	Br	15	15	15
(*S*)-9	HKB-01-72	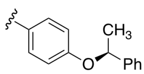	Br	-1	3	1
(*R*)-10	HKB-01-88	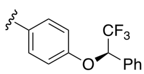	Br	1	2	1
(*S*)-10	HKB-01-90	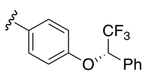	Br	8	9	9
(*rac*)-15	HKB-01-91	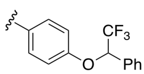	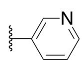	11	11	11

The six selected thienopyrimidines had overall low HER2 inhibitor activity. The parent compound **11** had mediocre inhibition of HER2, average of 23%. From the testing, introducing a stereocenter in compounds **(*R*)-9**, **(*S*)-9**, **(*R*)-10** and **(*S*)-10** obviously reduced the inhibitor activity even further. Thus, the effect of substitution of the benzylic carbon follows the trend H > (*R*)-CH_3 > (*S*)-CF_3

> (*S*)-CH_3 > (*R*)-CF_3. Modification of the scaffold structure to increase affinity towards HER2 must therefore be performed elsewhere. This could be other modifications of the aniline structure where the aromatic phenyl is replaced by the aliphatic cylcohexane, for which derivatives **8** and **14** has been prepared in this thesis.

Further, assay of compound **(*rac*)-15** hints that variation of the C-6 substituted aryl group is another possibility for increasing HER2 affinity. Although compound **(*rac*)-15** is a racemate, the inhibition is increased as compared to that expected from the data obtained from compounds **(*R*)-10** and **(*S*)-10**.

Cellular studies on selected derivatives are currently on-going. However, these data did not arrive in time to be included in this thesis.

Chapter 3

Conclusion

In total, 12 novel thieno[2,3-*d*]pyrimidine compounds have been synthesized, including seven 4-aniline substituted 6-bromo-thienopyrimidines and five 4-aniline substituted 6-aryl-thienopyrimidines. A selection of six compounds have been assayed for their HER2 inhibition activity.

The synthesis route consisted of preparing 4-alkoxylated anilines through ether synthesis, by either Williamson ether synthesis or nucleophilic aromatic substitution, and subsequently selective reduction of the nitro arenes. The target compounds were then formed by basic amination at C-4, followed by Suzuki-Miyaura cross-coupling at C-6.

The ether synthesis were performed in 38-81% yields. A series of test reactions showed that the Williamson ether synthesis proceeded best with 1.2 eq. K_2CO_3 and 0.1 eq. of nucleophilic catalyst KI, at 80 ℃. Another series of experiments revealed that nucleophilic aromatic substitution of ethers proceeded with fastest conversion rate using a 2.5 eq. K_2CO_3/DMF base/solvent system. The selective reduction of nitroarenes was carried out in high yields, 59-95%.

Selective amination was performed to introduce an aniline substituent, at C-4, on the thieno[2,3-*d*]pyrimidine in moderate yields, 32-56%. By performing the silica-gel chromatography before the extraction, the purification was easier and the product was obtained in a significantly higher yield, 81%.

To introduce C-6 aryl substituents, Suzuki-Miyaura cross-coupling was utilized. The Suzuki reaction proceeded mostly in good yields, 27-90%. The exception was synthesis of compound **14**.

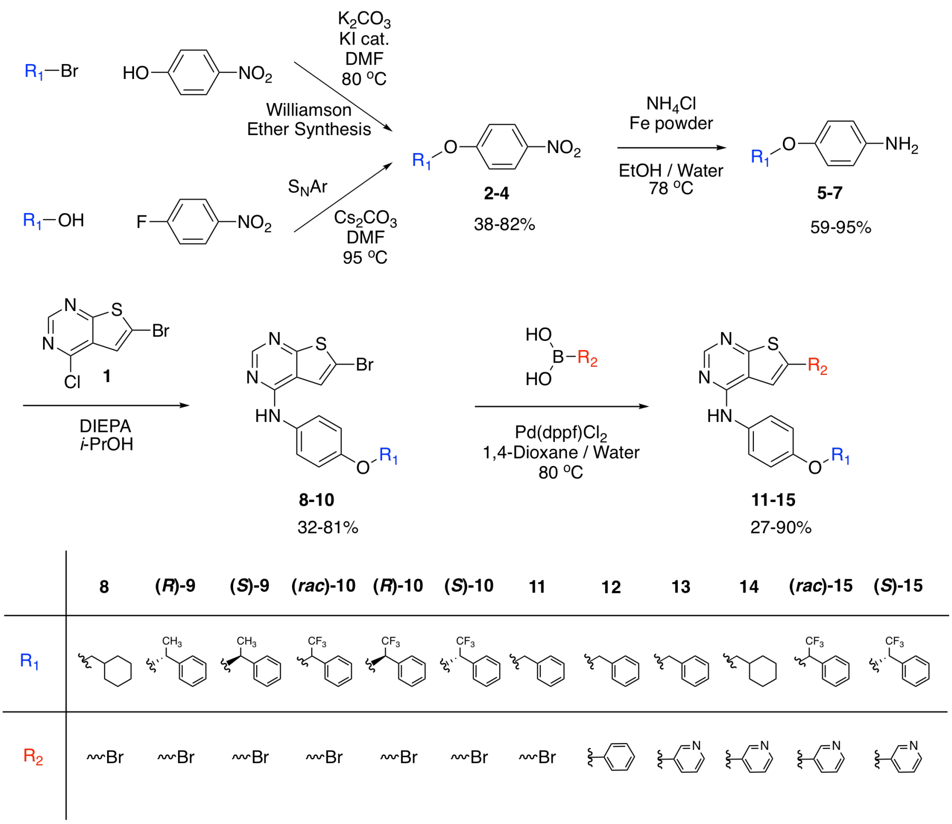

Biological evaluation of six selected thienopyrimidines **(*R*)-**, **(*S*)-9**, **(*R*)-**, **(*S*)-10**, **11** and **(*rac*)-15**, displayed moderate to low inhibitory effect of HER2. The biological data revealed that introducing a stereocenter at benzylic position, in the aniline, reduced the activity towards HER2. In addition, the activity data indicated that introducing a 3-pyridyl at C-6 in the thienopyrimidine increased the HER2 activity.

3.1 Future Work

In this Master thesis, 12 new 4-amine substituted thieno[2,3-*d*]pyrimidines have been synthesized. A selection of the synthesized target compounds has been sent to cellular breast cancer activity testing, beyond HER2 assays. The results from the breast cancer activity testing may affect the direction of future work on this project drastically.

The substrate anilines in this thesis were synthesized through ether synthesis and reduction. The ether synthesis through S_NAr reaction, showed promising results with the base/solvent system Cs_2CO_3/DMF. However, the syntheses employing Cs_2CO_3/DMF formed a lot of byproducts. Han *et al.* reported that the optimal base/solvent systems for nucleophilic aromatic substitution varied with the substitutients in the alcohol nucleophile.[37] To ensure less formation of byproducts, further investigation of the optimal base/solvent for the reagents utilized, is needed. Avoiding byproduct formation will help with the problematic purification of the nitro arene ether compounds.

The target compounds were formed through amination and Suzuki cross-coupling. The mediocre yields in the amination reaction, were due to the work up. The problems with loss of product seemed to be avoided by reversing the order of the work up, performing the silica-gel column chromatography first and then extraction. Further investigation of the loss of product is needed, to confirm whether or not the product is lost during of the extraction. The loss of product may have been avoided by the addition of HCl salt, from the reaction, which pH adjusted the eluent composition used in the silica-gel column. Further investigation may find that simple pH adjusting of the eluent may increase the yield.

The breast cancer activity study may indicate that the synthesized compounds inhibit other biological targets than HER2. If the compounds are primarily HER2 inhibitors, the study have provided valuable information for further work. The testing with stereocenters at benzylic position, for increasing the HER2 activity is not fruitful. Modifications to the inhibitors must be performed elsewhere in the compound. The addition of pyridine in C-6 position, increased the HER2 inhibitor activity. This suggests that modifications to the C-6 aryl are a possible target to increase the affinity towards HER2.

Chapter 4

Experimental Procedure

4.1 General Information

All commercially available solvents and reagents were purchased from Sigma Aldrich and used without any further purification. Compound **1** was previously made by the research group, and compound **11** was made during the pre-Master project. When dried solvents were required, they were obtained from MBraun SPS-800 solvent cleaner under N_2-atmosphere and stored over molecular sieves (4 Å). If reactions were carried out above room temperature, an oil bath was utilized to control the reaction temperature. A magnetic stirrer, coated with a teflon layer, was employed throughout all reactions.

4.1.1 Separation Techniques

Thin Layer Chromatography

Thin layer chromatography (TLC) was used to observe conversion of the reactions, as well as optimizing eluent systems utilized in silica-gel column chromatography purification. During TLC analysis, TLC Silica-gel 60 F_{254} aluminum plates from Merck were applied. UV-light (254 nm) was used to visualize TLC-plates.

Column Chromatography

During silica-gel column chromatography, silica-gel 40-63 μm from VWR chemicals was used as stationary phase. The eluent systems applied, are specified for the specific purification step. The utilized adsorbate was Celite®(545, 0.002-0.1 mm) from Merck.

4.1.2 Chromatography Analyses

To determine the purity of the final compounds, high-performance liquid chromatography was applied. HPLC was performed on an Agilent 1100-series instrument with G1379A degasser,G1313A ALS autosampler and Agilent G1315D diode array detector. The column used was an Agilant Poreshell 120 EC-18 (4,6 x 100 mm) with 2,7 μm pore size. The flow used was 1.0 mL/min with a gradient from ACN: water 10:90 to 100:0 over 5 minutes. The chromatograms were recorded at 254 nm using Agilent ChemStation as processing software.

Enantiomeric Purity

To analyze the enantiomeric excess of the final compounds, HPLC with chiral stationary phases was applied. The chiral analyses were performed on a Aligent 1100 series instrument with G1379A degasser, G1328B manual injector and Agilent G1315D diode array detector. The chromatograms were recorded at 254 nm using Agilent ChemStation as processing software.

Method 1: The column used was a OD ChiralCel (4.6 $\times$ 250 mm) with 5 μm pore size. The injection volume was 10 μL. The flow rate was 1.0 mL/min of isocratic *i*-PrOH: *n*-hexane (10:90).

Method 2: The column used was a Lux 5u Cellulose 1 (4.6 $\times$ 250 mm) with 5 μm pore size. The injection volume was 10 μL. The flow rate was 1.5 mL/min of isocratic *i*-PrOH: *n*-hexane (15:85).

Method 3: The column used was a OD ChiralCel (4.6 $\times$ 250 mm) with 5 μm pore size. The injection volume was 10 μL. The flow rate was 1.0 mL/min of isocratic EtOH (0.1% TFA): *n*-hexane (5:95).

4.1.3 Spectroscopic Analyses

Accurate mass determination in positive or negative mode was performed on a "Synapt G2-S" Q-TOF instrument from Water TM. Samples were ionized by the use of an ASAP probe (APCI) or ESI probe. No chromatographic separation was used previous to the mass analysis. Calculated exact mass and spectra processing was done using Waters TM Software Masslynx V4.1 SCN871.

^{1}H-NMR, ^{13}C-NMR and ^{19}F-NMR spectra were recorded on 600 MHz Bruker Avance III HD NMR and 400 MHz Bruker Avance III HD NMR spectrometers. ^{1}H-NMR were recorded at 400 MHz and 600 MHz, ^{13}C-NMR at 150 MHz and ^{19}F-NMR at 565 MHz. All NMR spectra were recorded using DMSO-d_6 as deuterated solvent. The chemical shifts are presented in δ, ppm, in relation to DMSO-d_6 solvent peaks (^{1}H-NMR: 2.50 ppm and ^{13}C-NMR: 39.52 ppm). Hexafluorobenzene (^{19}F-NMR: -162.65 ppm) was utilized as reference standard to calibrate the ^{19}F-NMR spectra. The splitting pattern of peaks are referred to based on their multiplicity; singlet; s, doublet; d, triplet; t, quartett; q and multiplet; m. Coupling constants, J, are reported in Hz.

The infrared absorption, IR, spectra were recorded employing a FTIR Thermo Nicolet Nexus FT-IR Spectrometer, using a Smart Endurance reflection cell. The IR spectra were recorded in the range of 4000 - 400 cm^{-1}. The OPUS 7.5 software was used to process the spectra.

4.1.4 Melting Point

Melting point analysis was performed employing a Stuart automatic melting point SMP40 instrument.

4.1.5 Specific Rotation

The specific rotations were recorded employing Anton Paar MCP 5100 polarimeter, with Anton Paar 10 mm, Ø 5 mm stainless steel cuvette. All specific rotations were recorded in a 1.00 g/100mL concentration in chloroform, at 20 ℃.

4.1.6 *In vitro* HER2 Inhibitory Potency

The compounds were supplied in a 10 mM DMSO solution, and enzymatic HER2 inhibition potency was determined by Invitrogen (TermoFisher) using their Z'-LYTE assay technology[130]. In short, the assay is based on fluorescence resonance energy transfer (FRET). In the primary reaction, the kinase transfers the gamma-phosphate of ATP to a single tyrosine residue in a synthetic FRET-peptide. In the secondary reaction, a site-specific protease recognizes and cleaves non-phosphorylated FRET-peptides. Thus, phosphorylation of FRET-peptides suppresses cleavage by the development reagent. Cleavage disrupts FRET between the donor (i.e.,coumarin) and acceptor (i.e., fluorescein) fluorophores on the FRET-peptide, whereas uncleaved, phosphorylated FRET-peptides maintain FRET. A ratiometric method, which calculates the ratio (the emission ratio) of donor emission to acceptor emission after excitation of the donor fluorophore at 400 nm, is used to quantitate inhibition. All compounds were first tested for their inhibitory activity at 500 nM in duplicates.

4.2 Synthesis of 1-(cyclohexylmethoxy)-4-nitrobenzene (2)[70]

4.2.1 100 mg Scale

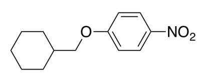

The reaction was performed five times. 4-Nitrophenol (100 mg, 0.719 mmol) and (bromomethyl)cyclohexane (127 mg, 0.719 mmol) were dissolved in DMF (3 mL). K_2CO_3 (119 mg, 0.863 mmol) was added while stirring. The reaction mixtures were stirred for 24 hours at 22 ℃. The reaction mixtures were extracted with EtOAc (20 mL) and water (4 × 10 mL). The organic phase was dried over Na_2SO_4, filtrated and concentrated in *vacuo*. The crude product was obtained as a yellow solid in 15% crude yield (25.4 mg, 0.108 mmol).

The reaction was repeated four times, with the addition of nucleophilic catalyst KI, at different temperatures. 4-Nitrophenol (100 mg, 0.719 mmol) and (bromomethyl)cyclohexane (127 mg, 0.719 mmol) were dissolved in DMF (3 mL). K_2CO_3 (119 mg, 0.863 mmol) and KI (potassiumiodid) (12 mg, 0.0719 mmol) were added while stirring. The reaction mixtures were stirred for 24 hours at 22 ℃, 60 ℃, 80 ℃ and 100 ℃. The reaction mixtures were extracted with EtOAc (20 mL) and water (4 × 10 mL). The organic phase was dried over Na_2SO_4, filtrated and concentrated in *vacuo*. The product from the reaction at 22 ℃ was obtained as a yellow oil in a 26% crude yield (43.8 mg, 0.186 mmol). The product from the reaction at 60 ℃ was obtained as a pale yellow solid in a 58% crude yield (98.8 mg, 0.420 mmol). The product from the reaction at 80 ℃ was obtained as a yellow solid in a 78% crude yield (131.2 mg, 0.560 mmol). The product from the reaction at 100 ℃ was isolated as a yellow solid in a 64% crude yield (107.9 mg, 0.459 mmol).

4.2.2 2.77 g Scale

The procedure described in Section 4.2.1 was repeated at the following scale: 4-Nitrophenol (**1**) (2.77 g, 19.9 mmol), (bromomethyl)cyclohexane (3.53 g, 19.9 mmol), K_2CO_3 (3.30 g, 23.9 mmol) and KI (0.33 g, 1.9 mmol). The reaction was performed in DMF (15 mL) at 80 ℃ for 24 hours. The reaction mixture was extracted with EtOAc (40 mL) and water (4 × 40 mL) and the organic phase was dried over Na_2SO_4, filtrated and concentrated in *vacuo*. The product was purified by extracting with EtOAc and water, which was pH adjusted with NaOH (5 M) to pH 11. The organic phase was dried over Na_2SO_4, filtrated and concentrated in *vacuo*. The product was isolated as a off-white solid in a 43% yield (2.01 g, 8.54 mmol) with Mp. 43.6-44.7 ℃

Spectroscopic data for compound (**2**) (Appendix .1.1): ^{1}H-NMR (600 MHz, DMSO-d_6) δ: 8.19 (d, ^3J =9.3 Hz, 2H), 7.14 (d, ^3J =9.3 Hz, 2H), 3.93 (d, ^3J =6.3 Hz, 2H), 1.79 (m, 2H), 1.76 (m, 1H), 1.71 (m, 2H), 1.64 (m, 1H), 1.24 (m, 2H), 1.17 (m, 1H), 1.06 (m, 2H); ^{13}C-NMR (150 MHz, DMSO-d_6) δ: 164.2, 140.6, 125.9 (2C), 115.0 (2C), 73.6, 36.9, 29.0 (2C), 25.9, 25.2 (2C); IR (cm^{-1}) ν: 2921 (m), 1593 (s), 1502 (s), 1451 (m), 1330 (s), 1299 (s), 1261 (s), 1223 (m), 1174 (m), 1105 (s), 1005 (s), 840 (s), 752 (s), 689 (m), 655 (s). HRMS (ASAP+, m/z): detected 236.1289, calculated for $C_{13}H_{18}NO_3$ $[M+H]^+$ 236.1287.

4.3 Synthesis of (*R*)-1-nitro-4-(1-phenylethoxy)-benzene ((*R*)-3)

4.3.1 Test Reactions

(*R*)-1-Phenylethan-1-ol (100 mg, 0.819 mmol) and 1-fluoro-4-nitrobenzene (115 mg, 0.819 mmol) and NaH 60 wt% in mineral oil (42.6 mg, 0.983 mmol) were stirred in DMF (5 mL) at 22 ℃ for 4.5 hours which gave 38% conversion.

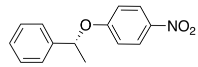

The reaction was repeated in the following scale: (R)-1-Phenylethan-1-ol (500 mg, 4.10 mmol) and 1-fluoro-4-nitrobenzene (592 mg, 4.10 mmol) and NaH 60 wt% in mineral oil (213 mg, 5.33 mmol) were stirred in DMF (20 mL) at 22 ℃ for 24 hours, which gave 36% conversion. The reaction was repeated, with a different base and solvent, at following scale: (R)-1-Phenylethan-1-ol (100 mg, 0.819 mmol), 1-fluoro-4-nitrobenzene (139 mg, 0.983 mmol) and Cs_2CO_3 (320 mg, 0.983 mmol) was stirred in acetonitrile (3 mL) for 24 hours at 95 ℃, which gave 53% conversion. The reaction was then repeated, with a different solvent and increased amount of base, at the following scale: (R)-1-Phenylethan-1-ol (100 mg, 0.819 mmol), 1-fluoro-4-nitrobenzene (139 mg, 0.983 mmol) and Cs_2CO_3 (667 mg, 2.05 mmol). The were stirred in DMF (3 mL) for 24 hours at 95 ℃, which gave 83% conversion.

4.3.2 1 gram Scale

(R)-1-Phenylethan-1-ol (1.0 g, 8.19 mmol), 1-fluoro-4-nitrobenzene (1.39 g, 9.83 mmol) and Cs_2CO_3 (6.67 g, 20.48 mmol) were stirred in DMF (20 mL) for 24 hours at 95 ℃. The reaction mixture was diluted with EtOAc (100 mL) and the organic phase was washed with saturated aq. $NaHCO_3$ (2 × 80 mL), water (3 × 80 mL) and brine (80 mL). The organic phase was dried over Na_2SO_4, filtrated and concentrated in *vacuo*. The crude product was purified by silica-gel column chromatography (n-pentane/EtOAc 6/4, Rf = 0.76). The product was isolated as a orange solid in a 82% yield (1.63 g, 6.70 mmol), with specific rotation $[\alpha]^{20}_{\mathrm{D}}$ = 63.70° and Mp. 45.6-47.8 ℃.

Spectroscopic data for Compound **(*R*)-3** (Appendix .1.2): ^{1}H-NMR (600 MHz, DMSO-d_6) δ: 8.12 (d, ^3J =9.3 Hz, 2H), 7.11 (d, ^3J =9.3 Hz, 2H), 7.42 (d, ^3J =7.1 Hz, 2H), 7.36 (t, ^3J =7.5 Hz, 2H), 7.27 (t, ^3J =7.3 Hz, 1H), 5.71 (d, ^3J =6.4 Hz, 2H), 1.59 (d, ^3J =6.4 Hz, 3H); ^{13}C-NMR (150 MHz, DMSO-d_6) δ: 162.8, 141.8, 140.7, 128.7 (2C), 127.8, 125.8 (2C), 125.7 (2C), 116.0 (2C), 75.8, 23.8; IR (cm^{-1}) ν: 3115 (w), 2980 (w), 2929 (w), 1911 (w), 1590 (s), 1503 (s), 1492 (s), 1338 (s), 1328 (s), 1295 (m), 1245 (s), 1210 (m), 1172 (m), 1107 (m), 1063 (s), 1026 (m), 1007 (m), 995 (m), 925 (m), 858 (m), 842 (s), 761 (s), 750 (s), 702 (s), 689 (m), 657 (s).

4.4 Synthesis of (S)-1-nitro-4-(1-phenylethoxy)-benzene ((S)-3)

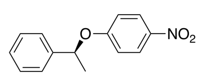

The reaction was performed following the procedure described in section 4.3.2 with the following compounds: (S)-1-phenylethan-1-ol (1.0 g, 8.19 mmol), 1-fluoro-4-nitrobenzene (1.39 g, 9.83 mmol) and Cs_2CO_3 (6.67 g, 20.5 mmol). The mixture was stirred in DMF (25 mL) for 24 hours at 95 ℃.

The reaction mixture was diluted with EtOAc (100 mL) and washed with saturated aq. $NaHCO_3$ (2 × 100 mL), water (3 × 100 mL) and brine (100 mL). The organic phase was dried over Na_2SO_4, filtrated and concentrated in *vacuo*. The crude product was purified by silica-gel column chromatography (*n*-pentane/EtOAc 6/4, R*f* = 0.82). The product was isolated as a orange solid in a 59% yield (1.17 g, 4.82 mmol), with specific rotation $[\alpha]^{20}_{\mathrm{D}}$ = - 52.95° and Mp. 43.1-45.4 °C.

Spectroscopic data for Compound **(*S*-)3** (Appendix .1.3): ^{1}H-NMR (600 MHz, DMSO-d_6) δ: 8.12 (d, ^3J =9.2 Hz, 2H), 7.42 (d, ^3J =7.3 Hz, 2H), 7.36 (t, ^3J =7.5 Hz, 2H), 7.27 (t, ^3J =7.3 Hz, 1H), 7.11 (d, ^3J =9.2 Hz, 2H), 5.71 (d, ^3J =6.4 Hz, 2H), 1.59 (d, ^3J =6.5 Hz, 3H); ^{13}C-NMR (150 MHz, DMSO-d_6) δ: 162.8, 141.8, 140.7, 128.7 (2C), 127.8, 125.7 (2C), 125.7 (2C), 116.1 (2C), 75.8, 23.8; IR (cm^{-1}) ν: 3115 (w), 2981 (w), 2929 (w), 1911 (w), 1590 (s), 1492 (s), 1451 (m), 1338 (s), 1245 (s), 1172 (s), 1107 (s), 1063 (s), 1026 (m), 995 (m), 925 (m), 842 (s), 750 (s), 702 (s), 657 (s), 562 (m), 530 (m), 498 (m).

4.5 Synthesis of 1-nitro-4-(2,2,2-trifluoro-1-phenylethoxy)benzene ((*rac*)-4)

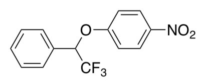

The synthesis of nitro compound **(*rac*)-4** was performed according to the procedure described in section 4.3.2, with the following compounds and scale: 2,2,2-trifluoro-1-phenylethanol (200 mg, 1.14 mmol), 1-fluoro-4-nitrobenzene (192 mg, 1.36 mmol) and Cs_2CO_3 (925 mg, 2.84 mmol). The mixture was stirred in DMF (6 mL) for 2.5 hours at 95 °C. The reaction mixture was diluted with EtOAc (50 mL) and washed with saturated aq. $NaHCO_3$ (2 × 50 mL), water (3 × 50 mL) and brine (50 mL). The organic phase was dried over Na_2SO_4, filtrated and concentrated in *vacuo*. The crude product was purified by silica-gel column chromatography (*n*-pentane/EtOAc 98/2 →9/1, R*f* = 0.40 at *n*-pentane/EtOAc 98/2). The product was isolated as colourless oil in a 38% yield (0.1286 g, 0.433 mmol).

The reaction was repeated at the following scale: 2,2,2-trifluoro-1-phenylethanol (2.0 g, 11.48 mmol), 1-fluoro-4-nitrobenzene (1.94 g, 13.78 mmol) and Cs_2CO_3 (9.36 g, 28.71 mmol). The mixture was stirred in DMF (30 mL) for 2.5 hours at 95 °C. The reaction mixture was diluted with EtOAc (100 mL) and washed with saturated aq. $NaHCO_3$ (2 × 100 mL), water (3 × 100 mL) and brine (100 mL). The organic phase was dried over Na_2SO_4, filtrated and concentrated in *vacuo*. The crude product was purified by silica-gel column chromatography (*n*-pentane/EtOAc 98/2 →9/1, R*f* = 0.40 at *n*-pentane/EtOAc 98/2). The product was isolated as pale yellow crystals in a 48% yield (1.661 g, 5.59 mmol) with Mp. 67.1-68.8 °C.

Spectroscopic data for Compound **(*rac*)-4** (Appendix .1.4): ^{1}H-NMR (600 MHz, DMSO-d_6) δ: 8.19 (d, ^3J = 9.3 Hz, 2H), 7.60 (d, ^3J = 6.5 Hz, 2H), 7.47 (m, 1H), 7.46 (m, 2H), 7.26 (d, ^3J = 9.2 Hz, 2H), 6.58 (q, ^3J = 6.4 Hz, 1H); ^{13}C-NMR (150 MHz, DMSO-d_6) δ: 160.6, 142.1, 130.8, 130.1 (2C), 129.0, 128.0 (2C), 125.9 (2C), 124.4 (q, $^{1}J_{CF}$ = 281.2 Hz), 116.4 (2C), 75.6 (q, $^{2}J_{CF}$ = 31.9 Hz); ^{19}F-NMR (565 MHz, DMSO-d_6, C_6F_6): -77.80; IR (cm^{-1}) ν: 3117 (w), 1588 (s), 1509 (s), 1493 (s), 1459 (m), 1337 (s), 1279 (m), 1268 (m), 1239 (s), 1174 (s), 1139 (s), 1126 (s), 1108 (s), 1042 (m), 1029 (m), 901 (m), 863 (m), 843 (s), 748 (m), 706 (s), 687 (s), 655 (m), 565 (m), 491 (m). HRMS (ASAP+, m/z): detected 298.0693, calculated for $C_{14}H_{11}NO_3F_3$ [M+H]$^+$ 298.0691.

4.6 Synthesis of (*R*)-1-nitro-4-(2,2,2-trifluoro-1-phenylethoxy)benzene ((*R*)-4)

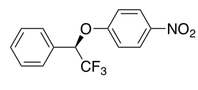

The synthesis was carried out according to the procedure described in section 4.3.2 with the following compounds and scale: (*R*)-2,2,2-trifluoro-1-phenylethanol (780 mg, 4.43 mmol), 1-fluoro-4-nitrobenzene (750 mg, 5.31 mmol) and Cs_2CO_3 (3600 mg, 11.1 mmol). The mixture was stirred in DMF (15 mL) for 2 hours at 60 ℃. The reaction mixture was diluted with EtOAc (75 mL) and washed with saturated aq. $NaHCO_3$ (2 × 75 mL), water (3 × 75 mL) and brine (75 mL). The organic phase was dried over Na_2SO_4, filtrated and concentrated in *vacuo*. The crude product was purified by silica-gel column chromatography (*n*-pentane/EtOAc 98/2 →8/2, R*f* = 0.14 at *n*-pentane/EtOAc 98/2). The product was isolated as pale yellow crystals in a 61% yield (805 mg, 2.71 mmol), with specific rotation $[\alpha]^{20}_{D}$ = -39.57° and Mp. 83.4-85.0 ℃.

Spectroscopic data for Compound **(*R*)-4** (Appendix .1.5): ^{1}H-NMR (600 MHz, DMSO-d_6) δ: 8.19 (d, ^{3}J = 9.2 Hz, 2H), 7.60 (d, ^{3}J = 6.7 Hz, 2H), 7.47 (m, 1H), 7.46 (m, 2H), 7.26 (d, ^{3}J = 9.2 Hz, 2H), 6.58 (q, ^{3}J = 6.3 Hz, 1H); ^{13}C-NMR (150 MHz, DMSO-d_6) δ: 160.6, 142.1, 130.8, 130.1 (2C), 129.0, 128.0 (2C), 125.9 (2C), 124.4 (q, $^{1}J_{CF}$ = 282.3 Hz), 116.4 (2C), 75.8 (q, $^{2}J_{CF}$ = 31.52 Hz); ^{19}F-NMR (565 MHz, DMSO-d_6, C_6F_6): -77.80; IR (cm^{-1}) ν: 3115 (w), 1736 (w), 1590 (s), 1508 (s), 1493 (s), 1341 (s), 1273 (m), 1241 (s), 1206 (m), 1192 (m), 1173 (s), 1132 (s), 1111 (s), 1044 (m), 1028 (m), 897 (m), 844 (s), 750 (s), 704 (s), 686 (s), 564 (w), 530 (w), 496 (w). HRMS (ASAP+, m/z): detected 298.0695, calculated for $C_{14}H_{11}NO_3F_3$ [M+H]$^+$ 298.0691.

4.7 Synthesis of (*S*)-1-nitro-4-(2,2,2-trifluoro-1-phenylethoxy)benzene ((*S*)-4)

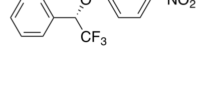

The synthesis was carried out according to the procedure described in section 4.3.2 with the following compounds and scale: (*S*)-2,2,2-trifluoro-1-phenylethanol (1.50 g, 8.71 mmol), 1-fluoro-4-nitrobenzene (1.44 g, 10.2 mmol) and Cs_2CO_3 (7.09 g, 21.8 mmol). The mixture was stirred in DMF (25 mL) for 3.5 hours at 60 ℃. The reaction mixture was diluted with EtOAc (100 mL) and the organic phase was washed with saturated aq. $NaHCO_3$ (2 × 100 mL), water (3 ×

100 mL) and brine (100 mL). The organic phase was dried over Na_2SO_4, filtrated and concentrated in *vacuo*. The crude product was purified by silica-gel column chromatography (*n*-pentane/EtOAc 98/2 →8/2, R*f* = 0.23 at *n*-pentane/EtOAc 98/2). The product was isolated as pale yellow crystals in a 71% yield (1.84 g, 6.19 mmol), with specific rotation $[\alpha]^{20}_{D}$ = 45.58° and Mp. 66.9-70.3 °C.

Spectroscopic data for Compound ***(S)*-4** (Appendix .1.6): ^{1}H-NMR (600 MHz, DMSO-d_6) δ: 8.20 (d, ^3J = 9.2 Hz, 2H), 7.61 (d, ^3J = 7.2 Hz, 2H), 7.48 (m, 1H), 7.47 (m, 2H), 7.27 (d, ^3J = 9.2 Hz, 2H), 6.59 (q, ^3J = 6.5 Hz, 1H); ^{13}C-NMR (150 MHz, DMSO-d_6) δ: 160.6, 142.1, 130.8, 130.1 (2C), 129.0, 128.0 (2C), 125.9 (2C), 124.4 (q, $^1J_{CF}$ = 281.7 Hz), 116.4 (2C), 75.8 (q, $^2J_{CF}$ = 32.5 Hz); ^{19}F-NMR (565 MHz, DMSO-d_6, C_6F_6): -77.80; IR (cm^{-1}) ν: 3448 (w), 3115 (w), 1734 (w), 1590 (s), 1493 (s), 1341 (s), 1241 (s), 1172 (s), 1130 (s), 1111 (s), 1044 (s), 896 (m), 845 (s), 750 (m), 704 (s), 629 (m), 492 (m); HRMS (ASAP+, m/z): detected 298.0692, calculated for $C_{14}H_{11}NO_3F_3$ [M+H]$^+$ 298.0691

4.8 Synthesis of 4-(cyclohexylmethoxy)aniline (5)

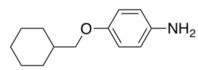

Nitro-compound **2** (500 mg, 2.13 mmol), NH_4Cl (1.02 g, 19.1 mmol) and iron powder (356 mg, 6.38 mmol) were mixed in degassed EtOH / water (4:1, 23.5 mL) under an N_2-atmosphere. The reaction mixture was stirred at 78 °C for 3 hours. The reaction mixture was filtrated through celite and extracted with DCM (60 mL) and water (2 × 60 mL). The organic phase was washed with brine (30 mL), dried over Na_2SO_4, filtrated and concentrated in *vacuo*. The product was isolated as a brown solid in a 95% yield (413 mg, 2.01 mmol).

The reaction was repeated with the procedure described above, in the following scale: Nitro-compound **2** (1.50 g, 6.35 mmol), NH_4Cl (3.06 g, 57.2 mmol) and iron powder (1.06 g, 19.1 mmol). The reaction was performed in degasssed EtOH / water (4:1, 73.5 mL) at 78 °C for 3 hours. The product was purified by silica-gel column chromatography (*n*-pentane/EtOAc 8/2 →0/10, R*f* = 0.32 at *n*-pentane/EtOAc 8/2). The product isolated as a brown solid in a 62% yield (810 mg, 3.95 mmol) with Mp. 52.4-53.0 °C

Spectroscopic data for Compound **5** (Appendix .1.7): ^{1}H-NMR (600 MHz, DMSO-d_6) δ: 6.62 (d, ^3J =8.8 Hz, 2H), 6.49(d, ^3J =8.8 Hz, 2H), 4.56 (s, 2H), 3.61 (d, ^3J =6.4 Hz, 2H), 1.78 (m, 2H), 1.70 (m, 2H), 1.65 (m, 1H), 1.63 (m, 2H), 1.21 (m, 2H), 1.16 (m, 1H), 0.99 (m, 2H); ^{13}C-NMR (150 MHz, DMSO-d_6) δ: 150.2, 142.2, 115.3 (2C), 114.9 (2C), 73.4, 37.2, 29.4 (2C), 25.3 (2C), 26.1; IR (cm^{-1}) ν: 3411 (w), 3311 (w), 3209 (w), 2915 (m), 2847 (m), 1611 (w), 1509 (s), 1466 (m), 1447 (m), 1238 (s), 1029 (s), 827 (s), 716 (m), 681 (m), 640 (m), 511 (s); HRMS (ASAP+, m/z): detected 206.1548, calculated for $C_{13}H_{20}NO$ [M+H]$^+$ 206.1545.

4.9 Synthesis of (*R*)-4-(1-phenylethoxy)aniline ((*R*)-6)

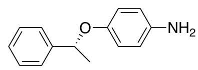

Synthesis of (*R*)-4-(1-phenylethoxy)aniline was performed following the procedure in Section 4.8 in the following scale: Nitro-compound **(*R*)-3** (700 mg, 2.88 mmol), NH_4Cl (1.39 g, 25.90 mmol) and iron powder (485 mg, 8.63 mmol) were mixed in degassed EtOH / water (4:1, 33.5 mL) under an N_2-atmosphere. The reaction mixture was stirred at 78 ℃ for 3.5 hours. The reaction mixture was filtrated through celite and concentrated in *vacuo*, extracted with DCM (60 mL) and water (2 × 60 mL). The product was isolated as a brown oil in a 62% yield (380 mg, 1.78 mmol), with specific rotation $[\alpha]^{20}_{\mathrm{D}} = 52.80°$.

Spectroscopic data for Compound **(*R*)-6** (Appendix .1.8): ^{1}H-NMR (600 MHz, DMSO-d_6) δ: 7.36 (d, ^3J =7.8 Hz, 2H), 7.31 (t, ^3J =7.5 Hz, 2H), 7.23 (t, ^3J =8.1 Hz, 1H), 6.61 (d, ^3J =8.6 Hz, 2H), 6.42 (d, ^3J =8.7 Hz, 2H), 5.23 (d, ^3J =6.3 Hz, 2H), 4.55 (s, 2H), 1.48 (d, ^3J =6.4 Hz, 3H); ^{13}C-NMR (150 MHz, DMSO-d_6) δ: 148.6, 143.7, 142.5, 128.3 (2C), 127.1, 125.8 (2C), 117.0 (2C), 114.7 (2C), 75.5, 24.1; IR (cm^{-1}) ν: 3355 (w), 2976 (w), 1730 (w), 1622 (w), 1507 (s), 1450 (w), 1228 (s), 1069 (s), 1011 (m), 931 (w), 823 (m), 762 (m), 700 (m), 514 (m); HRMS (ASAP+, m/z): detected 214.1236, calculated for $C_{14}H_{16}NO$ $[M+H]^+$ 214.1232.

4.10 Synthesis of (*S*)-4-(1-phenylethoxy)aniline ((*S*)-6)

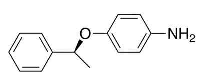

Synthesis of (*S*)-4-(1-phenylethoxy)aniline was performed following the procedure in Section 4.8 in the following scale: Nitro-compound **(*s*-)3** (800 mg, 3.29 mmol), NH_4Cl (1.58 g, 29.60 mmol) and iron powder (551 mg, 9.87 mmol) were mixed in degassed EtOH / water (4:1, 37.5 mL) under an N_2-atmosphere. The reaction mixture was stirred at 78 ℃ for 3.5 hours. The reaction mixture was filtrated through celite, concentrated in *vacuo* and extracted with DCM (60 mL) and water (2 × 60 mL). The product was isolated as a brown oil in a 62% yield, with specific rotation of $[\alpha]^{20}_{\mathrm{D}} = -60.47°$.

Spectroscopic data for Compound **(*S*)-6** (Appendix .1.9): ^{1}H-NMR (600 MHz, DMSO-d_6) δ: 7.36 (d, ^3J =7.1 Hz, 2H), 7.31 (t, ^3J =7.5 Hz, 2H), 7.23 (t, ^3J =7.1 Hz, 1H), 6.61 (d, ^3J =8.9 Hz, 2H), 6.42 (d, ^3J =8.9 Hz, 2H), 5.23 (d, ^3J =6.4 Hz, 2H), 4.56 (s, 2H), 1.47 (d, ^3J =6.5 Hz, 3H); ^{13}C-NMR (150 MHz, DMSO-d_6) δ: 148.6, 143.7, 142.5, 128.3 (2C), 127.1, 125.8 (2C), 117.0 (2C), 114.7 (2C), 75.5, 24.1; IR (cm^{-1}) ν: 3432 (w), 3358 (w), 2976 (w), 1612 (w), 1505 (s), 1450 (m), 1225 (s), 1067 (s), 1010 (m), 821 (s), 751 (m), 698 (s), 511 (s); HRMS (ASAP+, m/z): detected 214.1235, calculated for $C_{14}H_{16}NO$ $[M+H]^+$ 214.1232.

4.11 Synthesis of 4-(2,2,2-trifluoro-1-phenylethoxy) -aniline ((*rac*)-7)

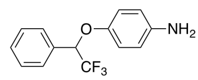

Synthesis of 4-(2,2,2-trifluoro-1-phenylethoxy)aniline was carried out according to the procedure in Section 4.8 with the following compounds and scale: Compound ***(rac)*-4** (989 mg, 3.33 mmol), NH_4Cl (1.62 g, 30.3 mmol), iron powder (564 mg, 10.1 mmol) were stirred in degassed EtOH / water (4:1, 50 mL) at 78 ℃ for 1.5 hours. The reaction mixture was filtrated through celite and concentrated in *vacuo*. The reaction mixture was diluted with EtOAc (100 mL) and washed with water (2 × 100 mL) and brine (100 mL). The organic phase was dried over Na_2SO_4, filtrated and concentrated in *vacuo*. The product was isolated as a brown oil in a 79% yield (0.694 g, 2.60 mmol)

Spectroscopic data for Compound ***(rac)*-7** (Appendix .1.10): ^{1}H-NMR (600 MHz, DMSO-d_6) δ: 7.55 (d, ^3J =6.4 Hz, 2H), 7.42 (m, 1H), 7.41 (m, 2H), 6.71 (d, ^3J =8.9 Hz, 2H), 6.44 (d, ^3J =8.9 Hz, 2H), 5.91 (q, ^3J =6.8 Hz, 1H), 4.72 (s, 2H); ^{13}C-NMR (150 MHz, DMSO-d_6) δ: 147.0 , 143.9, 132.6, 129.4 (2C), 128.5, 128.1 (2C), 124.9 (q, $^1J_{CF}$ = 282.2 Hz), 117.3 (2H), 114.5 (2C), 76.9 (q, $^2J_{CF}$ = 30.8 Hz); ^{19}F-NMR (565 MHz, DMSO-d_6, C_6F_6): -77.76; IR (cm^{-1}) ν: 3441 (w), 3361 (w), 3218 (w), 3039 (w), 2916 (w), 1624 (w), 1508 (s), 1455 (w), 1362 (w), 1267 (m), 1224 (s), 1173 (s), 1129 (s), 1085 (m), 1054 (m), 892 (m), 825 (m), 758 (m), 702 (s), 633 (m), 511 (m); HRMS (ASAP+, m/z): detected 268.0955, calculated for $C_{14}H_{13}NOF_3$ $[M+H]^+$ 268.0949.

4.12 Synthesis of (*R*)-4-(2,2,2-trifluoro-1-phenylethoxy)aniline (((*R*)-7))

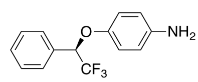

The synthesis of (*R*)-4-(2,2,2-trifluoro-1-phenylethoxy)aniline was performed according to the procedure in Section 4.8, with the following compounds and scale: Compound **(*R*)-4** (499 mg, 1.68 mmol), NH_4Cl (846 mg, 15.1 mmol), iron powder (270 mg, 5.05 mmol) were stirred in degassed EtOH / water (4:1, 30 mL) at 78 ℃ for 2 hours. The reaction mixture was filtrated through celite and concentrated in *vacuo*. The reaction mixture was diluted with EtOAc (100 mL) and washed with water (2 × 100 mL) and brine (100 mL). The organic phase was dried over Na_2SO_4, filtrated and concentrated in *vacuo*. The product was isolated as a brown oil in a 85% yield (0.383 g, 1.434 mmol) with Specific rotation $[\alpha]^{20}_{D}$ = -72.71 °.

Spectroscopic data for Compound **(*R*)-7** (Appendix .1.11): ^{1}H-NMR (600 MHz, DMSO-d_6) δ: 7.55 (d, ^3J =7.0 Hz, 2H), 7.42 (m, 1H), 7.41 (m, 2H), 6.71 (d, ^3J =8.9 Hz, 2H), 6.44 (d, ^3J =8.8 Hz, 2H), 5.92 (q, ^3J =6.8 Hz, 1H), 4.72 (s, 2H); ^{13}C-NMR (150 MHz, DMSO-d_6) δ: 147.1, 144.0, 132.6, 129.4 (2C), 128.5, 128.1 (2C), 124.9 (q, $^1J_{CF}$ = 280.0 Hz), 117.3 (2C), 114.5 (2C), 76.9 (q, $^2J_{CF}$ = 30.65, 1C); ^{19}F-NMR (565 MHz, DMSO-d_6, C_6F_6): -77.76; IR (cm^{-1}) ν: 3443 (w), 3365 (w), 3214 (w), 3040 (w), 2907 (w), 1624 (w), 1508 (s), 1455 (w), 1362 (w), 1267 (m), 1224 (s), 1173 (s), 1129 (s), 1086 (m), 1055 (m), 892 (m), 825 (m), 758 (m), 702 (s), 511 (s).

HRMS (ASAP+, m/z): detected 268.0954, calculated for $C_{14}H_{13}NOF_3$ [M+H]$^+$ 268.0949.

4.13 Synthesis of (*S*)-4-(2,2,2-trifluoro-1-phenyl-ethoxy)aniline ((*S*)-7)

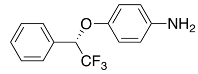

The synthesis of (S)-4-(2,2,2-trifluoro-1-phenylethoxy)aniline was performed according to the procedure in Section 4.8, with the following compounds and scale: Compound **(*S*)-4** (1.03 g, 3.47 mmol), NH_4Cl (1.69 g, 30.3 mmol), iron powder (540 mg, 10.1 mmol) were stirred in degassed EtOH / water (4:1, 60 mL) at 78 ℃ for 2.5 hours. The reaction mixture was filtrated through celite and concentrated in *vacuo*. The reaction mixture was diluted with EtOAc (150 mL) and washed with water (2 × 150 mL) and Brine (150 mL). The organic phase was dried over Na_2SO_4, filtrated and concentrated in *vacuo*. The product was isolated as a brown oil in a 86% yield (0.773 g, 2.90 mmol) with Specific rotation of $[\alpha]^{20}_{D}$ = 82.93.

Spectroscopic data for Compound **(*S*)-7** (Appendix **??**): ^{1}H-NMR (600 MHz, DMSO-d_6) δ: 7.55 (d, ^3J =7.0 Hz, 2H), 7.42 (m, 1H), 7.41 (m, 2H), 6.71 (d, ^3J =8.8 Hz, 2H), 6.44 (d, ^3J =8.8 Hz, 2H), 5.93 (q, ^3J =6.7 Hz, 1H), 4.72 (s, 2H); ^{13}C-NMR (150 MHz, DMSO-d_6) δ: 147.1, 144.0, 132.6, 129.4 (2C), 128.5, 128.1 (2C), 124.9 (q, $^1J_{CF}$ = 281.6 Hz), 117.3 (2C), 114.5 (2C), 77.0 (q, $^2J_{CF}$ = 30.3 Hz); ^{19}F-NMR (565 MHz, DMSO-d_6, C_6F_6): -77.76; IR (cm^{-1}) ν: 3451 (w), 3368 (w), 3220 (w), 3040 (w), 2917 (w), 1730 (w), 1625 (w), 1508 (s), 1456 (w), 1362 (w), 1267 (m), 1222 (s), 1173 (s), 1127 (s), 1053 (m), 892 (m), 824 (s), 757 (m), 701 (s), 633 (m), 510 (m).

HRMS (ASAP+, m/z): detected 268.0954, calculated for $C_{14}H_{13}NOF_3$ [M+H]$^+$ 268.0949.

4.14 Synthesis of 6-bromo-*N*-(4-(cyclohexyl-meth-oxy)phenyl)thieno[2,3-*d*]pyrimidin-4-amine (8)

Thienopyrimidine **1** (346 mg, 2.03 mmol), aniline-compound **5** (500 mg, 2.44 mmol) were dissolved in *i*-PrOH (16 mL) and DIPEA (595 mg, 4.06 mmol) under an N_2-atmosphere and stirred at 80 ℃ for 4 hours. The reaction mixture was concentrated in *vacuo*, extracted with EtOAc (40 mL) and water (2 × 40 mL). The organic phase was washed with brine (20 mL), dried over Na_2SO_4, filtrated and concentrated in *vacuo*. The crude product was purified by silica-gel column chromatography (*n*-pentane/EtOAc 9/1 →0/10, Rf = 0.13 at *n*-pentane/EtOAc 9/1). The product was isolated as off-white solid in a 48% yield (408 mg, 0.976 mmol), with HPLC purity of 99% and Mp. 189.5-190.1 ℃.

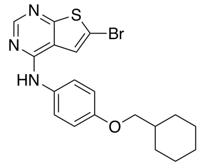

Spectroscopic data for Compound **8** (Appendix .1.13): ^{1}H-NMR (600 MHz, DMSO-d_6) δ: 9.51 (s, 1H), 8.40 (s, 1H), 8.00 (s, 1H), 7.62 (d, ^3J =9.0 Hz, 2H), 6.95 (d, ^3J =9.1 Hz, 2H), 3.77 (d, ^3J =6.4 Hz, 2H), 1.81 (m, 2H), 1.73 (m, 1H), 1.72 (m, 2H), 1.65 (m, 1H), 1.25 (m, 2H), 1.16 (m, 1H), 1.04 (m, 2H); ^{13}C-NMR (150 MHz, DMSO-d_6) δ: 166.9, 155.3, 153.8, 153.6, 131.5, 123.4 (2C), 122.7, 117.3, 114.4 (2C), 110.4, 72.9, 37.1, 29.3 (2C), 26.0, 25.3 (2C); IR (cm^{-1}) ν: 3071 (w), 2915 (m), 2848 (m), 1600 (m), 1570 (m), 1542 (m), 1504 (s), 1481 (m), 1465 (m), 1439 (s), 1411 (m), 1346 (s), 1297 (s), 1253 (m), 1235 (s), 1215 (m), 1204 (m), 1170 (m), 1022 (m), 849 (m), 827 (m), 773 (m), 684 (m), 518 (m).

HRMS (ASAP+, m/z): detected 418.0593, calculated for $C_{19}H_{21}N_3OS^{79}Br$ $[M+H]^+$ 418.0589.

4.15 Synthesis of (*R*)-6-bromo-*N*-(4-(1-phenylethoxy)phenyl)thieno[2,3-*d*]pyrimidin-4-amine ((*R*)-9)

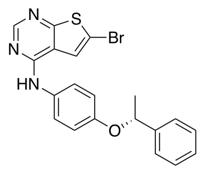

The procedure described in Section 4.14 was repeated with the following compounds: Aniline-compound **(*R*)-6** (200 mg, 0.938 mmol) and thienopyrimidine **1** (133 mg, 0.781 mmol), DIEPA (0.27 mL, 1.56 mmol) and *i*-PrOH (8 mL). The reaction was stirred at 80 ℃ for 4 hours. The crude product was purified with two rounds of silica-gel column chromatography (*n*-pentane: EtOAc: Et_3N; 1:1, R_f=0.33) (*n*-pentane: EtOAc: Et_3N; 7:3, R_f=0.67). The product was isolated as light brown solid with 32% yield (127 mg, 0.297 mmol) and HPLC purity 99%, specific rotation of $[\alpha]^{20}_{D}$ = 45.92 °, Mp. 156.7-157.7 ℃ and EE(%) = 99 (Method 1, t_R= 17.4 min, Rs= 4.7).

Spectroscopic data for Compound **(*R*)-9** (Appendix .1.14): ^{1}H-NMR (600 MHz, DMSO-d_6) δ: 9.46 (s, 1H), 8.37 (s, 1H), 7.96 (s, 1H), 7.53 (d, ^3J =9.0 Hz, 2H), 7.42 (d, ^3J =7.7 Hz, 2H), 7.34 (t, ^3J =7.8 Hz, 2H), 7.25 (t, ^3J =7.3 Hz, 1H), 6.92 (d, ^3J =9.0 Hz, 2H), 5.49 (q, ^3J =6.1 Hz, 2H), 1.56 (d, ^3J =6.4 Hz, 3H); ^{13}C-NMR (150 MHz, DMSO-d_6) δ: 167.0, 153.9, 153.7, 153.6, 143.0, 131.6, 128.5 (2C), 127.4, 125.7 (2C), 123.4 (2C), 122.6, 117.3, 115.8 (2C), 110.5, 74.9, 24.2; IR (cm^{-1}) ν: 3266 (w), 3073 (w), 2972 (w), 1607 (m), 1570 (m), 1540 (m), 1503 (s), 1442 (s), 1345 (s), 1305 (m), 1226 (s), 1201 (s), 1067 (m), 1002 (m), 932 (w), 823 (m), 773 (m), 752 (m), 696 (s), 582 (w), 517 (m), 469 (m).

HRMS (ASAP+, m/z): detected 426.0278, calculated for $C_{20}H_{17}N_3OS^{79}Br$ $[M+H]^+$ 426.0276.

4.16 Synthesis of (S)-6-bromo-*N*-(4-(1-phenylethoxy)phenyl)thieno[2,3-*d*]pyrimidin-4-amine ((*S*)-9)

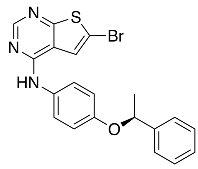

The procedure described in Section 4.14 was repeated with the following compounds: Aniline-compound **(*S*)-6** (200 mg , 0.938 mmol) and thienopyrimidine **1** (133 mg , 0.781 mmol), DIEPA (0.27 mL, 1.56 mmol) and *i*-PrOH (8 mL). The reaction was stirred at 80 ℃ for 4.5 hours. The crude product was purified with two rounds of silica-gel column chromatography (*n*-pentane: EtOAc: Et_3N; 6:4, R_f=0.34) (*n*-pentane: EtOAc; 8:2, R_f=0.38). The product was isolated as light brown solid with 41% yield (165 mg, 0.386 mmol) and HPLC purity 99%, with specific rotation of $[\alpha]^{20}_{D}$ = -37.85 °, Mp. 157.9-158.6 ℃ and EE(%) = 99 (Method 1, t_R= 21.5 min, Rs= 4.7).

Spectroscopic data for Compound **(*S*)-9** (Appendix .1.15): ^{1}H-NMR (600 MHz, DMSO-d_6) δ: 9.46 (s, 1H), 8.37 (s, 1H), 7.96 (s, 1H), 7.54 (d, ^3J =8.8 Hz, 2H), 7.42 (d, ^3J =6.7 Hz, 2H), 7.34 (t, ^3J =7.3 Hz, 2H), 7.25 (t, ^3J =7.1 Hz, 1H), 6.93 (d, ^3J =9.0 Hz, 2H), 5.49 (q, ^3J =6.1 Hz, 2H), 1.56 (d, ^3J =9.0 Hz, 3H); ^{13}C-NMR (150 MHz, DMSO-d_6) δ: 167.0, 153.9, 153.7, 153.6, 143.0, 131.6, 128.5 (2C), 127.4, 125.7 (2C), 123.4 (2C), 122.6, 117.3, 115.8 (2C), 110.5, 74.9, 24.2; IR (cm^{-1}) ν: 3265 (w), 3073 (w), 2971 (w), 2925 (w), 1608 (m), 1570 (m), 1540 (m), 1503 (s), 1482 (m), 1442 (s), 1408 (m), 1345 (s), 1305 (m), 1250 (m), 1226 (s), 1201 (m), 1067 (w), 1002 (m), 932 (m), 823 (m), 773 (m), 752 (m), 696 (s), 582 (w), 517 (w), 469 (m).

HRMS (ASAP+, m/z): detected 426.0278, calculated for $C_{20}H_{17}N_3OS^{79}Br$ $[M+H]^+$ 426.0276.

4.17 6-bromo-*N*-(4-(2,2,2-trifluoro-1-phenylethoxy)phenyl)thieno[2,3-*d*]pyrimidin-4-amine ((*rac*)-10)

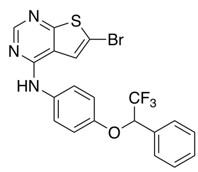

The synthesis of 6-bromo-*N*-(4-(2,2,2-trifluoro-1-phenylethoxy)-phenyl)thieno[2,3-*d*]pyrimidin-4-amine (**(*rac*)-10**) is performed following the procedure in Section 4.14 with the following compounds and scale: Compound **(*rac*)-7** (416 mg, 1.56 mmol), thienopyrimidine **1** (213 mg , 1.25 mmol) and

DIEPA (0.42 mL, 2.49 mmol) was stirred in *i*-PrOH (16 mL) at 80 ℃ for 6 hours. The crude product was purified by silica-gel column chromatography (*n*-pentane/EtOAc 6:4, Rf = 0.42). The product was isolated as off white crystals in a 51% yield (311 mg, 0.648 mmol) with HPLC purity 96% and Mp. 199.7-200.6 ℃.

Spectroscopic data for Compound **(*rac*)-10** (Appendix .1.16): ^{1}H-NMR (600 MHz, DMSO-d_6) δ: 9.52 (s, 1H), 8.39 (s, 1H), 7.98 (s, 1H), 7.62 (m, 2H), 7.60 (m, 2H), 7.46 (m, 1H), 7.45 (m, 2H), 7.06 (d, ^3J =8.9 Hz, 2H), 6.26 (q, ^3J =8.8 Hz, 1H); ^{13}C-NMR (150 MHz, DMSO-d_6) δ: 167.1, 153.7, 153.5, 152.1, 133.2, 131.9, 129.7 (2C), 128.7, 128.0 (2C), 124.8 (q, $^1J_{CF}$ = 281.2 Hz), 123.2 (2C), 122.6, 117.4, 116.1 (2C), 110.7, 76.0 (q, $^2J_{CF}$ = 31.3 Hz); ^{19}F-NMR (565 MHz, DMSO-d_6, C_6F_6): -77.75; IR (cm^{-1}) ν: 3280 (w), 3073 (w), 1619 (m), 1575 (m), 1541 (m), 1504 (s), 1482 (m), 1444 (s), 1412 (m), 1345 (s), 1306 (m), 1286 (m), 1274 (m), 1247 (s), 1230 (s), 1202 (s), 1167 (m), 1135 (s), 1055 (m), 896 (m), 850 (m), 833 (s), 774 (m), 756 (m), 700 (s), 520 (m), 473 (m).

HRMS (ASAP+, m/z): detected 479.9995, calculated for $C_{20}H_{14}N_3OS^{79}BrF_3$ $[M+H]^+$ 479.9993.

4.18 (*R*)-6-bromo-*N*-(4-(2,2,2-trifluoro-1-phenylethoxy)phenyl)thieno[2,3-*d*]pyrimidin-4-amine ((*R*)-10)

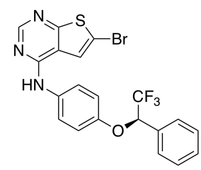

The synthesis of Compound **(*R*)-10** was carried out according to the procedure in Section 4.14 with following compounds: Compound **(*R*)-7** (204 mg, 0.763 mmol), thienopyrimidine **1** (108 mg , 0.633 mmol) and DIEPA (0.21 mL, 1.147 mmol) were stirred in *i*-PrOH (8 mL) at 80 ℃ for 6.5 hours. The crude product was purified by silica-gel column chromatography (*n*-pentane/EtOAc 8:2, Rf = 0.54). The product was isolated as off white crystals in a 56% yield (0.1699 g, 0.354 mmol) and HPLC purity 99%, with specific rotation of $[\alpha]^{20}_{D}$ = -61.49, Mp. 174.9-176.5 ℃ and EE(%) = 96 (Method 1, t_R= 19.9 min, Rs= 3.8).

Spectroscopic data for Compound **(*R*)-10** (Appendix .1.17): ^{1}H-NMR (600 MHz, DMSO-d_6) δ: 9.52 (s, 1H), 8.39 (s, 1H), 7.98 (s, 1H), 7.62 (m, 2H), 7.60 (m, 2H), 7.46 (m, 1H), 7.44 (m, 2H), 7.06 (d, ^3J =9.0 Hz, 2H), 6.25 (q, ^3J =5.4 Hz, 1H); ^{13}C-NMR (150 MHz, DMSO-d_6) δ: 167.1, 153.7, 153.5, 152.1, 133.2, 131.9, 129.7 (2C), 128.7, 128.1 (2C), 124.8 (q, $^1J_{CF}$ = 282.8 Hz), 123.2 (2C), 122.6, 117.4, 116.1 (2C), 110.7, 76.0 (q, $^2J_{CF}$ = 31.17 Hz); ^{19}F-NMR (565 MHz, DMSO-d_6, C_6F_6): -77.75; IR (cm^{-1}) ν: 3254 (w), 3203 (w), 3099 (w), 3071 (w), 3045 (w), 2923 (w), 1609 (m), 1573 (m), 1541 (m), 1504 (s), 1483 (m), 1443 (s), 1345 (m), 1260 (m), 1249 (m), 1222 (s), 1201 (s), 1176 (s), 1139 (s), 1126 (m), 1049 (m), 853 (m), 824 (m), 773 (m), 700 (s), 633 (w), 526 (w), 450 (w) HRMS (ASAP+, m/z): detected

479.9993, calculated for $C_{20}H_{14}N_3OS^{79}BrF_3$ $[M+H]^+$ 479.9993.

4.19 (*S*)-6-bromo-*N*-(4-(2,2,2-trifluoro-1-phenyl ethoxy)phenyl)thieno[2,3-*d*]pyrimidin-4-amine ((*S*)-10)

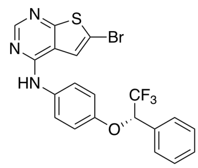

The synthesis of Compound **(*S*)-10** was carried out according to the procedure in Section 4.14 with following compounds: Compound **(*S*)-7** (415 mg, 1.55 mmol), thienopyrimidine **1** (217 mg , 1.27 mmol) and DIEPA (0.42 mL, 2.49 mmol) was stirred in *i*-PrOH (16 mL) at 80 ℃ for 24 hours. The crude product was purified by silica-gel column chromatography (*n*-pentane/EtOAc 4:1, Rf = 0.54). The product was isolated as off white crystals in a 52% yield (0.375 g, 0.780 mmol) with HPLC purity 99%, specific rotation $[\alpha]^{20}_{D} = 61.82$ °, Mp. 173.8-175.8 ℃ and EE (%) = 97 (Method 1, t_R= 16.0 min, Rs= 3.8).

Spectroscopic data for Compound **(*S*)-10** (Appendix .1.18): ^{1}H-NMR (600 MHz, DMSO-d_6) δ: 9.52 (s, 1H), 8.39 (s, 1H), 7.98 (s, 1H), 7.62 (m, 2H), 7.60 (m, 2H), 7.46 (m, 1H), 7.44 (m, 2H), 7.06 (d, ^3J =7.5 Hz, 2H), 6.25 (q, ^3J =6.5 Hz, 1H); ^{13}C-NMR (150 MHz, DMSO-d_6) δ: 167.1, 153.7, 153.5, 152.1, 133.2, 131.9, 129.7 (2C), 128.7, 128.1 (2C), 124.8 (q, $^1J_{CF}$ = 281.7 Hz), 123.2 (2C), 122.6, 117.4, 116.1 (2C, 110.7, 76.0 (q, $^2J_{CF}$ = 31.5 Hz); ^{19}F-NMR (565 MHz, DMSO-d_6, C_6F_6): -77.75; IR (cm^{-1}) ν:3252 (w), 3070 (w), 2960 (w), 2925 (w), 1609 (m), 1573 (m), 1540 (m), 1503 (s), 1482 (m), 1441 (s), 1344 (s), 1260 (m), 1248 (m), 1219 (s), 1199 (s), 1174 (s), 1137 (s), 1124 (s), 1083 (m), 1048 (m), 1001 (m), 852 (m), 823 (m), 773 (m), 754 (m), 698 (s), 633 (m), 506 (m), 469 (m).

HRMS (ASAP+, m/z): detected 479.9995, calculated for $C_{20}H_{14}N_3OS^{79}BrF_3$ $[M+H]^+$ 479.9993.

4.20 Synthesis of *N*-(4-(benzyloxy)phenyl)-6-bromo-thieno[2,3-*d*]pyrimidin-4-amine (11)

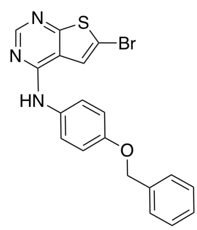

Thienopyrimidine **1** (1.01g , 4.01 mmol), 4-(benzyloxy)aniline hydrochloride (1.134 g, 4.81 mmol) were dissolved in *i*-PrOH (40 mL) and DIPEA (1.4 mL, 8.02 mmol) under an N_2-atmosphere and stirred at 80 ℃ for 6.5 hours. The mixture was concentrated in *vacuo*. An assay ^{1}H-NMR of the mixture (206 mg) was recorded with 4-chlorothieno[2,3-*d*]pyrimidine (159 mg) as standard, assay value of 58%. The crude product was purified with two parallel silica-gel column chromatography (*n*-pentane/EtOAc 3:2, Rf = 0.69). The product was further purified through extraction with EtOAc (100 mL × 3), $NaHCO_3$-brine (100 mL × 3), water (100 mL × 9) and brine (100 mL × 3. The product was isolated as an off-white solid, in a 81% yield (1.34g, 3.26 mmol) with HPLC purity of 99% and Mp. 174.9-177.6 ℃.

Spectroscopic data for Compound **11** (Appendix .1.19): ^{1}H-NMR (600 MHz, DMSO-d_6) δ: 9.53 (s, 1H), 8.41 (s, 1H), 8.01 (s, 1H), 7.63 (d, ^{3}J =7.4 Hz, 2H), 7.46 (d, ^{3}J =7.4 Hz, 2H), 7.40 (t, ^{3}J =7.5 Hz, 2H), 7.33 (t, ^{3}J =7.3 Hz, 1H), 7.05 (d, ^{3}J =8.9 Hz, 2H), 5.11 (s, 2H); ^{13}C-NMR (150 MHz, DMSO-d_6) δ: 167.0, 154.8, 153.8, 153.7, 137.2, 131.9, 128.5 (2C), 127.8, 127.7 (2C), 123.5 (2C), 122.7, 117.4, 114.8 (2C), 110.5, 69.4; IR (cm^{-1}) ν: 3264 (w), 3072 (w), 3008 (w), 2859 (w), 1618 (m), 1609 (m), 1540 (m), 1504 (s), 1481 (m), 1446 (s), 1344 (m), 1221 (s), 1201 (s), 1033 (m), 827 (s), 770 (m). HRMS (ASAP+, m/z): detected 334.1014, calculated for $C_{19}H_{14}N_3OS^{79}Br$ [M+H]$^+$ 334.1018

4.21 Synthesis of *N*-(4-(benzyloxy)phenyl)-6-phenyl-thieno[2,3-*d*]pyrimidin-4-amine (12)

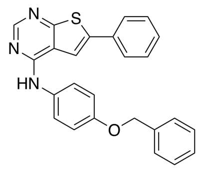

Compound **11** (75 mg, 0.182 mmol), phenylboronic acid (27 mg, 0.218 mmol), K_2CO_3 (75 mg, 0.546 mmol) and Pd(dppf)Cl_2 (6.7 mg, 0.0091 mmol) were dissolved in degassed ACN (2 mL) and water (1 mL). The reaction was stirred at 80 ℃ for 20 minutes. The reaction mixture was concentrated in *vacuo*, and extracted with water (10 mL) and EtOAc (3 × 10 mL). The combined organic phase were washed with brine (10 mL) and dried over Na_2SO_4, filtrated and concentrated in *vacuo*. The crude product was purified with silica-gel column chromatography (*n*-pentane: EtOAc; 1:1, R_f=0.64). The product was isolated as a white solid with 67% yield (50 mg, 0.122 mmol) with HPLC purity 99% and Mp. 211.2-211.4 ℃.

Spectroscopic data for Compound **12** (Appendix .1.20): ^{1}H-NMR (600 MHz, DMSO-d_6) δ: 9.58 (s, 1H), 8.43 (s, 1H), 8.23 (s, 1H), 7.73 (d, ^{3}J =7.9 Hz, 2H), 7.71 (d, ^{3}J =9.0 Hz, 2H), 7.53 (t, ^{3}J =7.7 Hz, 2H), 7.48 (d, ^{3}J =7.4 Hz, 2H), 7.43 (m, 1H), 7.40 (m, 2H), 7.34 (t, ^{3}J =7.4 Hz, 2H), 7.07 (d, ^{3}J =9.0 Hz, 2H), 5.12 (s, 1H); ^{13}C-NMR (150 MHz, DMSO-d_6) δ: 165.7, 154.7, 154.6, 153.5, 138.9, 137.2, 133.2, 132.2, 129.5 (2C), 128.8, 128.4 (2C), 127.8, 127.7 (2C), 125.8 (2C), 123.2 (2C), 118.0, 115.3, 114.8 (2C), 69.4; IR (cm^{-1}) ν: 3071 (w), 3029 (w), 2959 (w), 2857 (w), 1602 (m), 1571 (m), 1551 (m), 1504 (s), 1483 (m), 1451 (m), 1441 (m), 1414 (m), 1383 (m), 1353 (m), 1298 (m). 1236 (m), 1208 (s), 1028 (w), 992 (w), 860 (w), 754 (m), 733 (m), 690 (m), 544 (w), 516 (w), 463 (w).

HRMS (ASAP+, m/z): detected 410.1331, calculated for $C_{25}H_{20}N_3OS$ [M+H]$^+$ 410.1327.

4.22 Synthesis of *N*-(4-(benzyloxy)phenyl)-6-(pyridin-3-yl)thieno[2,3-*d*]pyrimidin-4-amine (13)

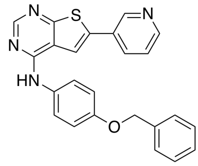

The procedure described in Section 4.21 was repeated with the following compounds: Compound **11** (75 mg, 0.182 mmol), pyridin-3-ylboronic acid (27 mg, 0.218 mmol), K_2CO_3 (75 mg, 0.546 mmol), Pd(dppf)Cl_2 (6.7 mg, 0.0091 mmol) in degassed ACN (2 mL) and water (1 mL). The reaction was stirred at 80 ℃ for 15 minutes. The crude product was purified with silica-gel column chromatography (*n*-pentane: EtOAc; 4:1, R_f=0.16). The product was isolated as a yellow solid with 64% yield (48 mg, 0.116 mmol), HPLC purity 99% and Mp. 216.2-218.1.

Spectroscopic data for Compound **13** (Appendix .1.21): ^{1}H-NMR (600 MHz, DMSO-d_6) δ: 9.64 (s, 1H), 8.96 (m, 1H), 8.62 (m, 1H), 8.45 (s, 1H), 8.31 (s, 1H), 8.10 (m, 1H), 7.70 (d, ^3J =9.0 Hz, 2H), 7.57 (q, ^3J =4.8 Hz, 1H), 7.48 (d, ^3J =7.1 Hz, 2H), 7.41 (t, ^3J =7.4 Hz, 2H), 7.34 (t, ^3J =7.3 Hz, 1H), 7.07 (d, ^3J =9.0 Hz, 2H), 5.12 (s, 1H); ^{13}C-NMR (150 MHz, DMSO-d_6) δ: 166.2, 154.74, 154.73, 153.9, 149.5, 146.4, 137.2, 135.2, 133.2, 132.2, 132.0, 129.2,128.4, 127.8 (2C), 127.7 (2C), 124.3, 123.3 (2C), 117.8, 116.8, 114.8 (2C), 69.4; IR (cm^{-1}) ν: 3247 (w), 3030 (w), 2919 (w), 2853 (w), 1741 (w), 1605 (m), 1568 (m), 1500 (s), 1440 (m), 1373 (m), 1347 (m), 1301 (m), 1231 (s), 1206 (m), 1006 (m), 989 (m), 858 (m), 795 (s), 767 (m), 755 (s), 732 (m), 702 (m), 690 (s), 625 (m), 616 (m), 539 (m), 524 (m), 460 (m).

HRMS (ASAP+, m/z): detected 411.1283, calculated for $C_{24}H_{19}N_4OS$ $[M+H]^+$ 411.1280.

4.23 Synthesis of *N*-(4-(cyclohexylmethoxy)phenyl)-6-(pyridin-3-yl)thieno[2,3-*d*]pyrimidin-4-amine (14)

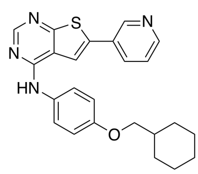

The procedure described in Section 4.21 was repeated with the following compounds: compound **8** (100 mg, 0.239 mmol), pyridin-3-ylboronic acid (35 mg, 0.287 mmol), K_2CO_3 (99 mg, 0.717 mmol), Pd(dppf)Cl_2 (8.7 mg, 0.012 mmol) in degassed ACN (4 mL) and water (2 mL). The reaction was stirred at 80 ℃ for 2.5 hours. The crude product was purified with silica-gel column chromatography (*n*-pentane: EtOAc; 8:2, R_f=0.11). The product was isolated as a off-white solid in a 27% yield (26.8 mg, 0.064 mmol) with HPLC purity 99% and Mp. 224.2-226.2 ℃

Spectroscopic data for Compound **14** (Appendix .1.22): ^{1}H-NMR (600 MHz, DMSO-d_6) δ: 9.63 (s, 1H), 8.97 (m, 1H), 8.62 (m, 1H), 8.46 (s, 1H), 8.32 (s, 1H), 8.10 (m, 1H), 7.69 (d, ^3J =8.9 Hz, 2H), 7.58 (q, ^3J =4.8 Hz, 1H), 6.98 (d, ^3J =9.0 Hz, 2H), 3.80 (d, ^3J =6.4 Hz, 2H), 1.81 (m, 2H), 1.74 (m, 3H), 1.67 (m, 1H), 1.26 (m, 2H), 1.19 (m, 1H), 1.05 (m, 2H); ^{13}C-NMR (150 MHz, DMSO-d_6) δ: 166.1, 155.3, 154.7, 153.9, 149.5, 146.4, 135.1, 133.2, 131.7, 129.2, 124.4, 123.3 (2C), 117.8, 116.9, 114.4 (2C), 72.9, 37.1, 29.3 (2C), 26.1, 25.3 (2C); IR (cm^{-1}) ν: 3280 (w), 3104 (w), 2905 (w), 2850 (w), 1627 (m), 1569 (m), 1543 (m), 1503 (s), 1468 (m), 1445 (s), 1418 (m), 1379 (m), 1350 (m), 1301 (m), 1251 (m), 1228 (m), 1203 (m), 1024 (m), 990 (m), 862 (m), 830 (m), 806 (m), 766 (m), 718 (m), 706 (m), 608 (m), 545 (m), 521 (m). HRMS (ASAP+, m/z): detected 417.1752, calculated for $C_{24}H_{25}N_4OS$ $[M+H]^+$ 417.1749.

4.24 Synthesis of 6-(pyridin-3-yl)-*N*-(4-(2,2,2-trifluoro-1-phenylethoxy)phenyl)thieno[2,3-*d*]-pyrimidin-4-amine (*rac*)-15

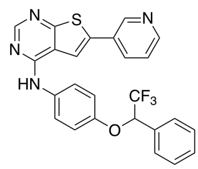

The synthesis of compound **(*rac*)-15** was carried out by the procedure described in Section 4.21, with the following compounds: compound **(*rac*)-9** (101 mg, 0.210 mmol), pyridin-3-ylboronic acid (32 mg, 0.260 mmol), K_2CO_3 (91 mg, 0.655 mmol), Pd(dppf)Cl_2 (7.2 mg, 0.098 mmol) in degassed ACN (4 mL) and water (2 mL).The reaction was stirred at 80 ℃ for 15 minutes. The crude product was purified with silica-gel column chromatography (*n*-pentane: EtOAc; 3:7, R_f=0.32). The product was isolated as a off-white solid in a 88% yield (87.4 mg, 0.183 mmol) and HPLC purity 99%, Mp. 217.7-218.6 ℃, Rs = 3.9 determined from method 3 in Section 4.1.2.

Spectroscopic data for Compound **(*rac*)-15** (Appendix .1.23): ^{1}H-NMR (600 MHz, DMSO-d_6) δ: 9.64 (s, 1H), 8.94 (s, 1H), 8.61 (s, 1H), 8.43 (s, 1H), 8.27 (s, 1H), 8.08 (d, ^3J =8.0 Hz, 1H), 7.67 (d, ^3J =7.7 Hz, 2H), 7.62 (d, ^3J =7.6 Hz, 2H), 7.55 (m, 1H), 7.47 (m, 1H), 7.45 (m, 2H), 7.08 (d, ^3J =7.8 Hz, 2H), 6.26 (q, ^3J =6.2 Hz, 2H); ^{13}C-NMR (150 MHz, DMSO-d_6) δ: 166.2, 154.6, 153.8, 152.0, 149.5, 146.4, 135.3, 133.4, 133.2, 132.0, 129.7 (2C), 129.2, 128.8, 128.1 (2C), 124.8 (q, ^3J =282.0 Hz), 124.3, 123.1 (2C), 117,9, 116.7, 116.1 (2C), 76.0 (q, ^3J =31.5 Hz); ^{19}F-NMR (565 MHz, DMSO-d_6, C_6F_6): -77.74; IR (cm^{-1}) ν: 3260 (w), 3037 (w), 2925 (w), 2854 (w), 1728 (m), 1612 (m), 1574 (m), 1501 (s), 1442 (s), 1350 (m), 1229 (s), 1205 (s), 1175 (s), 1131 (s), 1046 (m), 990 (m), 894 (m), 767 (s), 757 (m), 701 (s), 627 (m), 524 (m). HRMS (ASAP+, m/z): detected 479.1152, calculated for $C_{25}H_{18}N_4OF_3S$ $[M+H]^+$ 479.1153.

4.25 Synthesis of (*S*)-6-(pyridin-3-yl)-*N*-(4-(2,2,2-trifluoro-1-phenylethoxy)phenyl)thieno[2,3-*d*] pyrimidin-4-amine (*S*)-15

The synthesis of compound **(*S*)-15** was carried out by the procedure described in Section 4.21, with the following compounds: compound **(*S*)-9** (99.1 mg, 0.206 mmol), pyridin-3-ylboronic acid (30.5 mg, 0.248 mmol), K_2CO_3 (90.5 mg, 0.655 mmol), Pd(dppf)Cl_2 (7.8 mg, 0.011 mmol) in degassed ACN (4 mL) and water (2 mL). The reaction was stirred at 80 ℃ for 20 minutes. The crude product was purified with silica-gel column chromatography (*n*-pentane: EtOAc; 3:7, R_f=0.32). The product was isolated as a off-white solid in a 90% yield (89.0 mg, 0.186 mmol) and HPLC purity 99%, specific rotation $[\alpha]^{20}_{D}$ = 53.30 °, Mp. 166.7-167.8 ℃, EE (%) = 99 (Method 3, t_R= 63.4 min, Rs= 3.9).

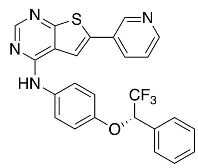

Spectroscopic data for Compound **(*S*)-15** (Appendix .1.24): ^{1}H-NMR (600 MHz, DMSO-d_6) δ: 9.64 (s, 1H), 8.94 (s, 1H), 8.61 (m, 1H), 8.43, 8.27, 8.08 (m, 1H), 7.67 (d, ^3J =9.0 Hz, 2H), 7.62 (d, ^3J =7.3 Hz, 2H), 7.55 (q, ^3J =4.7 Hz, 1H), 7.47 (m, 1H), 7.45 (m, 2H), 7.08 (d, ^3J =9.1 Hz, 2H), 6.26 (q, ^3J =6.5 Hz, 2H); ^{13}C-NMR (150 MHz, DMSO-d_6) δ:166.2, 154.6, 153.8, 152.0, 149.5, 146.4, 135.3, 133.4, 133.2, 132.0, 129.7 (2C), 129.2, 128.8, 128.1 (2C), 124.8 (q, ^3J =280.1 Hz), 124.3, 123.1 (2C), 117.9, 116.7, 116.1 (2C), 76.0 (q, ^3J =31.3 Hz); ^{19}F-NMR (565 MHz, DMSO-d_6, C_6F_6): -77.74; IR (cm^{-1}) ν: 3265 (w), 3037 (w), 2920 (w), 2851 (w), 1729 (w), 1613 (m), 1573 (m), 1501 (s), 1442 (m), 1228 (s), 1205 (s), 1174 (s), 1131 (s), 1047 (m), 990 (m), 767 (m), 701 (s), 627 (m), 524 (m). HRMS (ASAP+, m/z): detected 479.1153, calculated for $C_{25}H_{18}N_4OF_3S$ $[M+H]^+$ 479.1153.

Bibliography

[1] Amar Bennasroune, Anne Gardin, Dominique Aunis, Gérard Crémel, and Pierre Hubert. Tyrosine kinase receptors as attractive targets of cancer therapy. *Critical Reviews in Oncology/Hematology*, 50(1):23–38, 2004.

[2] Esther Zwick, Johannes Bange, and Axel Ullrich. Receptor tyrosine kinases as targets for anticancer drugs. *Trends in Molecular Medicine*, 8(1):17–23, 2002.

[3] I Rubin and Y Yarden. The basic biology of HER2. *Annals of Oncology*, 12:S3–S8, 2001.

[4] Ryan H Engel and Virginia G Kaklamani. HER2-Positive Breast Cancer. *Drugs*, 67(9):1329–1341, 2007.

[5] S Paik, R Hazan, E R Fisher, R E Sass, B Fisher, C Redmond, J Schlessinger, M E Lippman, and C R King. Pathologic findings from the National Surgical Adjuvant Breast and Bowel Project: prognostic significance of erbB-2 protein overexpression in primary breast cancer. *Journal of Clinical Oncology*, 8(1):103–112, 1990.

[6] Himanshu Joshi and Michael F Press. 22 - Molecular Oncology of Breast Cancer. In Kirby I Bland, Edward M Copeland, V Suzanne Klimberg, and William J Gradishar, editors, *The Breast*, pages 282–307. Elsevier, 5th edition, 2018.

[7] Adrienne G Waks and Eric P Winer. Breast Cancer Treatment: A Review. *JAMA*, 321(3):288–300, 2019.

[8] Aleix Prat, Estela Pineda, Barbara Adamo, Patricia Galván, Aranzazu Fernández, Lydia Gaba, Marc Díez, Margarita Viladot, Ana Arance, and Montserrat Muñoz. Clinical implications of the intrinsic molecular subtypes of breast cancer. *The Breast*, 24:S26–S35, 2015.

[9] Şerban Comşa, Anca Maria Cîmpean, and Marius Raica. The Story of MCF-

7 Breast Cancer Cell Line: 40 years of Experience in Research. *Anticancer Research*, 35(6):3147 – 3154, 2015.

[10] Tony Hunter. The Croonian Lecture 1997. The phosphorylation of proteins on tyrosine: its role in cell growth and disease. *Philosophical Transactions of the Royal Society of London. Series B: Biological Sciences*, 353(1368):583–605, 1998.

[11] Morris F White. Structure and function of tyrosine kinase receptors. *Journal of Bioenergetics and Biomembranes*, 23(1):63–82, 1991.

[12] Joseph Schlessinger. Cell Signaling by Receptor Tyrosine Kinases. *Cell*, 103(2):211–225, 2000.

[13] Manash K Paul and Anup K Mukhopadhyay. Tyrosine kinase - Role and significance in Cancer. *International Journal of Medical Sciences*, 1(2):101–115, 2004.

[14] Stevan R Hubbard and Jeffrey H Till. Protein Tyrosine Kinase Structure and Function. *Annual Review of Biochemistry*, 69(1):373–398, 2000.

[15] Kodappully S Siveen, Kirti S Prabhu, Iman W Achkar, Shilpa Kuttikrishnan, Sunitha Shyam, Abdul Q Khan, Maysaloun Merhi, Said Dermime, and Shahab Uddin. Role of Non Receptor Tyrosine Kinases in Hematological Malignances and its Targeting by Natural Products. *Molecular Cancer*, 17(1):31, 2018.

[16] A Levitzki and A Gazit. Tyrosine kinase inhibition: an approach to drug development. *Science*, 267(5205):1782–1788, 1995.

[17] Fleur Broekman, Elisa Giovannetti, and Godefridus J Peters. Tyrosine kinase inhibitors: Multi-targeted or single-targeted? *World Journal of Clinical Oncology*, 2(2):80–93, 2011.

[18] Srinivasan Madhusudan and Trivadi S Ganesan. *Tyrosine Kinase Inhibitors and Cancer Therapy*, pages 25–44. Springer Berlin Heidelberg, Berlin, Heidelberg, 2007.

[19] Toru Mukohara. Mechanisms of resistance to anti-human epidermal growth factor receptor 2 agents in breast cancer. *Cancer Science*, 102(1):1–8, 2011.

[20] Ronit Pinkas-Kramarski, Anne E G Lenferink, Sarah S Bacus, Ljuba Lyass, Monique L M van de Poll, Leah N Klapper, Eldad Tzahar, Michael Sela, Everardus J J van Zoelen, and Yosef Yarden. The oncogenic ErbB-2/ErbB-3 heterodimer is a surrogate receptor of the epidermal growth factor and betacellulin. *Oncogene*, 16(10):1249–1258, 1998.

[21] Ami Citri and Yosef Yarden. EGF–ERBB signalling: towards the systems level. *Nature Reviews Molecular Cell Biology*, 7(7):505–516, 2006.

[22] Rasha M Sareyeldin, Ishita Gupta, Israa Al-Hashimi, Hamda A Al-Thawadi, Halema F Al Farsi, Semir Vranic, and Ala-Eddin Al Moustafa. Gene Expres-

sion and miRNAs Profiling: Function and Regulation in Human Epidermal Growth Factor Receptor 2 (HER2)-Positive Breast Cancer. *Cancers*, 11(5), 2019.

[23] Rachel E Ellsworth, Darrell L Ellsworth, Heather L Patney, Brenda Deyarmin, Brad Love, Jeffrey A Hooke, and Craig D Shriver. Amplification of HER2 is a marker for global genomic instability. *BMC Cancer*, 8(1):297, 2008.

[24] Nida Iqbal and Naveed Iqbal. Human Epidermal Growth Factor Receptor 2 (HER2) in Cancers: Overexpression and Therapeutic Implications. *Molecular Biology International*, 2014:852748, 2014.

[25] Alexey A Larionov. Current Therapies for Human Epidermal Growth Factor Receptor 2-Positive Metastatic Breast Cancer Patients. *Frontiers in Oncology*, 8:89, 2018.

[26] Rutugandha Paranjpe, Dima Basatneh, Gabriel Tao, Carmine De Angelis, Sobia Noormohammed, Ekim Ekinci, Susan Abughosh, Romi Ghose, and Meghana V Trivedi. Neratinib in HER2-Positive Breast Cancer Patients. *Annals of Pharmacotherapy*, 53(6):612–620, 2019.

[27] David W Rusnak, Karen Lackey, Karen Affleck, Edgar R Wood, Krystal J Alligood, Nelson Rhodes, Barry R Keith, Doris M Murray, W Blaine Knight, Robert J Mullin, and Tona M Gilmer. The Effects of the Novel, Reversible Epidermal Growth Factor Receptor/ErbB-2 Tyrosine Kinase Inhibitor, GW2016, on the Growth of Human Normal and Tumor-derived Cell Lines in Vitro and in Vivo. *Molecular Cancer Therapeutics*, 1(2):85–94, 2001.

[28] Gottfried E Konecny, Mark D Pegram, Natarajan Venkatesan, Richard Finn, Guorong Yang, Martina Rahmeh, Michael Untch, David W Rusnak, Glenn Spehar, Robert J Mullin, Barry R Keith, Tona M Gilmer, Mark Berger, Karl C Podratz, and Dennis J Slamon. Activity of the Dual Kinase Inhibitor Lapatinib (GW572016) against HER-2-Overexpressing and Trastuzumab-Treated Breast Cancer Cells. *Cancer Research*, 66(3):1630–1639, 2006.

[29] Mohamed Abdel-Megid, Kamlia M Elmahdy, Azza M Elkazak, Magdy H Seada, and Osama F Mohamed. Chemistry of Thienopyrimidines and Their Biological Applications. *Journal of Pharmaceutical and Applied Chemistry*, 2(3), 2016.

[30] S Bugge, E M Skjønsfjell, F B Willumsen, E Sundby, and B H Hoff. Improved and Scalable Preparation of 6-Bromo-4-Chlorothieno[2,3-d]Pyrimidine. *Chemistry of Heterocyclic Compounds*, 50(8):1177–1187, 2014.

[31] Jennifer L Woodring, Gautam Patel, Jessey Erath, Ranjan Behera, Patricia J Lee, Susan E Leed, Ana Rodriguez, Richard J Sciotti, Kojo Mensa-Wilmot, and Michael P Pollastri. Evaluation of aromatic 6-substituted thienopyrimidines as scaffolds against parasites that cause trypanosomiasis{,} leishmaniasis{,} and malaria. *Med. Chem. Commun.*, 6(2):339–346, 2015.

[32] Safinaz E Abbas, Nagwa M Abdel Gawad, Riham F George, and Yahya A Akar. Synthesis, antitumor and antibacterial activities of some novel tetrahydrobenzo[4,5]thieno[2,3-d]pyrimidine derivatives. *European Journal of Medicinal Chemistry*, 65:195–204, 2013.

[33] Shrikant B Kanawade, Raghunath B Toche, and Dhanji P Rajani. Synthetic tactics of new class of 4-aminothieno[2,3-d]pyrimidine-6-carbonitrile derivatives acting as antimicrobial agents. *European Journal of Medicinal Chemistry*, 64:314–320, 2013.

[34] Mi-Yeon Jang, Steven De Jonghe, Kristien Van Belle, Thierry Louat, Mark Waer, and Piet Herdewijn. Synthesis, immunosuppressive activity and structure–activity relationship study of a new series of 4-N-piperazinyl-thieno[2,3-d]pyrimidine analogues. *Bioorganic & Medicinal Chemistry Letters*, 20(3):844–847, 2010.

[35] Michael Berger, Bettina Albrecht, Attila Berces, Peter Ettmayer, Wolfgang Neruda, and Maximilian Woisetschläger. S(+)-4-(1-Phenylethylamino)quinazolines as Inhibitors of Human Immunoglobuline E Synthesis: Potency Is Dictated by Stereochemistry and Atomic Point Charges at N-1. *Journal of Medicinal Chemistry*, 44(18):3031–3038, 2001.

[36] Wei Yang, Lixuan Li, Xun Ji, Xiaowei Wu, Mingbo Su, Li Sheng, Yi Zang, Jia Li, and Hong Liu. Design, synthesis and biological evaluation of 4-anilinothieno[2,3-d]pyrimidine-based hydroxamic acid derivatives as novel histone deacetylase inhibitors. *Bioorganic & Medicinal Chemistry*, 22(21):6146–6155, 2014.

[37] Fangbin Han, Songwen Lin, Peng Liu, Xiujie Liu, Jing Tao, Xiaobing Deng, Chongqin Yi, and Heng Xu. Discovery of a Novel Series of Thienopyrimidine as Highly Potent and Selective PI3K Inhibitors. *ACS Medicinal Chemistry Letters*, 6(4):434–438, 2015.

[38] Yongcong Lv, Mengyuan Li, Ting Liu, Linjiang Tong, Ting Peng, Lixin Wei, Jian Ding, Hua Xie, and Wenhu Duan. Discovery of a New Series of Naphthamides as Potent VEGFR-2 Kinase Inhibitors. *ACS Medicinal Chemistry Letters*, 5(5):592–597, 2014.

[39] Steffen Bugge, Svein Jacob Kaspersen, Synne Larsen, Unni Nonstad, Geir Bjørkøy, Eirik Sundby, and Bård Helge Hoff. Structure–activity study leading to identification of a highly active thienopyrimidine based EGFR inhibitor. *European Journal of Medicinal Chemistry*, 75:354–374, 2014.

[40] Steffen Bugge, Audun Formo Buene, Nathalie Jurisch-Yaksi, Ingri Ullestad Moen, Ellen Martine Skjønsfjell, Eirik Sundby, and Bård Helge Hoff. Extended structure–activity study of thienopyrimidine-based EGFR inhibitors with evaluation of drug-like properties. *European Journal of Medicinal Chemistry*, 107:255–274, 2016.

[41] Ailing Zhao, Xin Gao, Yuanxiang Wang, Jing Ai, Ying Wang, Yi Chen,

Meiyu Geng, and Ao Zhang. Discovery of novel c-Met kinase inhibitors bearing a thieno[2,3-d]pyrimidine or furo[2,3-d]pyrimidine scaffold. *Bioorganic & Medicinal Chemistry*, 19(13):3906–3918, 2011.

[42] A A Gryshchenko, V G Bdzhola, A O Balanda, N V Briukhovetska, I M Kotey, A G Golub, T P Ruban, L L Lukash, and S M Yarmoluk. Design, synthesis and biological evaluation of N-phenylthieno[2,3-d]pyrimidin-4-amines as inhibitors of FGFR1. *Bioorganic & Medicinal Chemistry*, 23(9):2287–2293, 2015.

[43] Tara R Rheault, Thomas R Caferro, Scott H Dickerson, Kelly H Donaldson, Michael D Gaul, Aaron S Goetz, Robert J Mullin, Octerloney B McDonald, Kimberly G Petrov, David W Rusnak, Lisa M Shewchuk, Glenn M Spehar, Anne T Truesdale, Dana E Vanderwall, Edgar R Wood, and David E Uehling. Thienopyrimidine-based dual EGFR/ErbB-2 inhibitors. *Bioorganic & Medicinal Chemistry Letters*, 19(3):817–820, 2009.

[44] Eman F Abdelhaleem, Mohammed K Abdelhameid, Asmaa E Kassab, and Manal M Kandeel. Design and synthesis of thienopyrimidine urea derivatives with potential cytotoxic and pro-apoptotic activity against breast cancer cell line MCF-7. *European Journal of Medicinal Chemistry*, 143:1807–1825, 2018.

[45] Eman Z Elrazaz, Rabah A T Serya, Nasser S M Ismail, Dalal A Abou El Ella, and Khaled A M Abouzid. Thieno[2,3-d]pyrimidine based derivatives as kinase inhibitors and anticancer agents. *Future Journal of Pharmaceutical Sciences*, 1(2):33–41, 2015.

[46] Steffen Bugge, Ingri Ullestad Moen, Kent-Ove Kragseth Sylte, Eirik Sundby, and Bård Helge Hoff. Truncated structures used in search for new lead compounds and in a retrospective analysis of thienopyrimidine-based EGFR inhibitors. *European Journal of Medicinal Chemistry*, 94:175–194, 2015.

[47] Giorgio Caravatti and Andrea Vaupel. Pyrrolo [2, 3-d] pyrimidines as protein tyrosine kinase inhibitors, December 1 2009. US Patent 7,625,894.

[48] Hans-Joachim Böhm, David Banner, Stefanie Bendels, Manfred Kansy, Bernd Kuhn, Klaus Müller, Ulrike Obst-Sander, and Martin Stahl. Fluorine in Medicinal Chemistry. *ChemBioChem*, 5(5):637–643, 2004.

[49] David C Lankin, Nizal S Chandrakumar, Shashidhar N Rao, Dale P Spangler, and James P Snyder. Protonated 3-fluoropiperidines: an unusual fluoro directing effect and a test for quantitative theories of solvation. *Journal of the American Chemical Society*, 115(8):3356–3357, 1993.

[50] Henrik Helligsø Jensen, Laila Lyngbye, Astrid Jensen, and Mikael Bols. Stereoelectronic Substituent Effects in Polyhydroxylated Piperidines and Hexahydropyridazines. *Chemistry – A European Journal*, 8(5):1218–1226, 2002.

[51] Monique B van Niel, Ian Collins, Margaret S Beer, Howard B Broughton, Susan K F Cheng, Simon C Goodacre, Anne Heald, Karen L Locker, Angus M

MacLeod, Denise Morrison, Christopher R Moyes, Desmond O'Connor, Andrew Pike, Michael Rowley, Michael G N Russell, Balbinder Sohal, Josephine A Stanton, Steven Thomas, Hugh Verrier, Alan P Watt, and José L Castro. Fluorination of 3-(3-(Piperidin-1-yl)propyl)indoles and 3-(3-(Piperazin-1-yl)propyl)indoles Gives Selective Human 5-HT1D Receptor Ligands with Improved Pharmacokinetic Profiles. *Journal of Medicinal Chemistry*, 42(12):2087–2104, 1999.

[52] William K Hagmann. The Many Roles for Fluorine in Medicinal Chemistry. *Journal of Medicinal Chemistry*, 51(15):4359–4369, 2008.

[53] Jean-Pierre Bégué and Danièle Bonnet-Delpon. Recent advances (1995–2005) in fluorinated pharmaceuticals based on natural products. *Journal of Fluorine Chemistry*, 127(8):992–1012, 2006.

[54] Gang Wang, Shuo Yuan, Zhiqiang Wu, Wanyi Liu, Haijuan Zhan, Yanping Liang, Xiaoyan Chen, Baojun Ma, and Shuxian Bi. Ultra-low-loading palladium nanoparticles stabilized on nanocrystalline Polyaniline (Pd@PANI): A efficient, green, and recyclable catalyst for the reduction of nitroarenes. *Applied Organometallic Chemistry*, 33(11):e5159, 2019.

[55] Stephen D Roughley and Allan M Jordan. The Medicinal Chemist's Toolbox: An Analysis of Reactions Used in the Pursuit of Drug Candidates. *Journal of Medicinal Chemistry*, 54(10):3451–3479, 2011.

[56] G Majetich and R Hicks. Applications of microwave accelerated organic chemistry. *Research on Chemical Intermediates*, 20(1):61, 1994.

[57] Liuqing Yang, Wei Liu, Hanbing Mei, Yuan Zhang, Xiaojuan Yu, Yufang Xu, Honglin Li, Jin Huang, and Zhenjiang Zhao. Synthesis and biological evaluation of pentanedioic acid derivatives as farnesyltransferase inhibitors. *MedChemComm*, 6(4):671–676, 2015.

[58] Robert W Holman. Strategic Applications of Named Reactions in Organic Synthesis: Background and Detailed Mechanisms (Kürti, László; Czakó, Barbara). *Journal of Chemical Education*, 82(12):484, 2005.

[59] S N Tan, Robert A Dryfe, and Hubert H Girault. Electrochemical Study of Phase-Transfer Catalysis Reactions: The Williamson ether synthesis. *Helvetica Chimica Acta*, 77(1):231–242, 1994.

[60] Edgar Fuhrmann and Jörg Talbiersky. Synthesis of Alkyl Aryl Ethers by Catalytic Williamson Ether Synthesis with Weak Alkylation Agents. *Organic Process Research & Development*, 9(2):206–211, 2005.

[61] Jong Chan Lee, Jong Yeob Yuk, and Sung Hye Cho. Facile Synthesis of Alkyl Phenyl Ethers Using Cesium Carbonate. *Synthetic Communications*, 25(9):1367–1370, 1995.

[62] George W. Gokel (auth.) William P. Weber. *Phase Transfer Catalysis in*

Organic Synthesis. Reactivity and Structure: Concepts in Organic Chemistry 4. Springer-Verlag Berlin Heidelberg, 1 edition, 1977.

[63] Yanqing Peng and Gonghua Song. Combined microwave and ultrasound assisted Williamson ether synthesis in the absence of phase-transfer catalysts. *Green Chemistry*, 4(4):349–351, 2002.

[64] Selena R Boothroyd and Michael A Kerr. A mild and efficient method for the preparation of anilines from nitroarenes. *Tetrahedron Letters*, 36(14):2411–2414, 1995.

[65] Patrica Lara and Karine Philippot. The hydrogenation of nitroarenes mediated by platinum nanoparticles: an overview. *Catalysis Science Technology*, 4(8):2445–2465, 2014.

[66] Ateeq Rahman and S B Jonnalagadda. Swift and Selective Reduction of Nitroaromatics to Aromatic Amines with Ni–Boride–Silica Catalysts System at Low Temperature. *Catalysis Letters*, 123(3):264–268, 2008.

[67] Anthony R Cartolano and Gamini A Vedage. *Amines by Reduction*. American Cancer Society, 2004.

[68] Fengyu Zhao, Shin-ichio Fujita, Jianmin Sun, Yutaka Ikushima, and Masahiko Arai. Hydrogenation of nitro compounds with supported platinum catalyst in supercritical carbon dioxide. *Catalysis Today*, 98(4):523–528, 2004.

[69] Hari K Kadam and Santosh G Tilve. Advancement in methodologies for reduction of nitroarenes. *RSC Advances*, 5(101):83391–83407, 2015.

[70] Seul Ki Yeon, Ji Won Choi, Jong-Hyun Park, Ye Rim Lee, Hyeon Jeong Kim, Su Jeong Shin, Bo Ko Jang, Siwon Kim, Yong-Sun Bahn, Gyoonhee Han, Yong Sup Lee, Ae Nim Pae, and Ki Duk Park. Synthesis and evaluation of biaryl derivatives for structural characterization of selective monoamine oxidase B inhibitors toward Parkinson's disease therapy. *Bioorganic & Medicinal Chemistry*, 26(1):232–244, 2018.

[71] Yukihiro Motoyama, Kazuyuki Kamo, and Hideo Nagashima. Catalysis in Polysiloxane Gels: Platinum-Catalyzed Hydrosilylation of Polymethylhydrosiloxane Leading to Reusable Catalysts for Reduction of Nitroarenes. *Organic Letters*, 11(6):1345–1348, 2009.

[72] Yasumasa Takenaka, Takahiro Kiyosu, Jun-Chul Choi, Toshiyasu Sakakura, and Hiroyuki Yasuda. Selective synthesis of N-aryl hydroxylamines by the hydrogenation of nitroaromatics using supported platinum catalysts. *Green Chemistry*, 11(9):1385–1390, 2009.

[73] Mohamed Anouar Harrad, Brahim Boualy, Larbi El Firdoussi, Ahmad Mehdi, Claudio Santi, Stefano Giovagnoli, Morena Nocchetti, and Mustapha Ait Ali. Colloidal nickel(0)-carboxymethyl cellulose particles: A biopolymer-

inorganic catalyst for hydrogenation of nitro-aromatics and carbonyl compounds. *Catalysis Communications*, 32:92–100, 2013.

[74] Yi-Si Feng, Jing-Jing Ma, Yu-Mei Kang, and Hua-Jian Xu. PdCu nanoparticles supported on graphene: an efficient and recyclable catalyst for reduction of nitroarenes. *Tetrahedron*, 70(36):6100–6105, 2014.

[75] Samuel Piña, Diana M Cedillo, Carlos Tamez, Nezhueyotl Izquierdo, Jason G Parsons, and Jose J Gutierrez. Reduction of nitrobenzene derivatives using sodium borohydride and transition metal sulfides. *Tetrahedron Letters*, 55(40):5468–5470, 2014.

[76] Hari K Kadam and Santosh G Tilve. Copper(ii) bromide as a procatalyst for in situ preparation of active Cu nanoparticles for reduction of nitroarenes. *RSC Advances*, 2(14):6057–6060, 2012.

[77] Fang Li, Brendan Frett, and Hong-Yu Li. Selective Reduction of Halogenated Nitroarenes with Hydrazine Hydrate in the Presence of Pd/C. *Synlett*, 25(10):1403–1408, 2014.

[78] David Cantillo, Mojtaba Mirhosseini Moghaddam, and C Oliver Kappe. Hydrazine-mediated Reduction of Nitro and Azide Functionalities Catalyzed by Highly Active and Reusable Magnetic Iron Oxide Nanocrystals. *The Journal of Organic Chemistry*, 78(9):4530–4542, 2013.

[79] Raju Dey, Nirmalya Mukherjee, Sabir Ahammed, and Brindaban C Ranu. Highly selective reduction of nitroarenes by iron(0) nanoparticles in water. *Chemical Communications*, 48(64):7982–7984, 2012.

[80] Krishnamurthy Ramadas and Natarajan Srinivasan. Iron-Ammonium Chloride - A Convenient and Inexpensive Reductant. *Synthetic Communications*, 22(22):3189–3195, 1992.

[81] Zhu-Ping Xiao, Ying-Chun Wang, Gao-Yu Du, Jun Wu, Tao Luo, and Shou-Fu Yi. Efficient Reducing System Based on Iron for Conversion of Nitroarenes to Anilines. *Synthetic Communications*, 40(5):661–665, 2010.

[82] Viktor Zimmermann, Frank Avemaria, and Stefan Bräse. Chemoselective Reduction of Nitroarenes in the Presence of Acid-Sensitive Functional Groups: Solid-Phase Syntheses of Amino Aryl Azides and Benzotriazoles. *Journal of Combinatorial Chemistry*, 9(2):200–203, 2007.

[83] Yoshiro Ogata. Steric acceleration by ortho substituents of the stannous chloride reduction of nitrobenzenes in aqueous ethanol. *The Journal of Organic Chemistry*, 47(18):3577–3581, 1982.

[84] Ganesha Rai, Jae Min Jeong, Yun-Sang Lee, Hyung Woo Kim, Dong Soo Lee, June-Key Chung, and Myung Chul Lee. Ionic liquid mediated efficient reduction of nitroarenes using stannous chloride under sonication. *Tetrahedron Letters*, 46(23):3987–3990, 2005.

[85] Allan B Gamble, James Garner, Christopher P Gordon, Sean M J O'Conner, and Paul A Keller. Aryl Nitro Reduction with Iron Powder or Stannous Chloride under Ultrasonic Irradiation. *Synthetic Communications*, 37(16):2777–2786, 2007.

[86] Francesco Pietra. Mechanisms for nucleophilic and photonucleophilic aromatic substitution reactions. *Quarterly Reviews Chemical Society*, 23(4):504–521, 1969.

[87] Mieczysław Mąkosza. Electrophilic and nucleophilic aromatic substitution: Analogous and complementary processes. *Russian Chemical Bulletin*, 45(3):491–504, 1996.

[88] Nicholas J Venditto and David A Nicewicz. Cation Radical-Accelerated Nucleophilic Aromatic Substitution for Amination of Alkoxyarenes. *Organic Letters*, 22(12):4817–4822, 2020.

[89] Joseph F Bunnett. Mechanism and reactivity in aromatic nucleophilic substitution reactions. *Quarterly Reviews Chemical Society*, 12(1):1–16, 1958.

[90] Mieczysław Mąkosza. Nucleophilic substitution of hydrogen in electron-deficient arenes, a general process of great practical value. *Chemical Society Reviews*, 39(8):2855–2868, 2010.

[91] Francis A Carey and Richard J Sundberg. *Advanced Organic Chemistry Part A: Structure and Mechanisms / by Francis A. Carey, Richard J. Sundberg.* Part A: Structure and Mechanisms. Springer US : Imprint: Springer, New York, NY, 5th edition, 2007.

[92] Israel Fernández, Gernot Frenking, and Einar Uggerud. Rate-Determining Factors in Nucleophilic Aromatic Substitution Reactions. *The Journal of Organic Chemistry*, 75(9):2971–2980, 2010.

[93] Francois Terrier. Rate and equilibrium studies in Jackson-Meisenheimer complexes. *Chemical Reviews*, 82(2):77–152, 1982.

[94] Francis A Carey. *Advanced organic chemistry. Part B, Reaction and synthesis.* Springer, New York, 5th edition, 2007.

[95] John A Zoltewicz. New directions in aromatic nucleophilic substitution. In R D Rieke, J A Zoltewicz, H G Aurich, W Weiss, and K P C Vollhardt, editors, *Organic Syntheses*, pages 33–64, Berlin, Heidelberg, 1975. Springer Berlin Heidelberg.

[96] John O Edwards and Ralph G Pearson. The Factors Determining Nucleophilic Reactivities. *Journal of the American Chemical Society*, 84(1):16–24, 1962.

[97] John A Joule and Keith Mills. *Heterocyclic Chemistry.* John Wiley & Sons, 2010.

[98] Michael R Crampton, Thomas A Emokpae, Judith A K Howard, Chukwuemeka Isanbor, and Raju Mondal. Leaving group effects on the mechanism of aromatic nucleophilic substitution (SNAr) reactions of some phenyl 2,4,6-trinitrophenyl ethers with aniline in acetonitrile. *Journal of Physical Organic Chemistry*, 17(1):65–70, 2004.

[99] Jin Han, Eirik Sundby, and Bård Helge Hoff. Solvent selection in synthesis of 4-(1-arylfluoroethoxy)quinazolines and thienopyrimidines. *Journal of Fluorine Chemistry*, 153:82–88, 2013.

[100] Sonali Kurup, Bradley McAllister, Pavlina Liskova, Trusha Mistry, Anthony Fanizza, Dan Stanford, Jolanta Slawska, Ulrich Keller, and Alexander Hoellein. Design, synthesis and biological activity of N4-phenylsubstituted-7H-pyrrolo[2,3-d]pyrimidin-4-amines as dual inhibitors of aurora kinase A and epidermal growth factor receptor kinase. *Journal of Enzyme Inhibition and Medicinal Chemistry*, 33(1):74–84, 2018.

[101] Janis Louie and John F Hartwig. Palladium-catalyzed synthesis of arylamines from aryl halides. Mechanistic studies lead to coupling in the absence of tin reagents. *Tetrahedron Letters*, 36(21):3609–3612, 1995.

[102] Ylva Sunesson, Elaine Limé, Sten O Nilsson Lill, Rebecca E Meadows, and Per-Ola Norrby. Role of the Base in Buchwald–Hartwig Amination. *The Journal of Organic Chemistry*, 79(24):11961–11969, 2014.

[103] David S Surry and Stephen L Buchwald. Biaryl Phosphane Ligands in Palladium-Catalyzed Amination. *Angewandte Chemie International Edition*, 47(34):6338–6361, 2008.

[104] L Kürti, Barbara Czako, E Corey, and K C Nicolaou. Strategic applications of named reactions in organic synthesis: background and detailed mechanisms. 2005.

[105] John F Hartwig. Transition Metal Catalyzed Synthesis of Arylamines and Aryl Ethers from Aryl Halides and Triflates: Scope and Mechanism. *Angewandte Chemie International Edition*, 37(15):2046–2067, 1998.

[106] Ruth Dorel, Christian P Grugel, and Alexander M Haydl. The Buchwald–Hartwig Amination After 25 Years. *Angewandte Chemie International Edition*, 58(48):17118–17129, 2019.

[107] J F Hartwig. Approaches to catalyst discovery. New carbon–heteroatom and carbon–carbon bond formation. *Pure and Applied Chemistry*, 71(8):1417–1423, 1999.

[108] Diego Gonzàlez Cabrera, Frederic Douelle, Claire Le Manach, Ze Han, Tanya Paquet, Dale Taylor, Mathew Njoroge, Nina Lawrence, Lubbe Wiesner, David Waterson, Michael J Witty, Sergio Wittlin, Leslie J Street, and Kelly Chibale. Structure–Activity Relationship Studies of Orally Active Anti-

malarial 2,4-Diamino-thienopyrimidines. *Journal of Medicinal Chemistry*, 58(18):7572–7579, 2015.

[109] Akira Suzuki. Recent advances in the cross-coupling reactions of organoboron derivatives with organic electrophiles, 1995–1998. *Journal of Organometallic Chemistry*, 576(1):147–168, 1999.

[110] John P Wolfe, Robert A Singer, Bryant H Yang, and Stephen L Buchwald. Highly Active Palladium Catalysts for Suzuki Coupling Reactions. *Journal of the American Chemical Society*, 121(41):9550–9561, 1999.

[111] Christian Torborg and Matthias Beller. Recent Applications of Palladium-Catalyzed Coupling Reactions in the Pharmaceutical, Agrochemical, and Fine Chemical Industries. *Advanced Synthesis & Catalysis*, 351(18):3027–3043, 2009.

[112] Christian Amatore, Gaëtan LeDuc, and Anny Jutand. Mechanism of Palladium-Catalyzed Suzuki–Miyaura Reactions: Multiple and Antagonistic Roles of Anionic "Bases" and Their Countercations. *Chemistry – A European Journal*, 19(31):10082–10093, 2013.

[113] Akira Suzuki. Organoborane coupling reactions (Suzuki coupling). *Proceedings of the Japan Academy, Series B*, 80(8):359–371, 2004.

[114] Timothy E Barder, Shawn D Walker, Joseph R Martinelli, and Stephen L Buchwald. Catalysts for SuzukiMiyaura Coupling Processes: Scope and Studies of the Effect of Ligand Structure. *Journal of the American Chemical Society*, 127(13):4685–4696, 2005.

[115] Marcial Moreno-Mañas, Montserrat Pérez, and Roser Pleixats. Palladium-Catalyzed Suzuki-Type Self-Coupling of Arylboronic Acids. A Mechanistic Study. *The Journal of Organic Chemistry*, 61(7):2346–2351, 1996.

[116] Christian Amatore and Anny Jutand. Anionic Pd(0) and Pd(II) Intermediates in Palladium-Catalyzed Heck and Cross-Coupling Reactions. *Accounts of Chemical Research*, 33(5):314–321, 2000.

[117] Sambasivarao Kotha, Kakali Lahiri, and Dhurke Kashinath. Recent applications of the Suzuki–Miyaura cross-coupling reaction in organic synthesis. *Tetrahedron*, 58(48):9633–9695, 2002.

[118] Brad P Carrow and John F Hartwig. Distinguishing Between Pathways for Transmetalation in SuzukiMiyaura Reactions. *Journal of the American Chemical Society*, 133(7):2116–2119, 2011.

[119] Norio Miyaura, Kinji Yamada, and Akira Suzuki. A new stereospecific cross-coupling by the palladium-catalyzed reaction of 1-alkenylboranes with 1-alkenyl or 1-alkynyl halides. *Tetrahedron Letters*, 20(36):3437–3440, 1979.

[120] Norio. Miyaura and Akira. Suzuki. Palladium-Catalyzed Cross-Coupling Re-

actions of Organoboron Compounds. *Chemical Reviews*, 95(7):2457–2483, 1995.

[121] Joshua Almond-Thynne, David C Blakemore, David C Pryde, and Alan C Spivey. Site-selective Suzuki-Miyaura coupling of heteroaryl halides - understanding the trends for pharmaceutically important classes. *Chemical Science*, 8(1):40–62, 2017.

[122] Ruben Martin and Stephen L Buchwald. Palladium-Catalyzed SuzukiMiyaura Cross-Coupling Reactions Employing Dialkylbiaryl Phosphine Ligands. *Accounts of Chemical Research*, 41(11):1461–1473, 2008.

[123] Fabio Bellina, Adriano Carpita, and Renzo Rossi. Palladium Catalysts for the Suzuki Cross-Coupling Reaction: An Overview of Recent Advances. *Synthesis*, 2004(15):2419–2440, 2004.

[124] Adam F Littke and Gregory C Fu. Palladium-Catalyzed Coupling Reactions of Aryl Chlorides. *Angewandte Chemie International Edition*, 41(22):4176–4211, 2002.

[125] Irene Maluenda and Oscar Navarro. Recent Developments in the Suzuki-Miyaura Reaction: 2010–2014, 2015.

[126] Steffen Bugge, Svein Jacob Kaspersen, Eirik Sundby, and Bård Helge Hoff. Route selection in the synthesis of C-4 and C-6 substituted thienopyrimidines. *Tetrahedron*, 68(45):9226–9233, 2012.

[127] Haakon Kristvik Bye. Synthesis of 4-amine substitutedthieno[2,3-d]pyrimidines for breastcancer activity testing. Pre-Master project, NTNU, 2020.

[128] Gregory R Fulmer, Alexander J M Miller, Nathaniel H Sherden, Hugo E Gottlieb, Abraham Nudelman, Brian M Stoltz, John E Bercaw, and Karen I Goldberg. NMR Chemical Shifts of Trace Impurities: Common Laboratory Solvents, Organics, and Gases in Deuterated Solvents Relevant to the Organometallic Chemist. *Organometallics*, 29(9):2176–2179, 2010.

[129] Arthur S Wexler. Integrated Intensities of Absorption Bands in Infrared Spectroscopy. *Applied Spectroscopy Reviews*, 1(1):29–98, 1967.

[130] Svein Jacob Kaspersen, Jin Han, Kristin G Nørsett, Line Rydså, Eli Kjøbli, Steffen Bugge, Geir Bjørkøy, Eirik Sundby, and Bård Helge Hoff. Identification of new 4-N-substituted 6-aryl-7H-pyrrolo[2,3-d]pyrimidine-4-amines as highly potent EGFR-TK inhibitors with Src-family activity. *European Journal of Pharmaceutical Sciences*, 59:69–82, 2014.

Appendix

.1 Spectroscopic Data

.1.1 Spectroscopic data for Compound 2

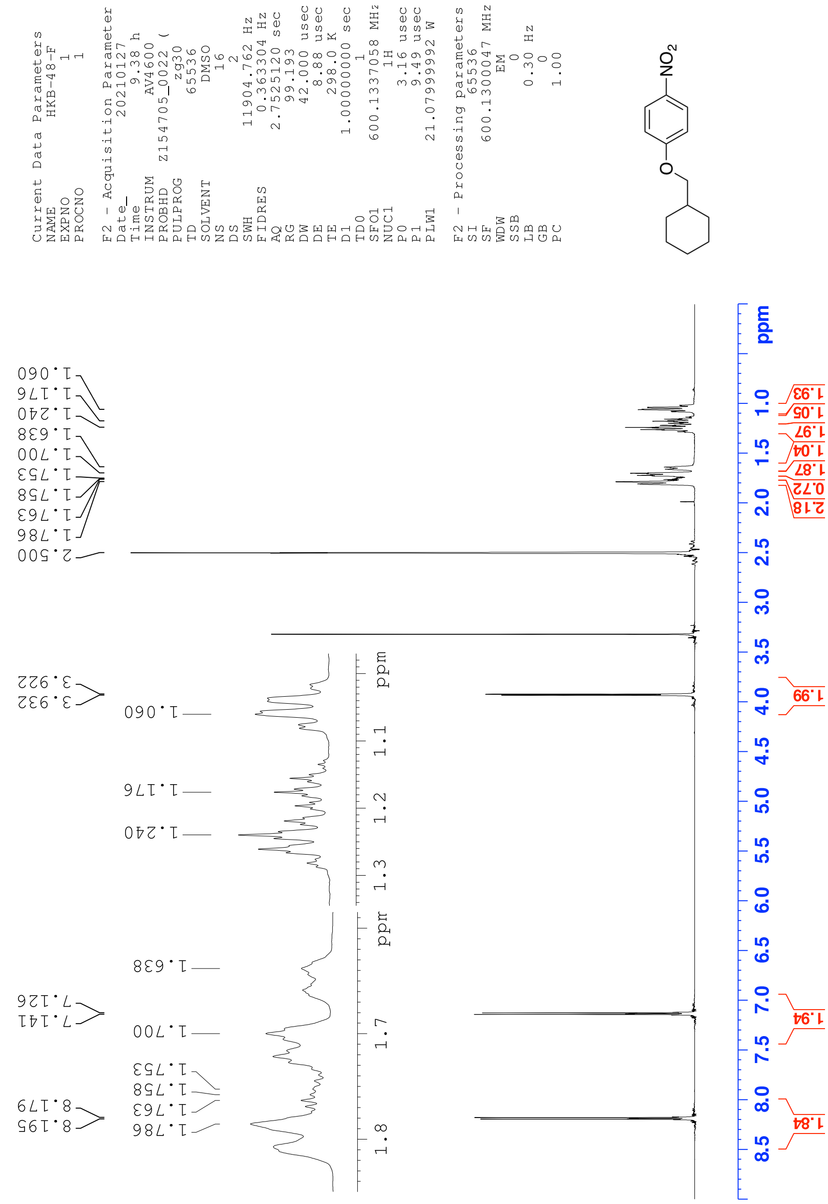

Figure 1: ^{1}H-NMR specter of compound **2**

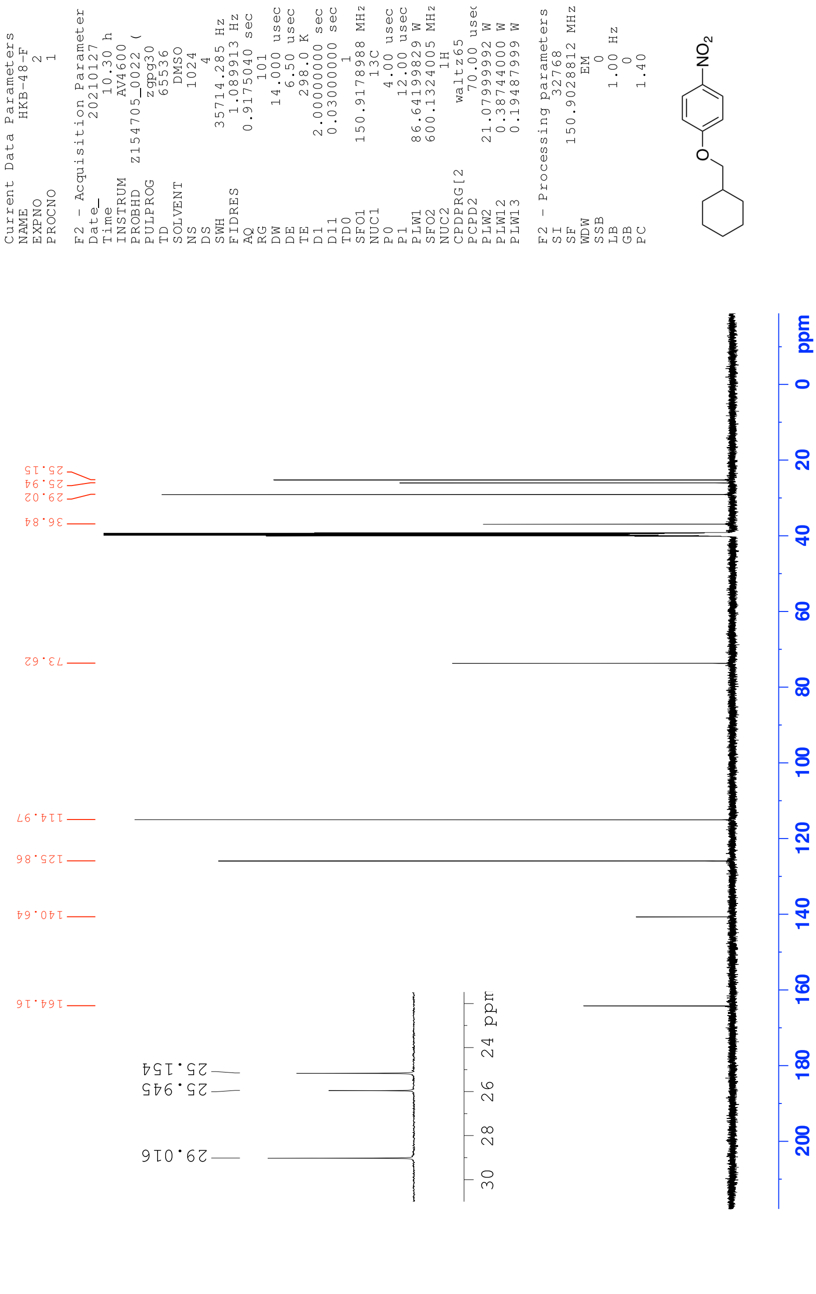

Figure 2: ^{13}C-NMR specter of compound **2**

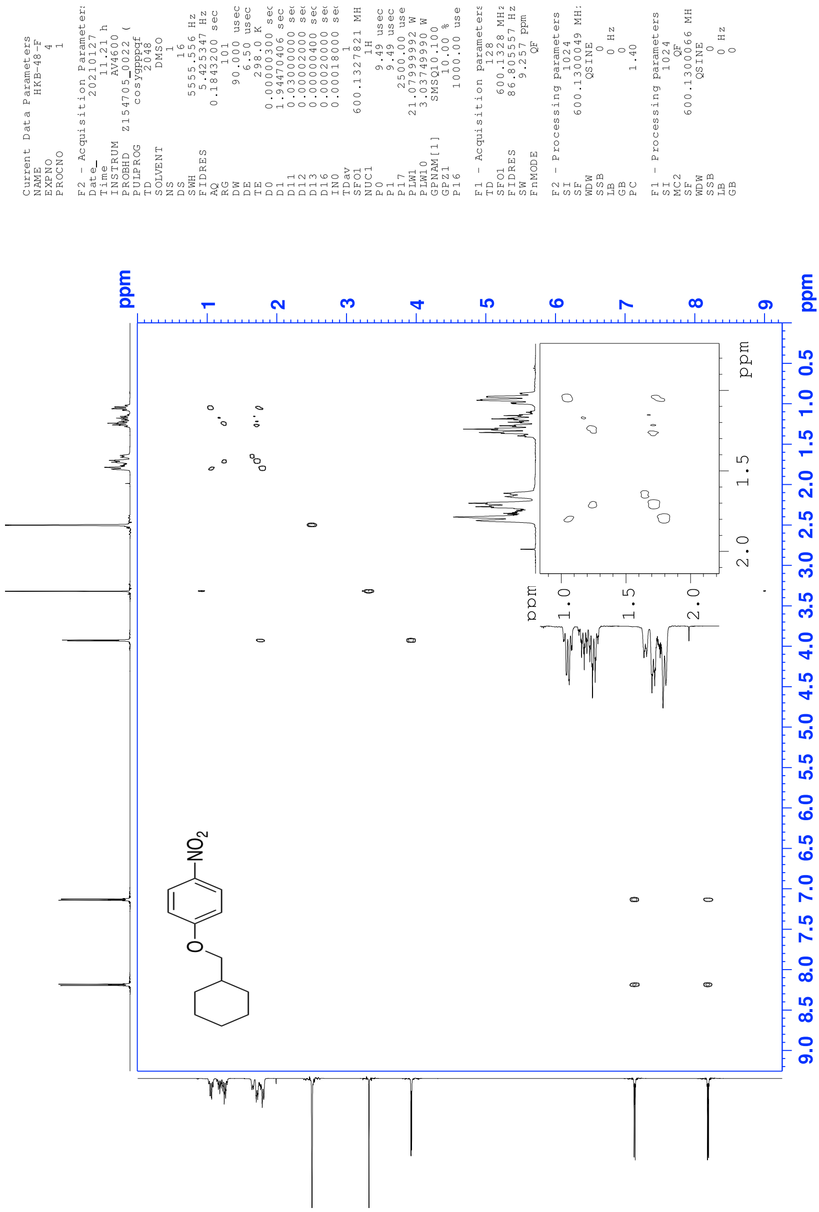

Figure 3: COSY specter of compound **2**

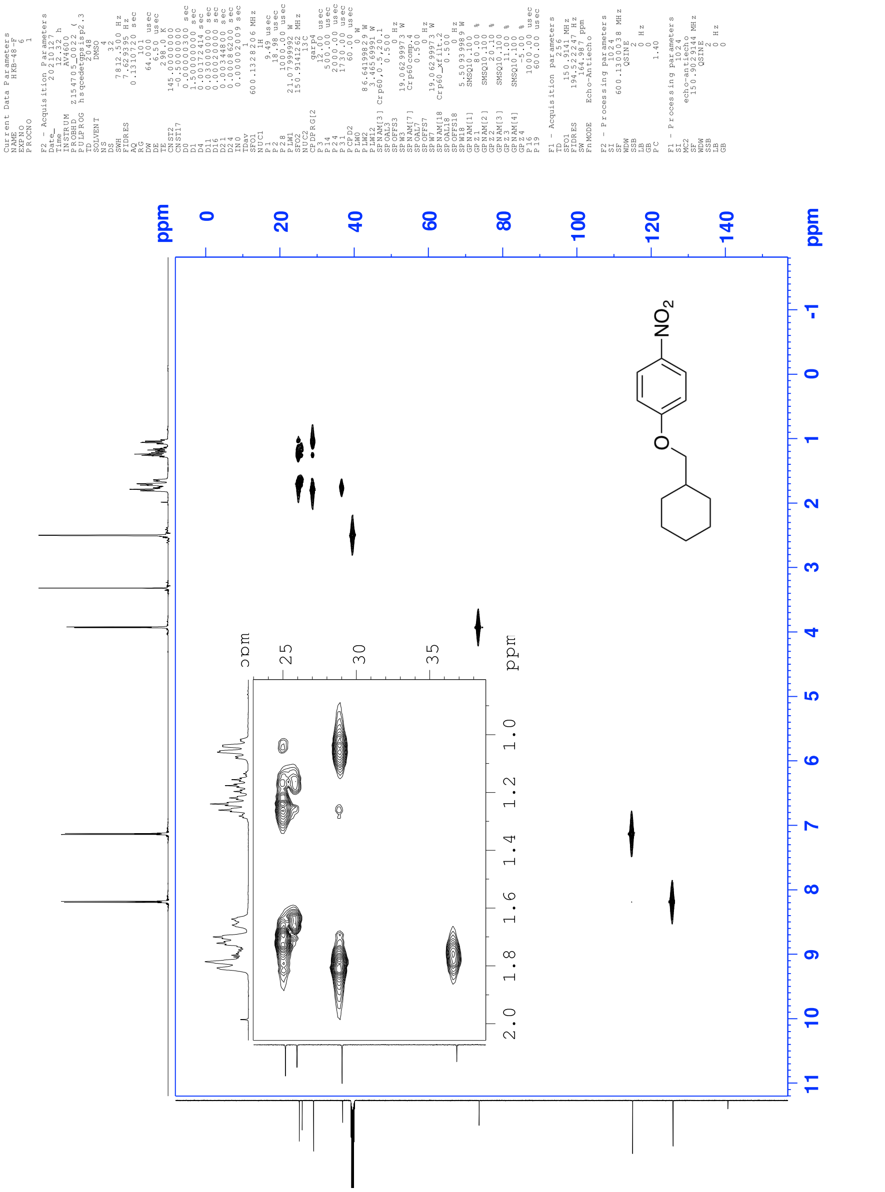

Figure 4: HSQC specter of compound **2**

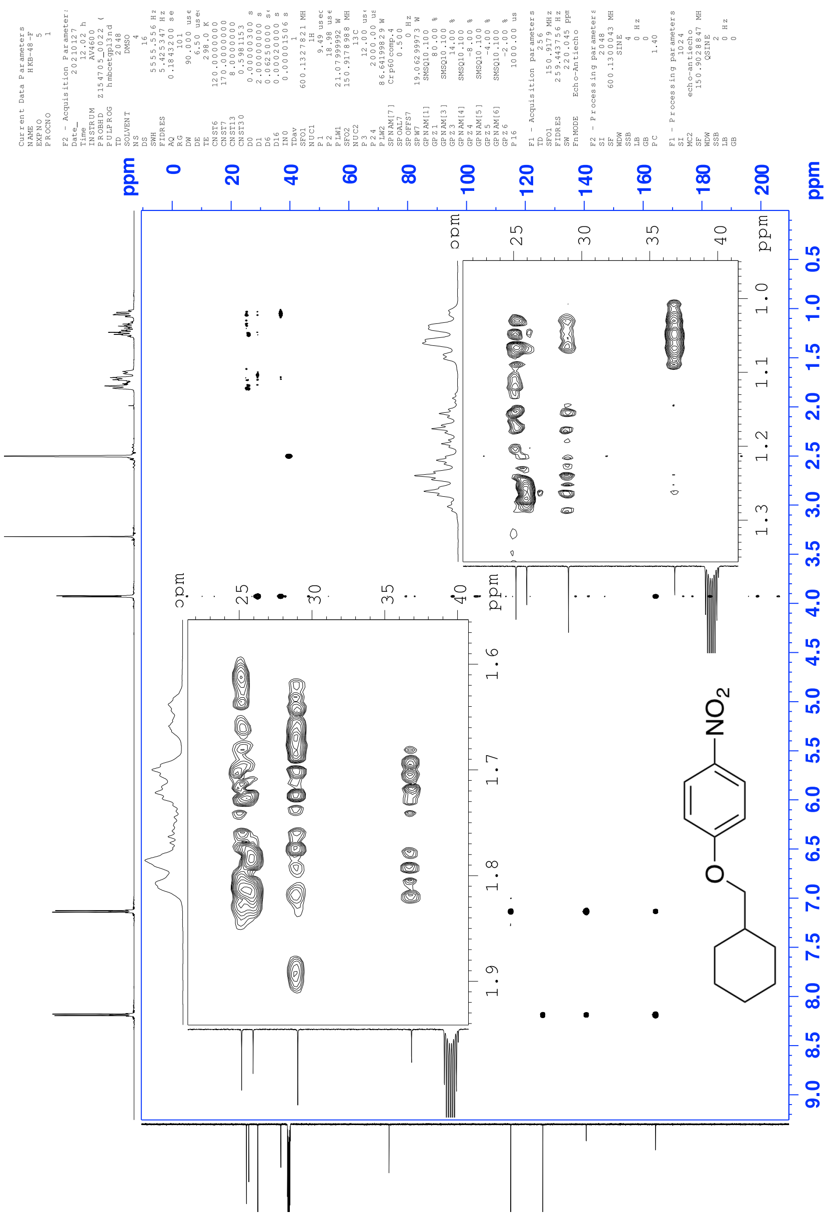

Figure 5: HMBC specter of compound **2**

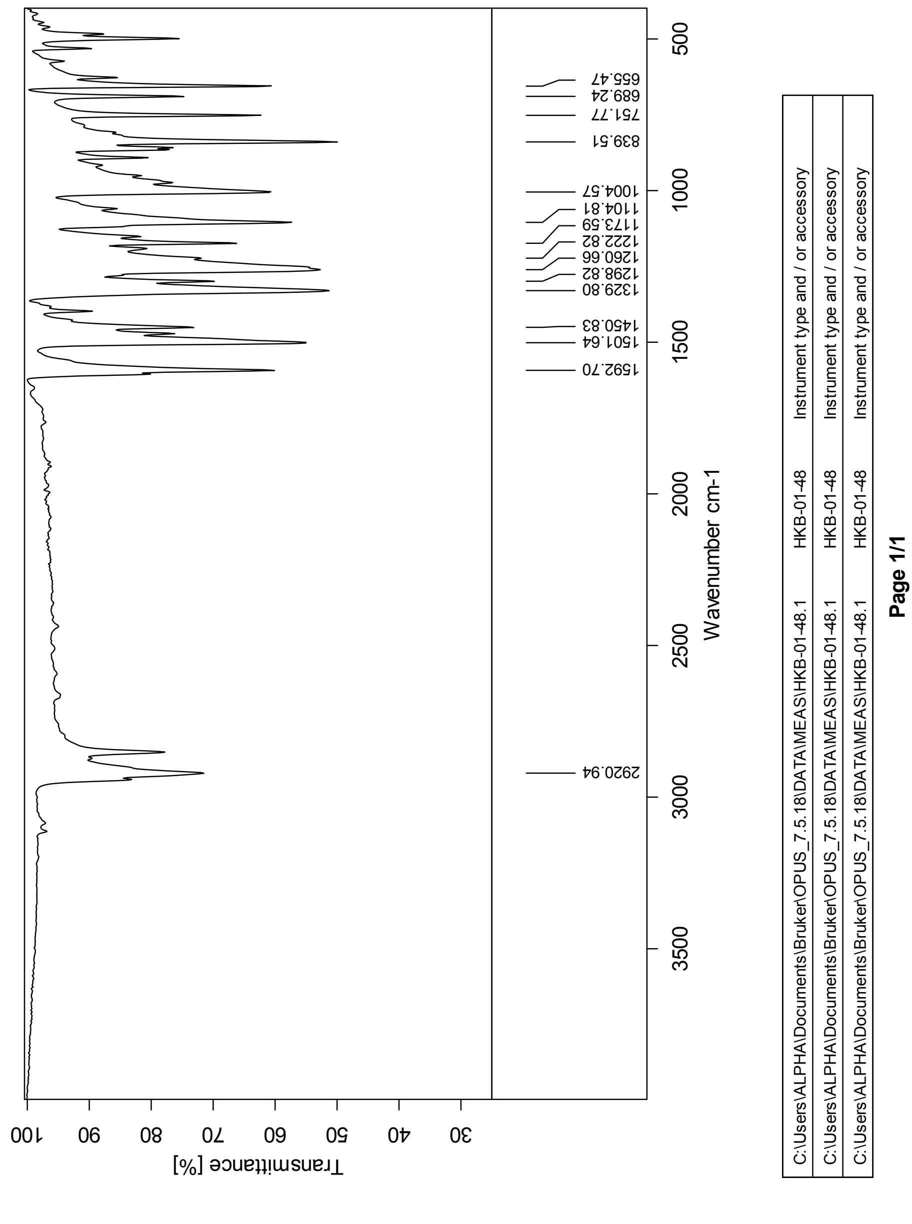

Figure 6: IR-spectrum of compound **2**

Elemental Composition Report **Page 1**

Single Mass Analysis
Tolerance = 2.0 PPM / DBE: min = -10.0, max = 50.0
Element prediction: Off
Number of isotope peaks used for i-FIT = 6

Monoisotopic Mass, Even Electron Ions
787 formula(e) evaluated with 2 results within limits (all results (up to 1000) for each mass)
Elements Used:
C: 0-100 H: 0-100 N: 0-6 O: 0-6 S: 0-5
2021-195 89 (1.759) AM2 (Ar,35000.0,0.00,0.00); Cm (87:89)
1: TOF MS ASAP+

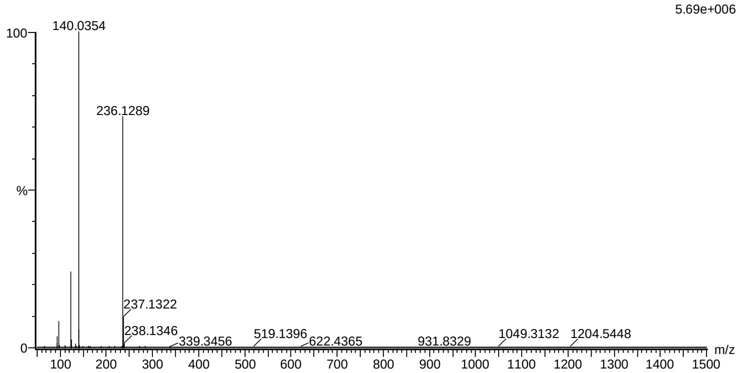

Minimum:				-10.0				
Maximum:		5.0	2.0	50.0				
Mass	Calc. Mass	mDa	PPM	DBE	i-FIT	Norm	Conf(%)	Formula
236.1289	236.1287	0.2	0.8	5.5	3557.7	0.000	100.00	C13 H18 N O3
	236.1289	0.0	0.0	-4.5	3589.6	31.908	0.00	C6 H26 N3 S3

Figure 7: MS specter of compound **2**

.1.2 Spectroscopic data for Compound (*R*)-3

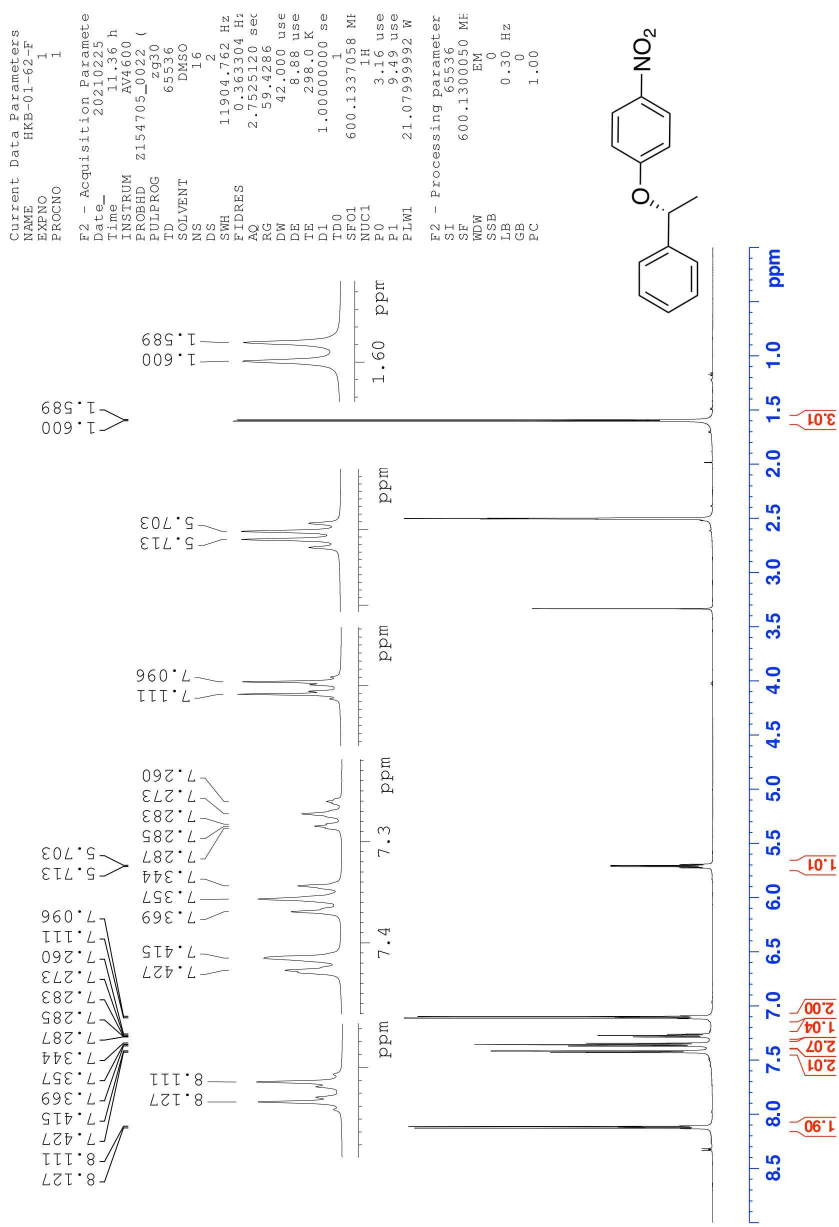

Figure 8: ^{1}H-NMR specter of compound **(*R*)-3**

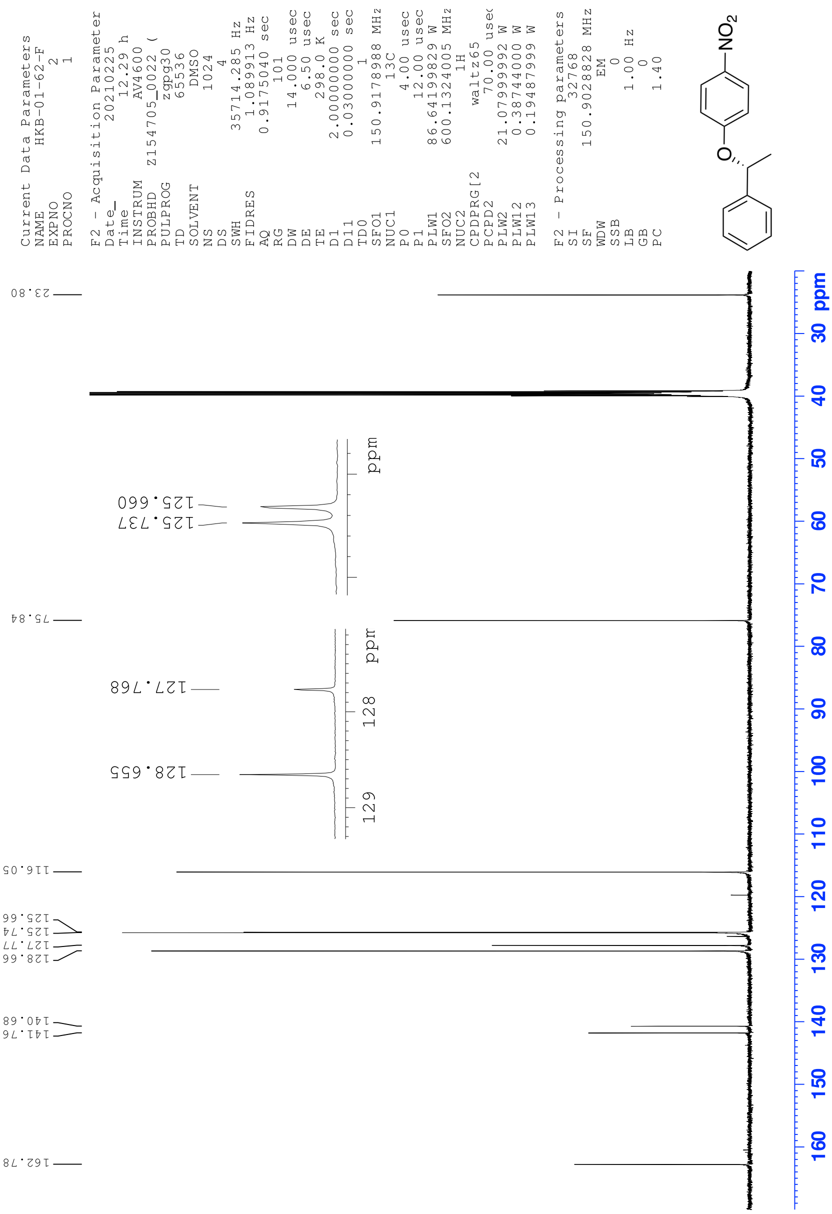

Figure 9: ^{13}C-NMR specter of compound ***(R)*-3**

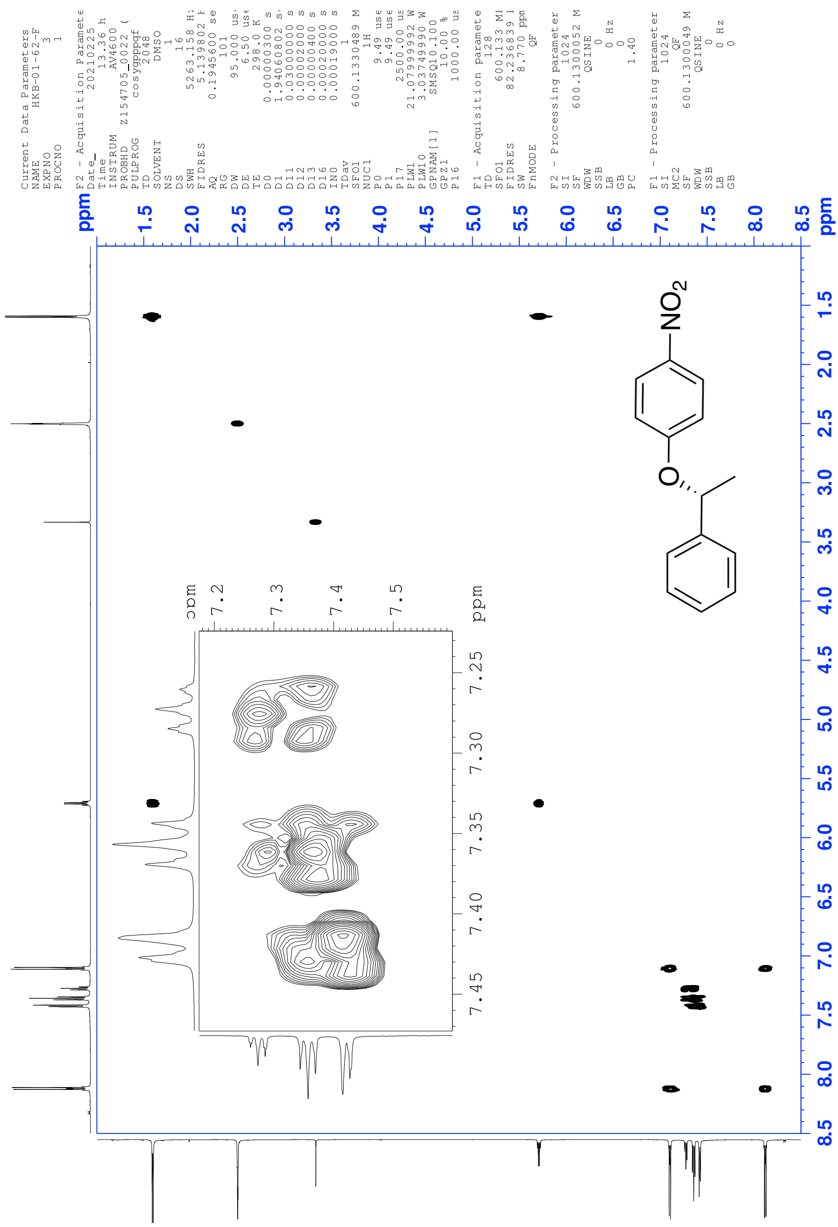

Figure 10: COSY specter of compound ***(R)*-3**

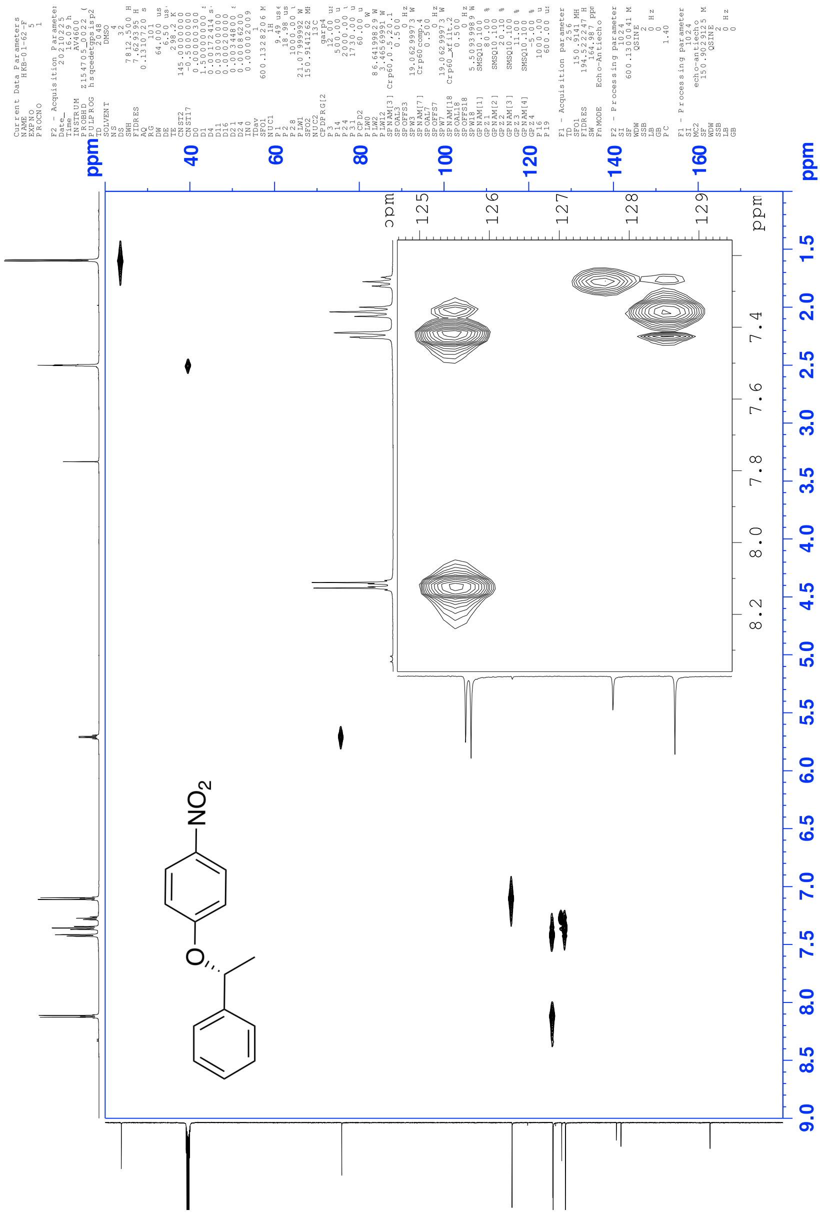

Figure 11: HSQC specter of compound **(*R*)-3**

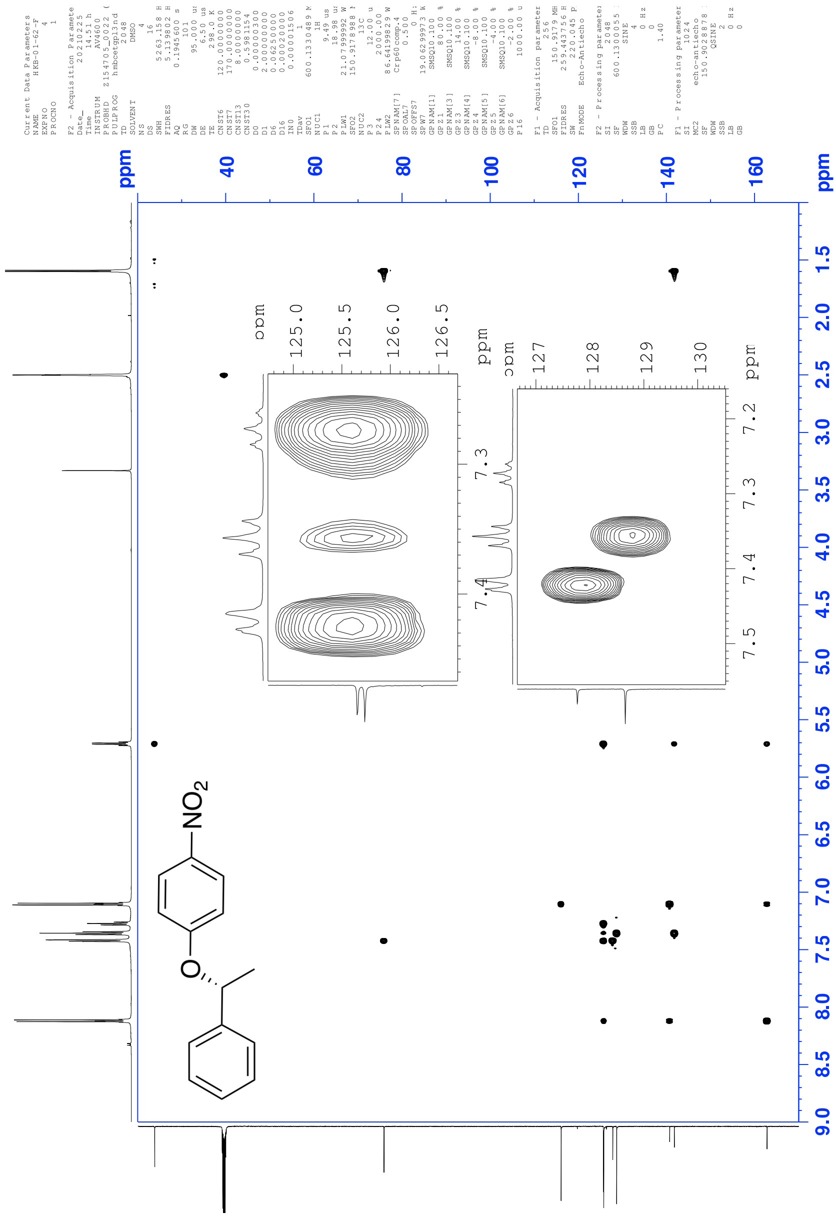

Figure 12: HMBC specter of compound **(*R*)-3**

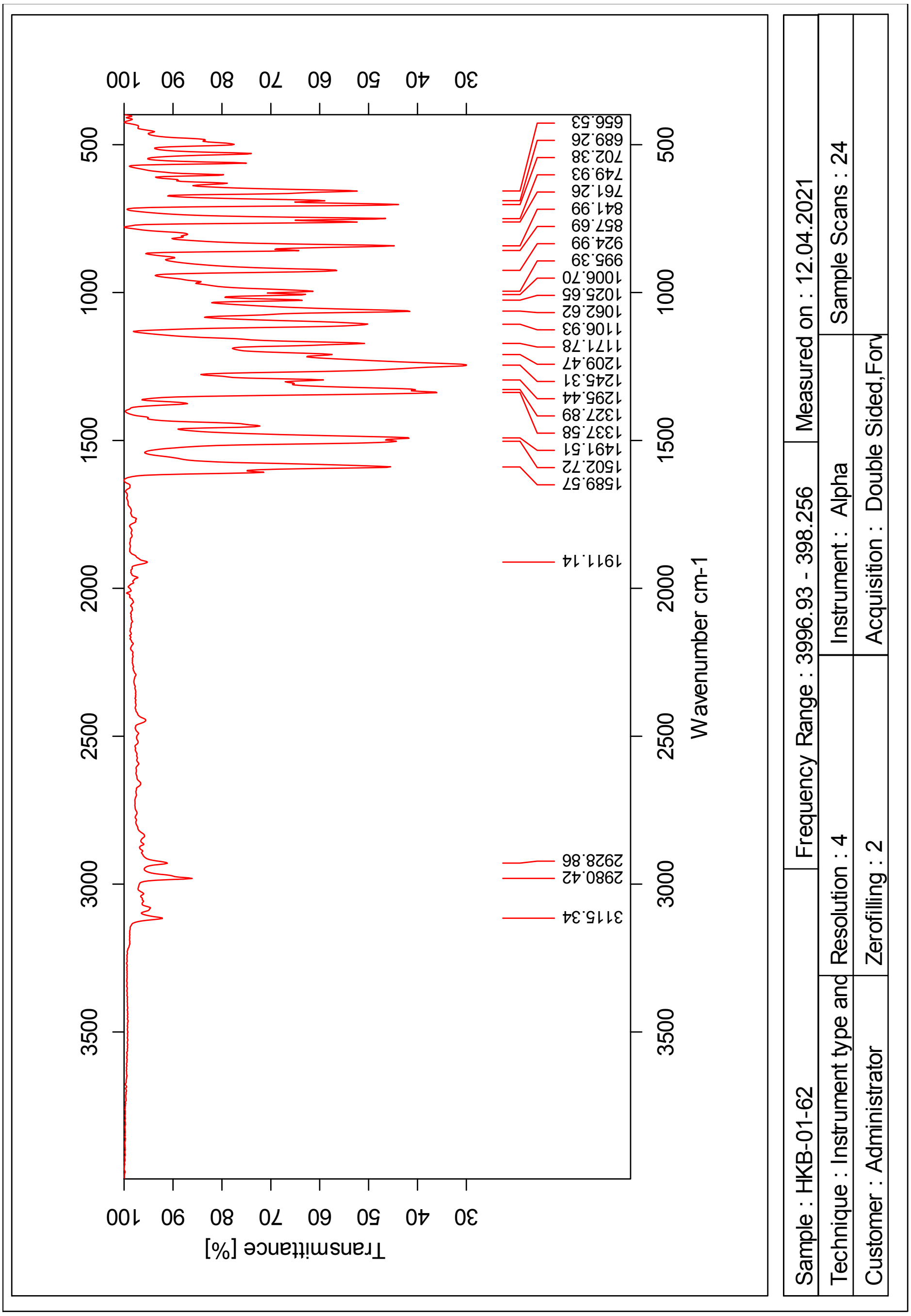

Figure 13: IR-spectrum of compound **(*R*)-3**

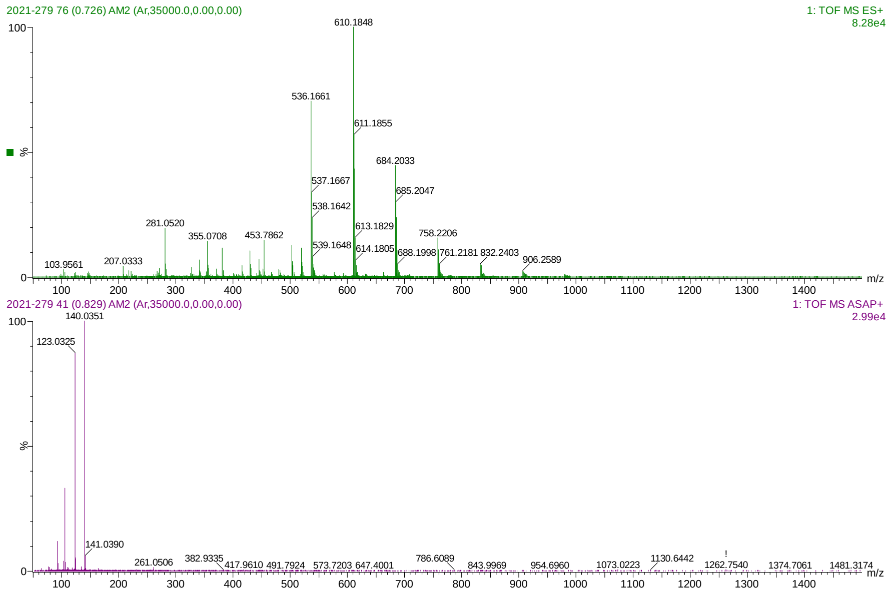

Figure 14: MS specter of compound **(*R*)-3**

.1.3 Spectroscopic data for Compound (*S*)-3

Figure 15: ^{1}H-NMR specter of compound **(*S*)-3**

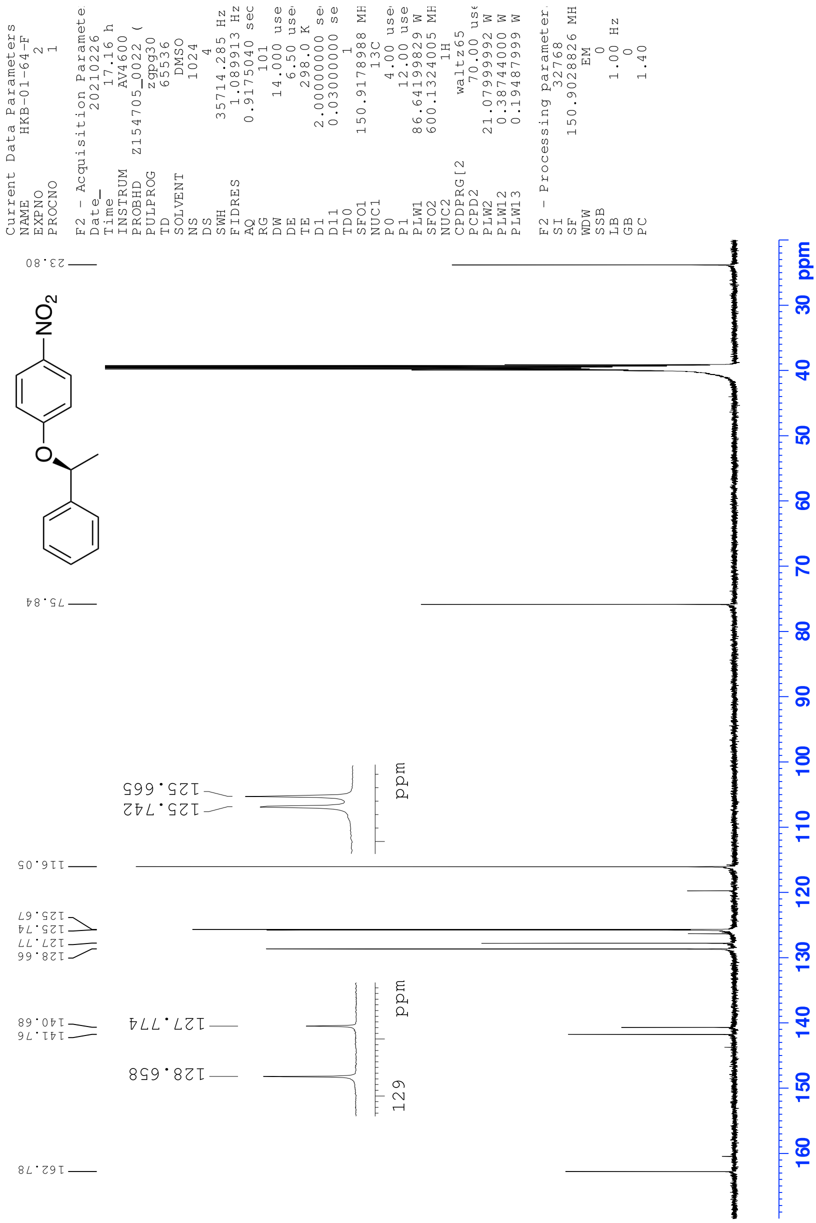

Figure 16: ^{13}C-NMR specter of compound **(*S*)-3**

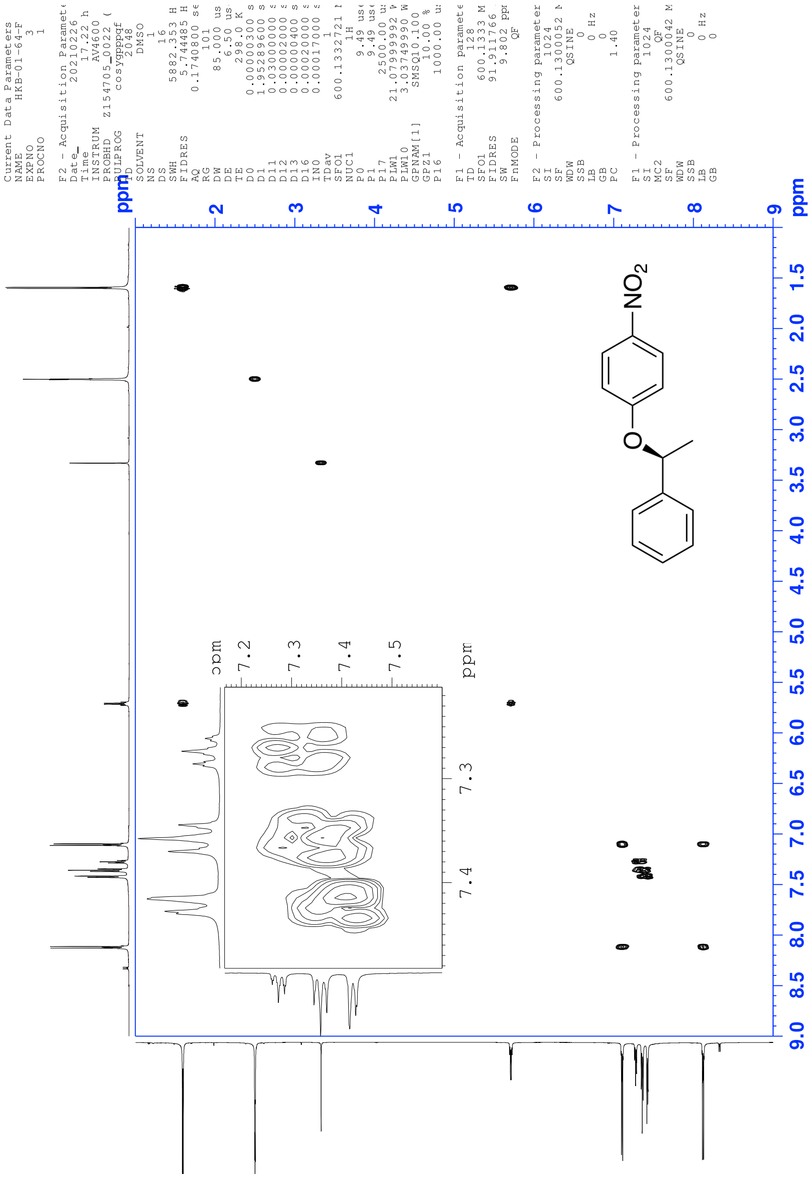

Figure 17: COSY specter of compound **(*S*)-3**

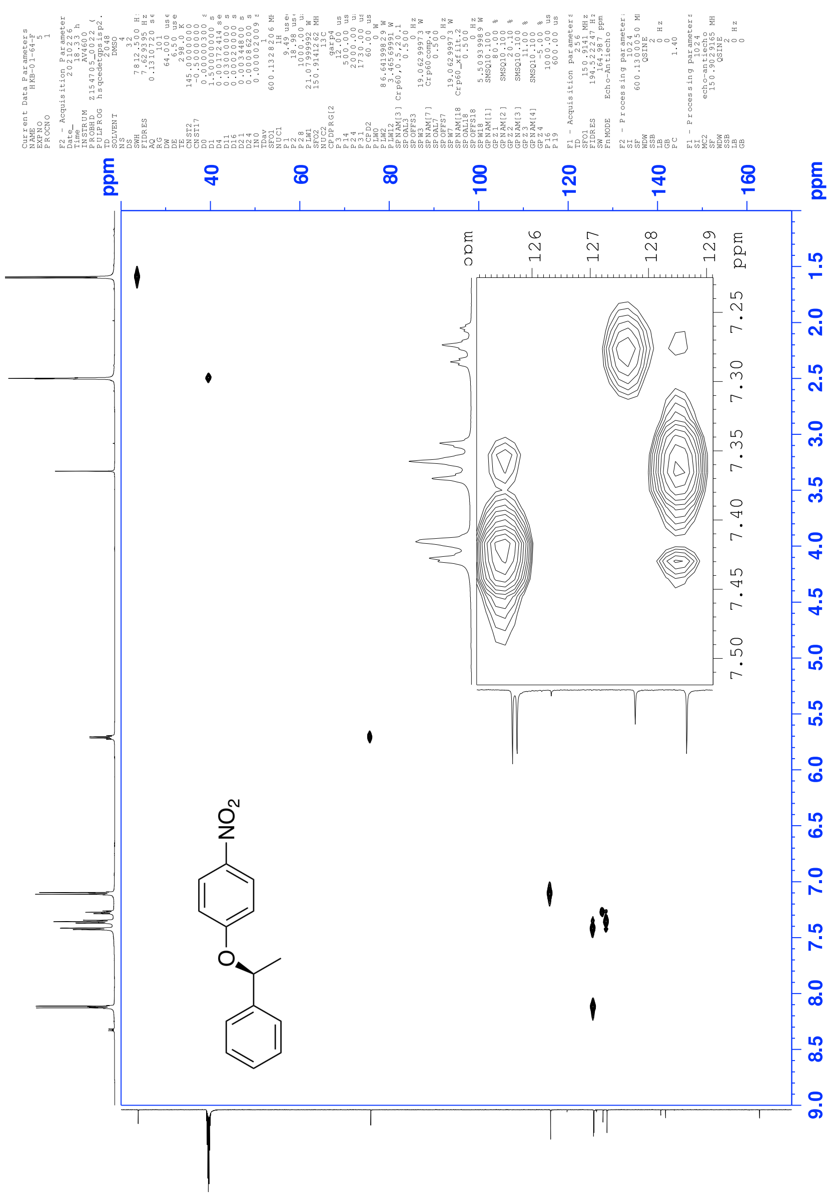

Figure 18: HSQC specter of compound ***(S)*-3**

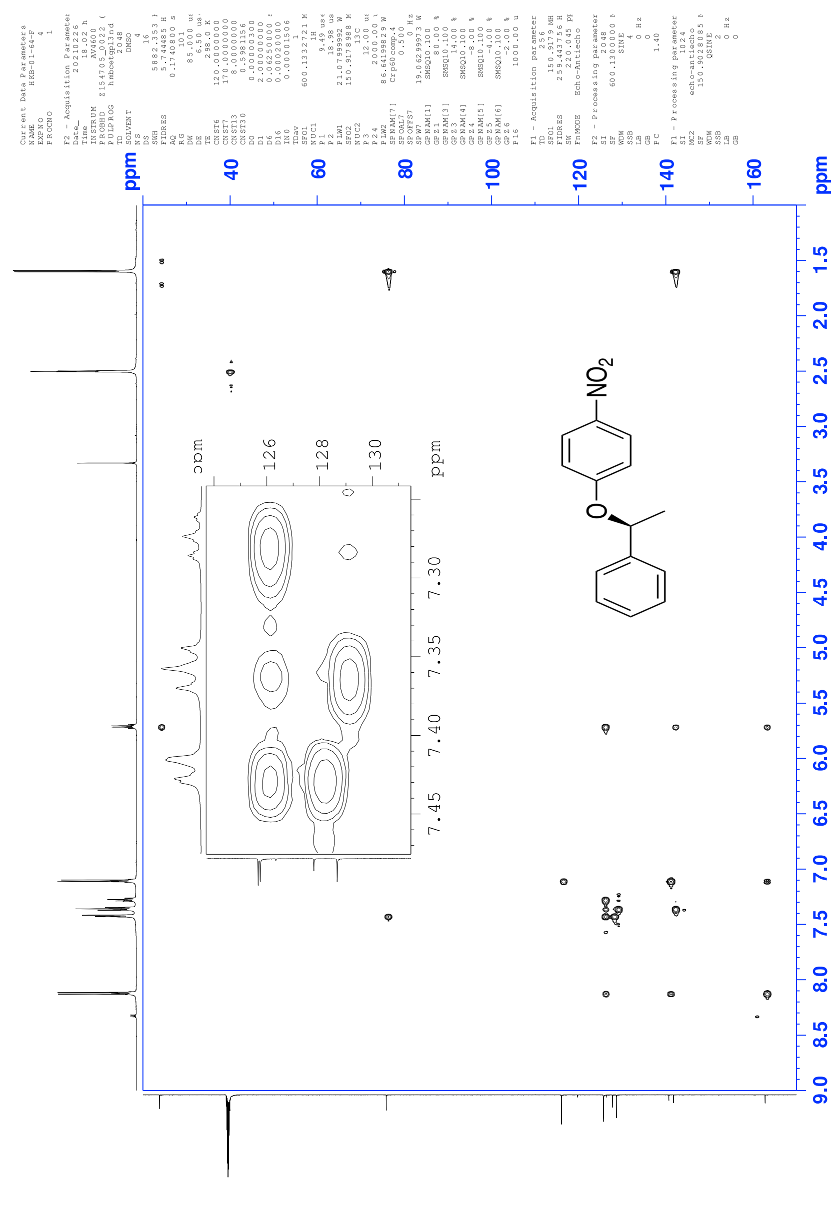

Figure 19: HMBC specter of compound **(*S*)-3**

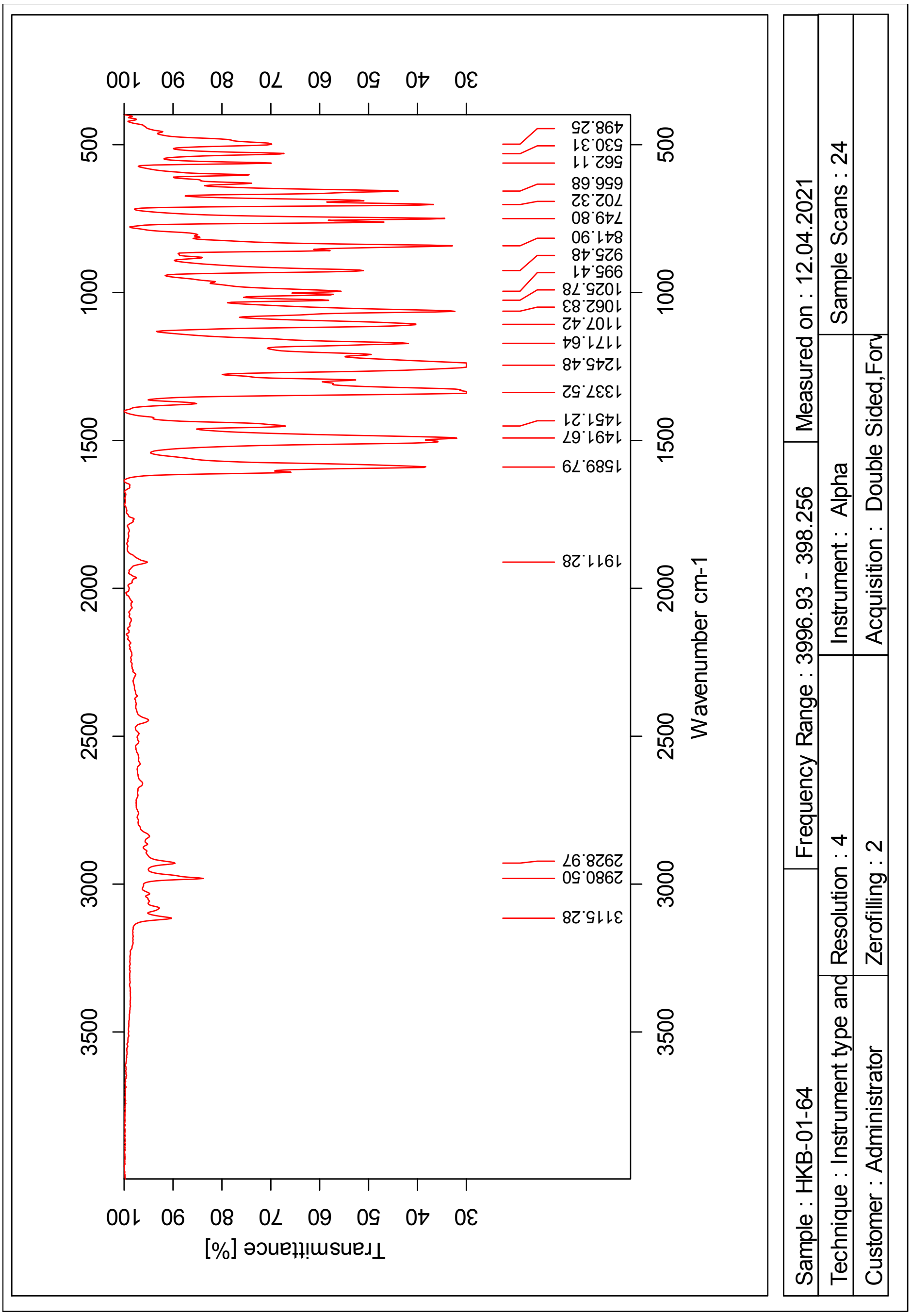

Figure 20: IR-spectrum of compound **(*S*)-3**

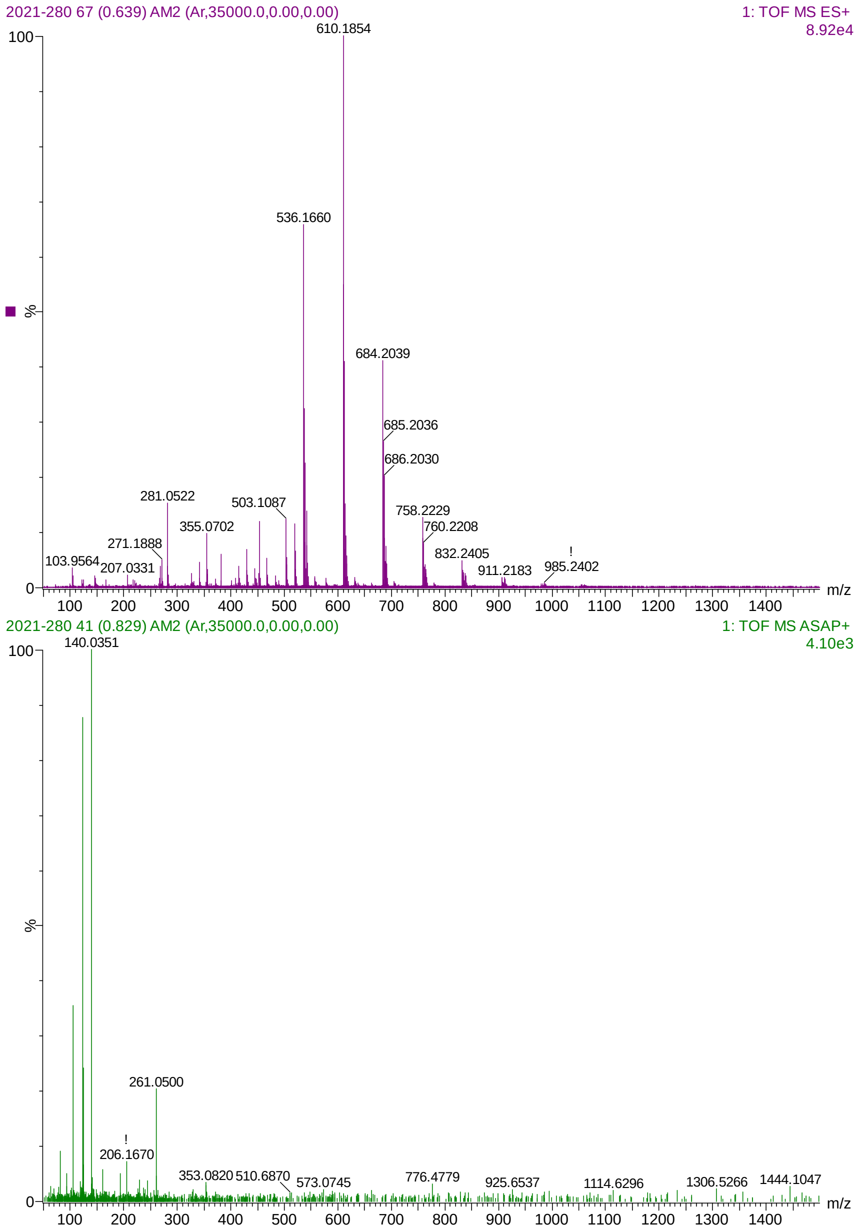

Figure 21: MS specter of compound **(*S*)-3**

.1.4 Spectroscopic data for Compound (*rac*)-4

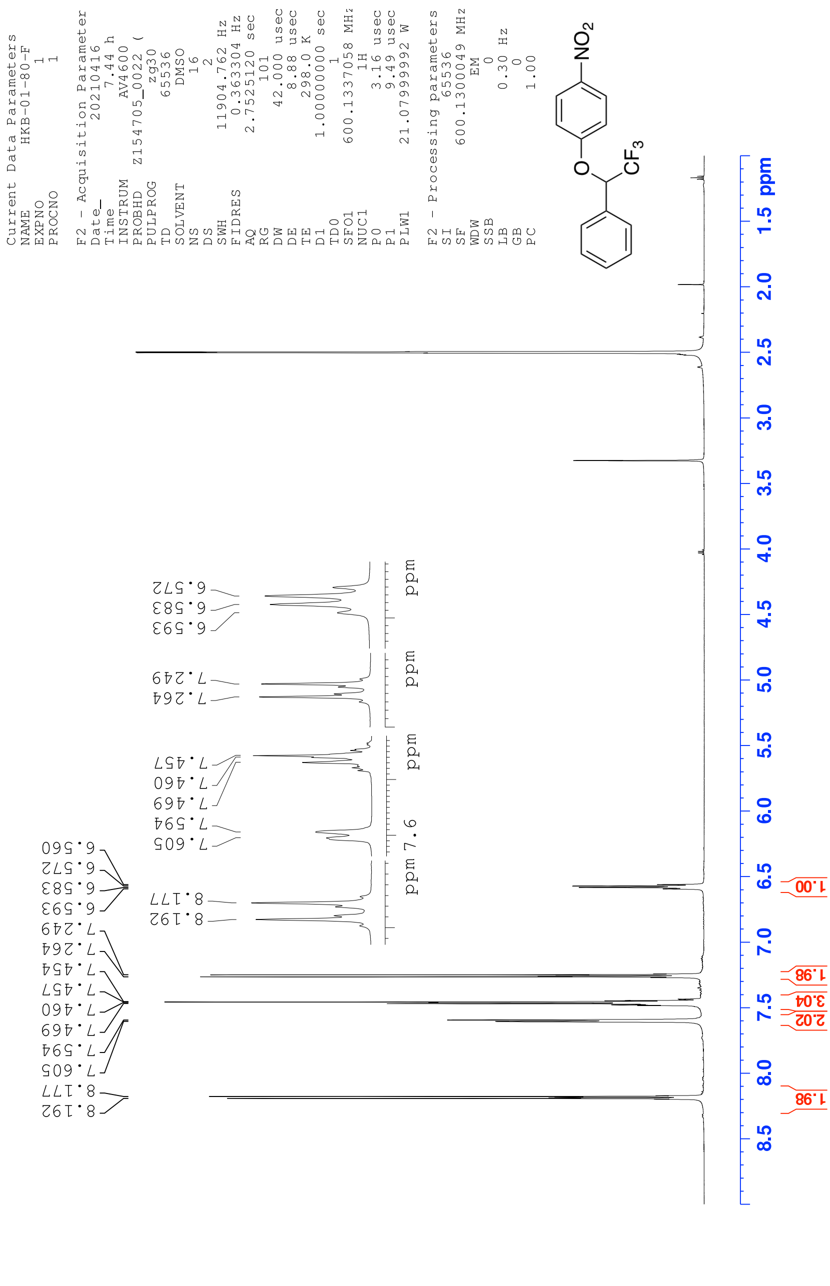

Figure 22: ^{1}H-NMR specter of compound **(*rac*)-4**

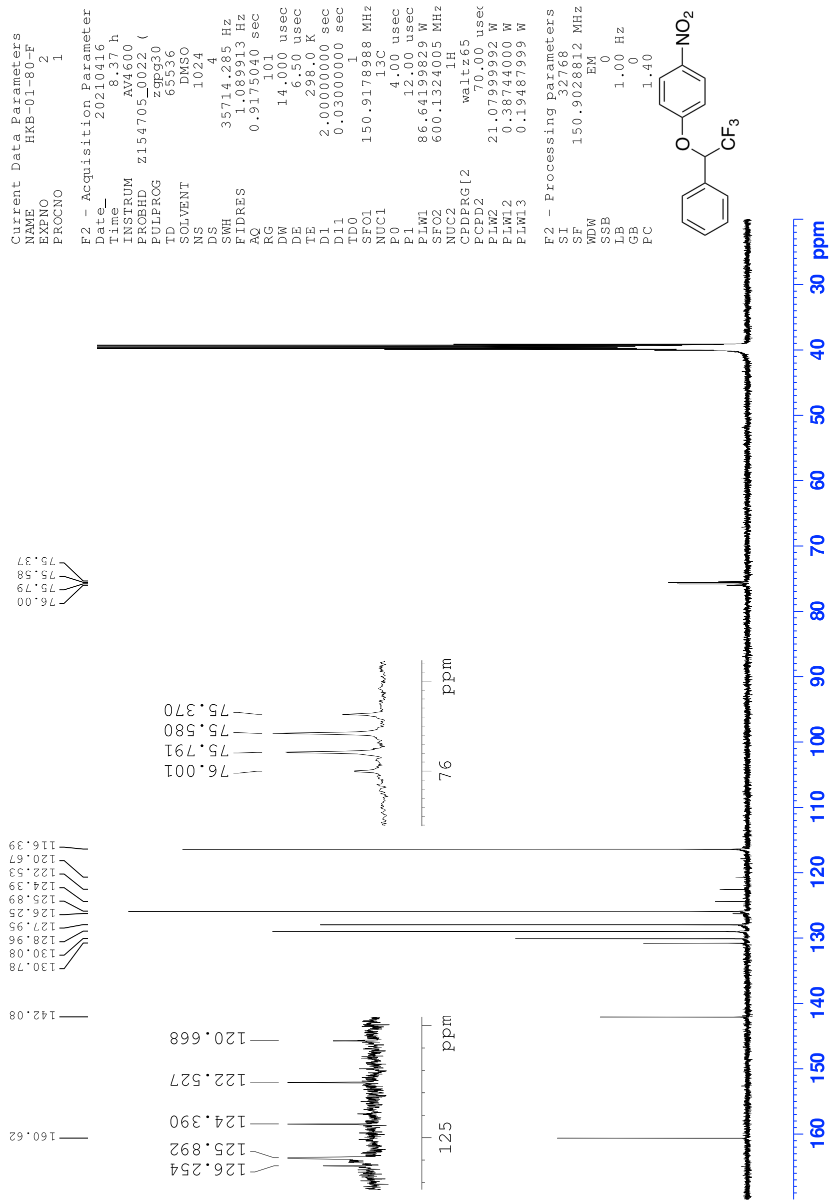

Figure 23: ^{13}C-NMR specter of compound ***(rac)*-4**

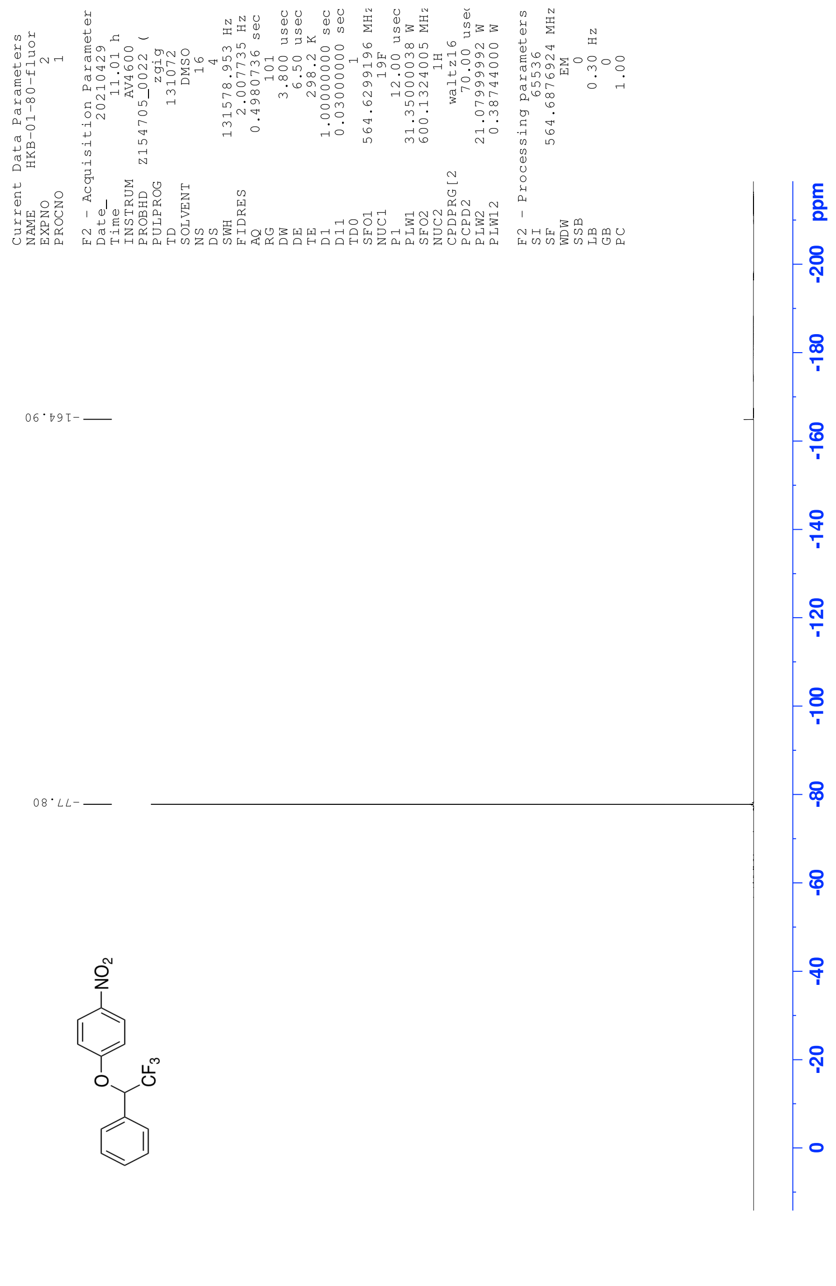

Figure 24: ^{19}F-NMR specter of compound ***(rac)*-4**

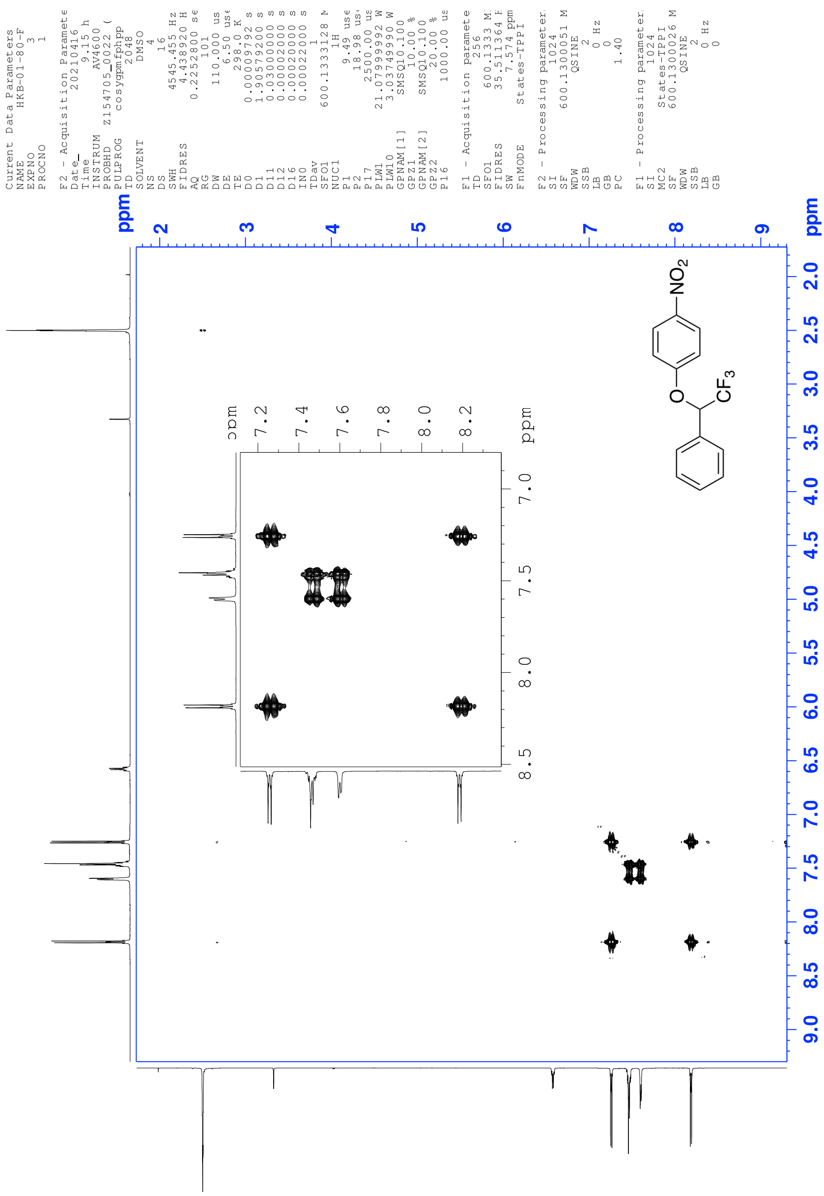

Figure 25: COSY specter of compound ***(rac)*-4**

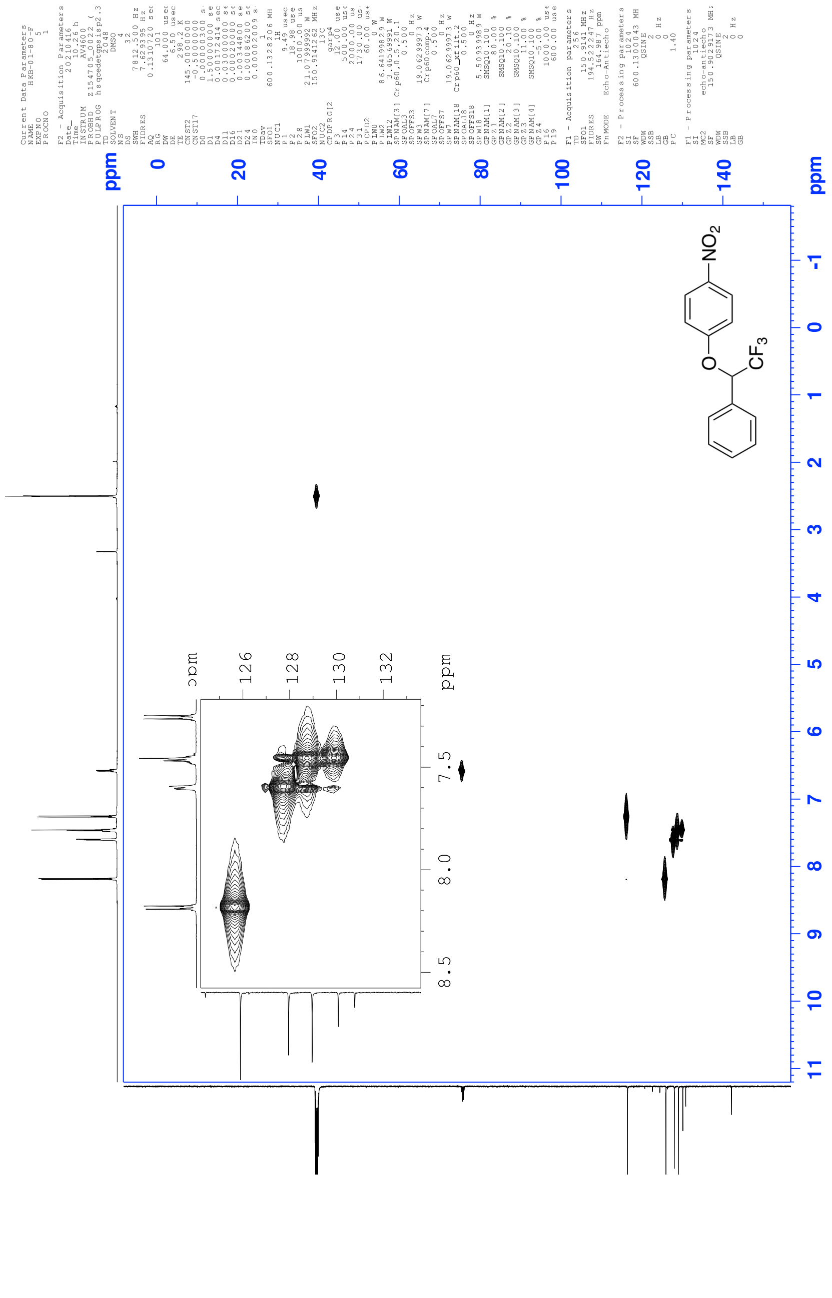

Figure 26: HSQC specter of compound ***(rac)*-4**

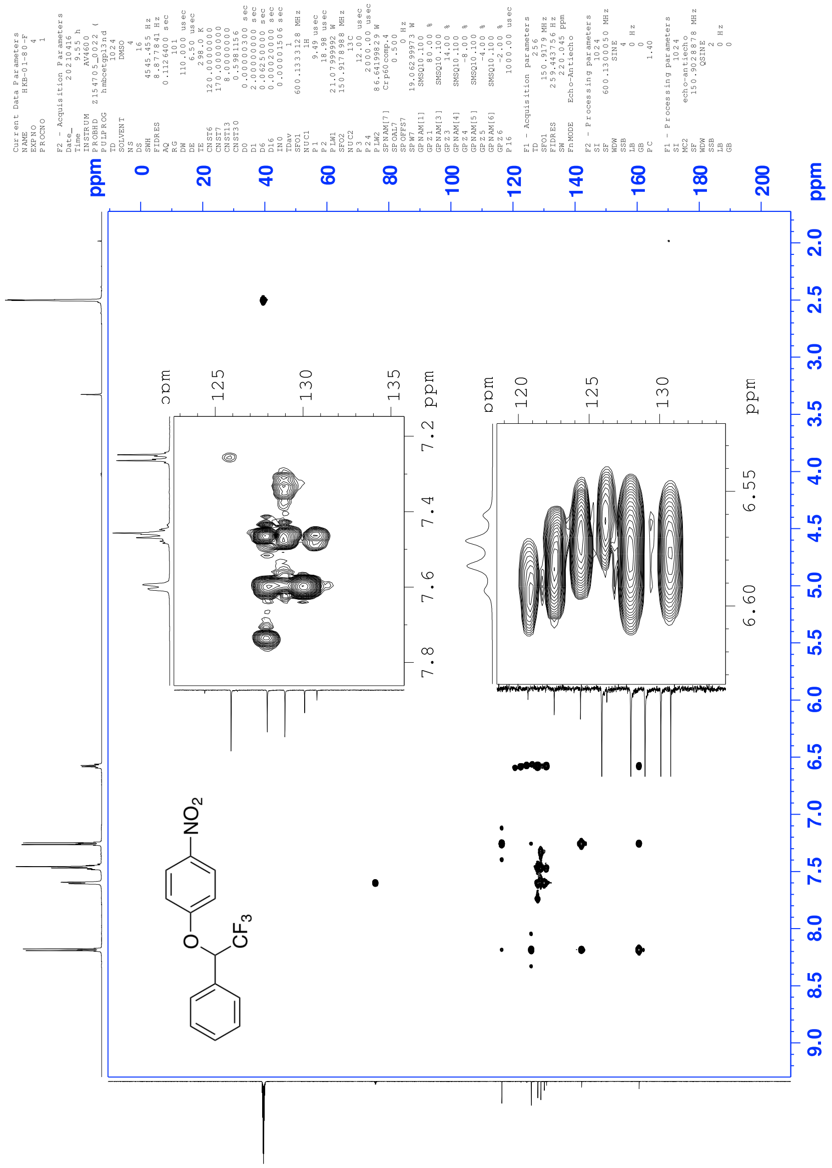

Figure 27: HMBC specter of compound ***(rac)*-4**

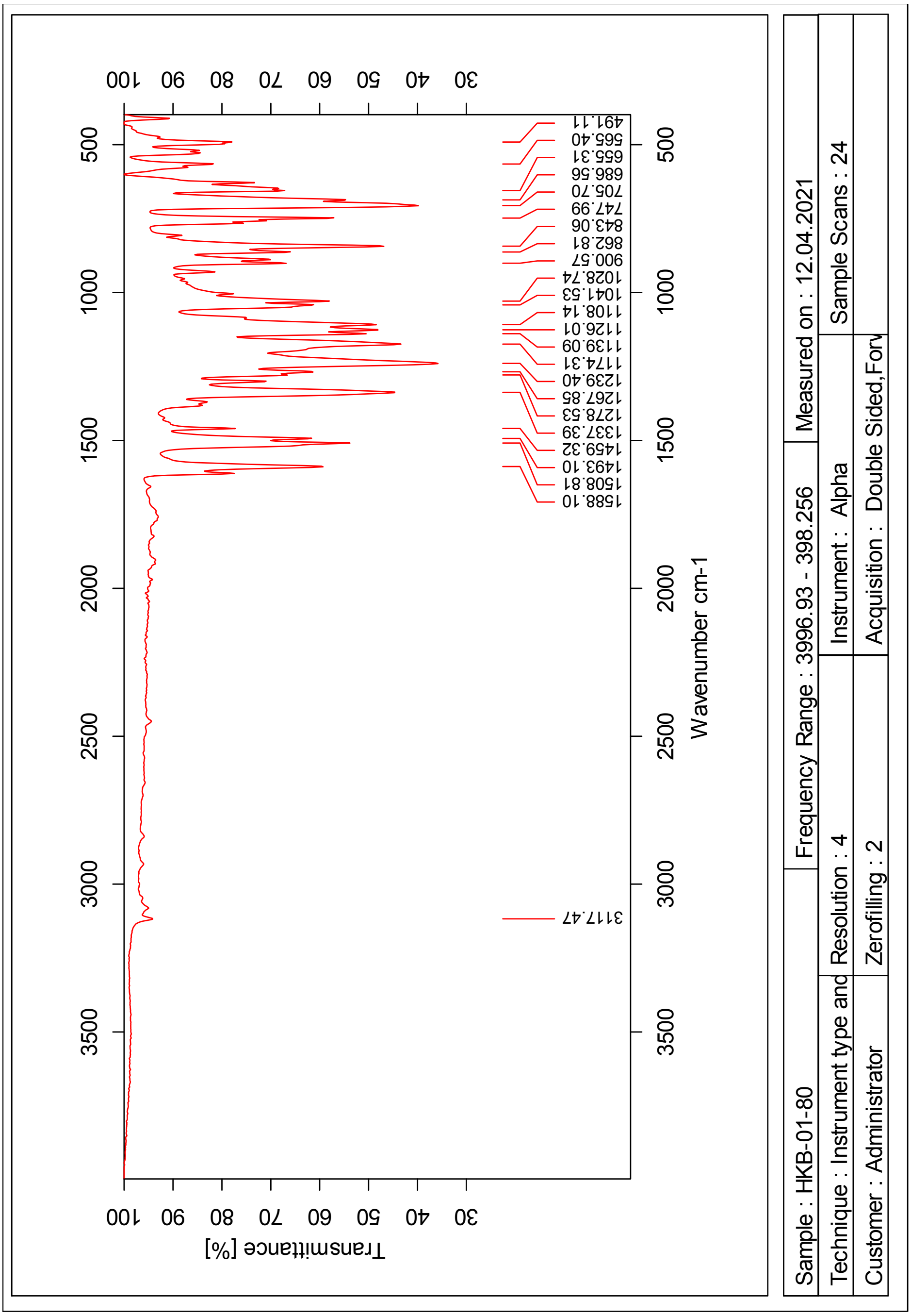

Figure 28: IR-spectrum of compound **(*rac*)-4**

Elemental Composition Report **Page 1**

Single Mass Analysis
Tolerance = 5.0 PPM / DBE: min = -10.0, max = 50.0
Element prediction: Off
Number of isotope peaks used for i-FIT = 6

Monoisotopic Mass, Even Electron Ions
3891 formula(e) evaluated with 14 results within limits (all results (up to 1000) for each mass)
Elements Used:
C: 0-100 H: 0-100 N: 0-6 O: 0-6 F: 0-3 S: 0-1 Br: 0-1 I: 0-2

2021-210 82 (1.621) AM2 (Ar,35000.0,0.00,0.00); Cm (78:82)
1: TOF MS ASAP+

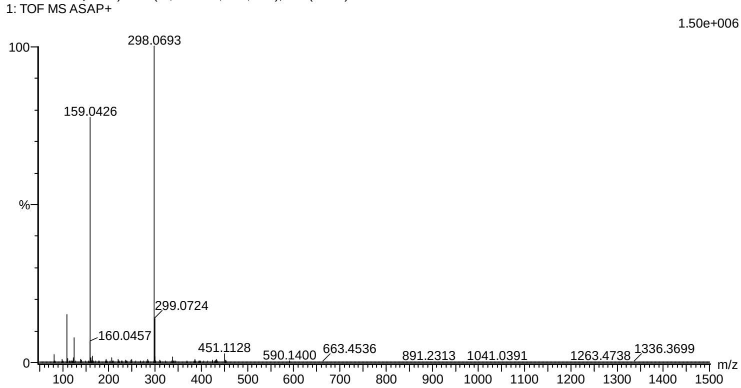

Minimum:				-10.0				
Maximum:		5.0	5.0	50.0				
Mass	Calc. Mass	mDa	PPM	DBE	i-FIT	Norm	Conf(%)	Formula
298.0693	298.0691	0.2	0.7	8.5	2525.2	0.006	99.36	C14 H11 N O3 F3
	298.0691	0.2	0.7	-7.5	2535.7	10.522	0.00	C4 H23 N O3 F2 I
	298.0690	0.3	1.0	15.5	2544.1	18.952	0.00	C20 H12 N S
	298.0690	0.3	1.0	-2.5	2551.3	26.080	0.00	C5 H19 N5 O2 F2 Br
	298.0688	0.5	1.7	-4.5	2552.9	27.688	0.00	C7 H25 N O4 S Br
	298.0699	-0.6	-2.0	-8.5	2552.9	27.681	0.00	C4 H26 N O5 F S Br
	298.0701	-0.8	-2.7	0.5	2552.5	27.361	0.00	C8 H21 N5 S Br
	298.0685	0.8	2.7	-0.5	2543.3	18.153	0.00	C6 H15 N3 O5 F3 S
	298.0702	-0.9	-3.0	11.5	2543.5	18.344	0.00	C17 H13 N O F S
	298.0702	-0.9	-3.0	-4.5	2542.6	17.405	0.00	C7 H25 N O S I
	298.0702	-0.9	-3.0	-6.5	2551.3	26.106	0.00	C2 H20 N5 O3 F3 Br
	298.0680	1.3	4.4	12.5	2530.4	5.196	0.55	C17 H10 N O2 F2
	298.0679	1.4	4.7	1.5	2551.2	26.004	0.00	C8 H18 N5 O F Br
	298.0679	1.4	4.7	-3.5	2532.2	7.061	0.09	C7 H22 N O2 F I

Figure 29: MS specter of compound **(*rac*)-4**

.1.5 Spectroscopic data for Compound (*R*)-4

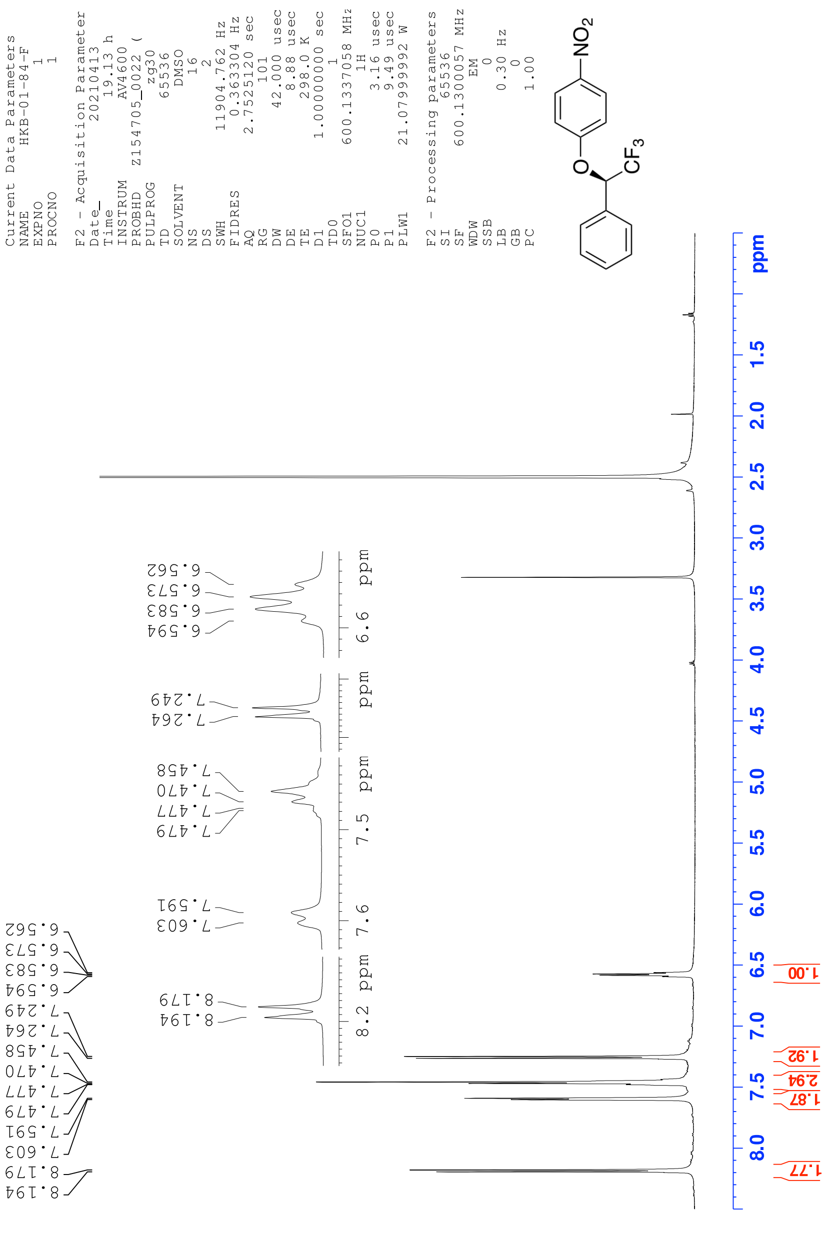

Figure 30: ^{1}H-NMR specter of compound **(*R*)-4**

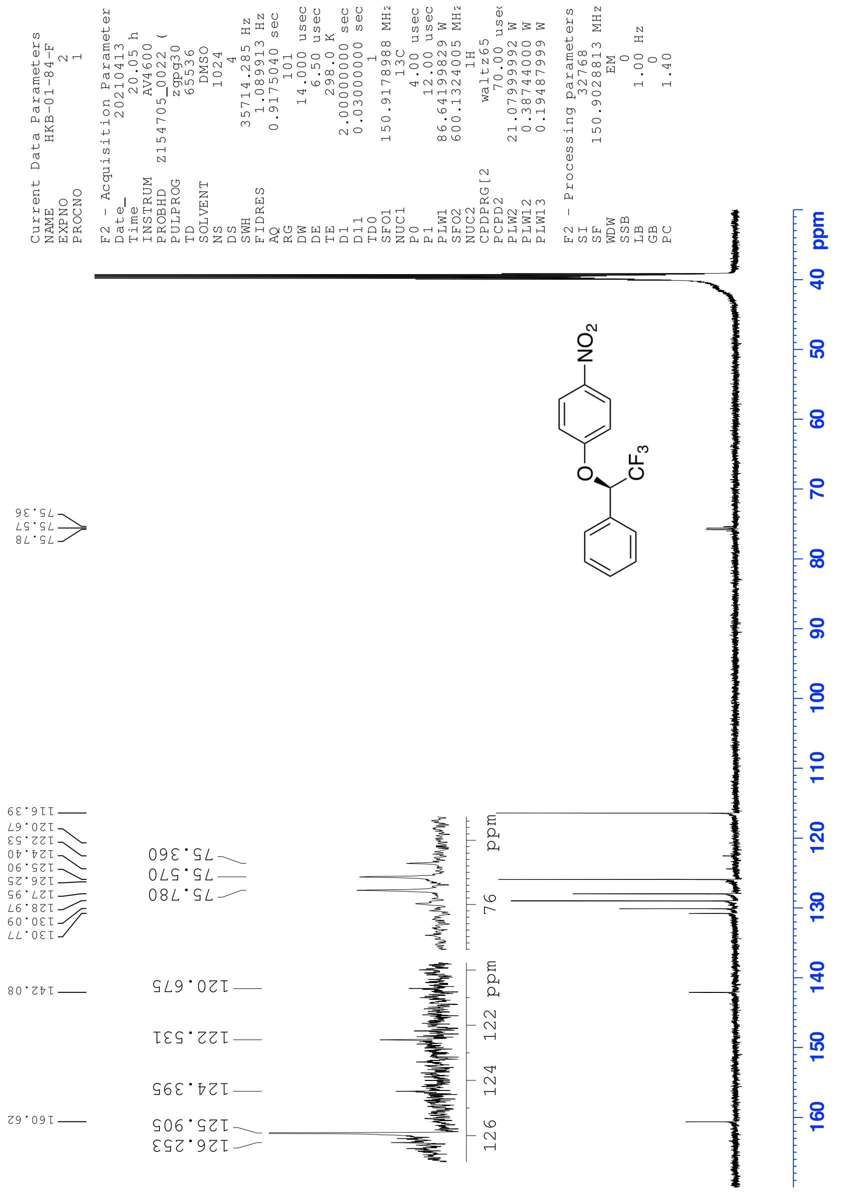

Figure 31: ^{13}C-NMR specter of compound **(*R*)-4**

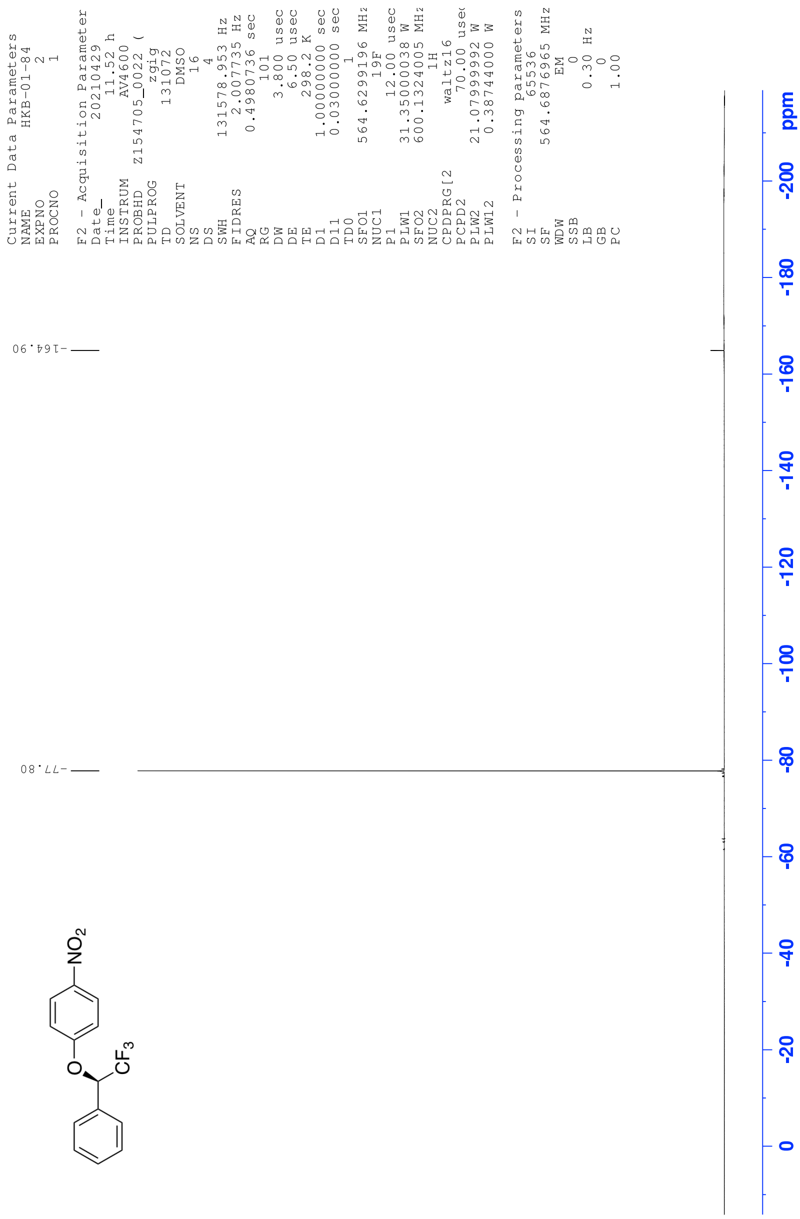

Figure 32: ^{19}F-NMR specter of compound **(*R*)-4**

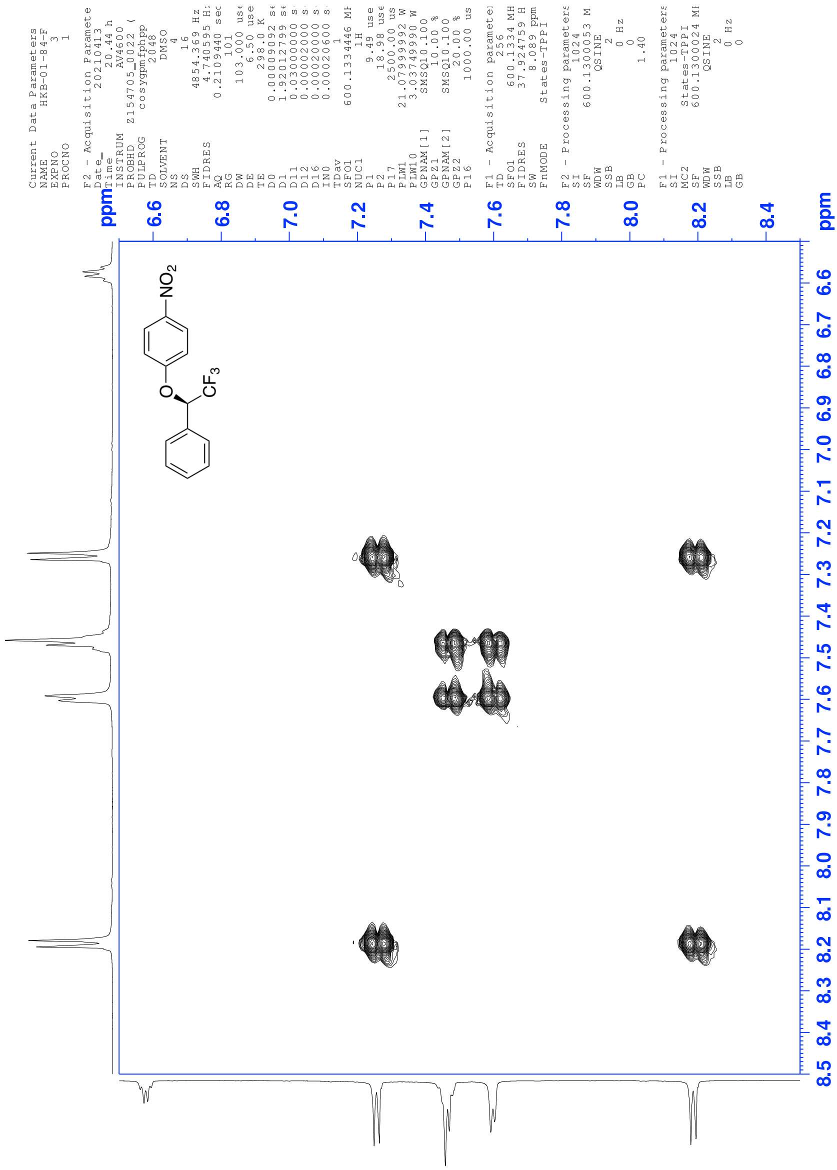

Figure 33: COSY specter of compound ***(R)*-4**

Figure 34: HSQC specter of compound ***(R)*-4**

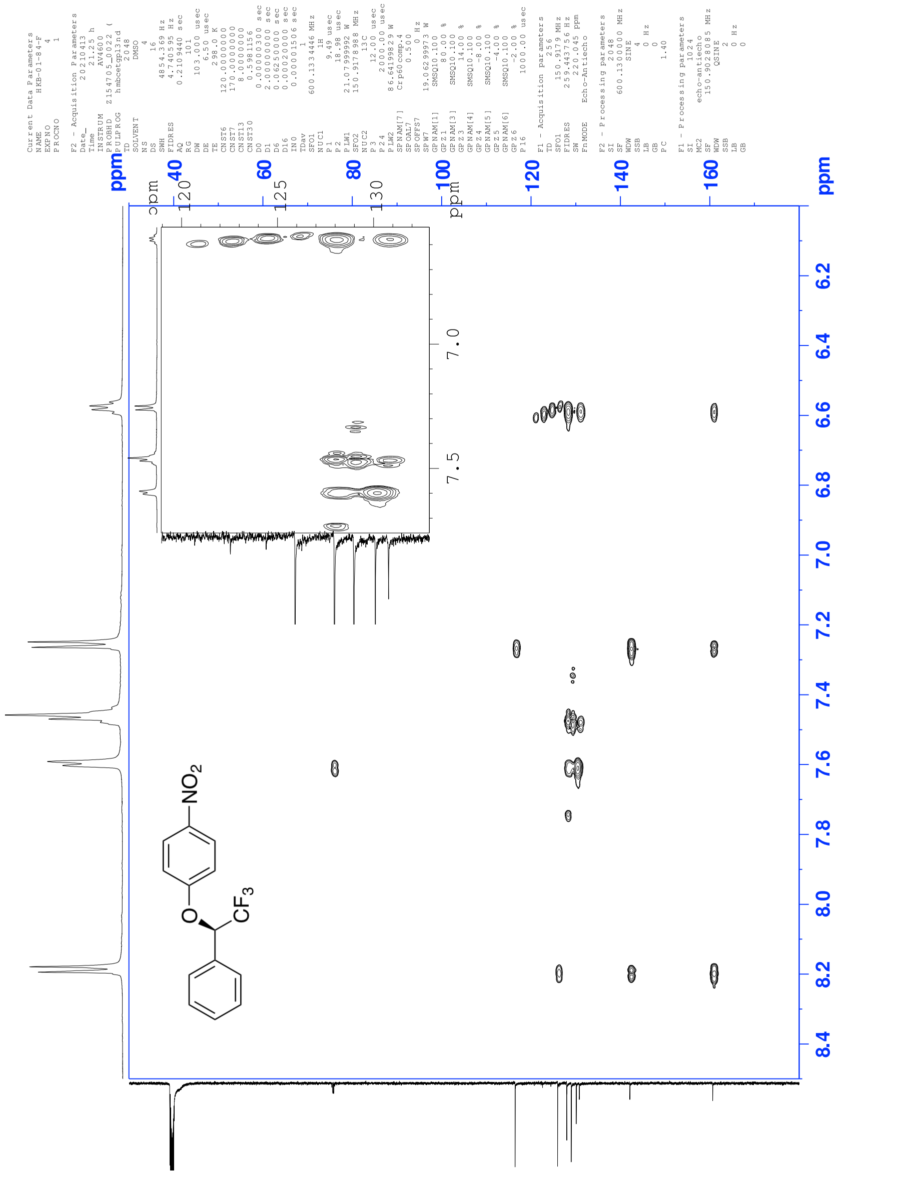

Figure 35: HMBC specter of compound ***(R)*-4**

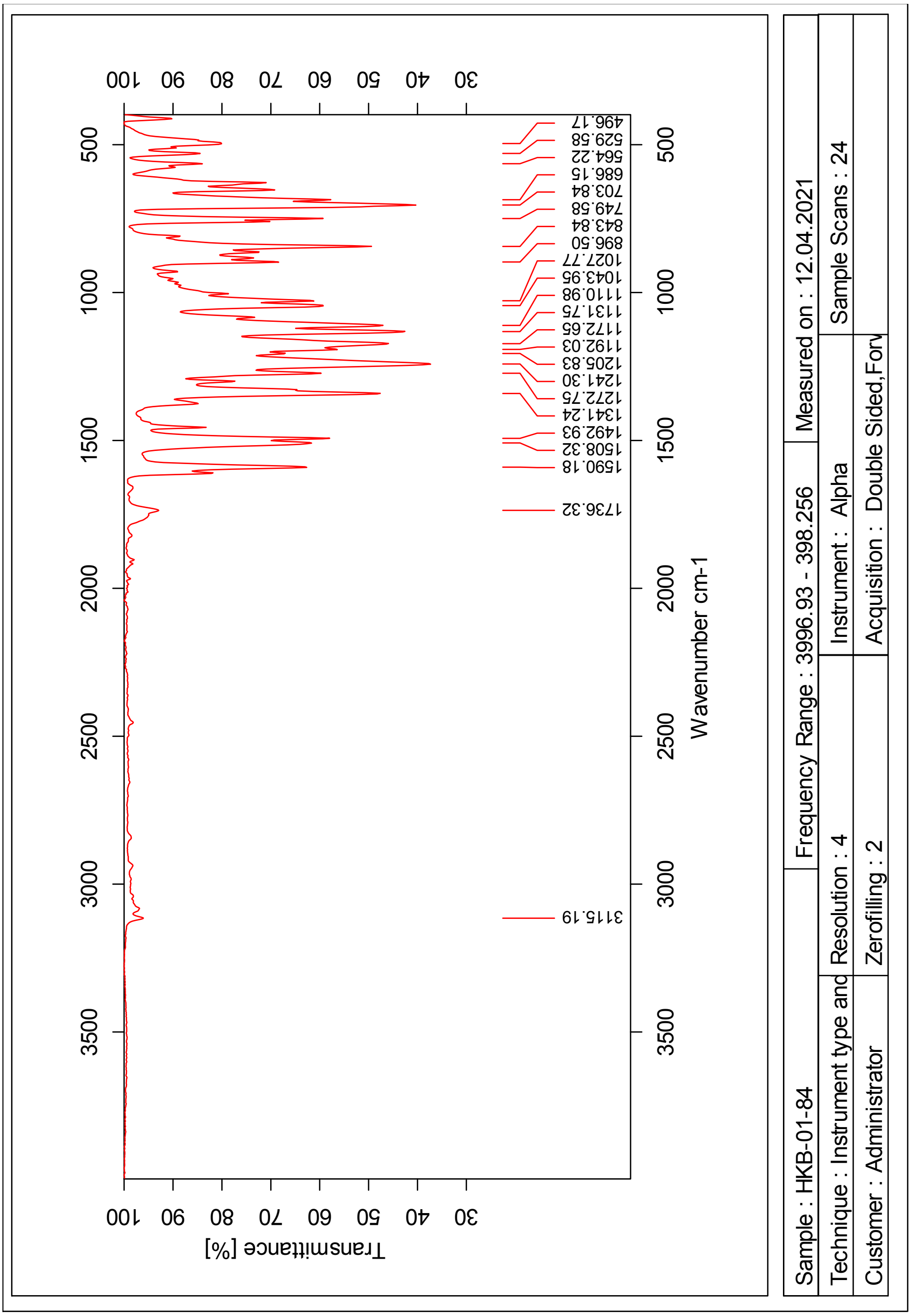

Figure 36: IR-spectrum of compound ***(R)*-4**

Elemental Composition Report **Page 1**

Single Mass Analysis
Tolerance = 5.0 PPM / DBE: min = -10.0, max = 50.0
Element prediction: Off
Number of isotope peaks used for i-FIT = 6

Monoisotopic Mass, Even Electron Ions
3891 formula(e) evaluated with 11 results within limits (all results (up to 1000) for each mass)
Elements Used:
C: 0-100 H: 0-100 N: 0-6 O: 0-6 F: 0-3 S: 0-1 Br: 0-1 I: 0-2

2021-212 64 (1.257) AM2 (Ar,35000.0,0.00,0.00); Cm (64)
1: TOF MS ASAP+

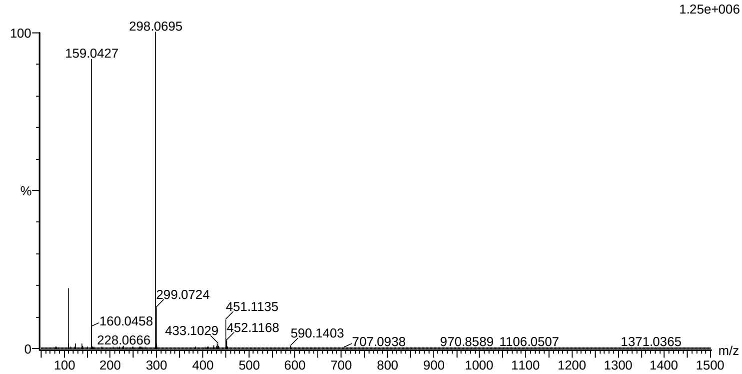

Mass	Calc. Mass	mDa	PPM	DBE	i-FIT	Norm	Conf(%)	Formula
Minimum:				-10.0				
Maximum:		5.0	5.0	50.0				
298.0695	298.0691	0.4	1.3	8.5	2304.1	0.002	99.76	C14 H11 N O3 F3
	298.0691	0.4	1.3	-7.5	2310.2	6.077	0.23	C4 H23 N O3 F2 I
	298.0702	-0.7	-2.3	-4.5	2314.1	10.013	0.00	C7 H25 N O S I
	298.0685	1.0	3.4	-0.5	2314.8	10.718	0.00	C6 H15 N3 O5 F3 S
	298.0702	-0.7	-2.3	11.5	2315.4	11.298	0.00	C17 H13 N O F S
	298.0690	0.5	1.7	15.5	2316.0	11.858	0.00	C20 H12 N S
	298.0699	-0.4	-1.3	-8.5	2322.4	18.291	0.00	C4 H26 N O5 F S Br
	298.0701	-0.6	-2.0	0.5	2322.5	18.346	0.00	C8 H21 N5 S Br
	298.0688	0.7	2.3	-4.5	2322.5	18.401	0.00	C7 H25 N O4 S Br
	298.0690	0.5	1.7	-2.5	2323.4	19.313	0.00	C5 H19 N5 O2 F2 Br
	298.0702	-0.7	-2.3	-6.5	2323.5	19.361	0.00	C2 H20 N5 O3 F3 Br

Figure 37: MS specter of compound ***(R)*-4**

.1.6 Spectroscopic data for Compound (*S*)-4

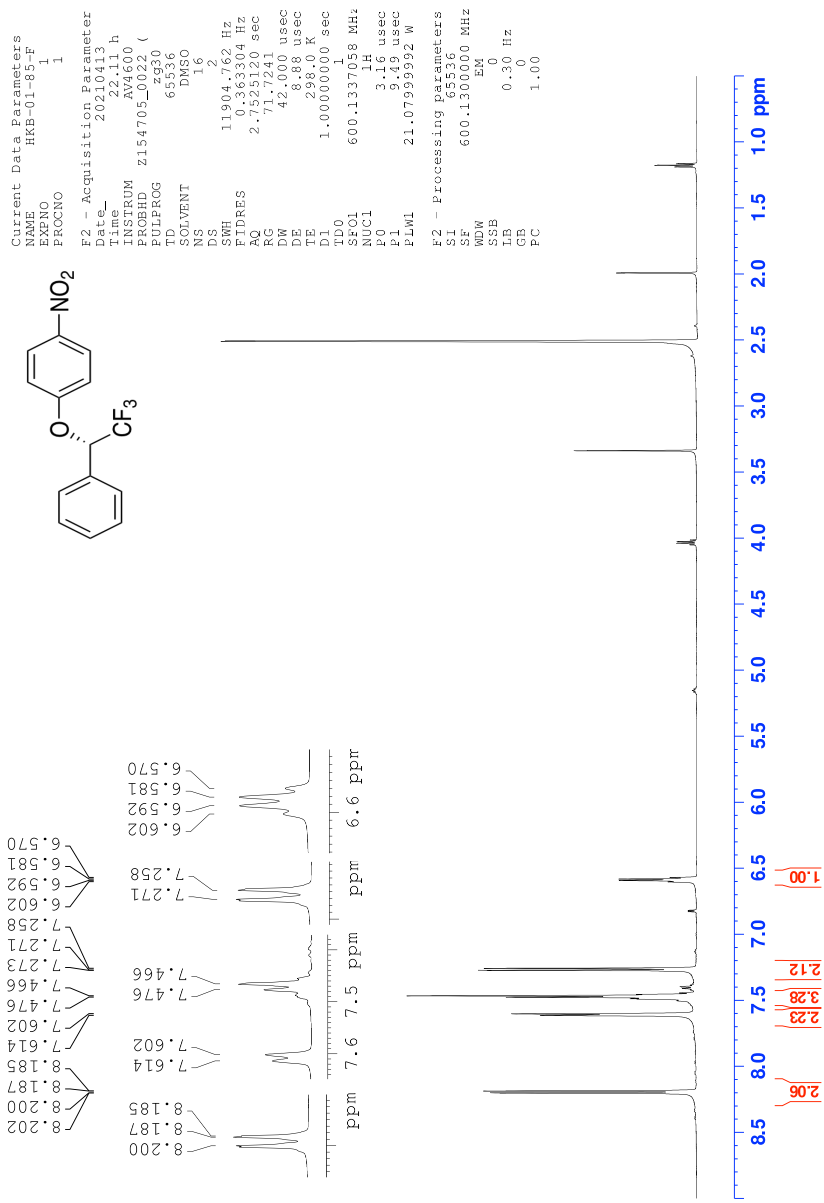

Figure 38: ^{1}H-NMR specter of compound **(*S*)-4**

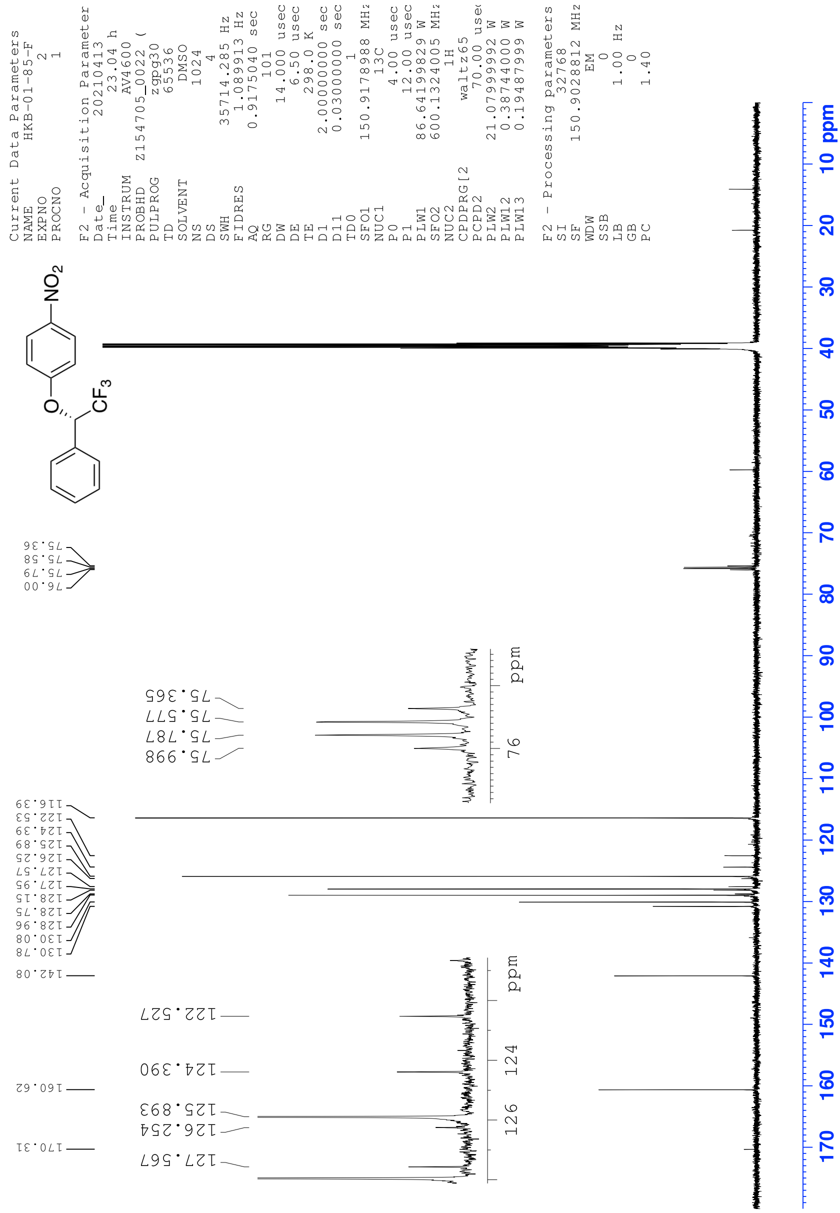

Figure 39: ^{13}C-NMR specter of compound **(*S*)-4**

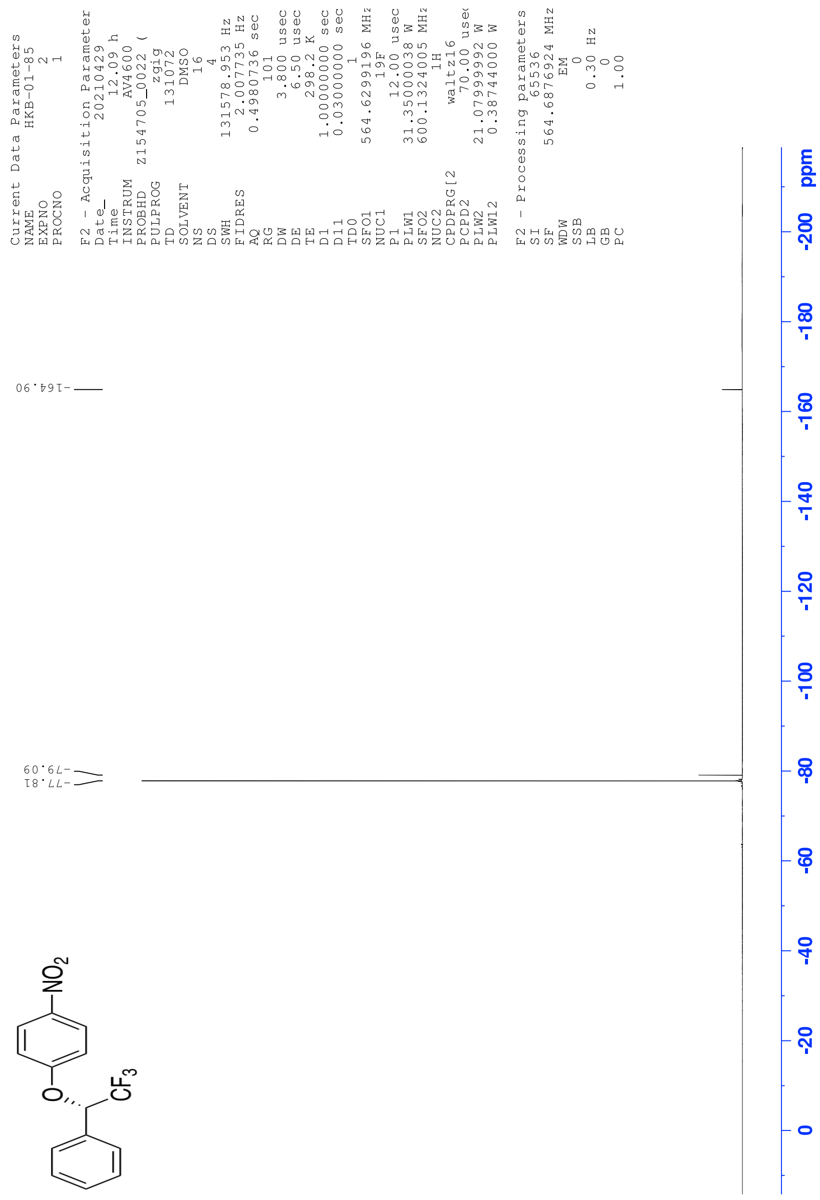

Figure 40: ^{19}F-NMR specter of compound **(*S*)-4**

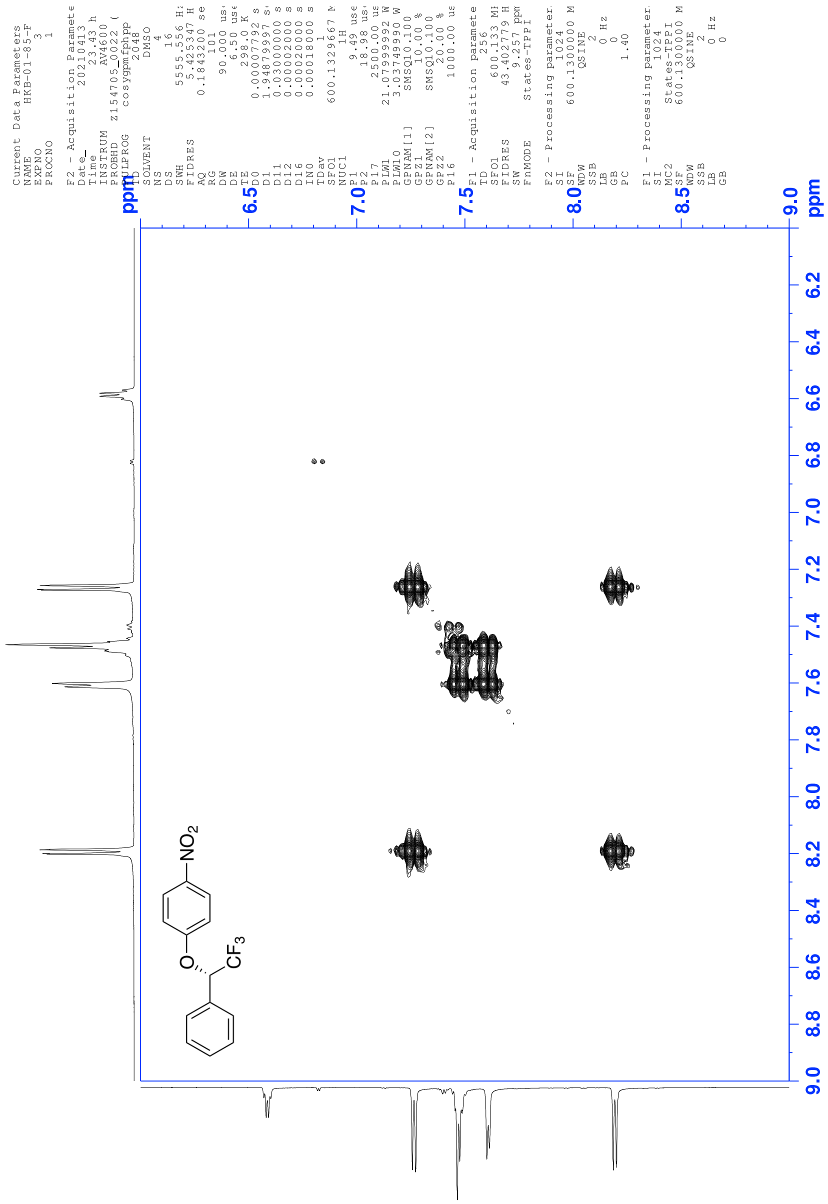

Figure 41: COSY specter of compound **(*S*)-4**

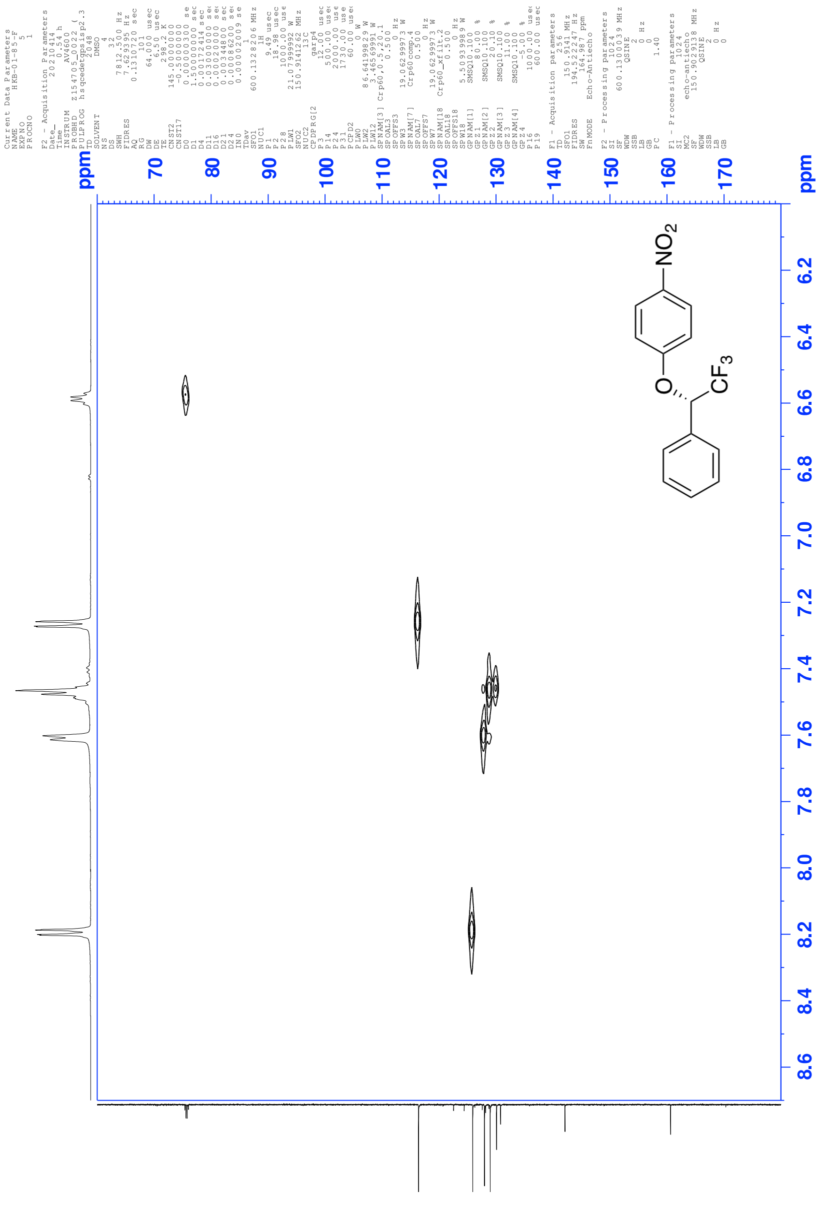

Figure 42: HSQC specter of compound **(*S*)-4**

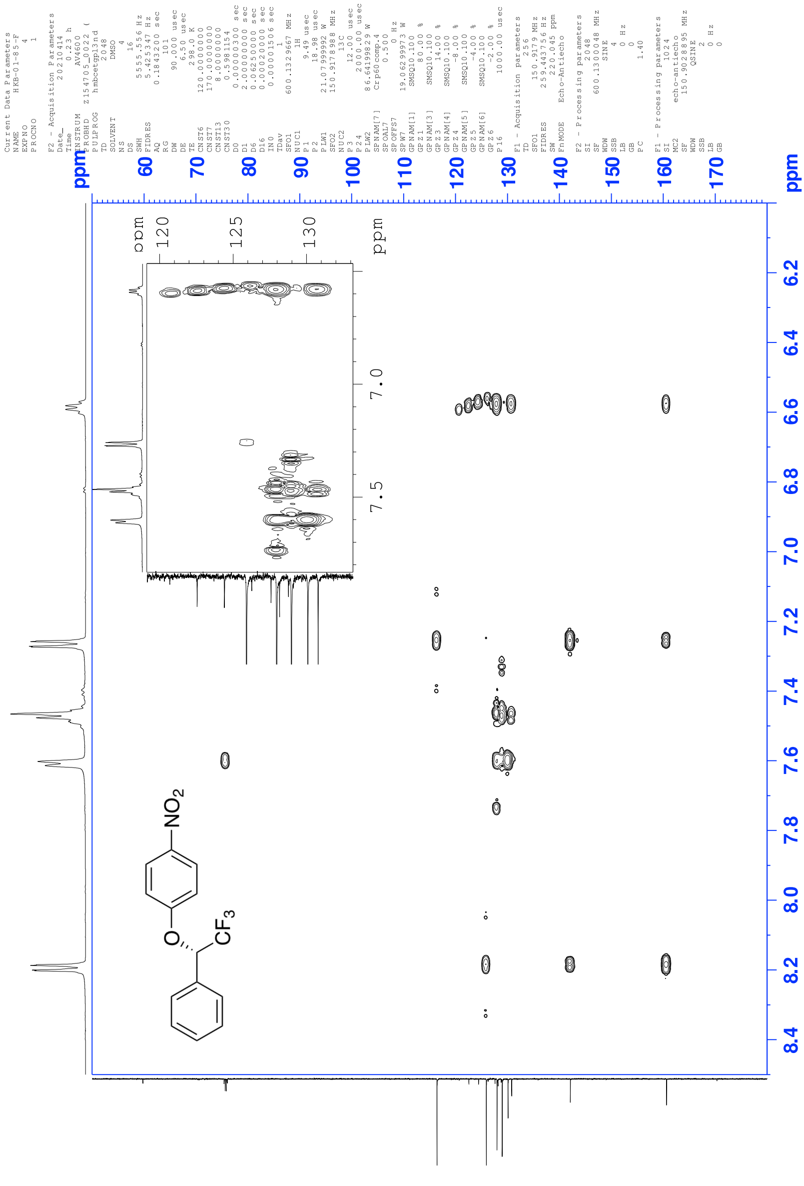

Figure 43: HMBC specter of compound **(*S*)-4**

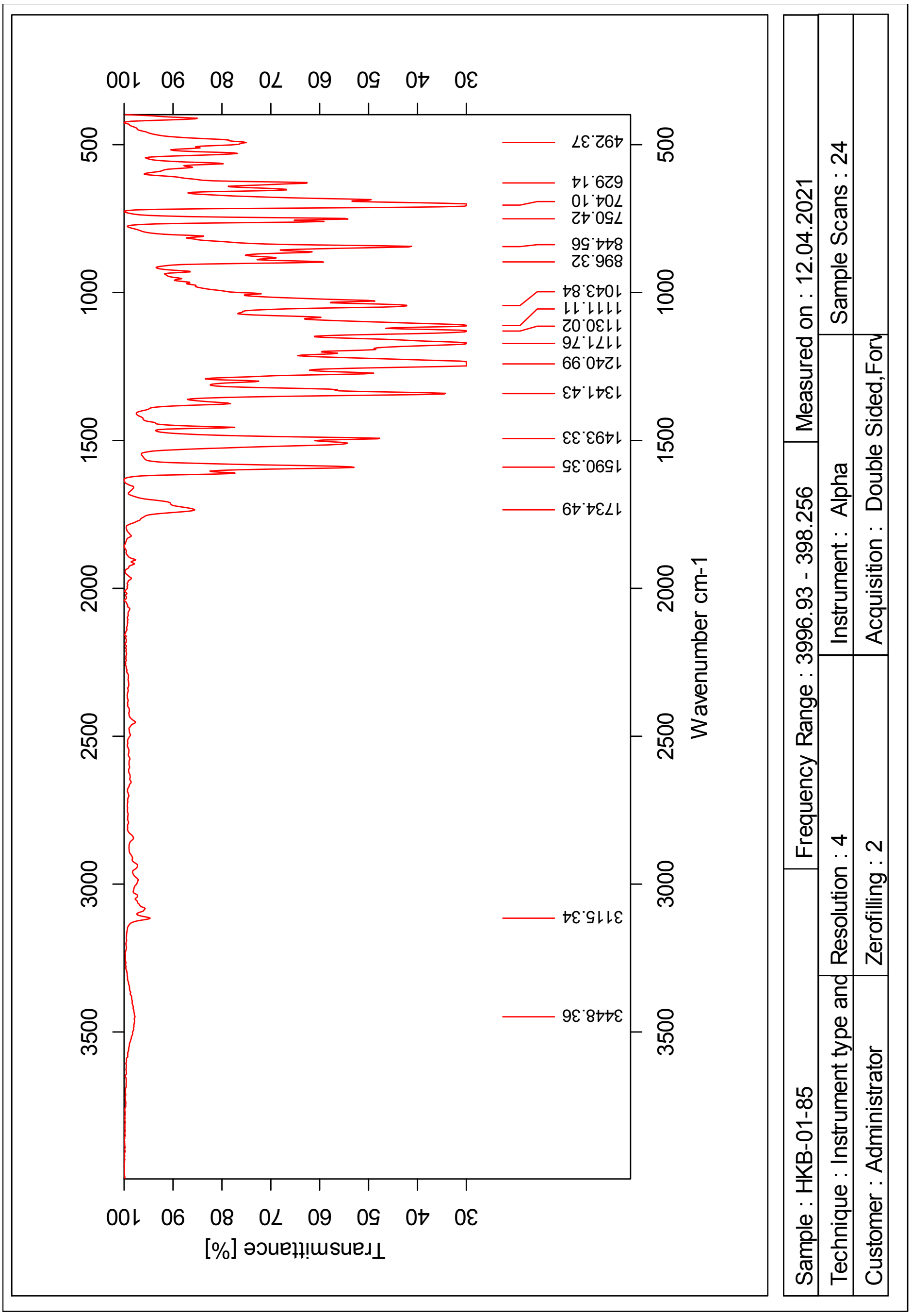

Figure 44: IR-spectrum of compound **(*S*)-4**

Elemental Composition Report

Page 1

Single Mass Analysis

Tolerance = 5.0 PPM / DBE: min = -10.0, max = 50.0
Element prediction: Off
Number of isotope peaks used for i-FIT = 6

Monoisotopic Mass, Even Electron Ions
3891 formula(e) evaluated with 14 results within limits (all results (up to 1000) for each mass)
Elements Used:
C: 0-100 H: 0-100 N: 0-6 O: 0-6 F: 0-3 S: 0-1 Br: 0-1 I: 0-2

2021-215A 83 (1.638) AM2 (Ar,35000.0,0.00,0.00); Cm (83:91)
1: TOF MS ASAP+

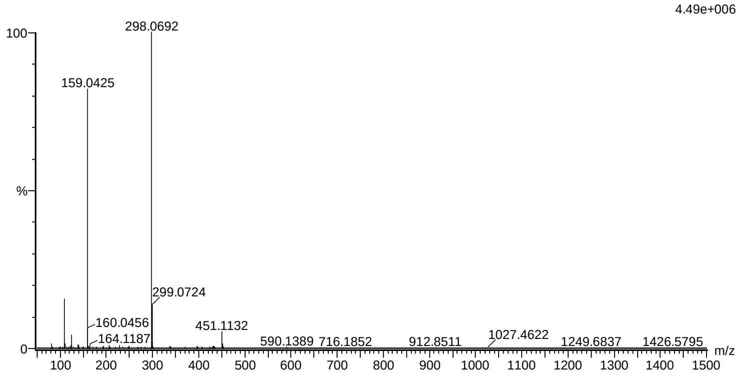

Minimum:				-10.0				
Maximum:		5.0	5.0	50.0				
Mass	Calc. Mass	mDa	PPM	DBE	i-FIT	Norm	Conf(%)	Formula
298.0692	298.0691	0.1	0.3	8.5	2986.1	0.005	99.46	C14 H11 N O3 F3
	298.0691	0.1	0.3	-7.5	2997.5	11.341	0.00	C4 H23 N O3 F2 I
	298.0690	0.2	0.7	15.5	3006.7	20.602	0.00	C20 H12 N S
	298.0690	0.2	0.7	-2.5	3014.1	28.031	0.00	C5 H19 N5 O2 F2 Br
	298.0688	0.4	1.3	-4.5	3014.5	28.420	0.00	C7 H25 N O4 S Br
	298.0685	0.7	2.3	-0.5	3005.4	19.242	0.00	C6 H15 N3 O5 F3 S
	298.0699	-0.7	-2.3	-8.5	3014.4	28.310	0.00	C4 H26 N O5 F S Br
	298.0701	-0.9	-3.0	0.5	3015.0	28.868	0.00	C8 H21 N5 S Br
	298.0702	-1.0	-3.4	11.5	3006.1	19.959	0.00	C17 H13 N O F S
	298.0702	-1.0	-3.4	-4.5	3004.6	18.495	0.00	C7 H25 N O S I
	298.0702	-1.0	-3.4	-6.5	3014.4	28.322	0.00	C2 H20 N5 O3 F3 Br
	298.0680	1.2	4.0	12.5	2991.4	5.327	0.49	C17 H10 N O2 F2
	298.0679	1.3	4.4	1.5	3014.2	28.066	0.00	C8 H18 N5 O F Br
	298.0679	1.3	4.4	-3.5	2993.6	7.501	0.06	C7 H22 N O2 F I

Figure 45: MS specter of compound ***(S)*-4**

.1.7 Spectroscopic data for Compound 5

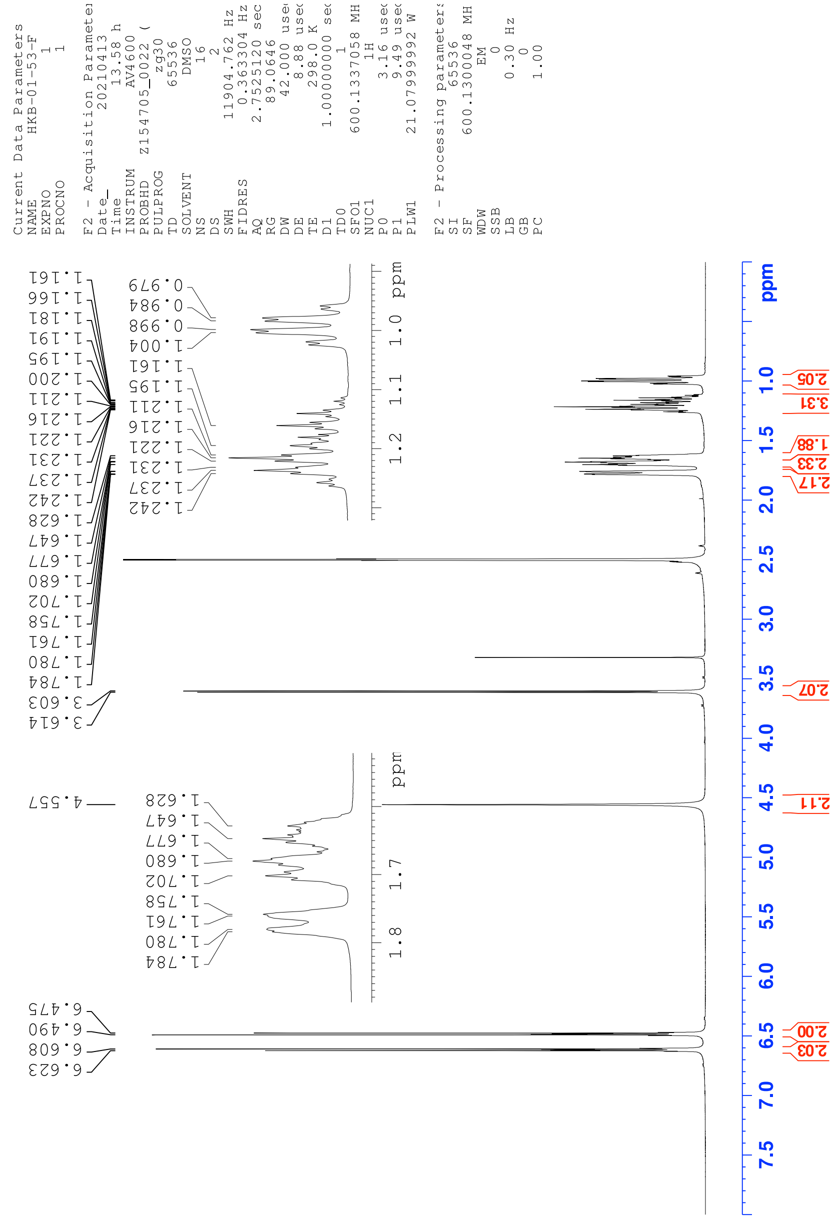

Figure 46: ^{1}H-NMR specter of compound **5**

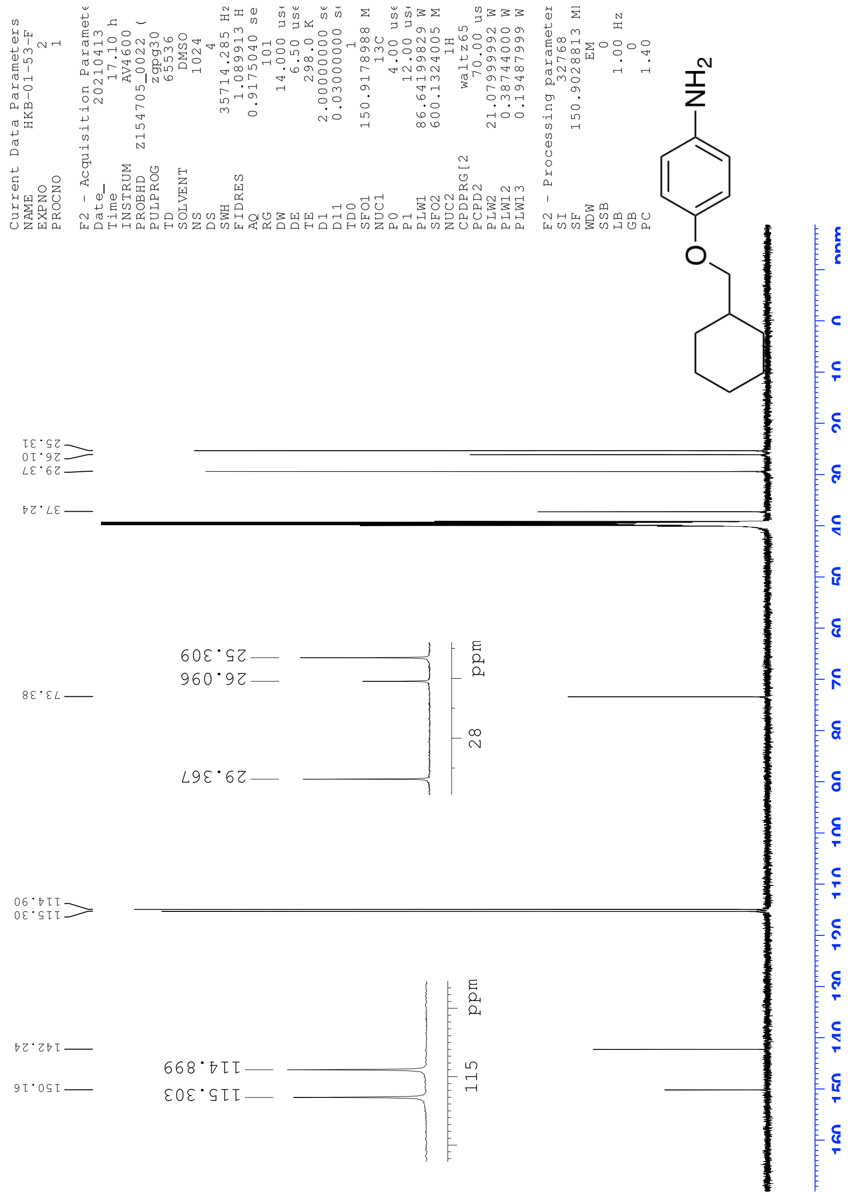

Figure 47: ^{13}C-NMR specter of compound **5**

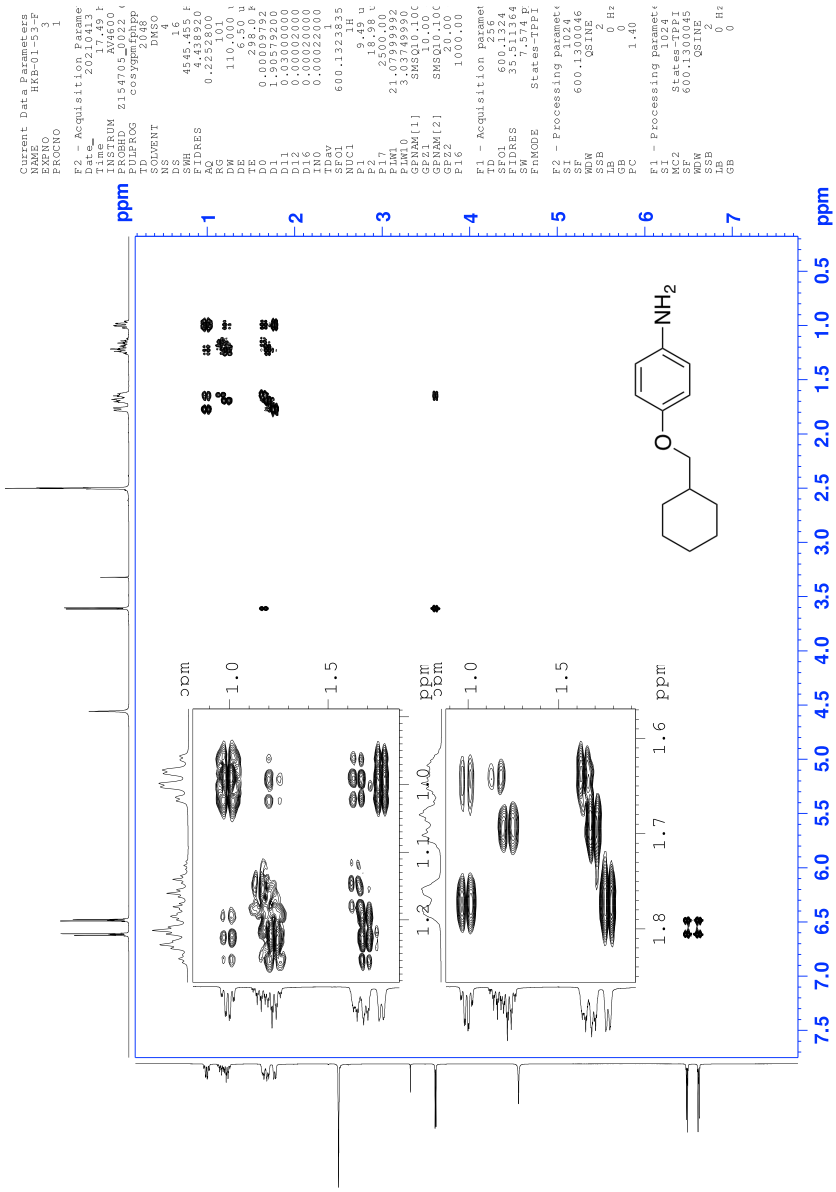

Figure 48: COSY specter of compound **5**

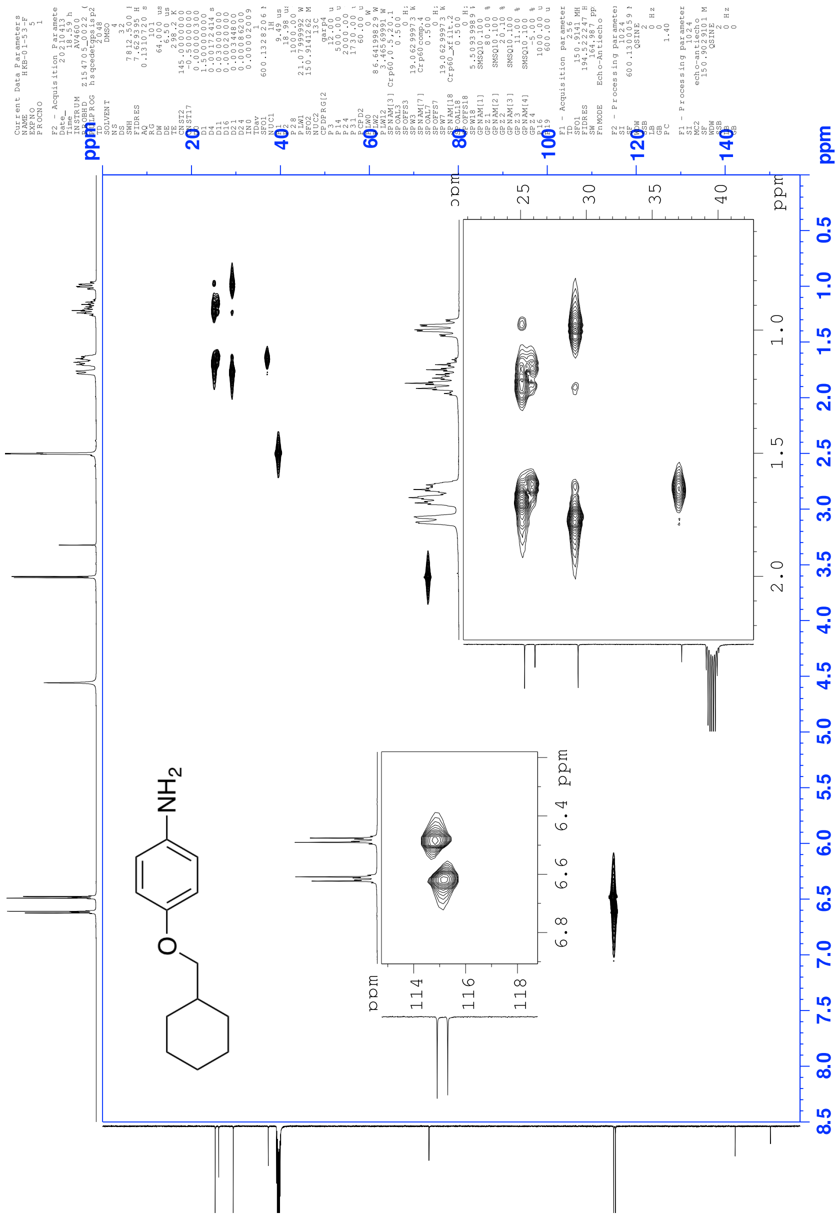

Figure 49: HSQC specter of compound **5**

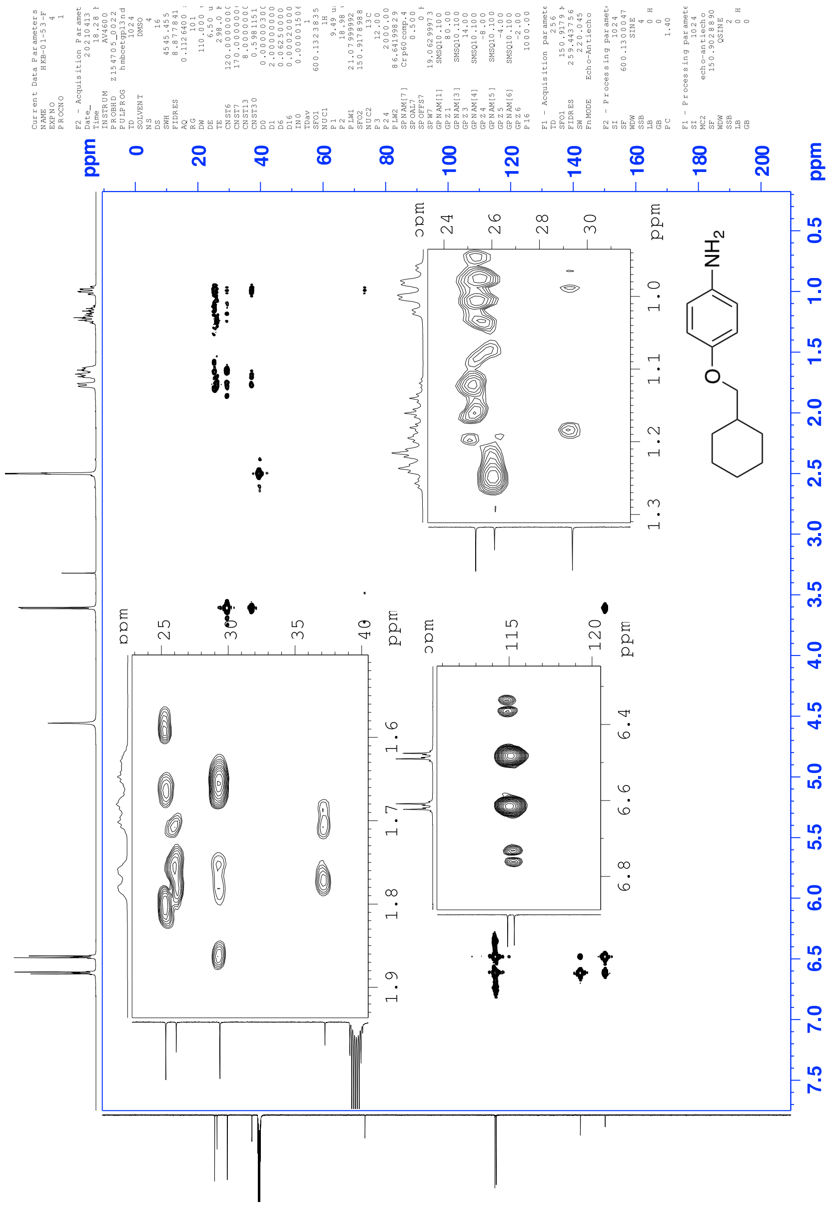

Figure 50: HMBC specter of compound **5**

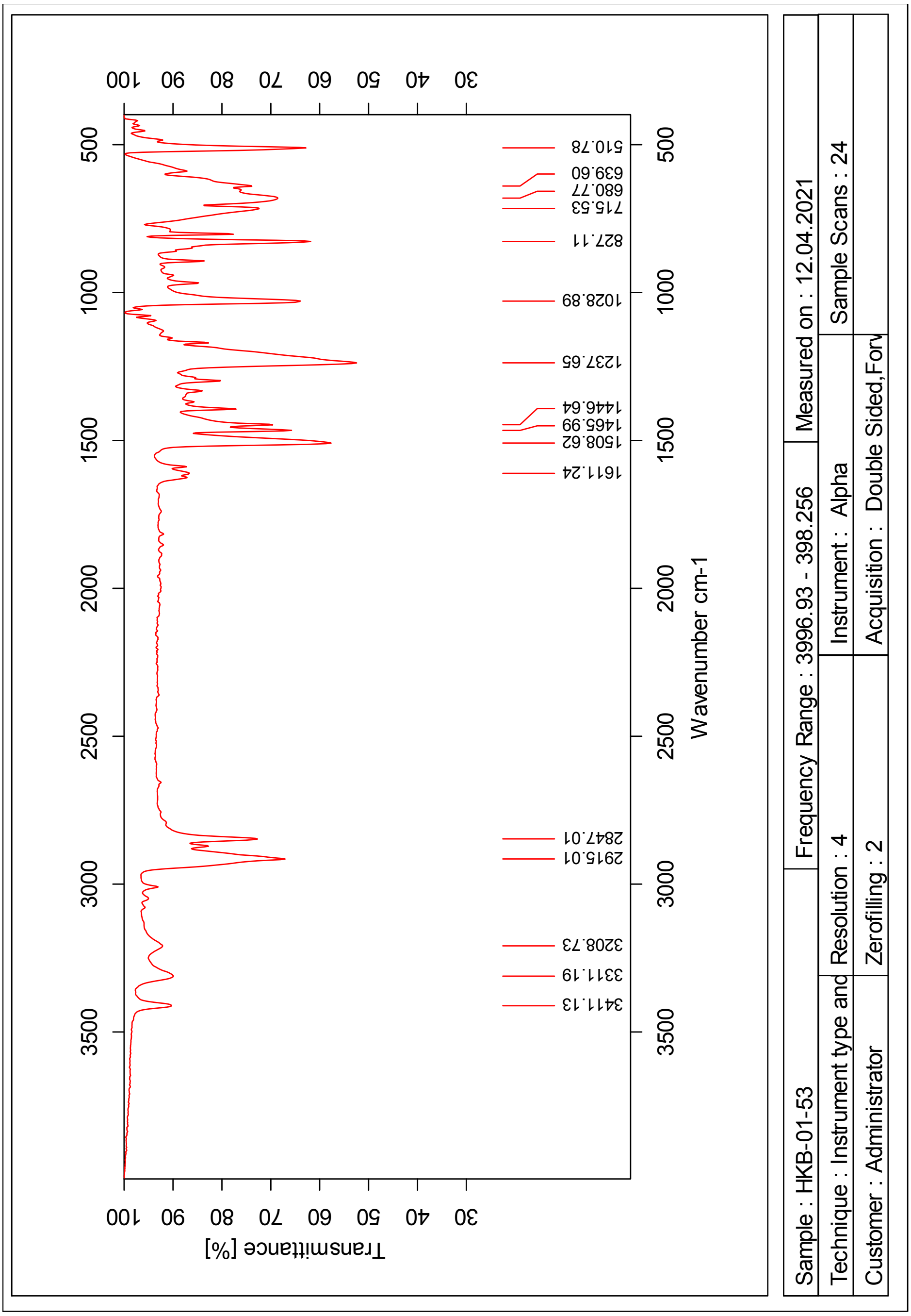

Figure 51: IR-spectrum of compound **5**

Elemental Composition Report **Page 1**

Single Mass Analysis
Tolerance = 2.0 PPM / DBE: min = -10.0, max = 50.0
Element prediction: Off
Number of isotope peaks used for i-FIT = 6

Monoisotopic Mass, Even Electron Ions
612 formula(e) evaluated with 1 results within limits (all results (up to 1000) for each mass)
Elements Used:
C: 0-100 H: 0-100 N: 0-6 O: 0-6 S: 0-5
2021-196 58 (0.553) AM2 (Ar,35000.0,0.00,0.00); Cm (55:58)
1: TOF MS ES+

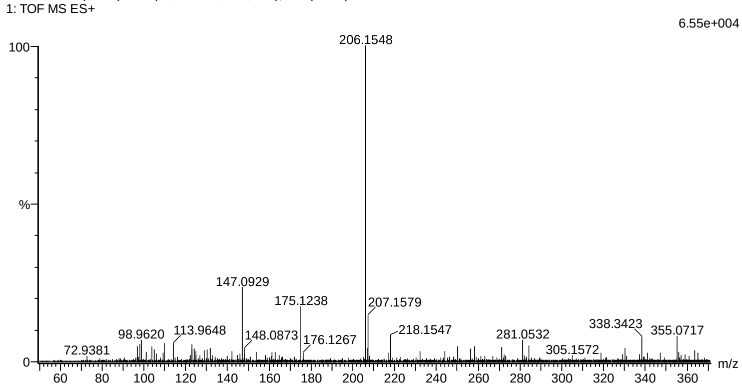

	Mass	Calc. Mass	mDa	PPM	DBE	i-FIT	Norm	Conf(%)	Formula
Minimum:					-10.0				
Maximum:			5.0	2.0	50.0				
	206.1548	206.1545	0.3	1.5	4.5	1726.8	n/a	n/a	C13 H20 N O

Figure 52: MS specter of compound **5**

.1.8 Spectroscopic data for Compound (*R*)-6

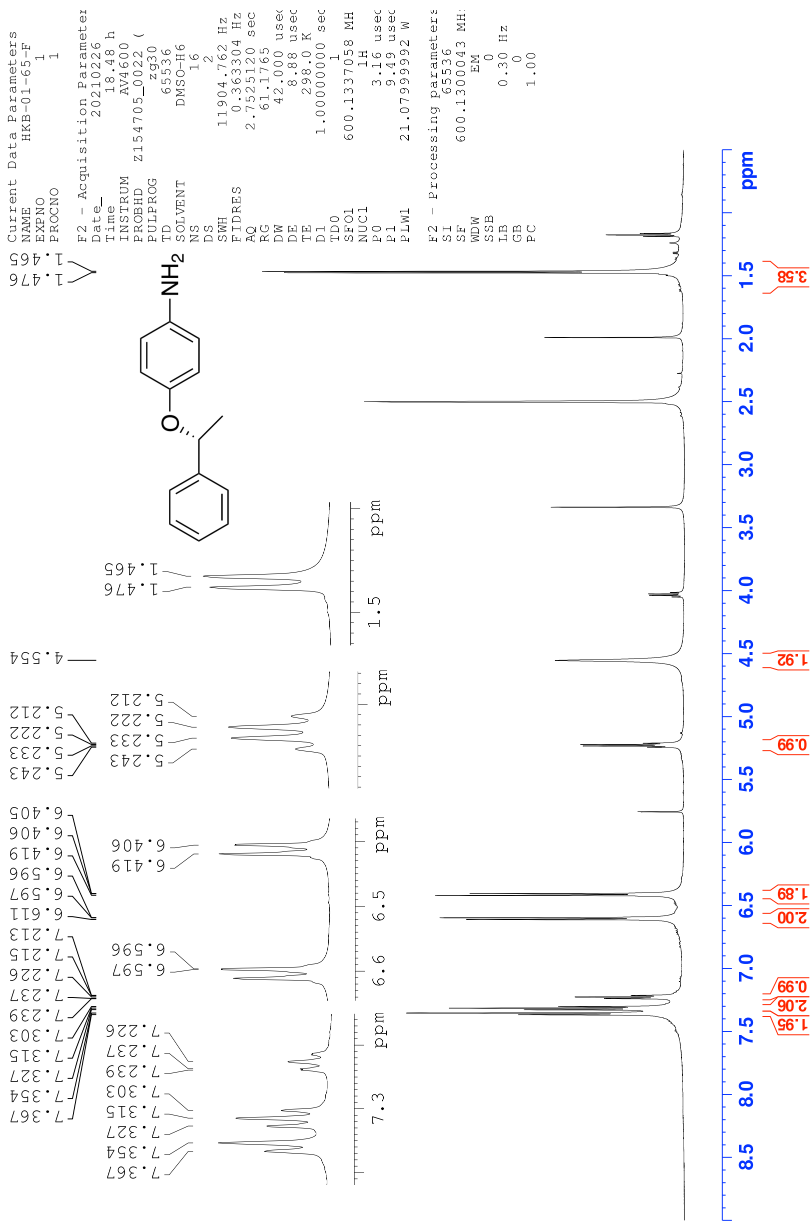

Figure 53: ^{1}H-NMR specter of compound **(*R*)-6**

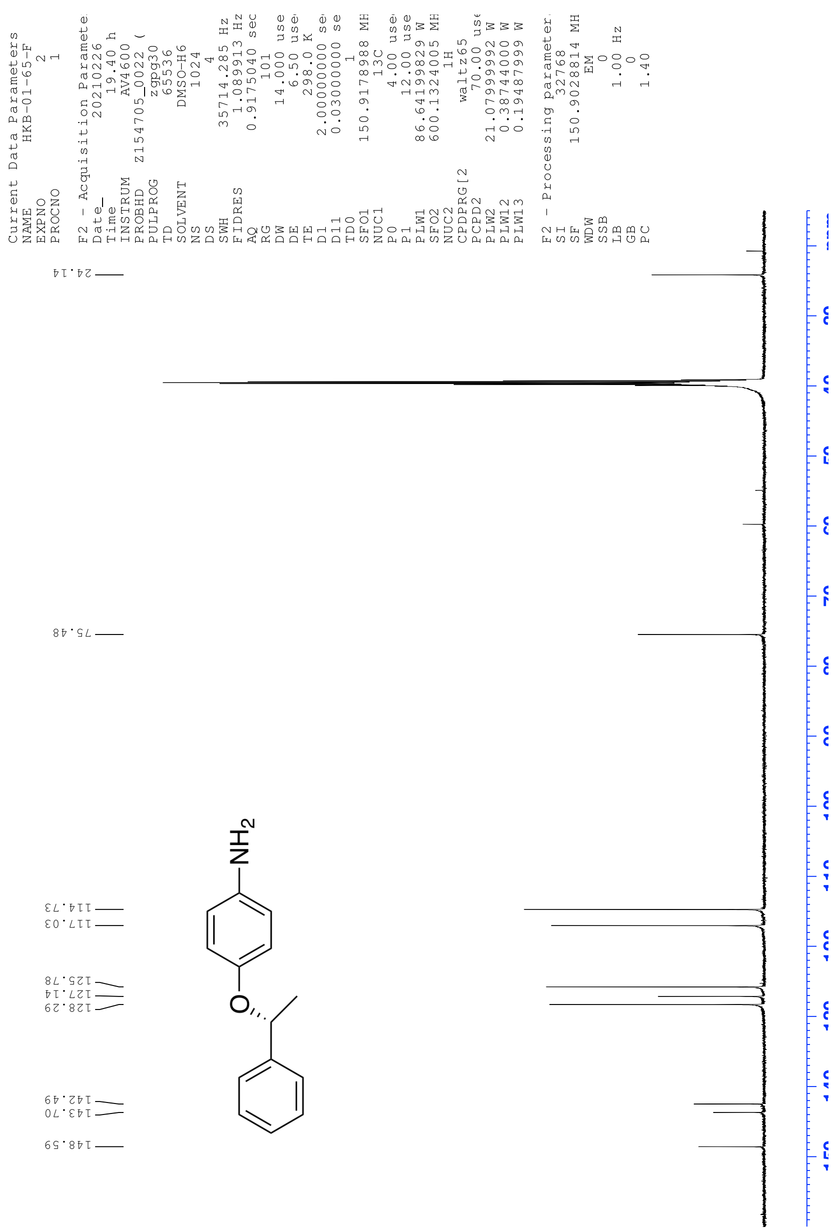

Figure 54: ^{13}C-NMR specter of compound ***(R)*-6**

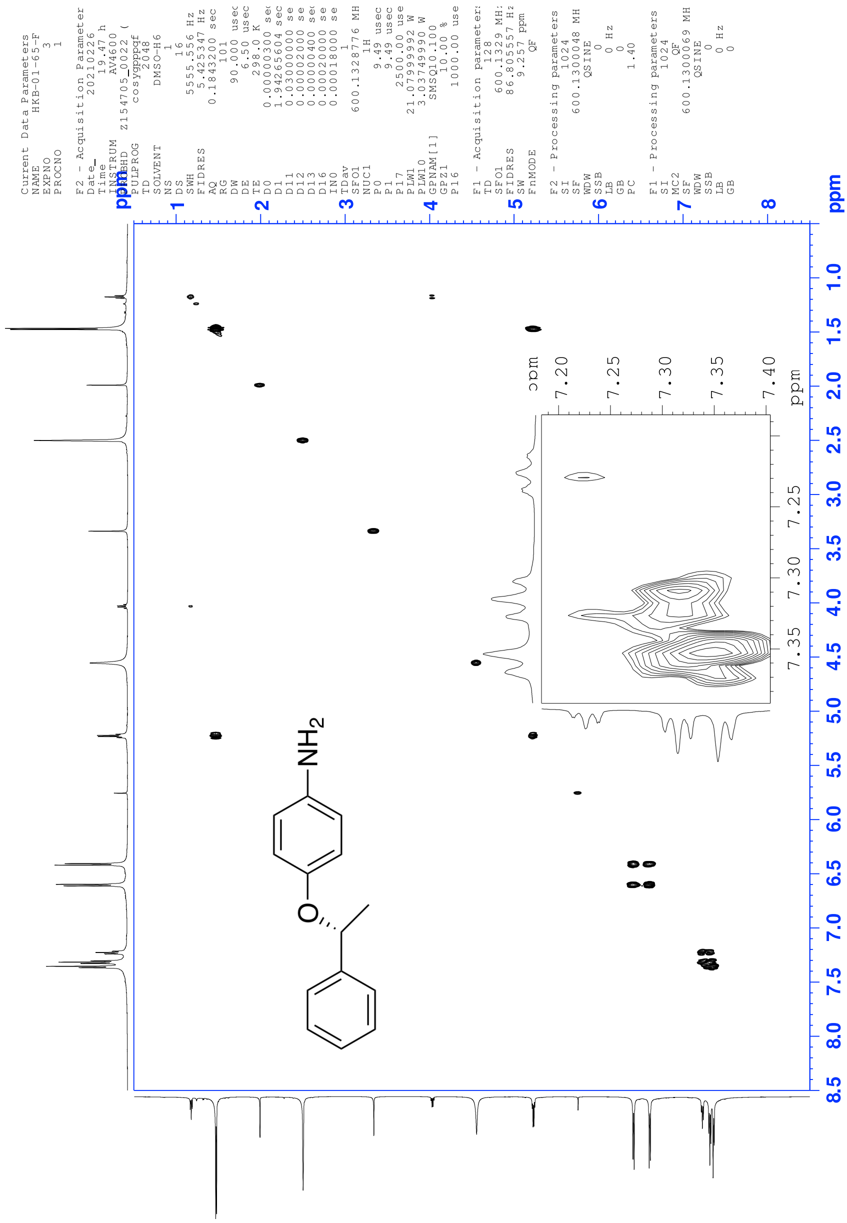

Figure 55: COSY specter of compound ***(R)*-6**

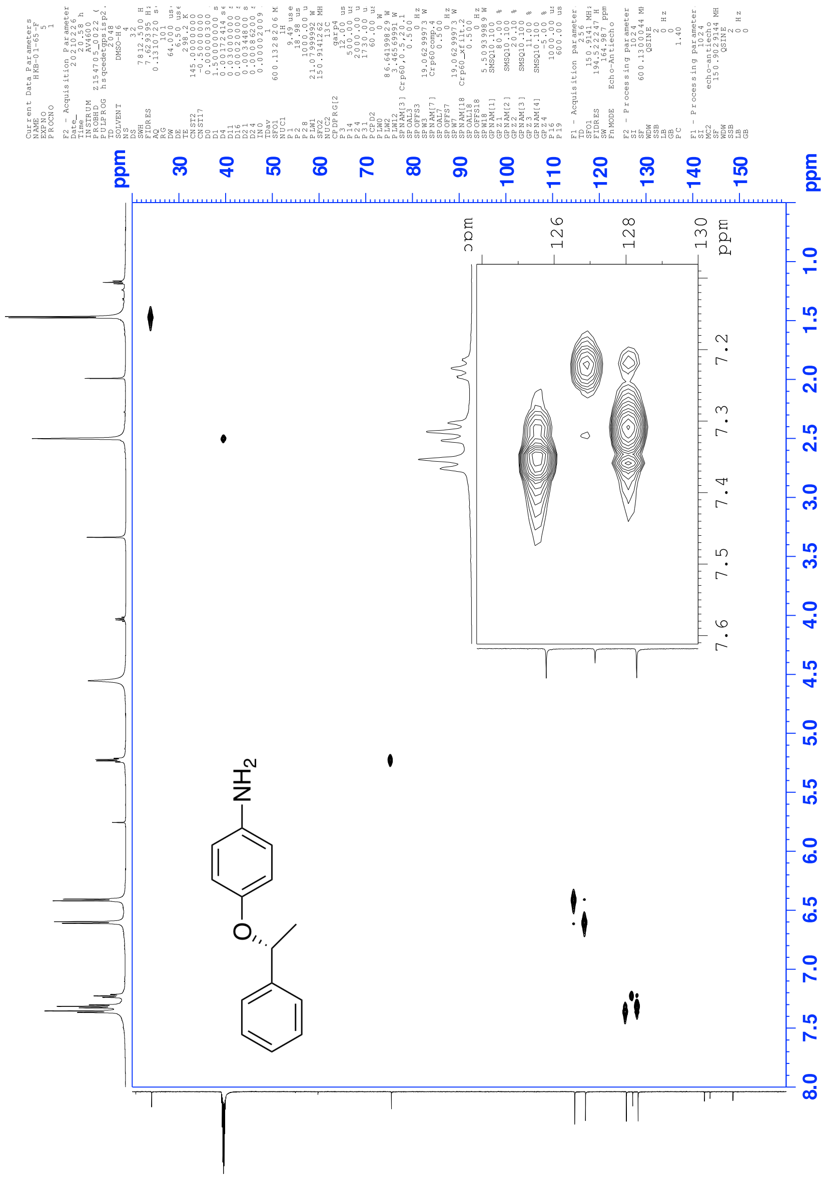

Figure 56: HSQC specter of compound **(*R*)-6**

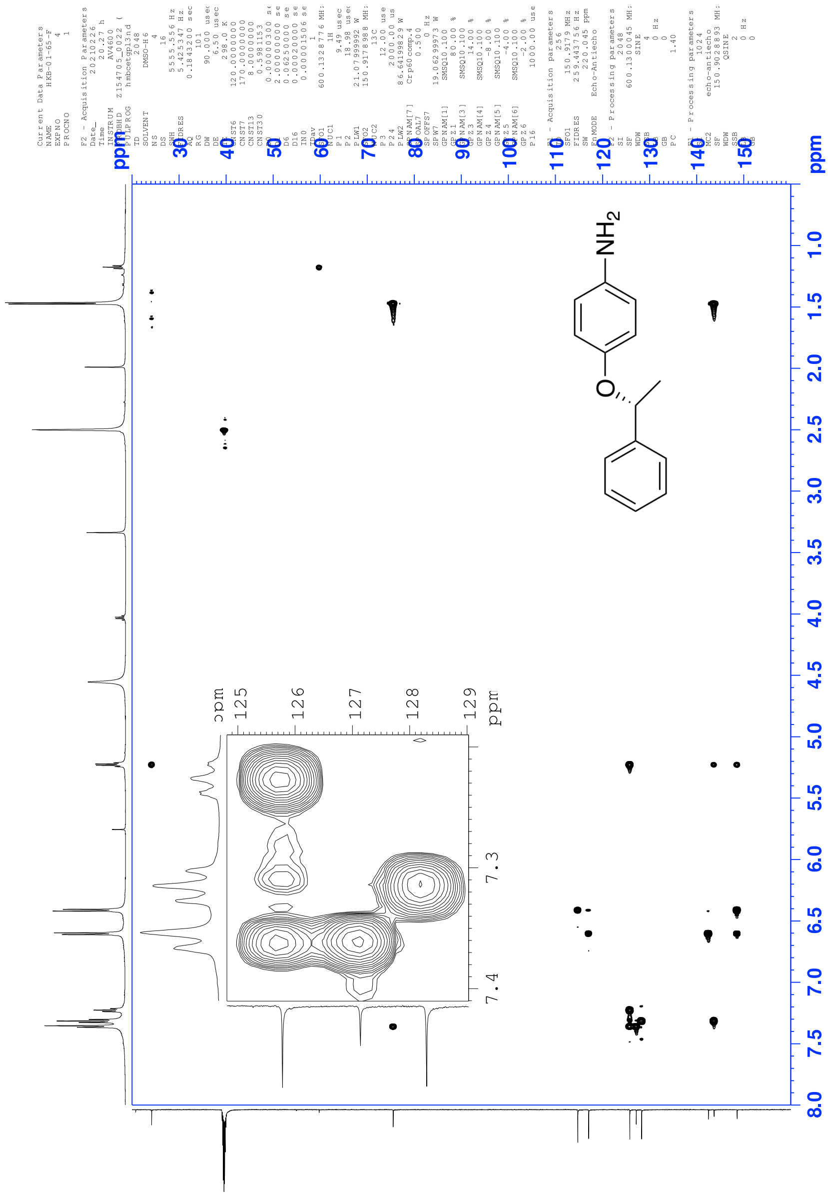

Figure 57: HMBC specter of compound **(*R*)-6**

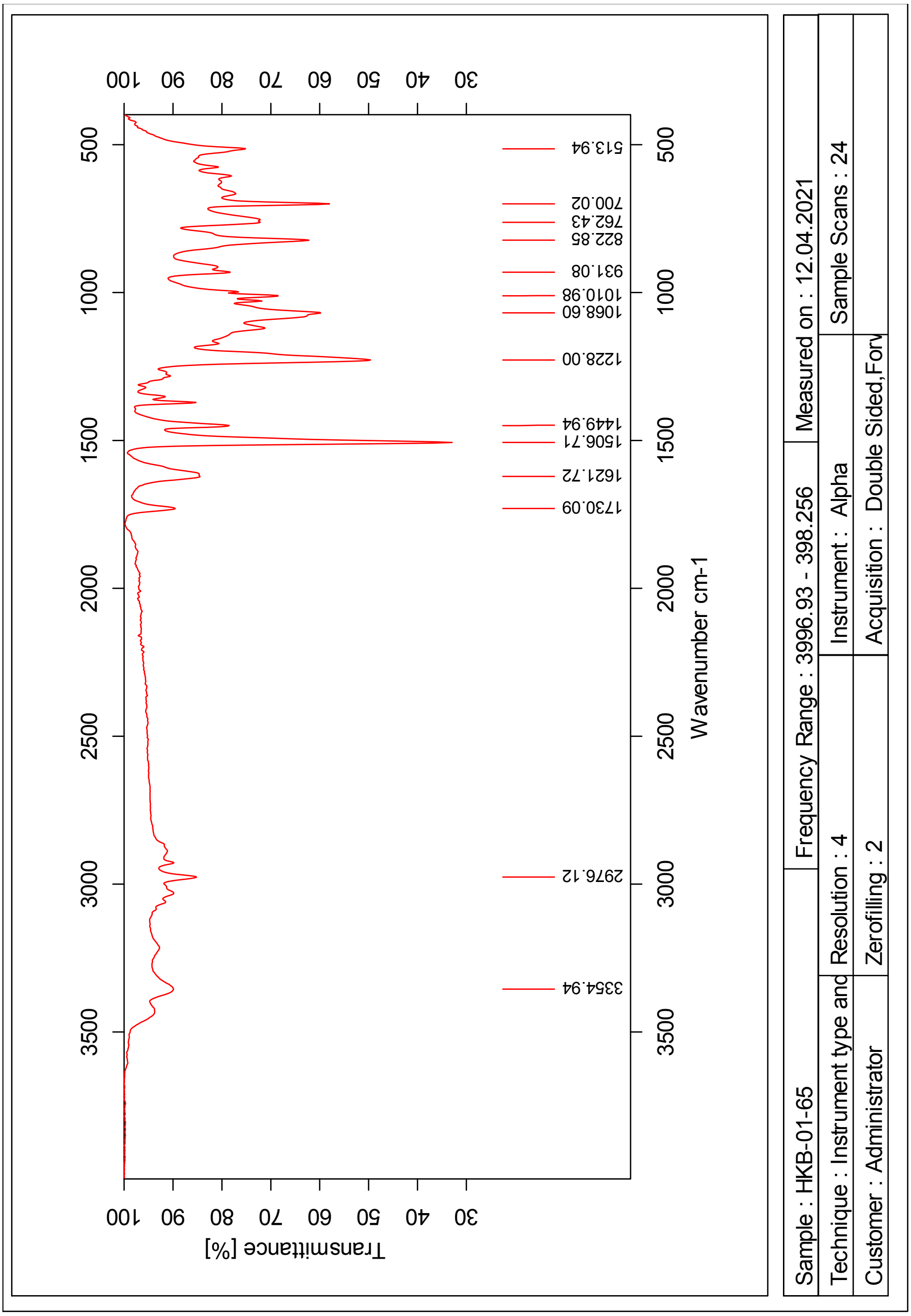

Figure 58: IR-spectrum of compound **(*R*)-6**

Elemental Composition Report **Page 1**

Single Mass Analysis
Tolerance = 5.0 PPM / DBE: min = -10.0, max = 50.0
Element prediction: Off
Number of isotope peaks used for i-FIT = 6

Monoisotopic Mass, Even Electron Ions
245 formula(e) evaluated with 1 results within limits (all results (up to 1000) for each mass)
Elements Used:
C: 0-100 H: 0-100 N: 0-6 O: 0-6 I: 0-2

2021-201 160 (1.502) AM2 (Ar,35000.0,0.00,0.00)
1: TOF MS ES+

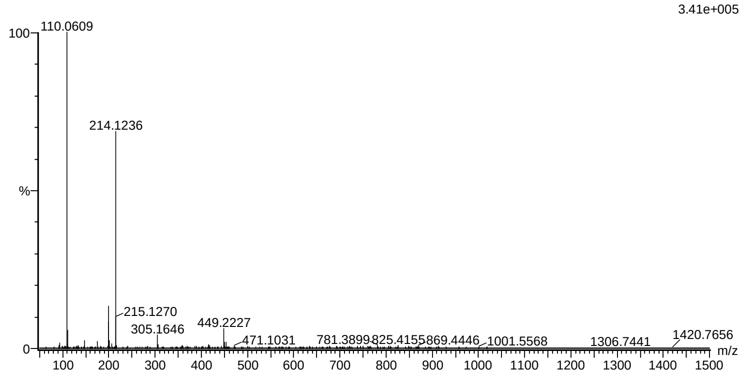

Minimum:				-10.0				
Maximum:		5.0	5.0	50.0				
Mass	Calc. Mass	mDa	PPM	DBE	i-FIT	Norm	Conf(%)	Formula
214.1236	214.1232	0.4	1.9	7.5	2025.0	n/a	n/a	C14 H16 N O

Figure 59: MS specter of compound ***(R)*-6**

.1.9 Spectroscopic data for Compound (*S*)-6

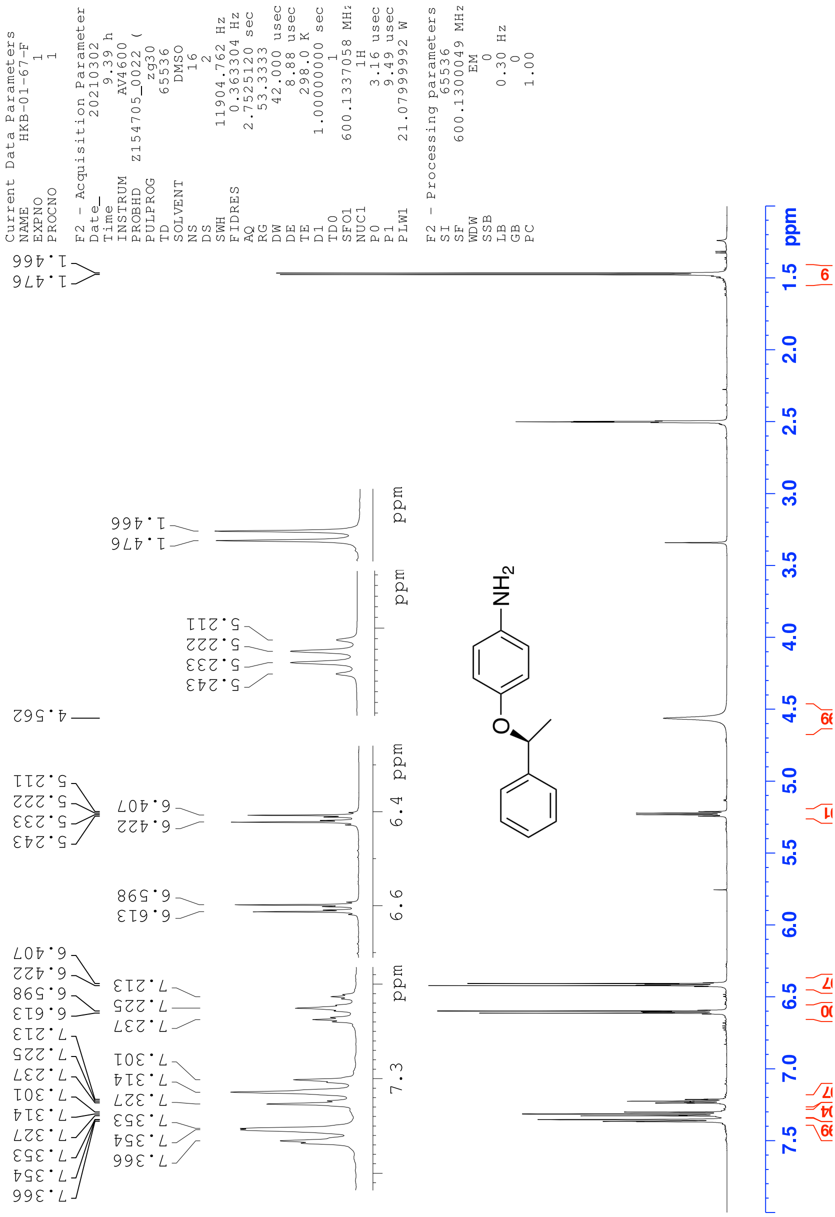

Figure 60: ^{1}H-NMR specter of compound **(*S*)-6**

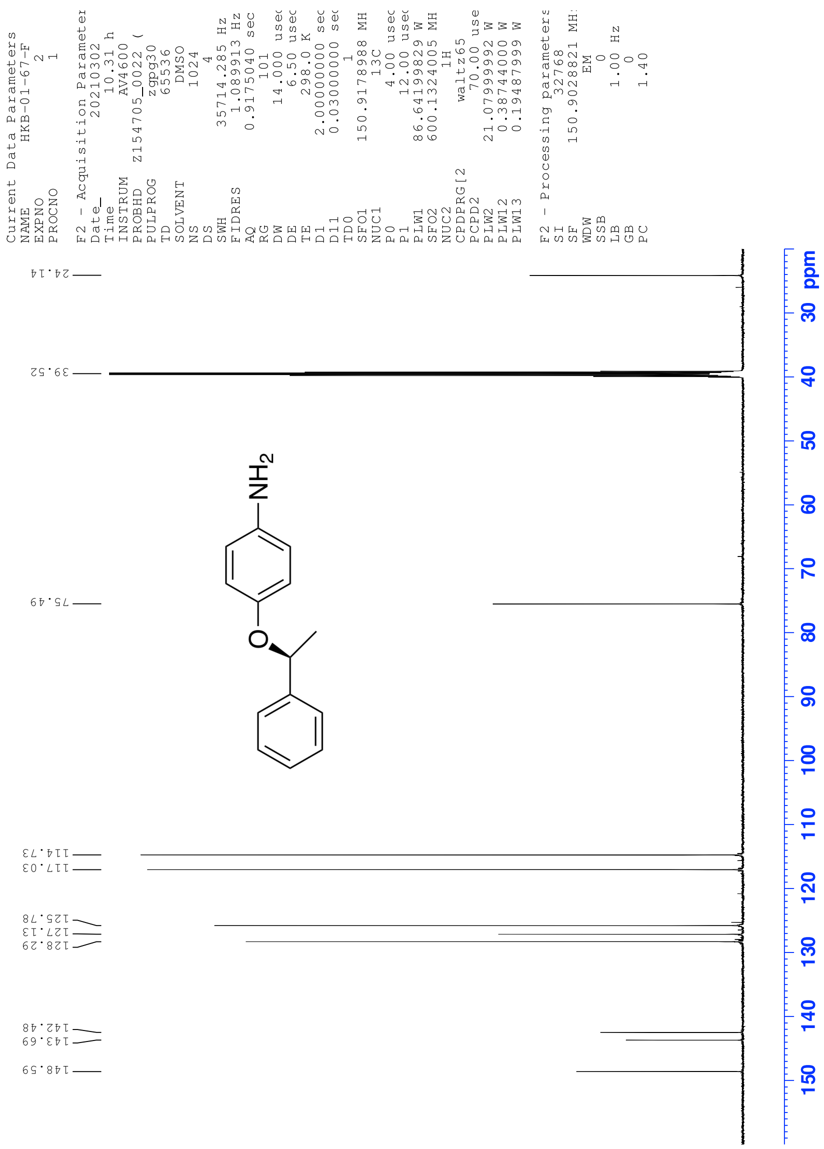

Figure 61: ^{13}C-NMR specter of compound ***(S)*-6**

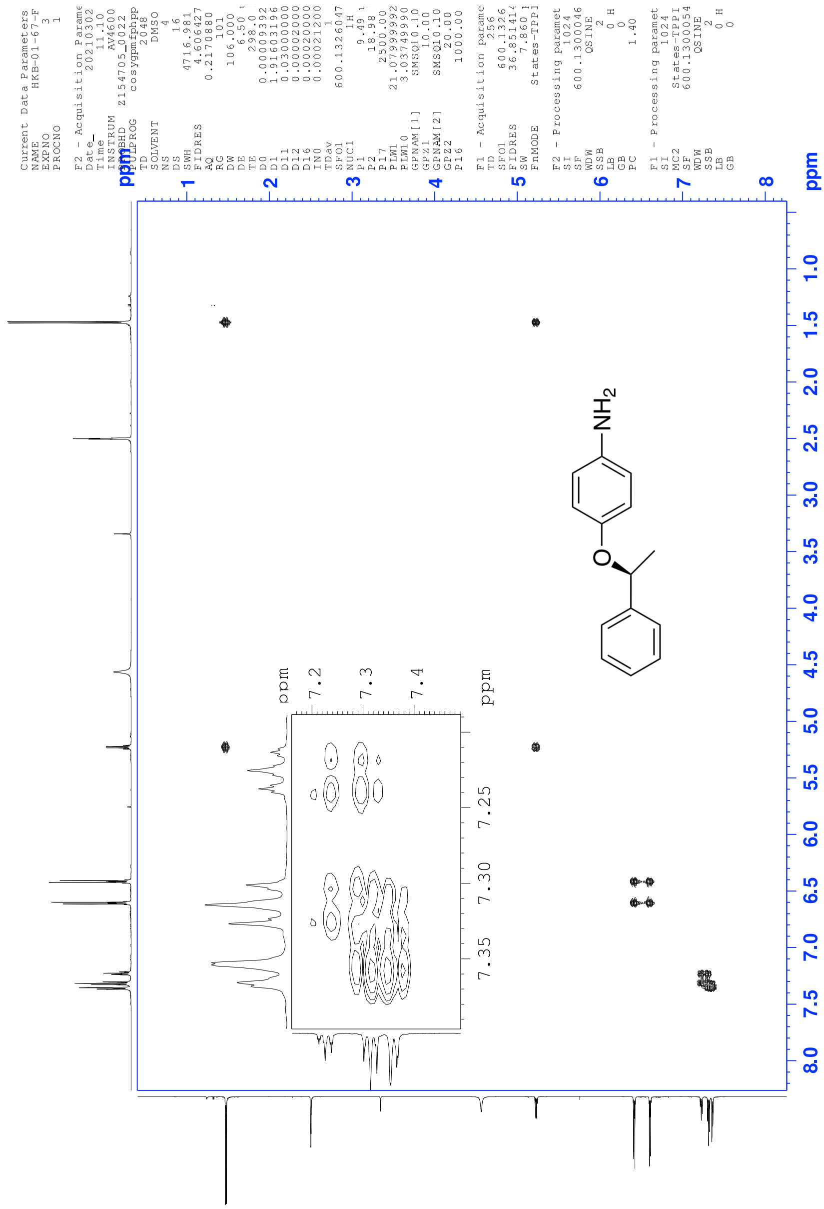

Figure 62: COSY specter of compound **(*S*)-6**

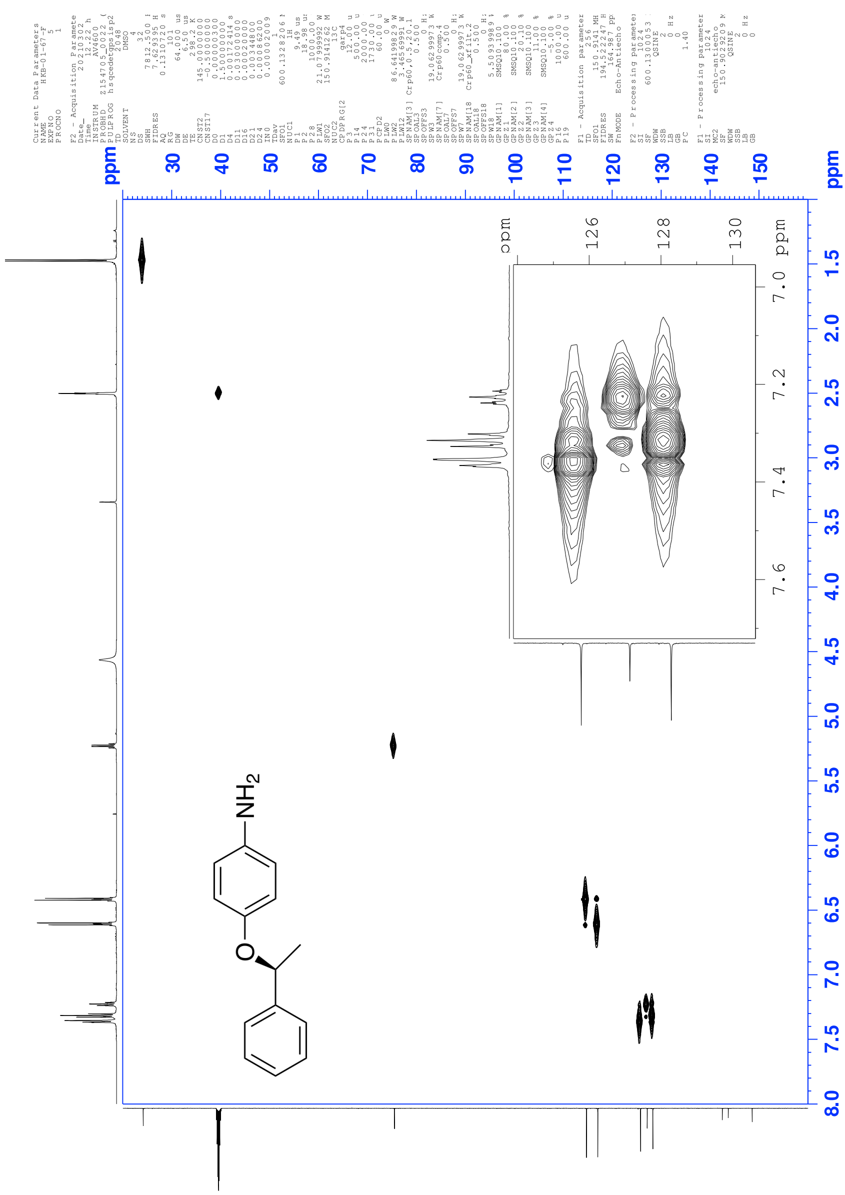

Figure 63: HSQC specter of compound **(*S*)-6**

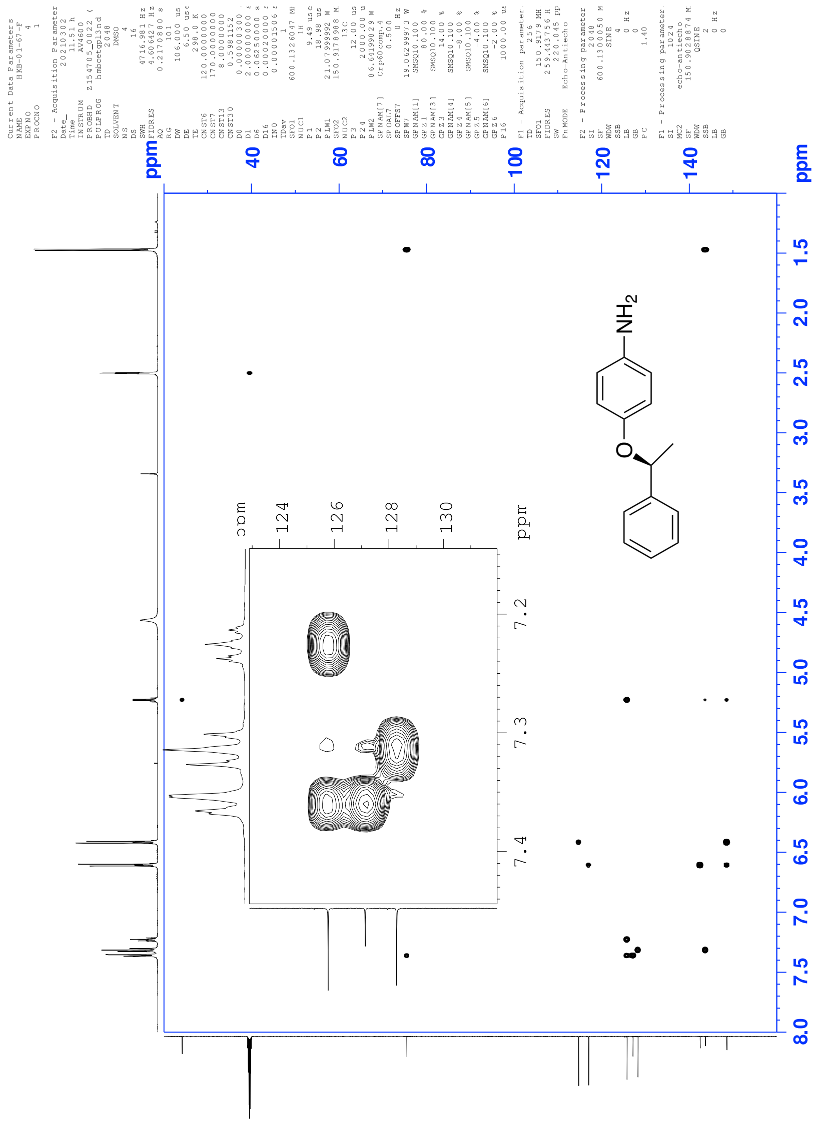

Figure 64: HMBC specter of compound **(*S*)-6**

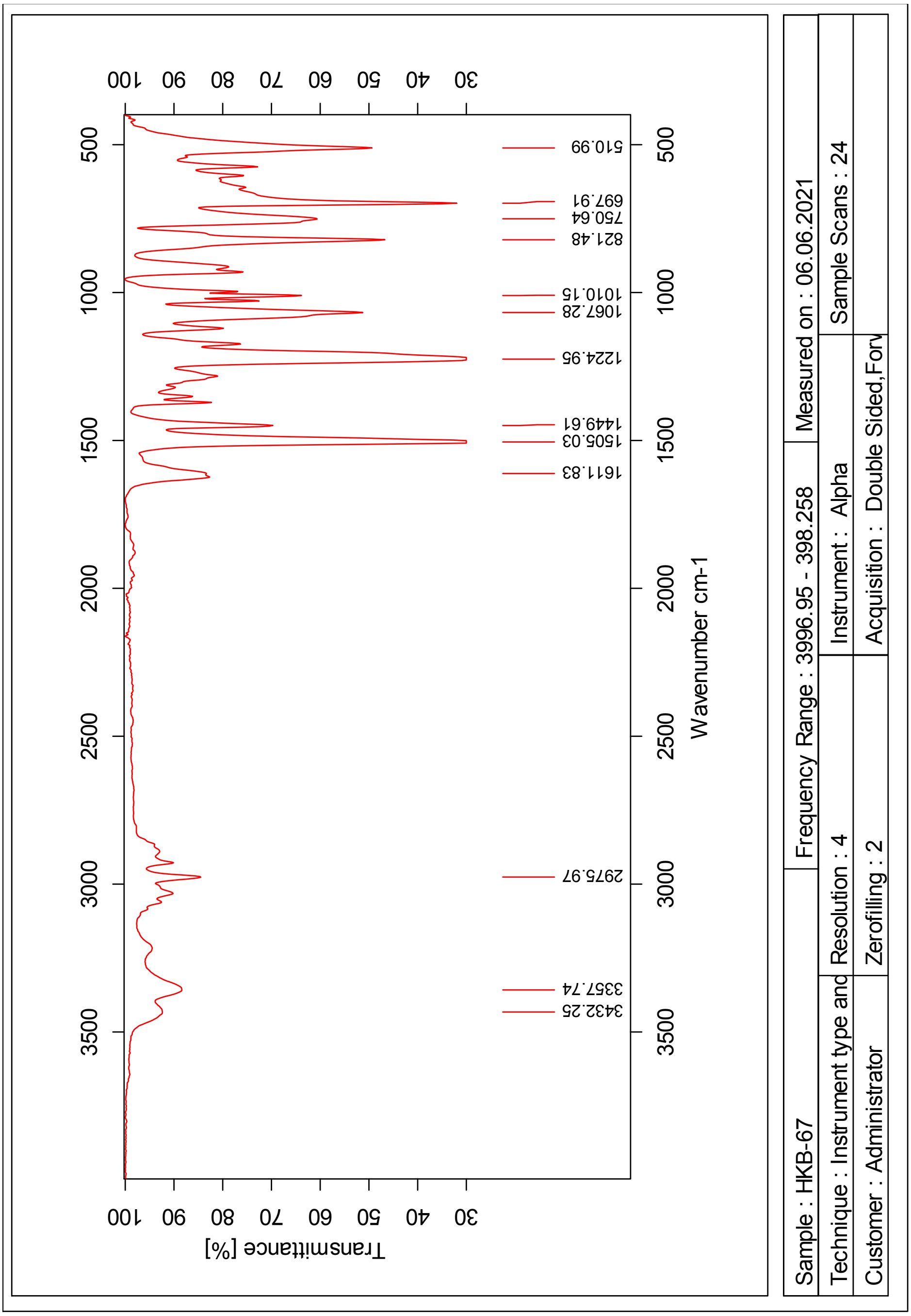

Figure 65: IR-spectrum of compound **(*S*)-6**

Elemental Composition Report **Page 1**

Single Mass Analysis
Tolerance = 5.0 PPM / DBE: min = -10.0, max = 50.0
Element prediction: Off
Number of isotope peaks used for i-FIT = 6

Monoisotopic Mass, Even Electron Ions
245 formula(e) evaluated with 1 results within limits (all results (up to 1000) for each mass)
Elements Used:
C: 0-100 H: 0-100 N: 0-6 O: 0-6 I: 0-2

2021-202 61 (0.586) AM2 (Ar,35000.0,0.00,0.00)
1: TOF MS ES+

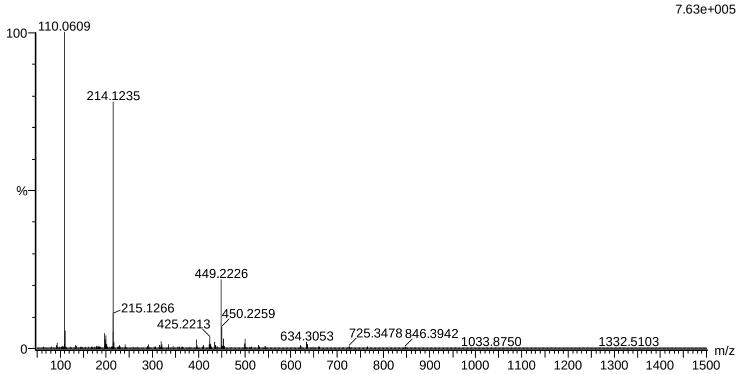

	Calc. Mass	mDa	PPM	DBE	i-FIT	Norm	Conf(%)	Formula
Minimum:				-10.0				
Maximum:		5.0	5.0	50.0				
Mass	Calc. Mass	mDa	PPM	DBE	i-FIT	Norm	Conf(%)	Formula
214.1235	214.1232	0.3	1.4	7.5	2635.4	n/a	n/a	C14 H16 N O

Figure 66: MS specter of compound **(*S*)-6**

.1.10 Spectroscopic data for Compound (*rac*)-7

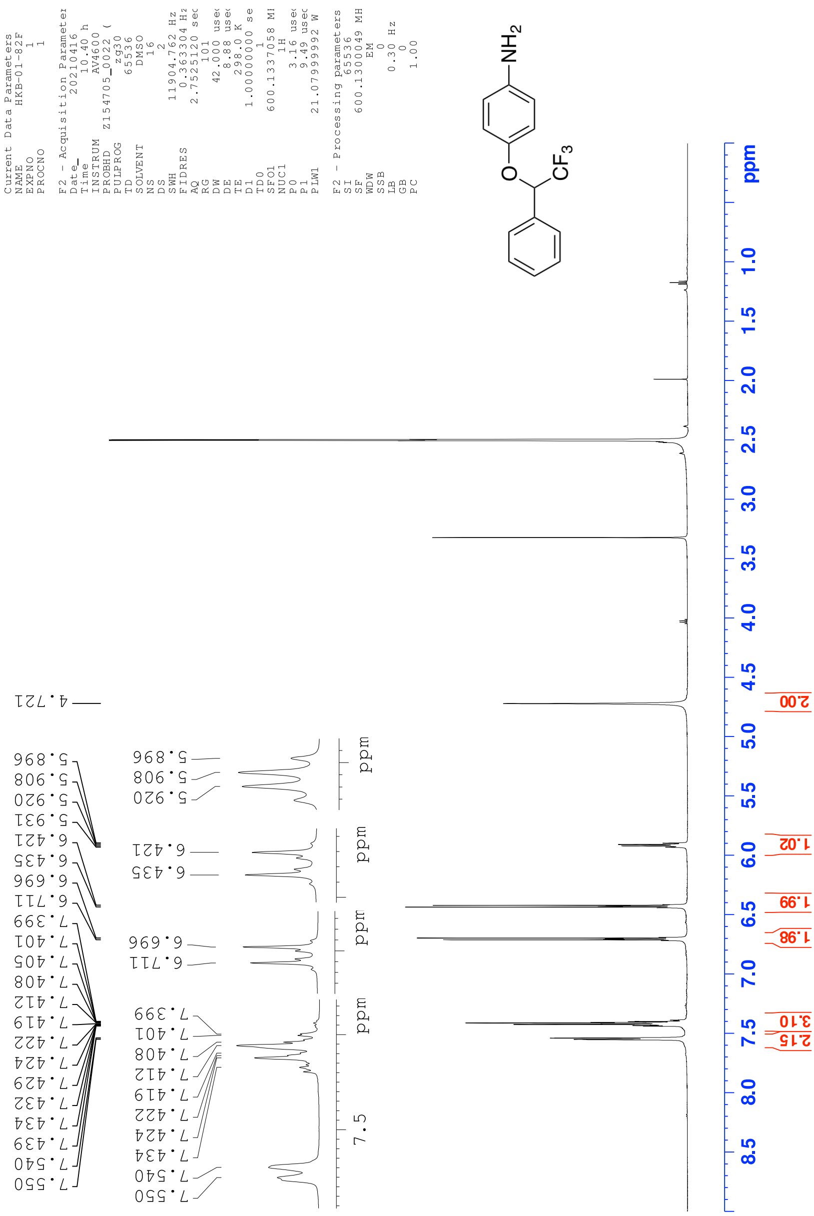

Figure 67: ^{1}H-NMR specter of compound (***rac***)-**7**

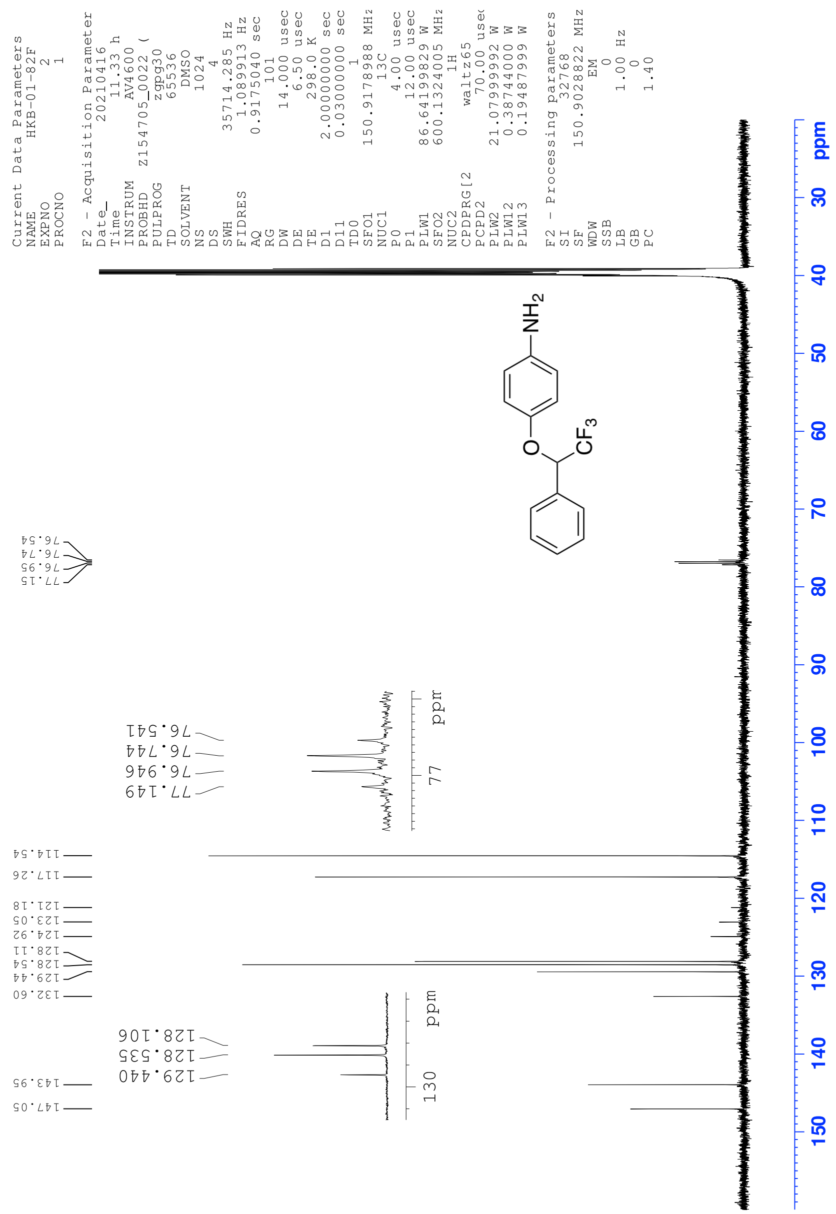

Figure 68: ^{13}C-NMR specter of compound ***(rac)*-7**

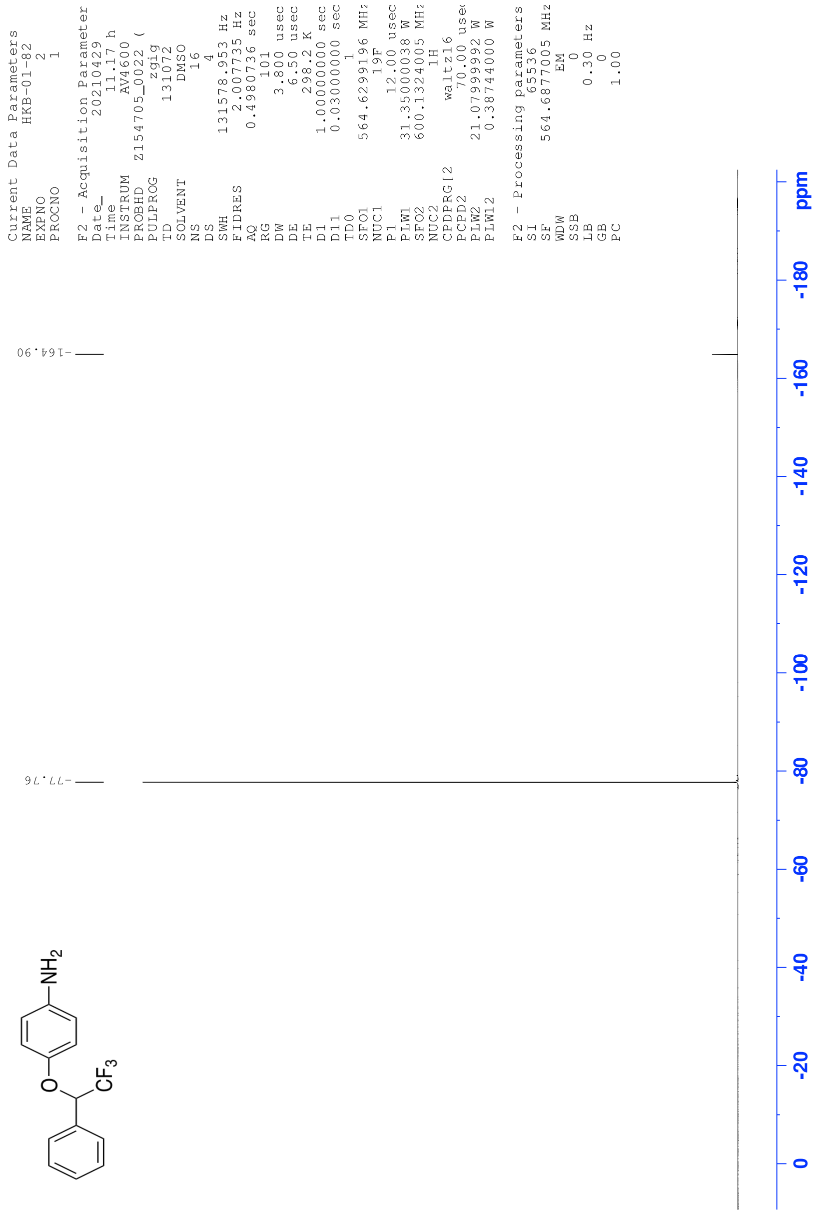

Figure 69: ^{19}F-NMR specter of compound ***(rac)*-7**

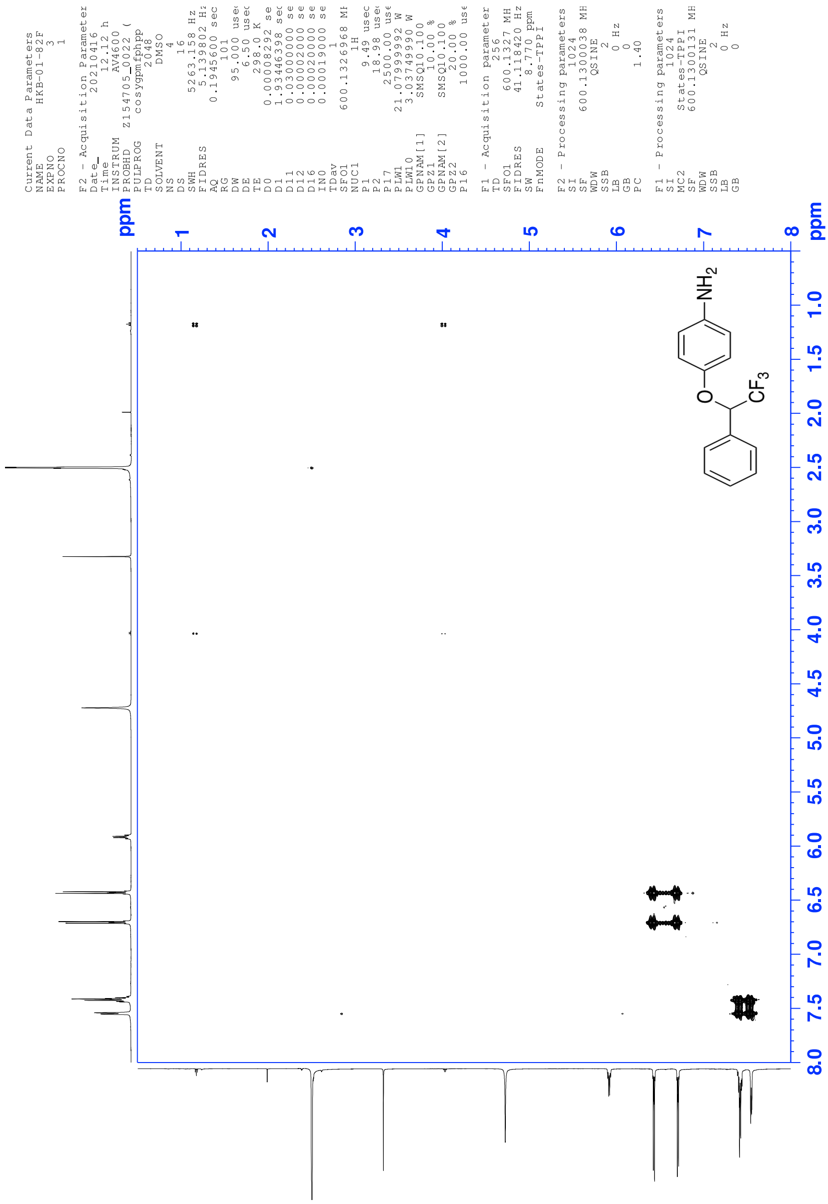

Figure 70: COSY specter of compound ***(rac)*-7**

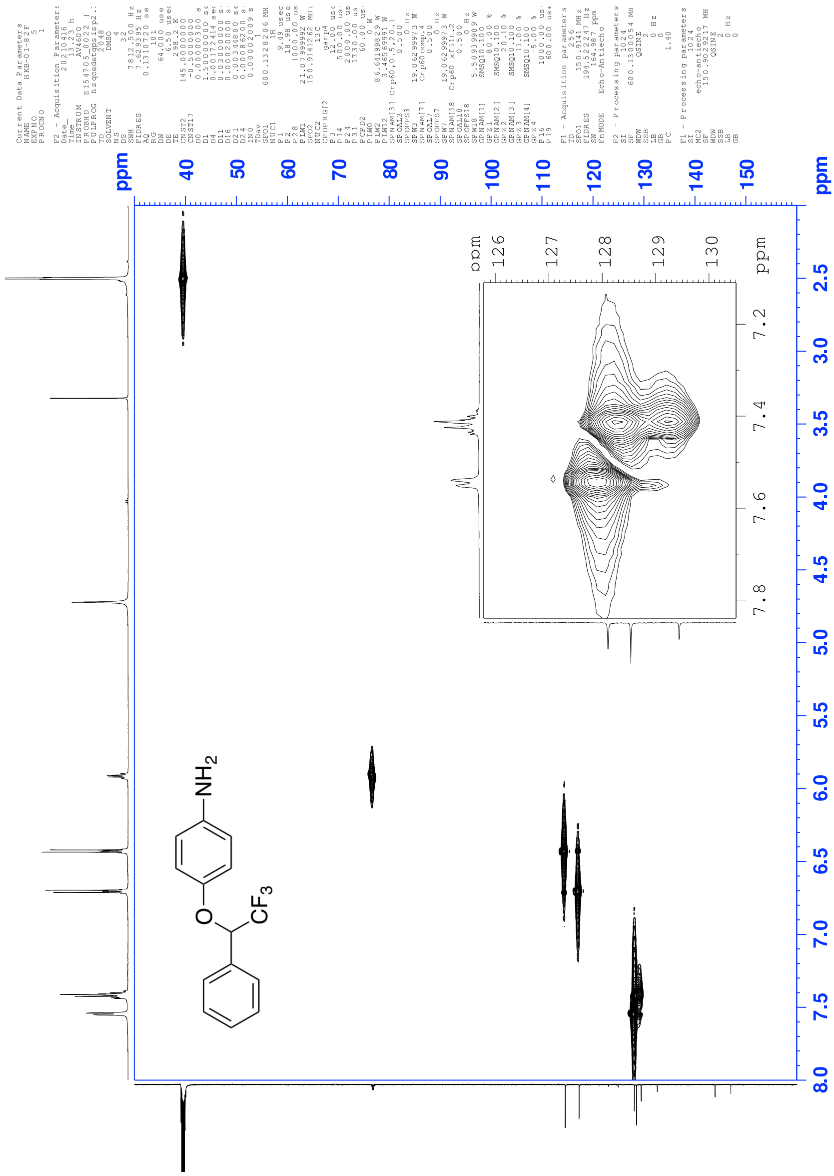

Figure 71: HSQC specter of compound **(*rac*)-7**

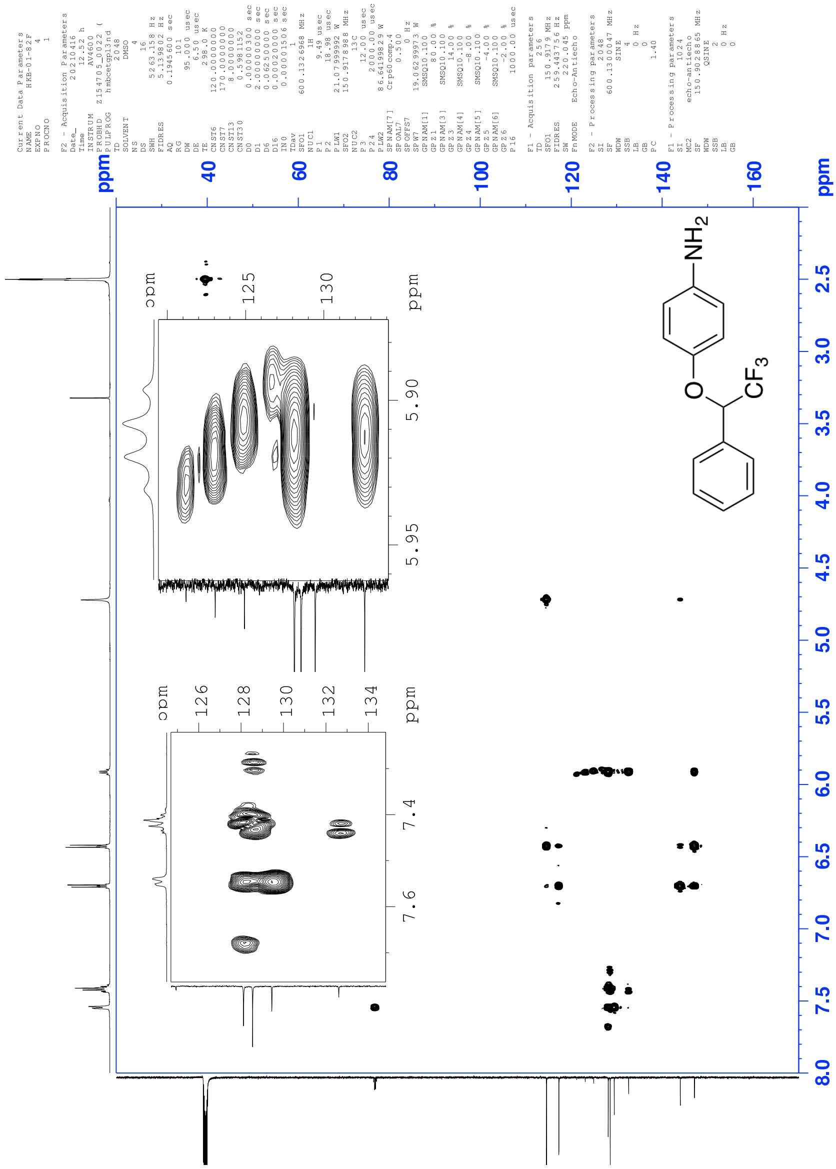

Figure 72: HMBC specter of compound **(*rac*)-7**

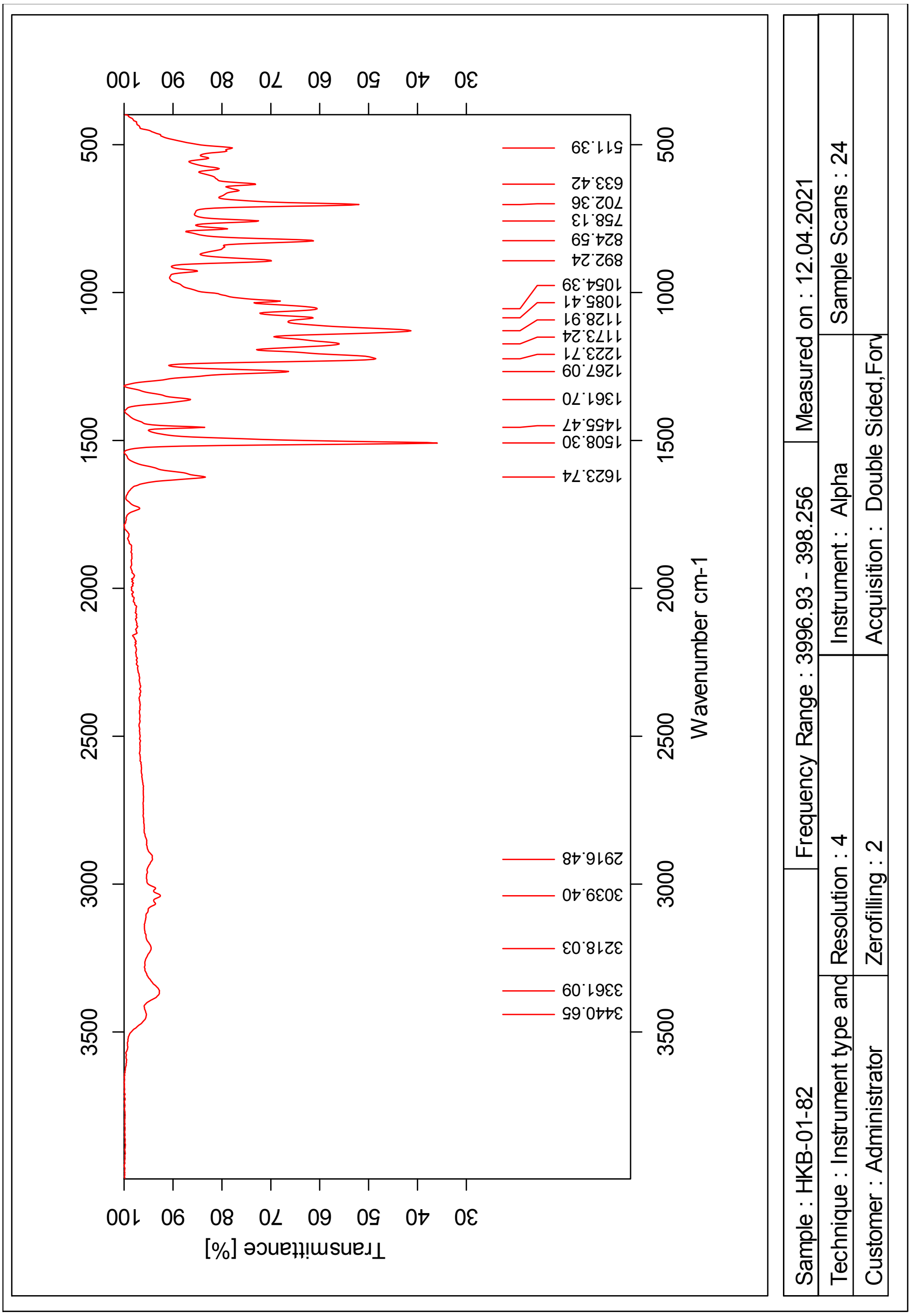

Figure 73: IR-spectrum of compound **(*rac*)-7**

Elemental Composition Report **Page 1**

Single Mass Analysis
Tolerance = 5.0 PPM / DBE: min = -10.0, max = 50.0
Element prediction: Off
Number of isotope peaks used for i-FIT = 6

Monoisotopic Mass, Even Electron Ions
3084 formula(e) evaluated with 9 results within limits (all results (up to 1000) for each mass)
Elements Used:
C: 0-100 H: 0-100 N: 0-6 O: 0-6 F: 0-3 S: 0-1 Br: 0-1 I: 0-2

2021-211 73 (1.449) AM2 (Ar,35000.0,0.00,0.00); Cm (73:79)
1: TOF MS ASAP+

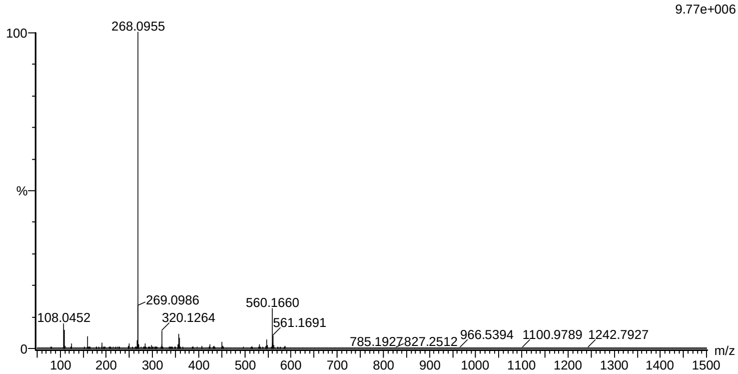

Mass	Calc. Mass	mDa	PPM	DBE	i-FIT	Norm	Conf(%)	Formula
Minimum:				-10.0				
Maximum:		5.0	5.0	50.0				
268.0955	268.0949	0.6	2.2	7.5	3635.5	0.491	61.17	C14 H13 N O F3
	268.0960	-0.5	-1.9	-7.5	3659.7	24.698	0.00	C2 H22 N5 O F3 Br
	268.0949	0.6	2.2	-8.5	3643.6	8.525	0.02	C4 H25 N O F2 I
	268.0957	-0.2	-0.7	-9.5	3661.2	26.178	0.00	C4 H28 N O3 F S Br
	268.0948	0.7	2.6	-3.5	3659.7	24.672	0.00	C5 H21 N5 F2 Br
	268.0943	1.2	4.5	-1.5	3652.8	17.780	0.00	C6 H17 N3 O3 F3 S
	268.0946	0.9	3.4	-5.5	3661.3	26.270	0.00	C7 H27 N O2 S Br
	268.0945	1.0	3.7	2.5	3636.0	0.947	38.81	C8 H15 N3 O6 F
	268.0967	-1.2	-4.5	1.5	3652.4	17.417	0.00	C8 H18 N3 O5 S

Figure 74: MS specter of compound **(*rac*)-7**

.1.11 Spectroscopic data for Compound (*R*)-7

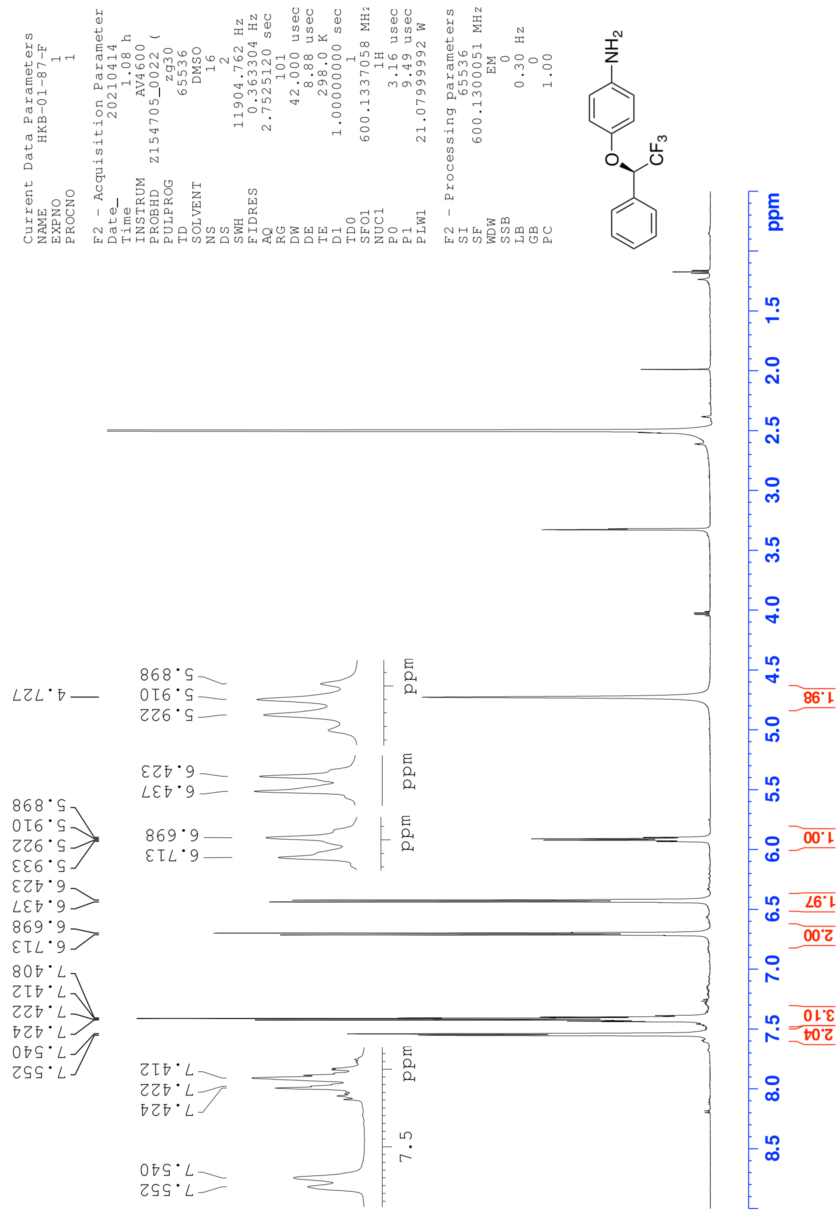

Figure 75: ^{1}H-NMR specter of compound **(*R*)-7**

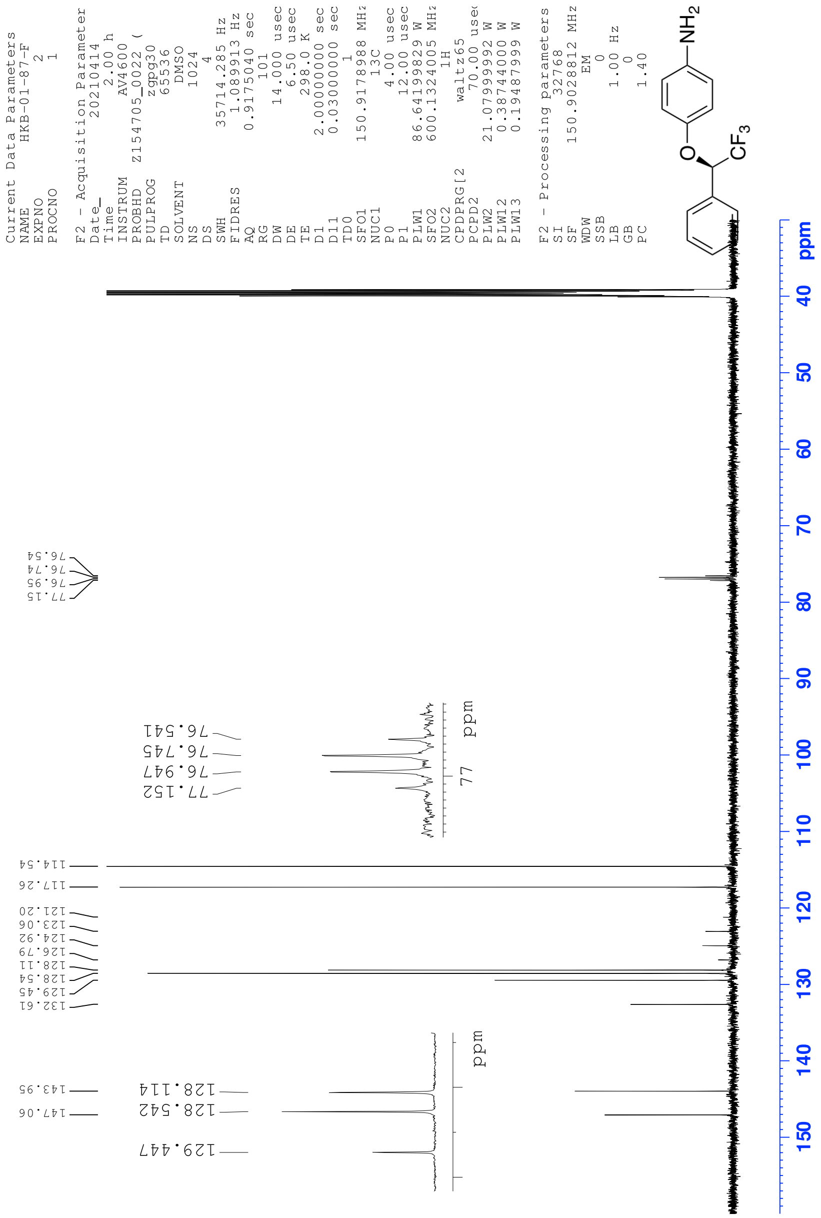

Figure 76: ^{13}C-NMR specter of compound **(*R*)-7**

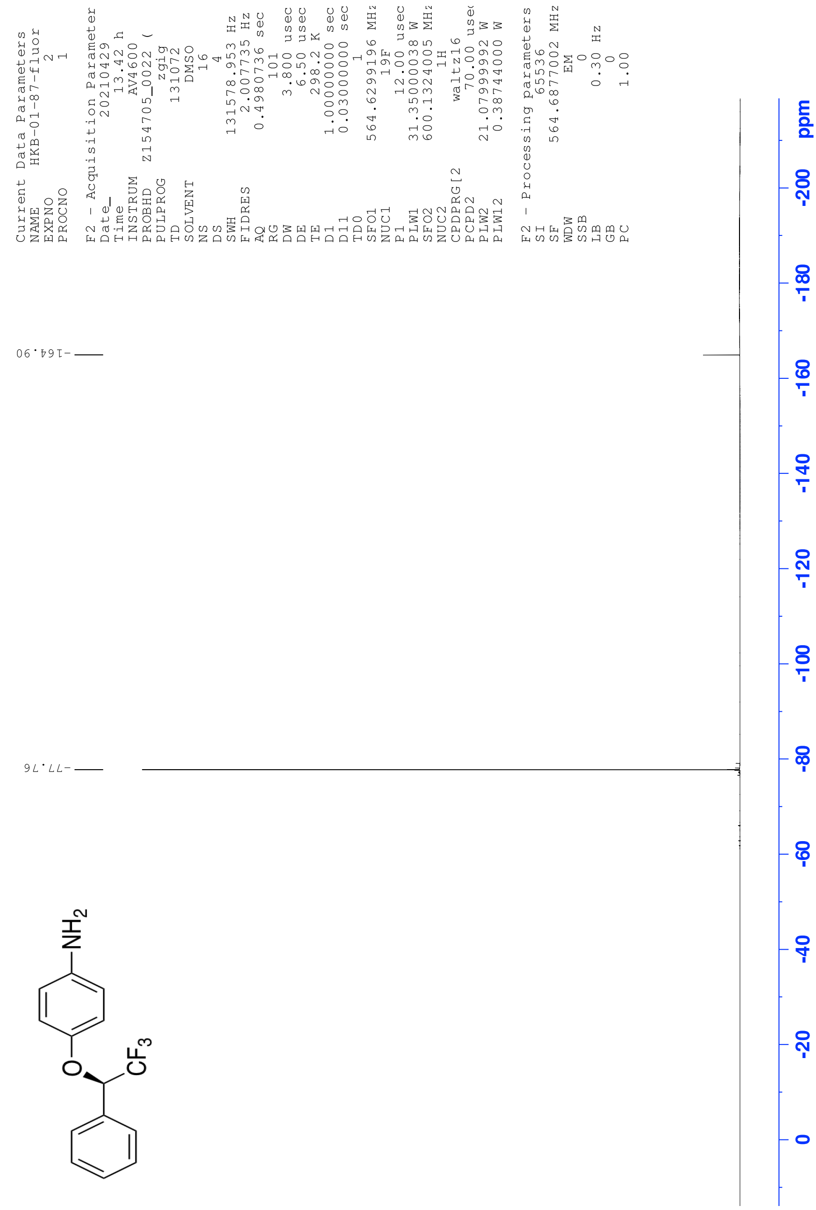

Figure 77: ^{19}F-NMR specter of compound **(*R*)-7**

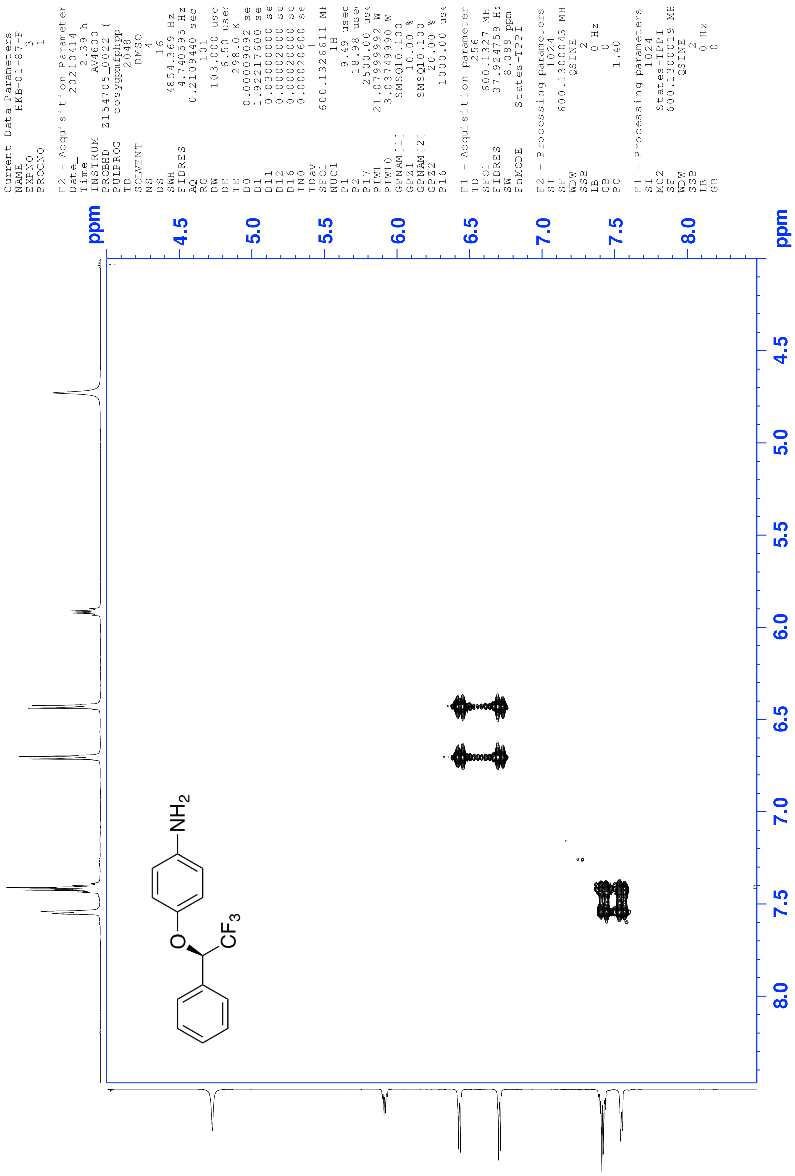

Figure 78: COSY specter of compound **(*R*)-7**

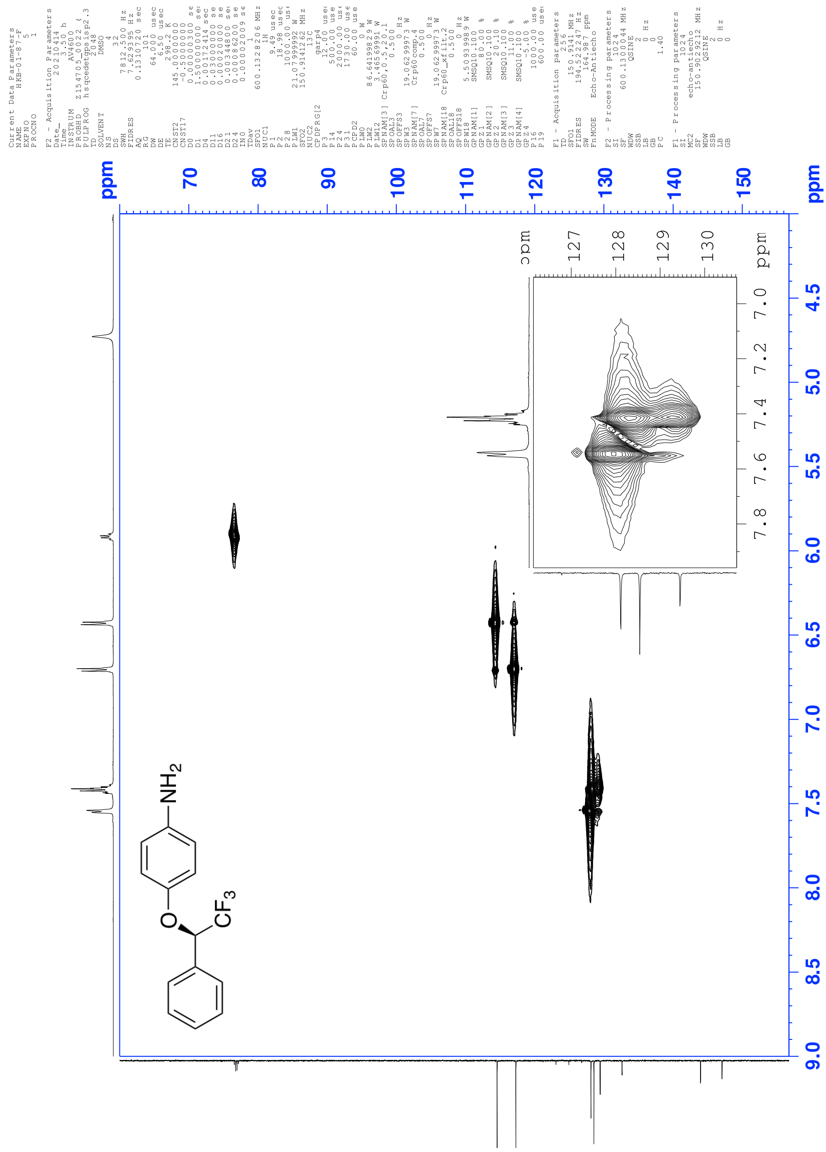

Figure 79: HSQC specter of compound **(*R*)-7**

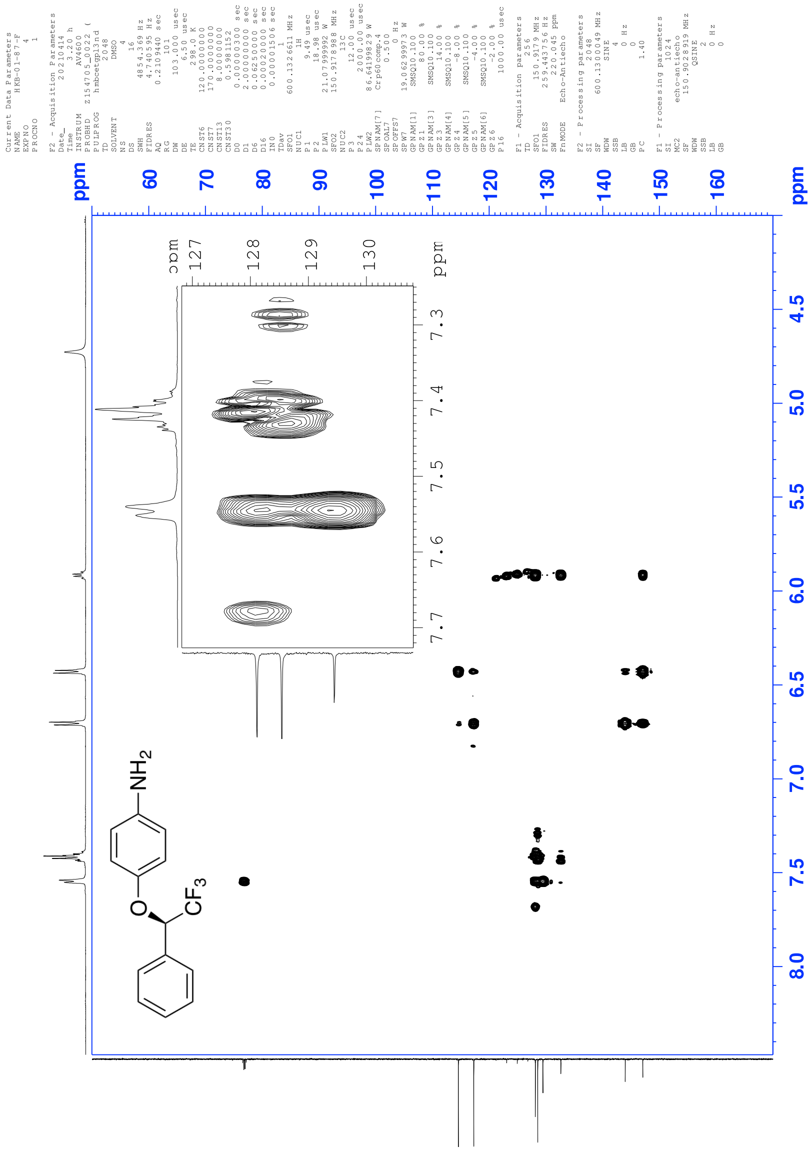

Figure 80: HMBC specter of compound **(*R*)-7**

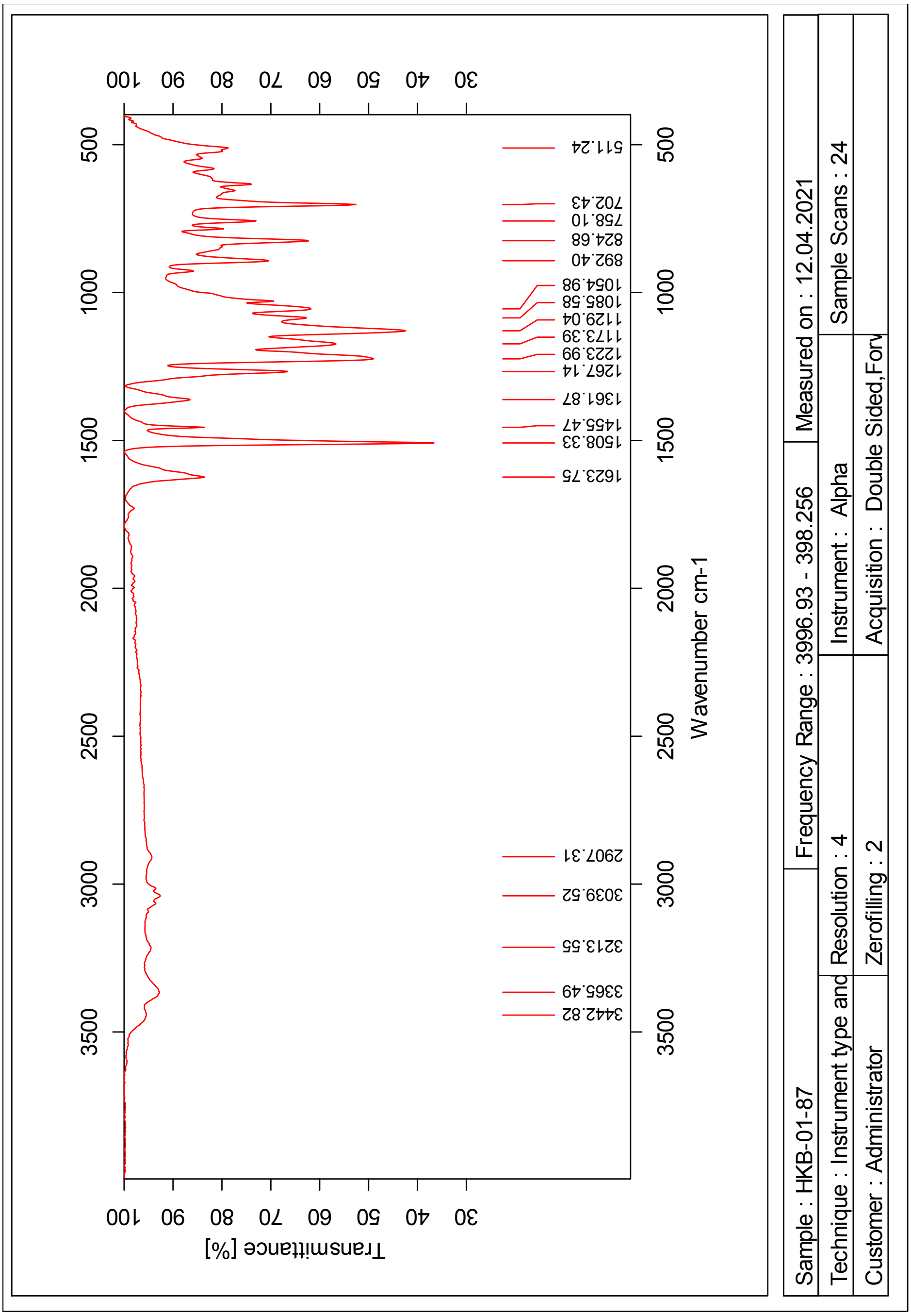

Figure 81: IR-spectrum of compound **(*R*)-7**

Elemental Composition Report

Page 1

Single Mass Analysis

Tolerance = 5.0 PPM / DBE: min = -10.0, max = 50.0
Element prediction: Off
Number of isotope peaks used for i-FIT = 6

Monoisotopic Mass, Even Electron Ions
3084 formula(e) evaluated with 9 results within limits (all results (up to 1000) for each mass)
Elements Used:
C: 0-100 H: 0-100 N: 0-6 O: 0-6 F: 0-3 S: 0-1 Br: 0-1 I: 0-2

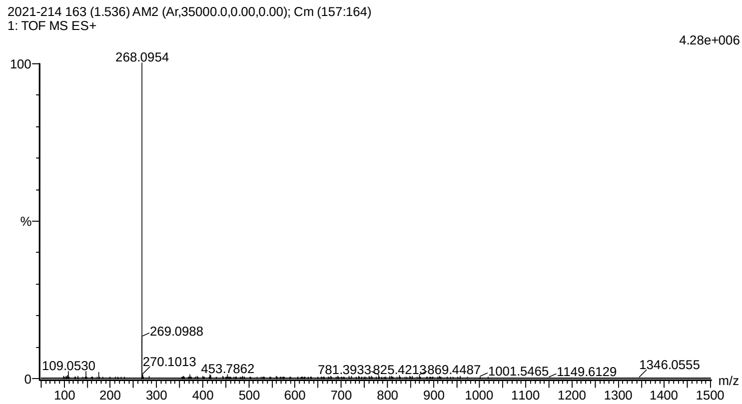

Minimum:				-10.0				
Maximum:		5.0	5.0	50.0				
Mass	Calc. Mass	mDa	PPM	DBE	i-FIT	Norm	Conf(%)	Formula
268.0954	268.0949	0.5	1.9	7.5	2873.5	0.076	92.66	C14 H13 N O F3
	268.0945	0.9	3.4	2.5	2876.0	2.617	7.30	C8 H15 N3 O6 F
	268.0949	0.5	1.9	-8.5	2881.3	7.924	0.04	C4 H25 N O F2 I
	268.0943	1.1	4.1	-1.5	2888.0	14.583	0.00	C6 H17 N3 O3 F3 S
	268.0967	-1.3	-4.8	1.5	2888.2	14.806	0.00	C8 H18 N3 O5 S
	268.0957	-0.3	-1.1	-9.5	2895.1	21.695	0.00	C4 H28 N O3 F S Br
	268.0946	0.8	3.0	-5.5	2895.1	21.735	0.00	C7 H27 N O2 S Br
	268.0948	0.6	2.2	-3.5	2895.7	22.280	0.00	C5 H21 N5 F2 Br
	268.0960	-0.6	-2.2	-7.5	2895.8	22.449	0.00	C2 H22 N5 O F3 Br

Figure 82: MS specter of compound ***(R)*-7**

.1.12 Spectroscopic data for Compound (*S*)-7

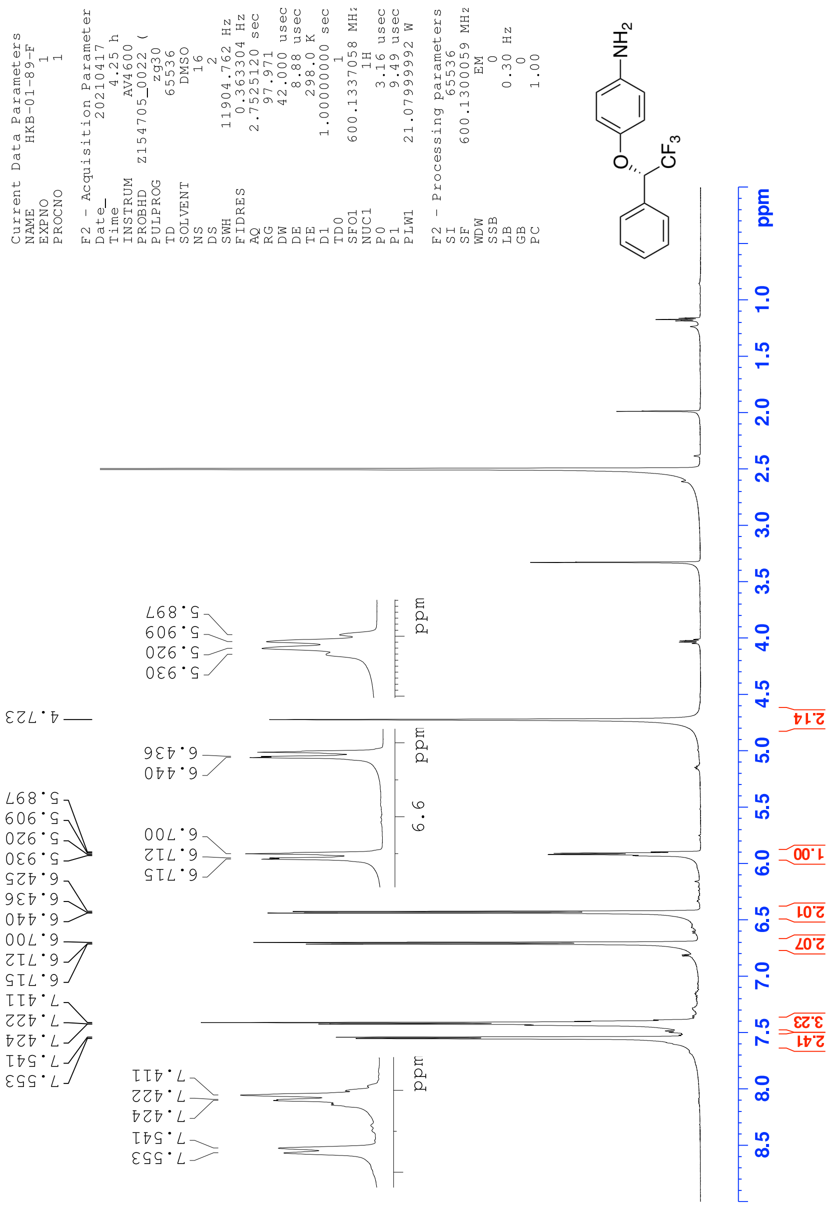

Figure 83: ^{1}H-NMR specter of compound **(*S*)-7**

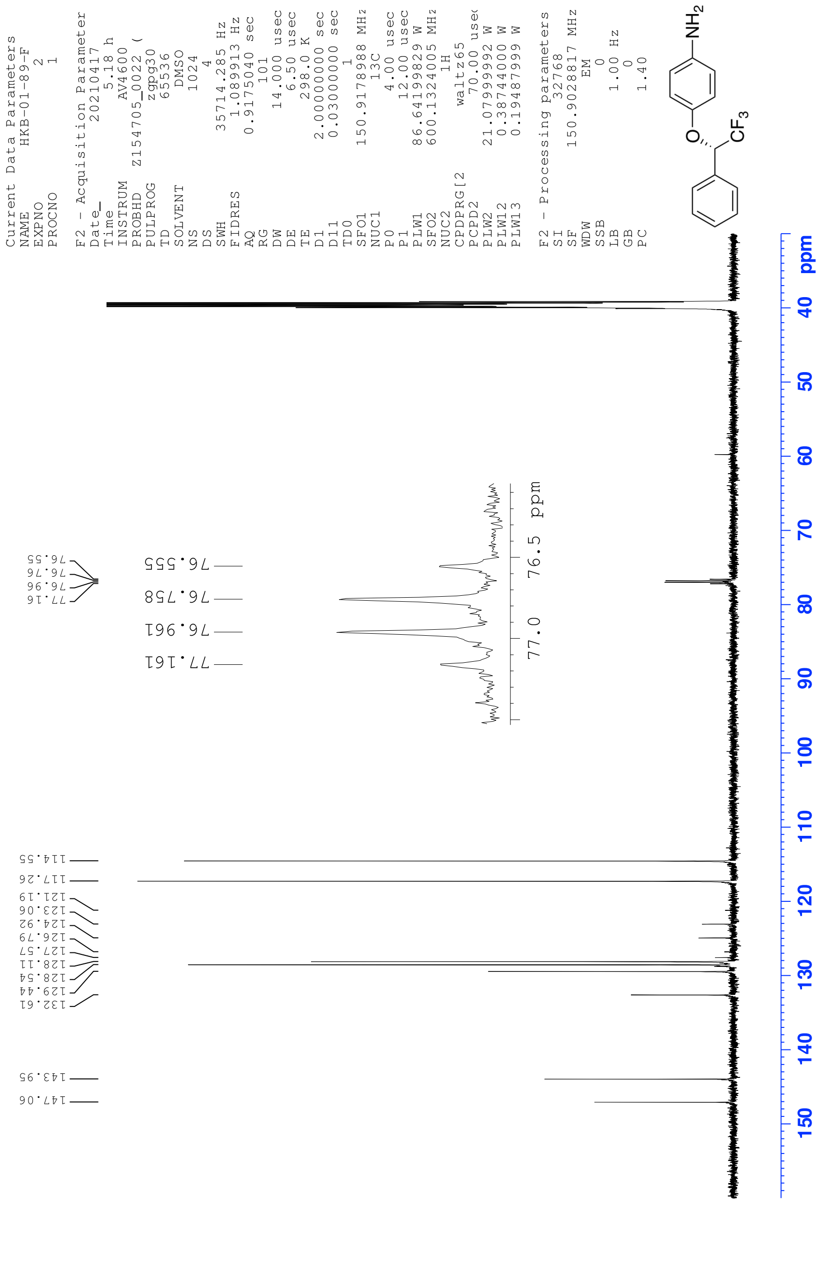

Figure 84: ^{89}C-NMR specter of compound ***(S)*-7**

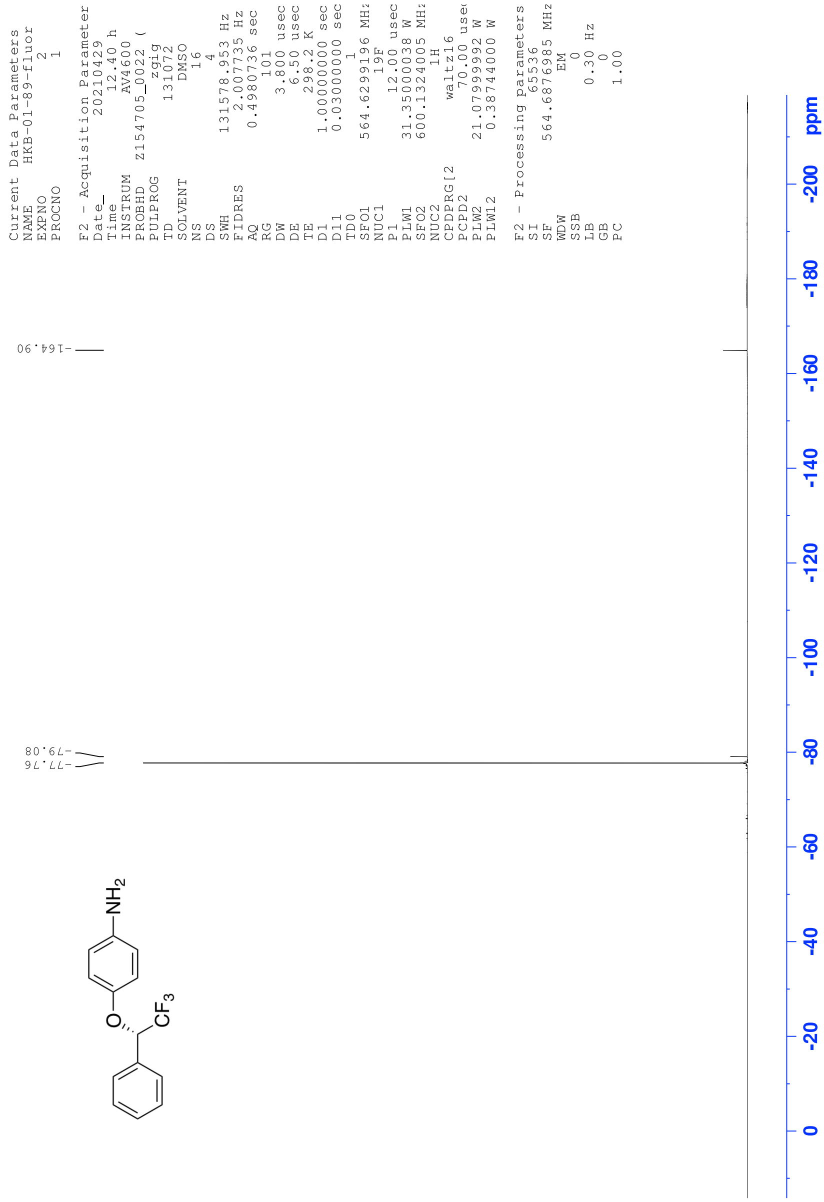

Figure 85: ^{19}F-NMR specter of compound ***(S)*-7**

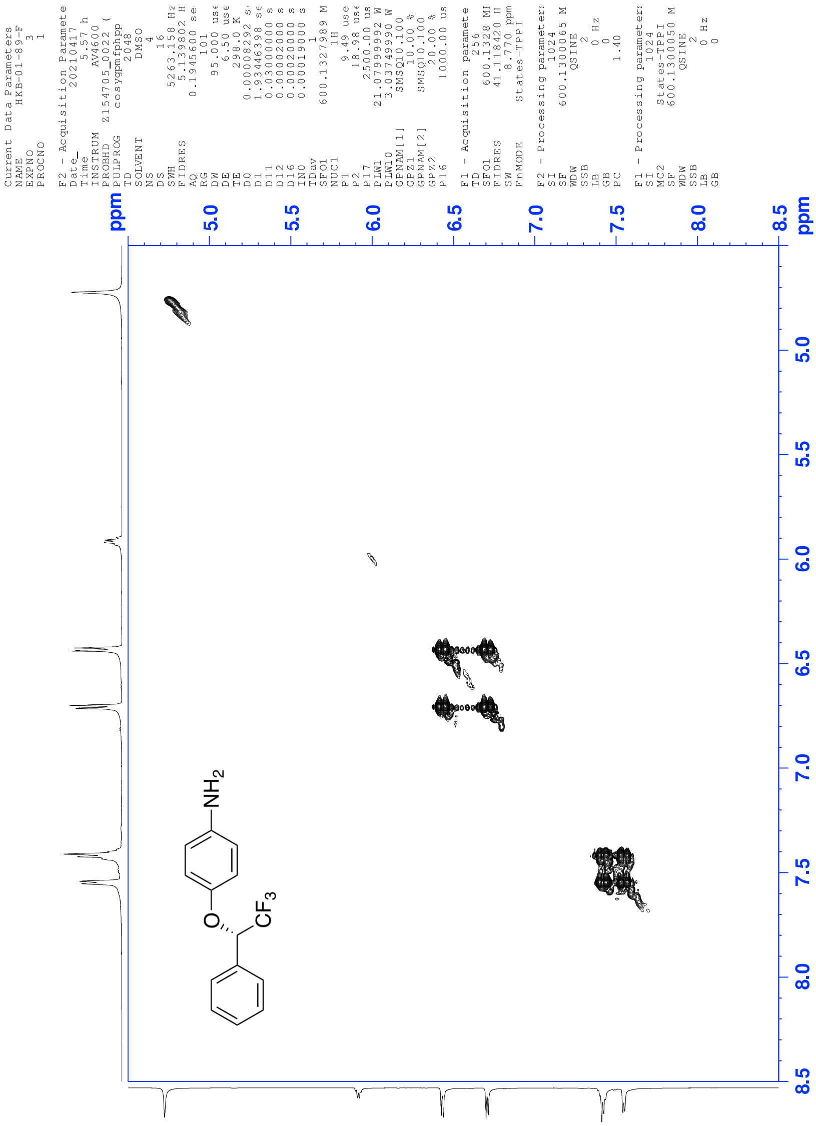

Figure 86: COSY specter of compound ***(S)*-7**

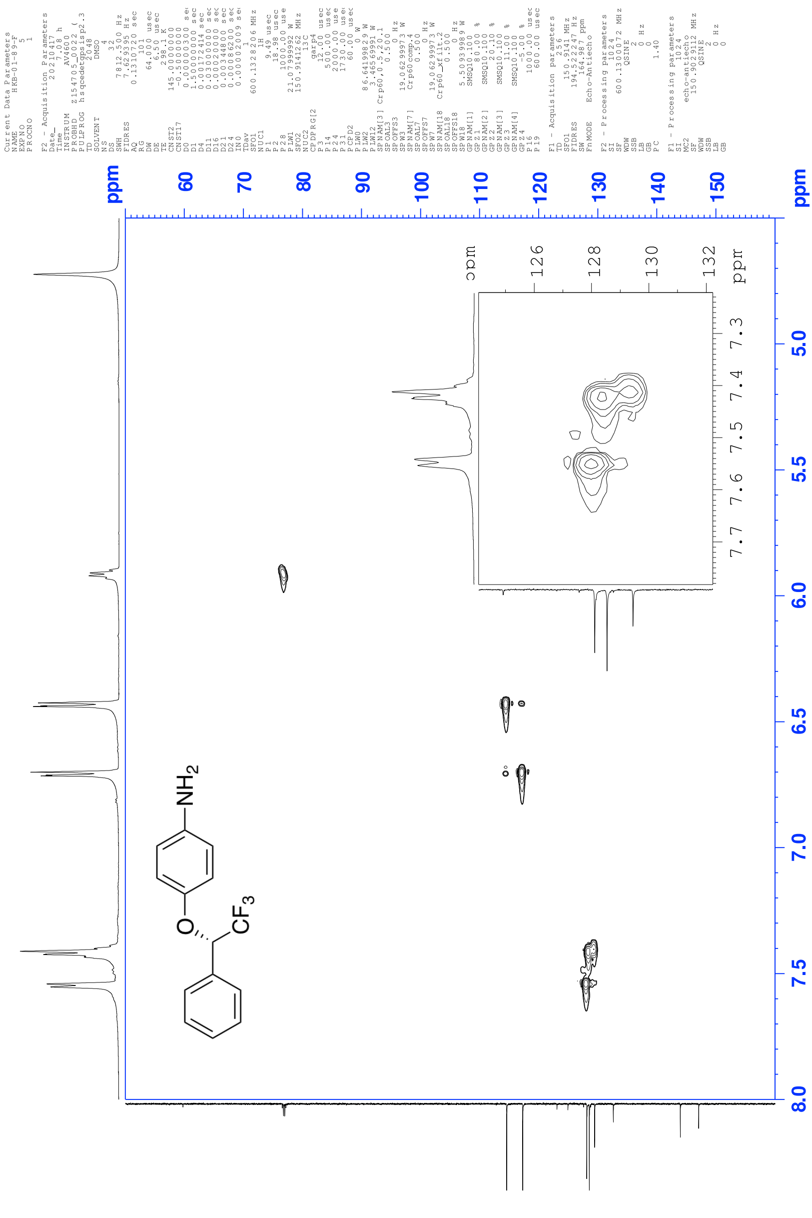

Figure 87: HSQC specter of compound ***(S)*-7**

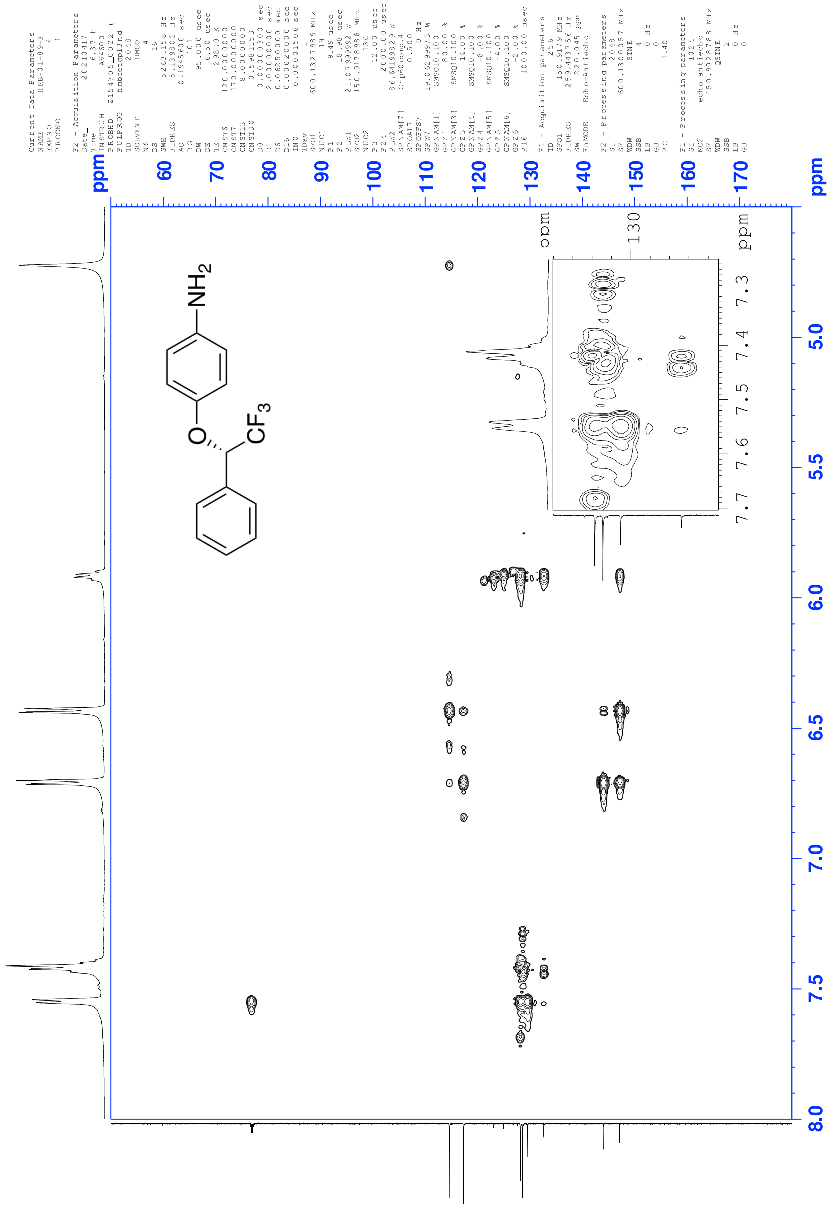

Figure 88: HMBC specter of compound **(*S*)-7**

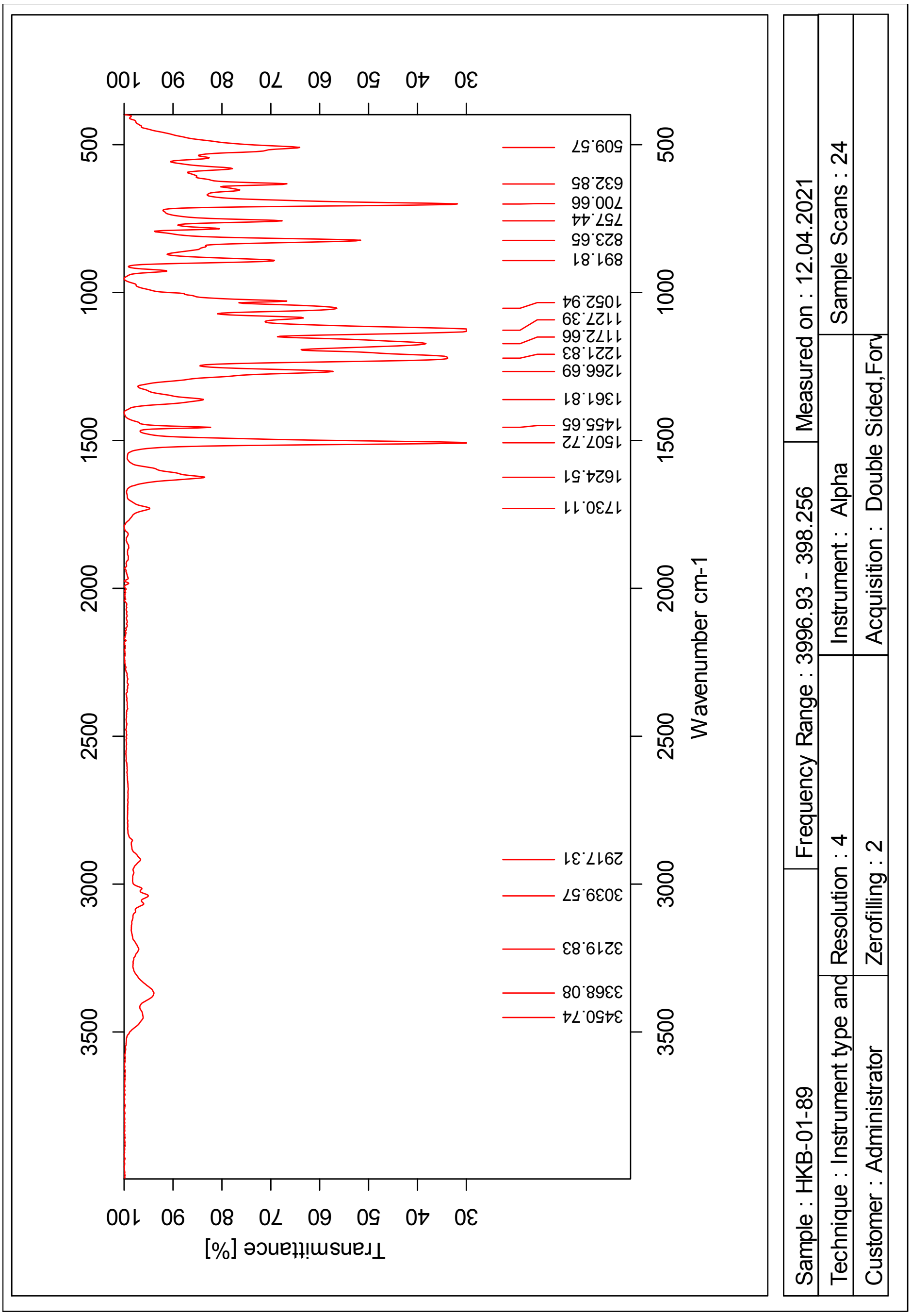

Figure 89: IR-spectrum of compound **(*S*)-7**

Elemental Composition Report **Page 1**

Single Mass Analysis
Tolerance = 5.0 PPM / DBE: min = -10.0, max = 50.0
Element prediction: Off
Number of isotope peaks used for i-FIT = 6

Monoisotopic Mass, Even Electron Ions
1070 formula(e) evaluated with 3 results within limits (all results (up to 1000) for each mass)
Elements Used:
C: 0-100 H: 0-100 N: 0-5 O: 0-12 F: 0-3
2021-281 176 (1.657) AM2 (Ar,35000.0,0.00,0.00); Cm (176:180)
1: TOF MS ES+

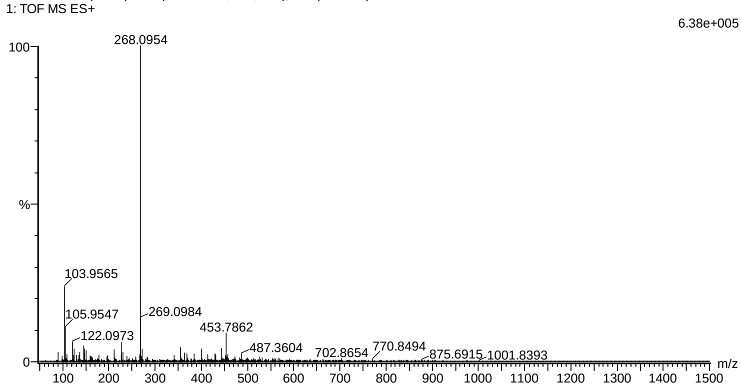

Mass	Calc. Mass	mDa	PPM	DBE	i-FIT	Norm	Conf(%)	Formula
Minimum:				-10.0				
Maximum:		5.0	5.0	50.0				
268.0954	268.0956	-0.2	-0.7	-1.5	2623.1	4.983	0.69	C5 H16 N3 O7 F2
	268.0949	0.5	1.9	7.5	2618.2	0.124	88.31	C14 H13 N O F3
	268.0945	0.9	3.4	2.5	2620.3	2.207	11.00	C8 H15 N3 O6 F

Figure 90: MS specter of compound **(*S*)-7**

.1.13 Spectroscopic data for Compound 8

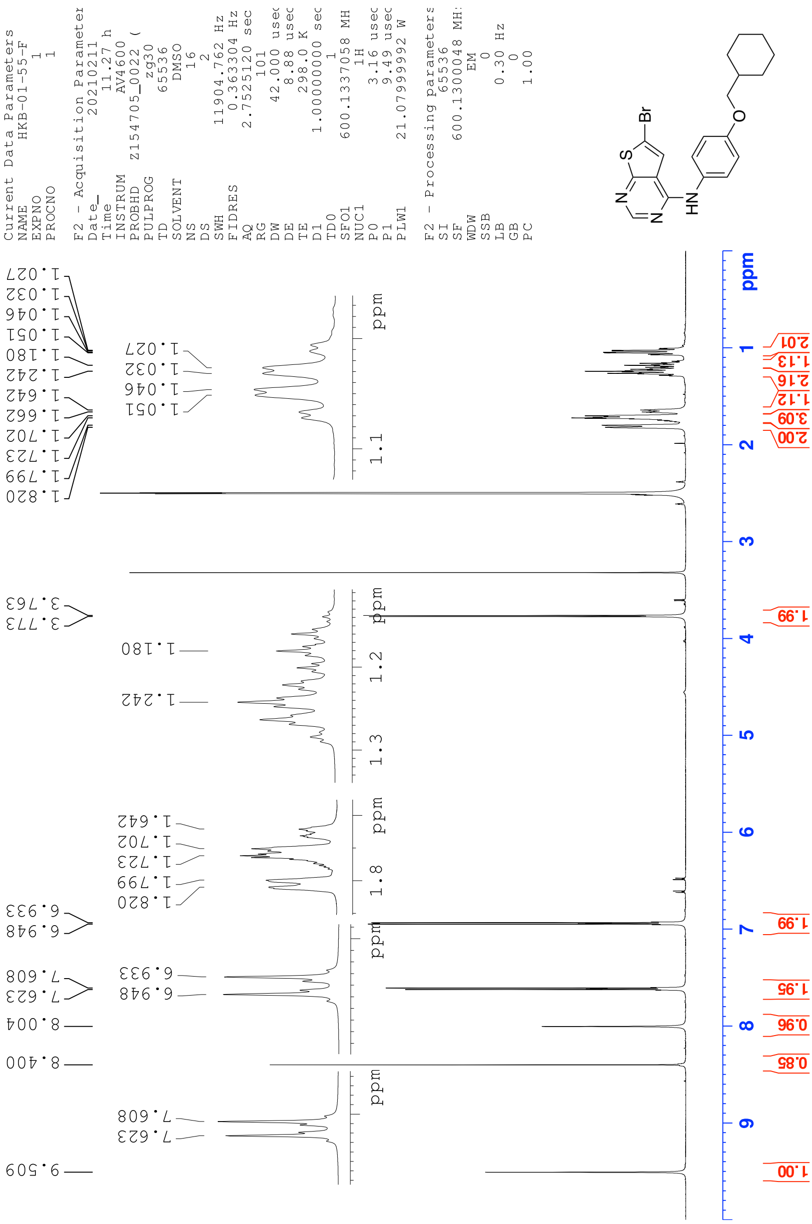

Figure 91: ^{1}H-NMR specter of compound **8**

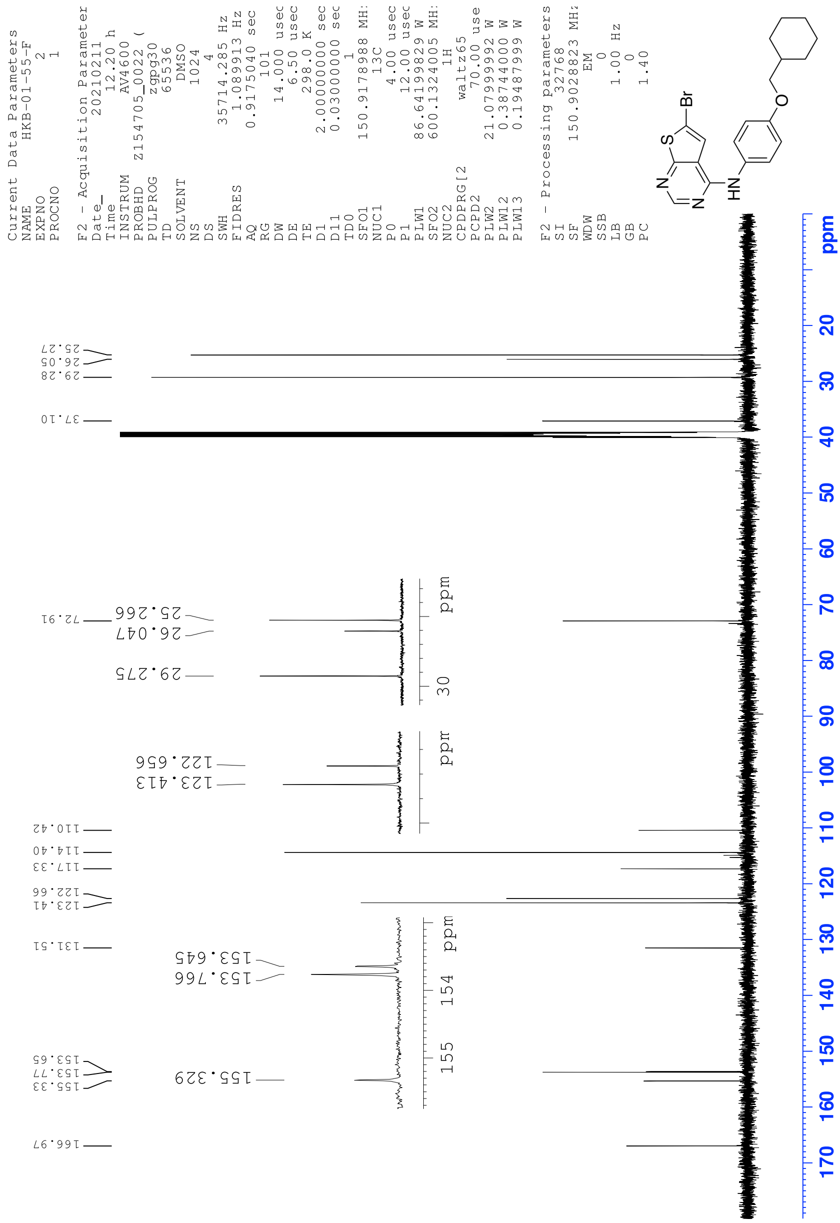

Figure 92: ^{13}C-NMR specter of compound **8**

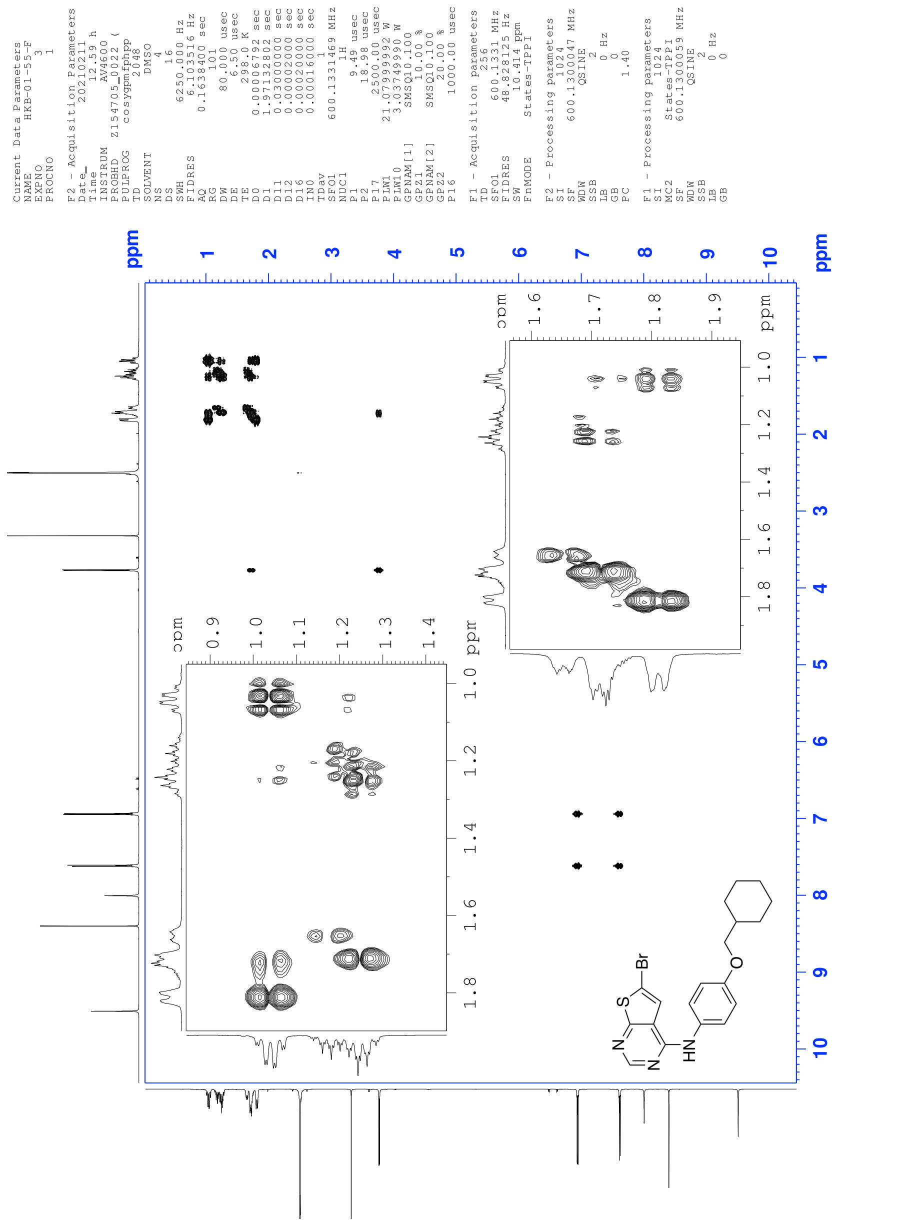

Figure 93: COSY specter of compound **8**

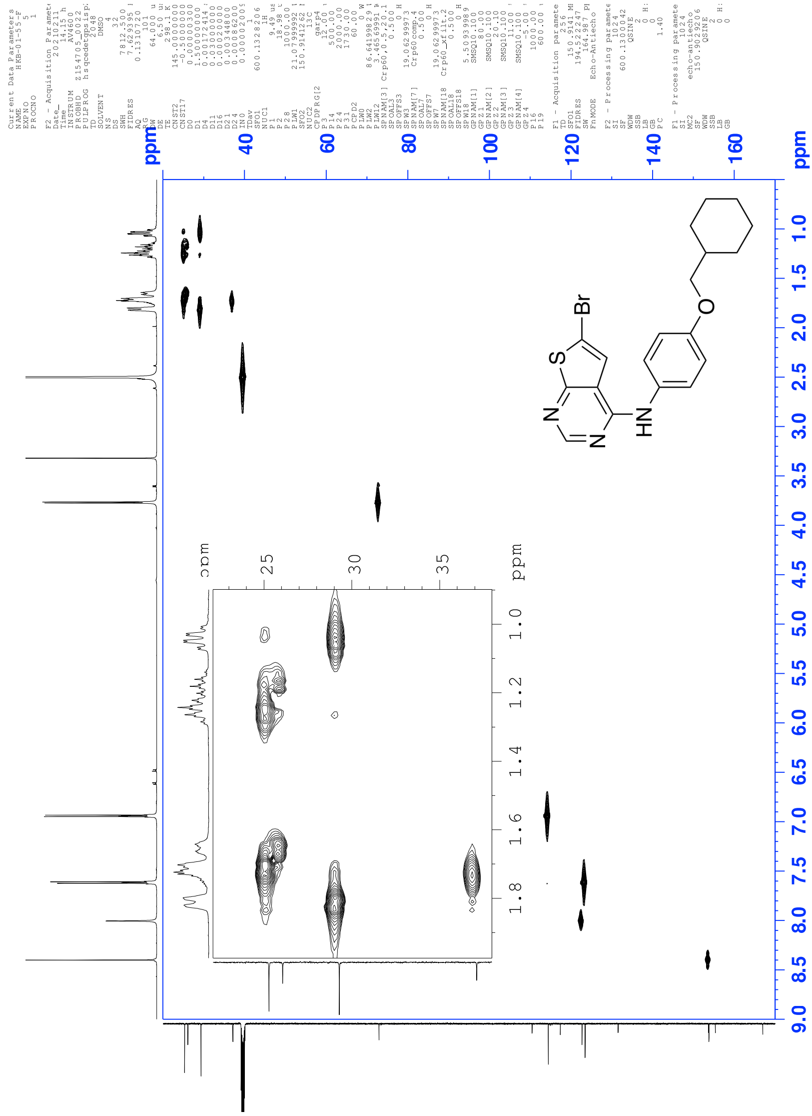

Figure 94: HSQC specter of compound **8**

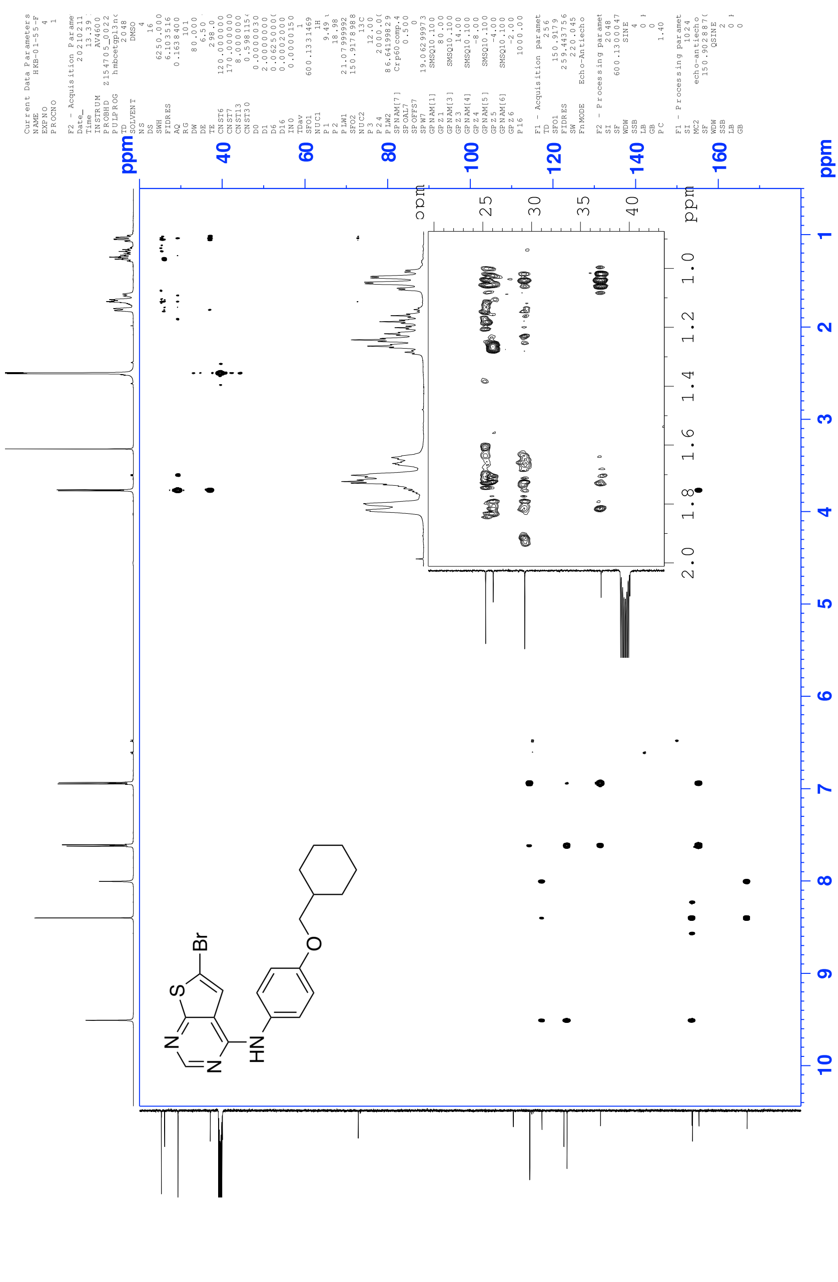

Figure 95: HMBC specter of compound **8**

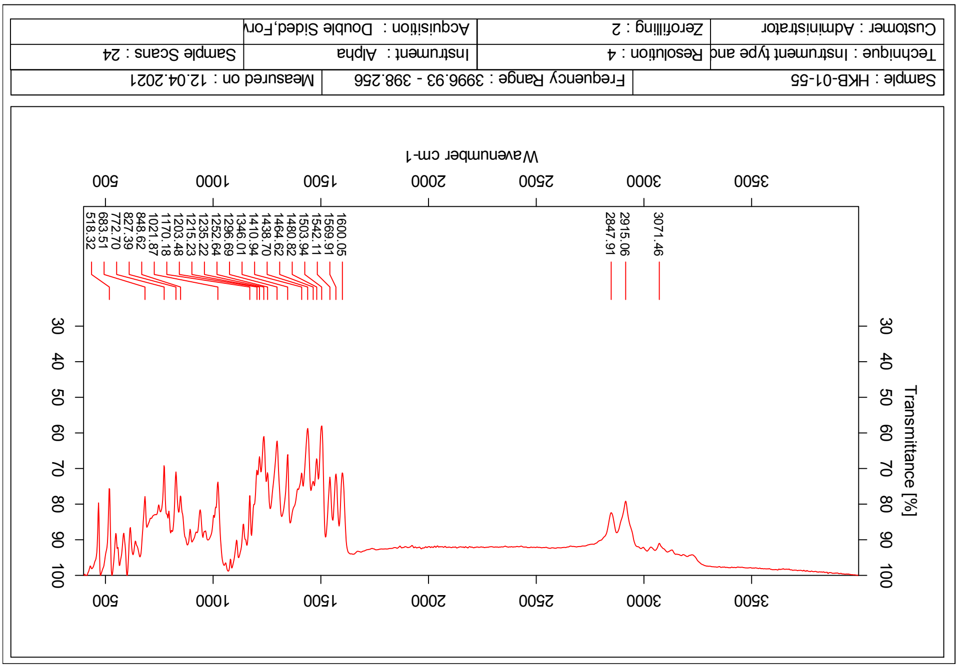

Figure 96: IR-spectrum of compound **8**

Elemental Composition Report **Page 1**

Single Mass Analysis
Tolerance = 2.0 PPM / DBE: min = -10.0, max = 50.0
Element prediction: Off
Number of isotope peaks used for i-FIT = 6

Monoisotopic Mass, Even Electron Ions
1509 formula(e) evaluated with 3 results within limits (all results (up to 1000) for each mass)
Elements Used:
C: 0-100 H: 0-100 N: 0-6 O: 0-6 S: 0-1 Br: 0-2

2021-197 119 (1.126) AM2 (Ar,35000.0,0.00,0.00); Cm (118:126)
1: TOF MS ES+

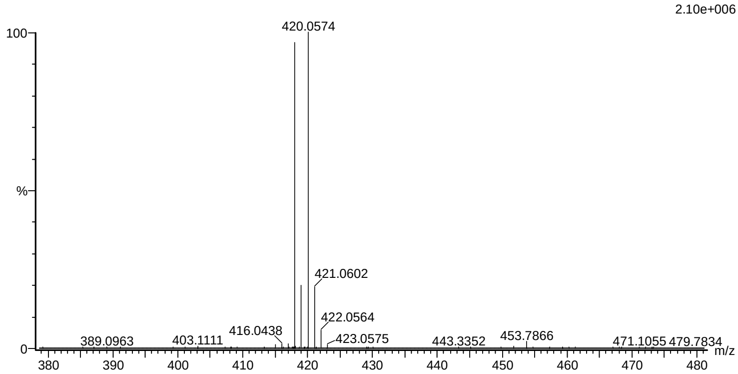

Mass	Calc. Mass	mDa	PPM	DBE	i-FIT	Norm	Conf(%)	Formula
Minimum:				-10.0				
Maximum:		5.0	2.0	50.0				
418.0593	418.0589	0.4	1.0	10.5	2444.9	0.000	100.00	C19 H21 N3 O S Br
	418.0586	0.7	1.7	-9.5	2469.4	24.489	0.00	C6 H34 N3 O5 S Br2
	418.0592	0.1	0.2	-0.5	2469.5	24.662	0.00	C14 H30 N O3 Br2

Figure 97: MS specter of compound **8**

.1.14 Spectroscopic data for Compound (*R*)-9

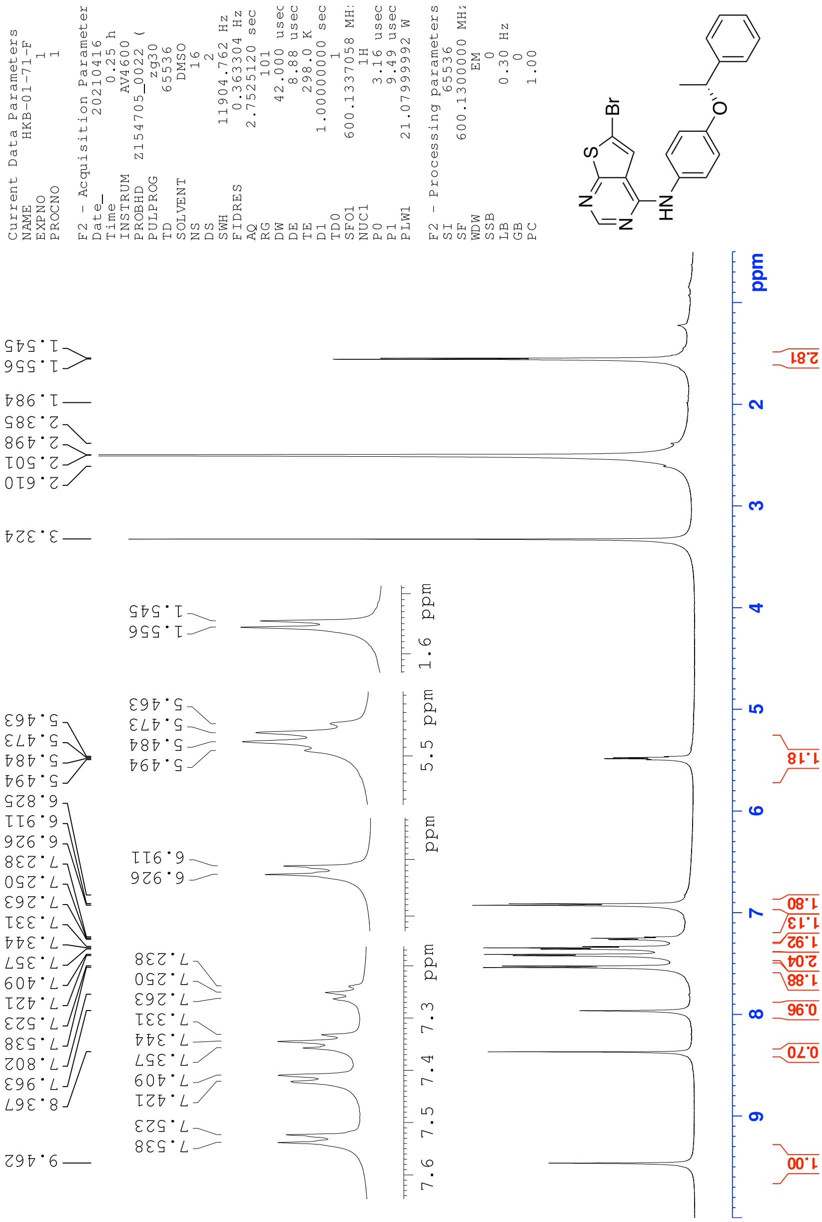

Figure 98: ^{1}H-NMR specter of compound **(*R*)-9**

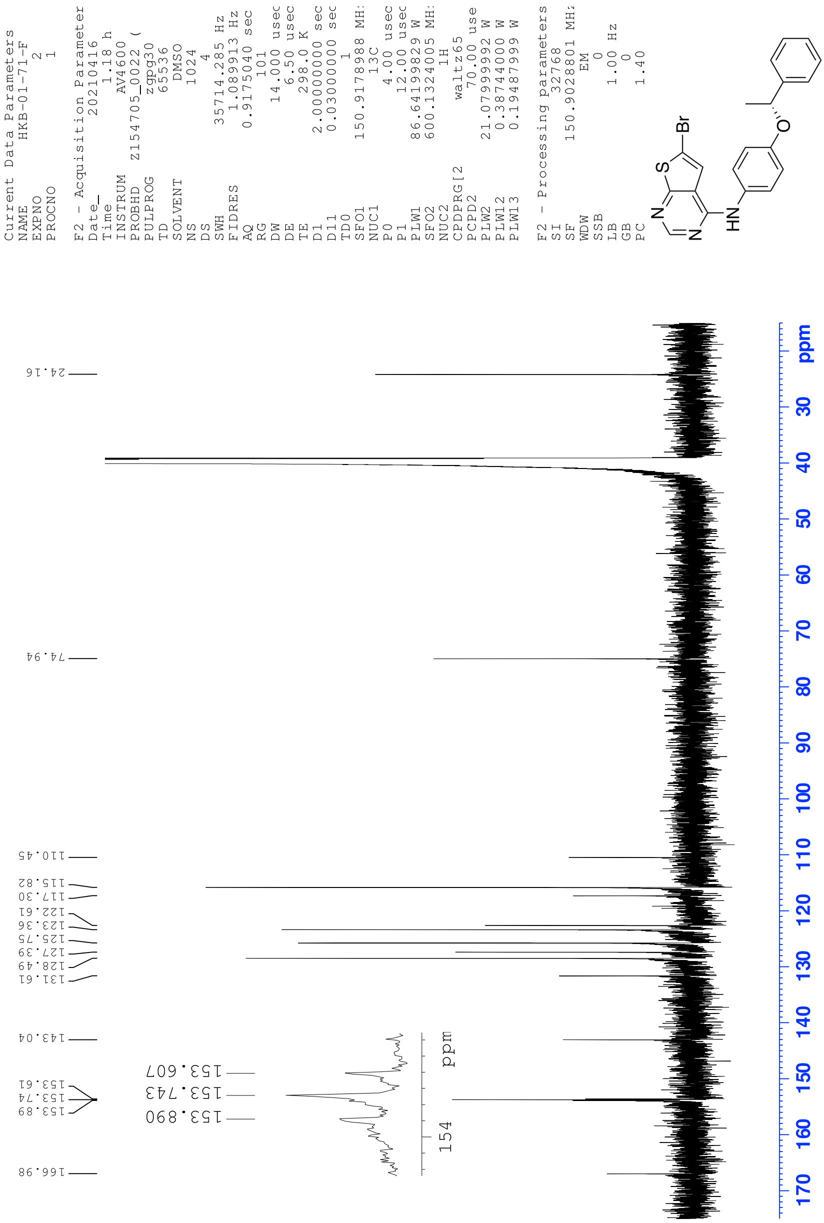

Figure 99: ^{13}C-NMR specter of compound ***(R)*-9**

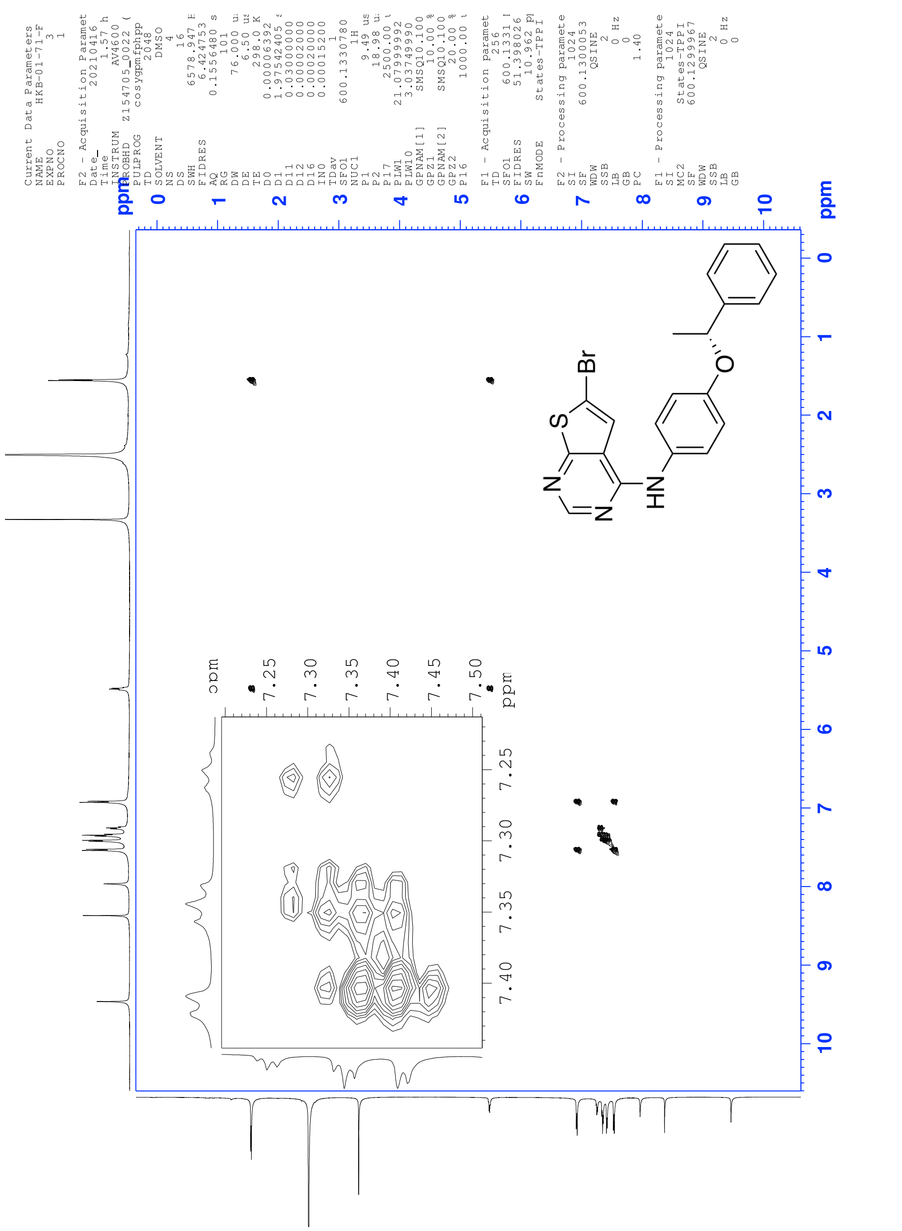

Figure 100: COSY specter of compound ***(R)*-9**

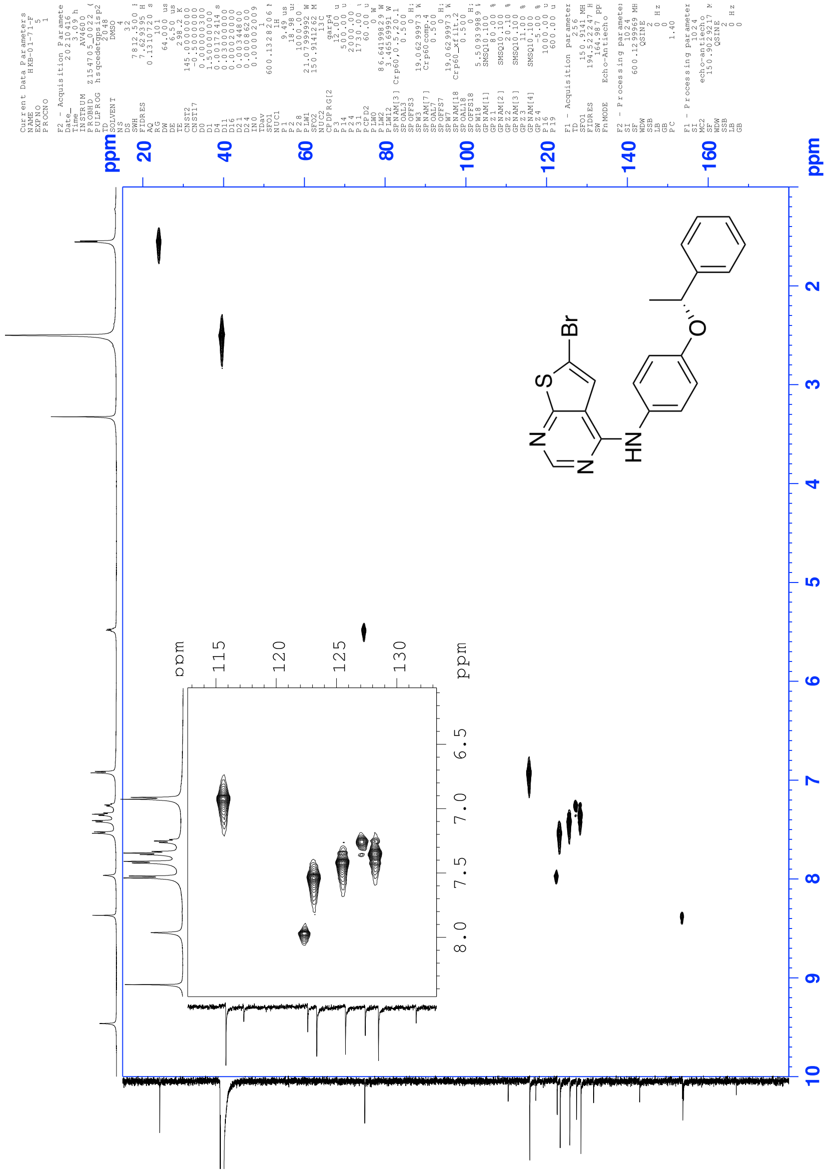

Figure 101: HSQC specter of compound **(*R*)-9**

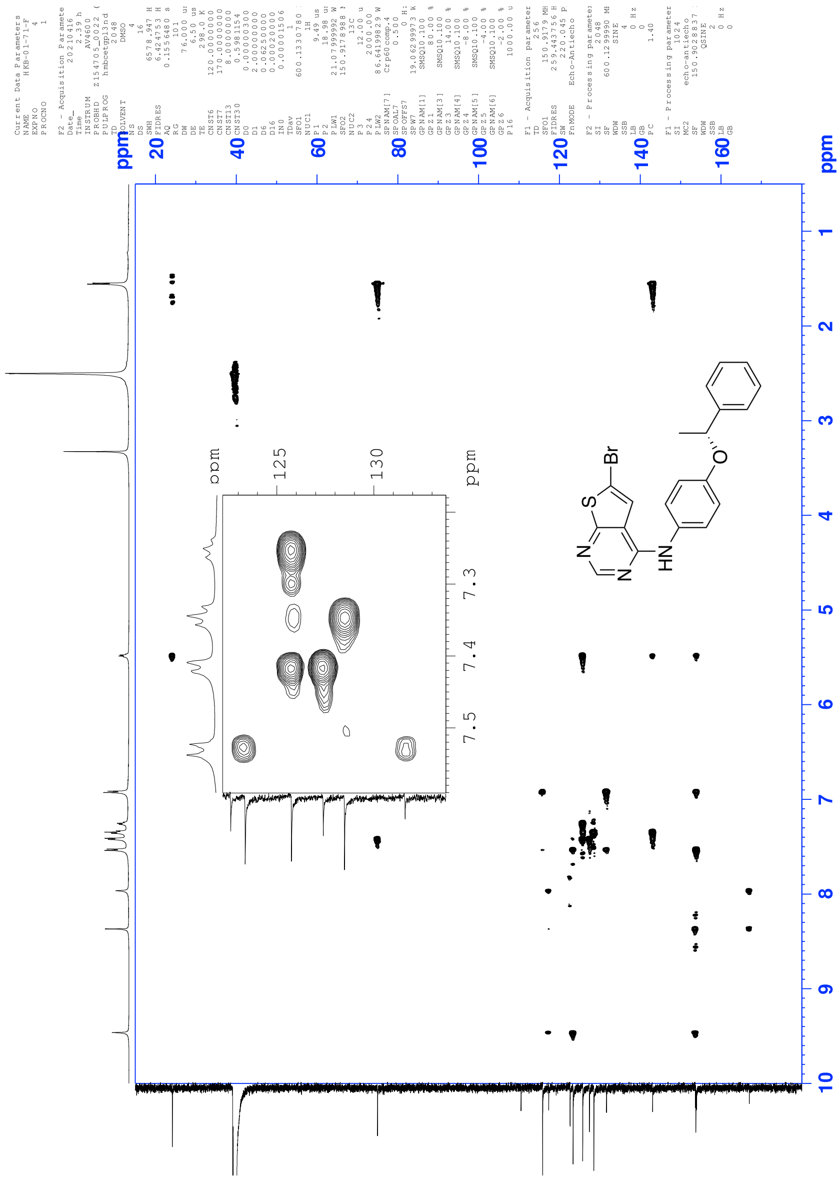

Figure 102: HMBC specter of compound **(*R*)-9**

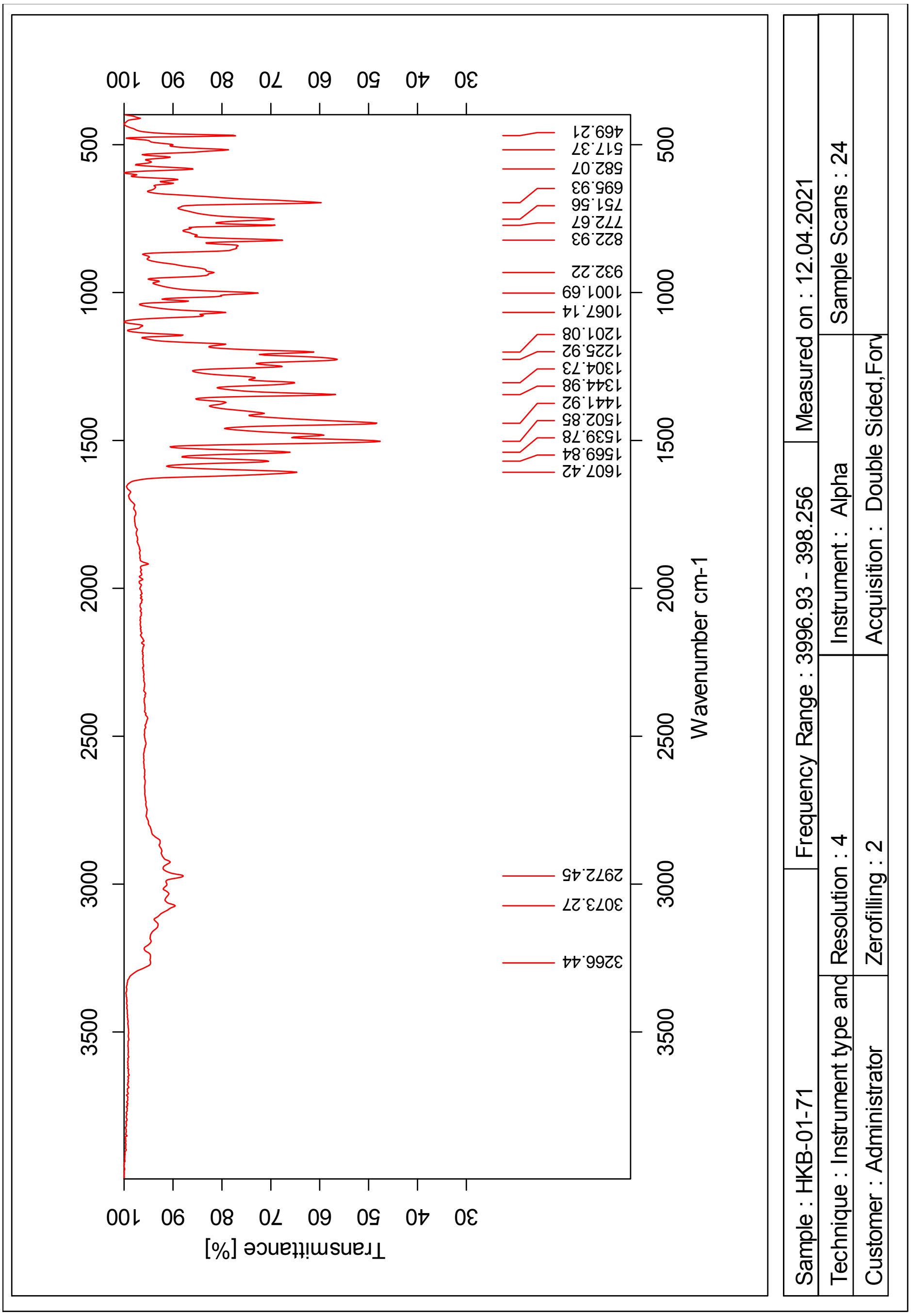

Figure 103: IR-spectrum of compound **(*R*)-9**

Elemental Composition Report

Page 1

Single Mass Analysis

Tolerance = 5.0 PPM / DBE: min = -10.0, max = 50.0
Element prediction: Off
Number of isotope peaks used for i-FIT = 6

Monoisotopic Mass, Even Electron Ions
2919 formula(e) evaluated with 8 results within limits (all results (up to 1000) for each mass)
Elements Used:
C: 0-100 H: 0-100 N: 0-6 O: 0-6 S: 0-1 Br: 0-2 I: 0-2

2021-203 89 (0.848) AM2 (Ar,35000.0,0.00,0.00); Cm (89:100)
1: TOF MS ES+

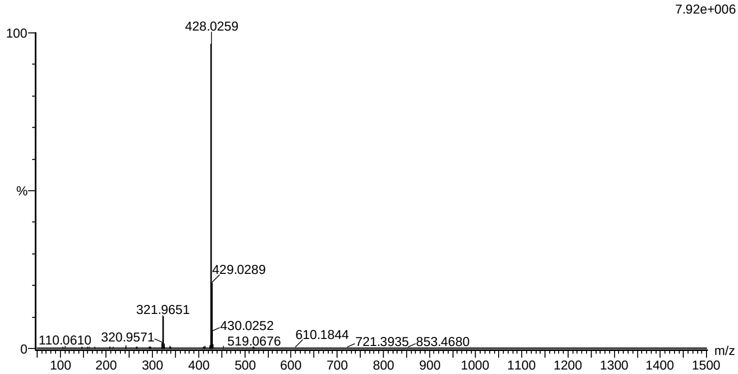

Mass	Calc. Mass	mDa	PPM	DBE	i-FIT	Norm	Conf(%)	Formula
Minimum:				-10.0				
Maximum:		5.0	5.0	50.0				
426.0278	426.0276	0.2	0.5	13.5	2580.3	0.000	100.00	C20 H17 N3 O S Br
	426.0287	-0.9	-2.1	-6.5	2594.2	13.953	0.00	C7 H30 N3 O2 S Br I
	426.0273	0.5	1.2	-6.5	2603.0	22.725	0.00	C7 H30 N3 O5 S Br2
	426.0293	-1.5	-3.5	2.5	2603.6	23.296	0.00	C15 H26 N Br I
	426.0279	-0.1	-0.2	2.5	2603.6	23.340	0.00	C15 H26 N O3 Br2
	426.0297	-1.9	-4.5	20.5	2611.7	31.439	0.00	C21 H8 N5 O4 S
	426.0274	0.4	0.9	5.5	2617.1	36.829	0.00	C11 H17 N5 O5 I
	426.0263	1.5	3.5	25.5	2617.6	37.351	0.00	C24 H4 N5 O4

Figure 104: MS specter of compound **(*R*)-9**

.1.15 Spectroscopic data for Compound (*S*)-9

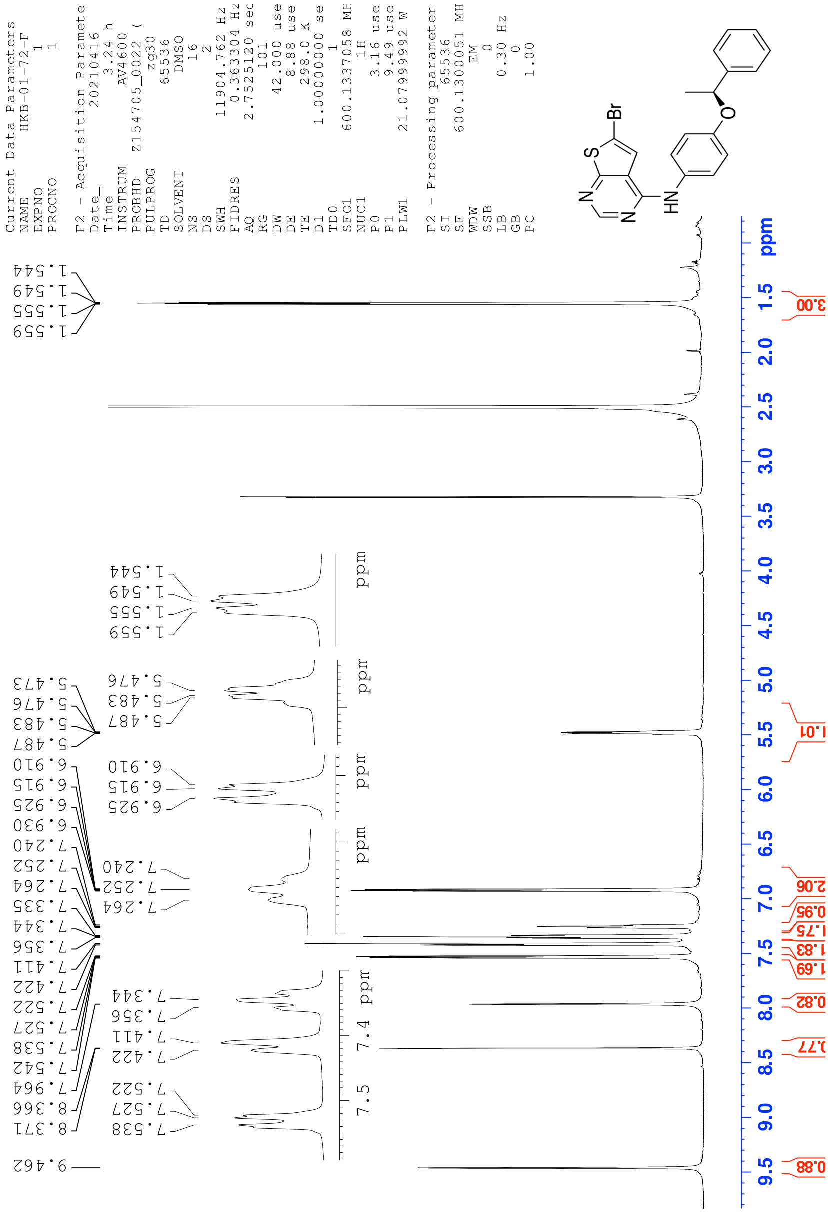

Figure 105: ^{1}H-NMR specter of compound **(*S*)-9**

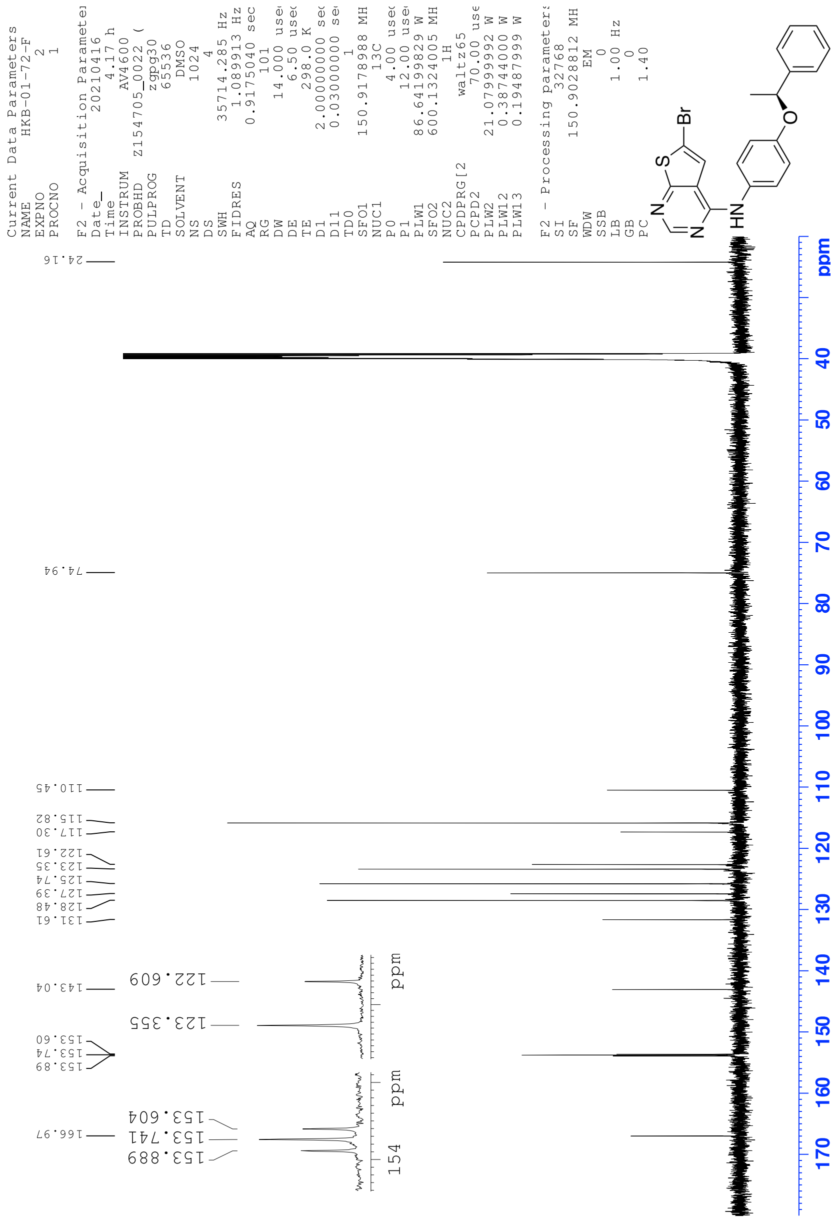

Figure 106: ^{13}C-NMR specter of compound ***(S)*-9**

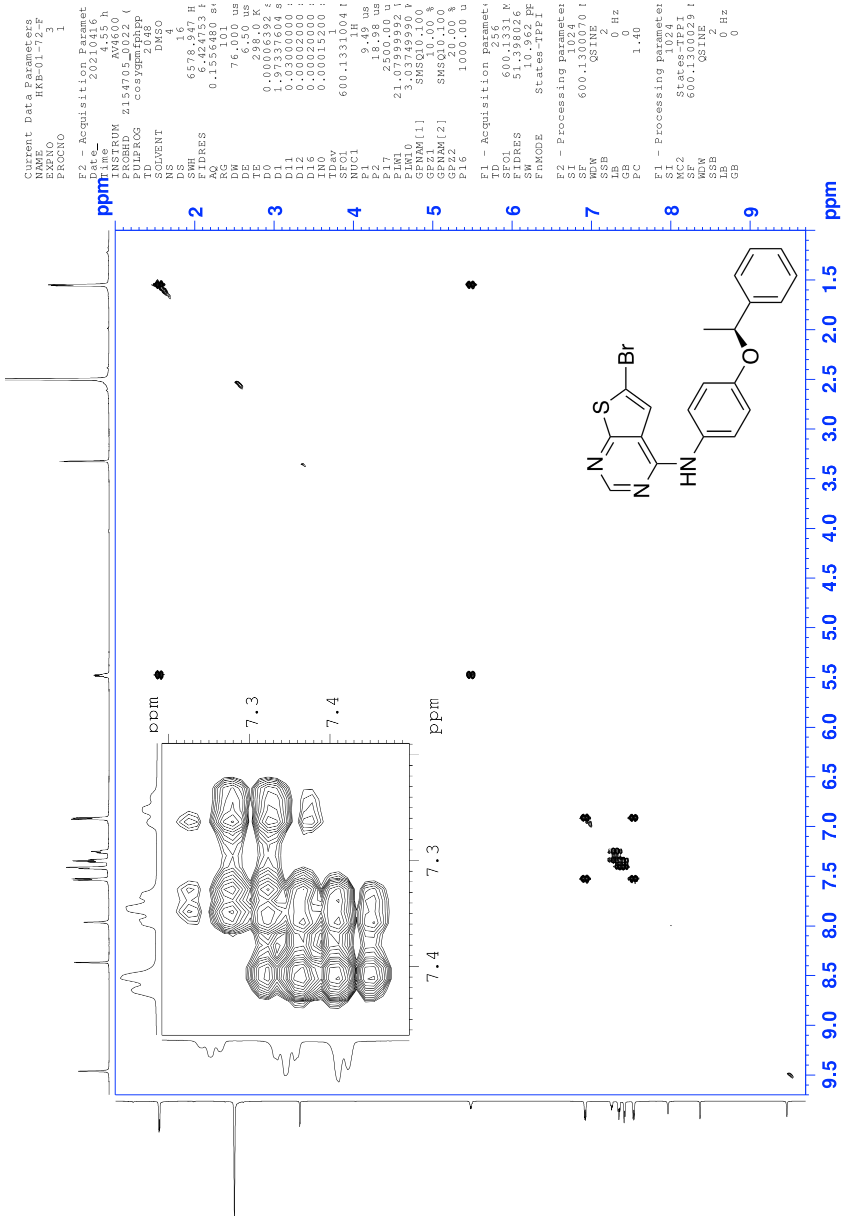

Figure 107: COSY specter of compound ***(S)*-9**

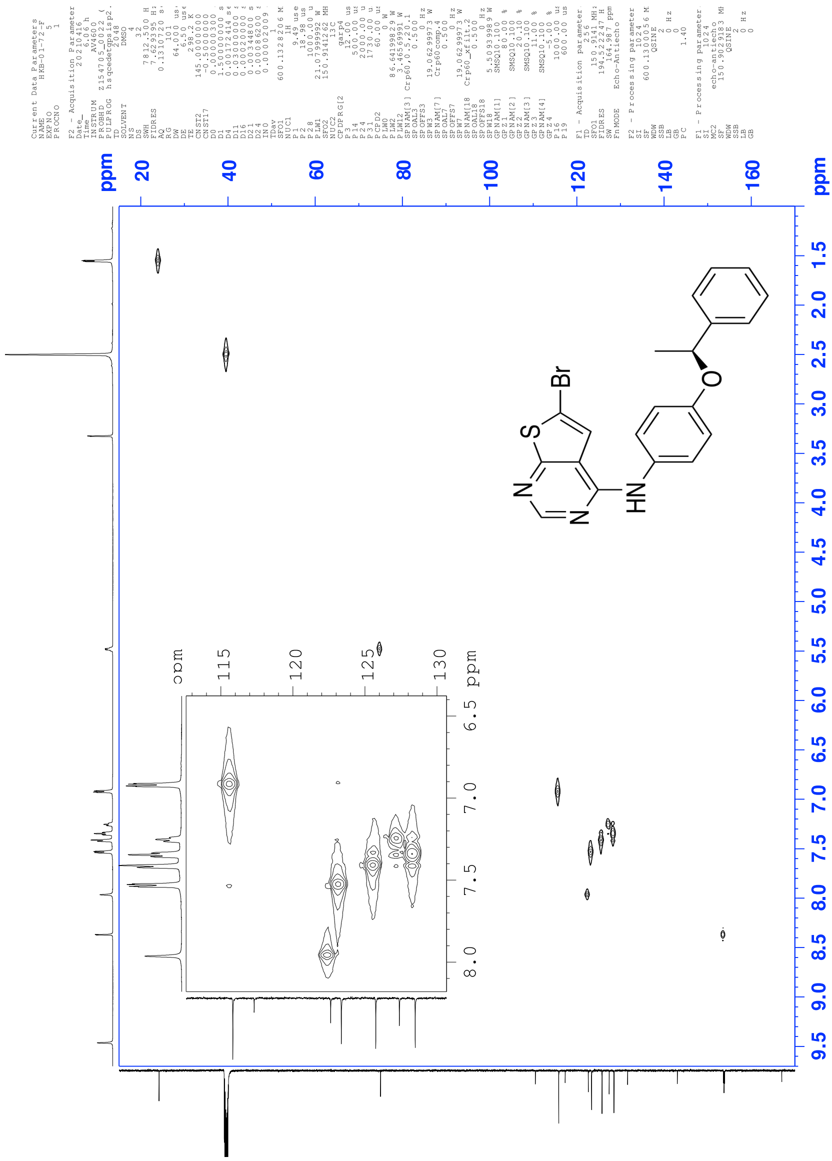

Figure 108: HSQC specter of compound ***(S)*-9**

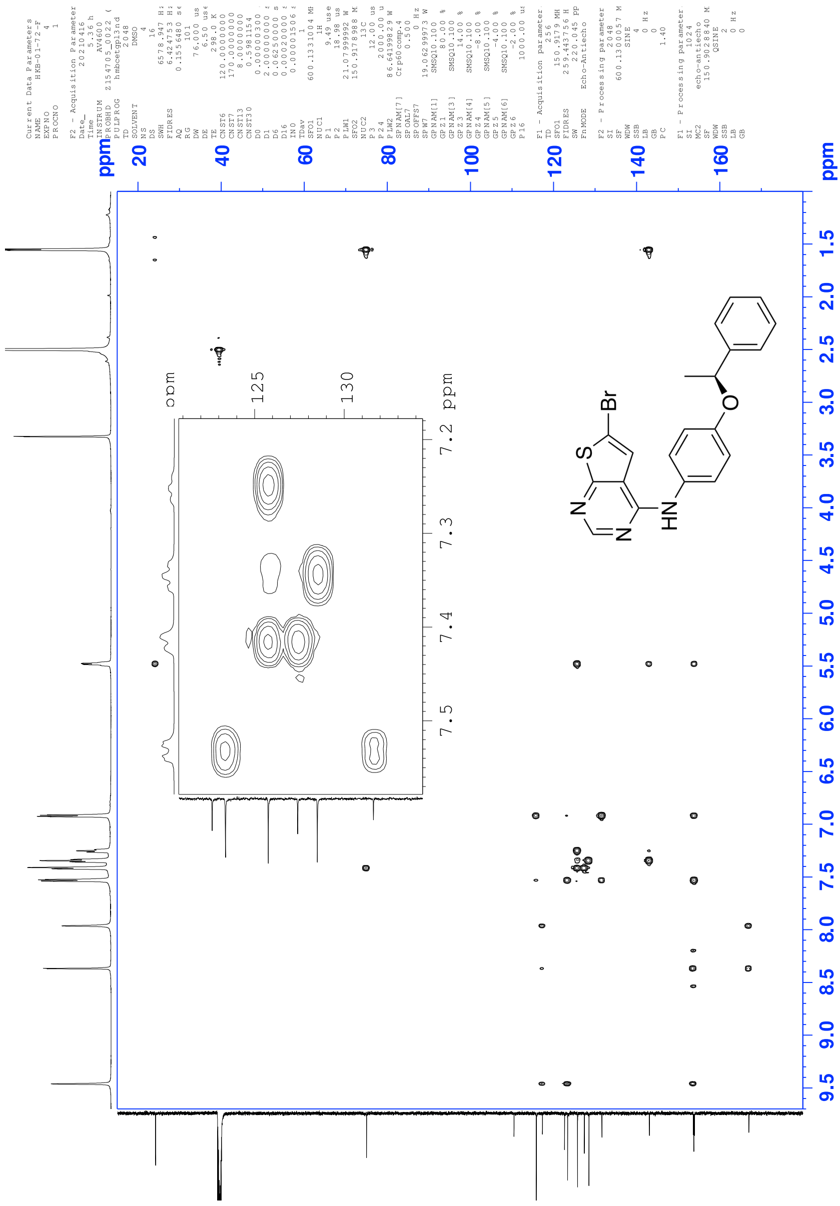

Figure 109: HMBC specter of compound **(*S*)-9**

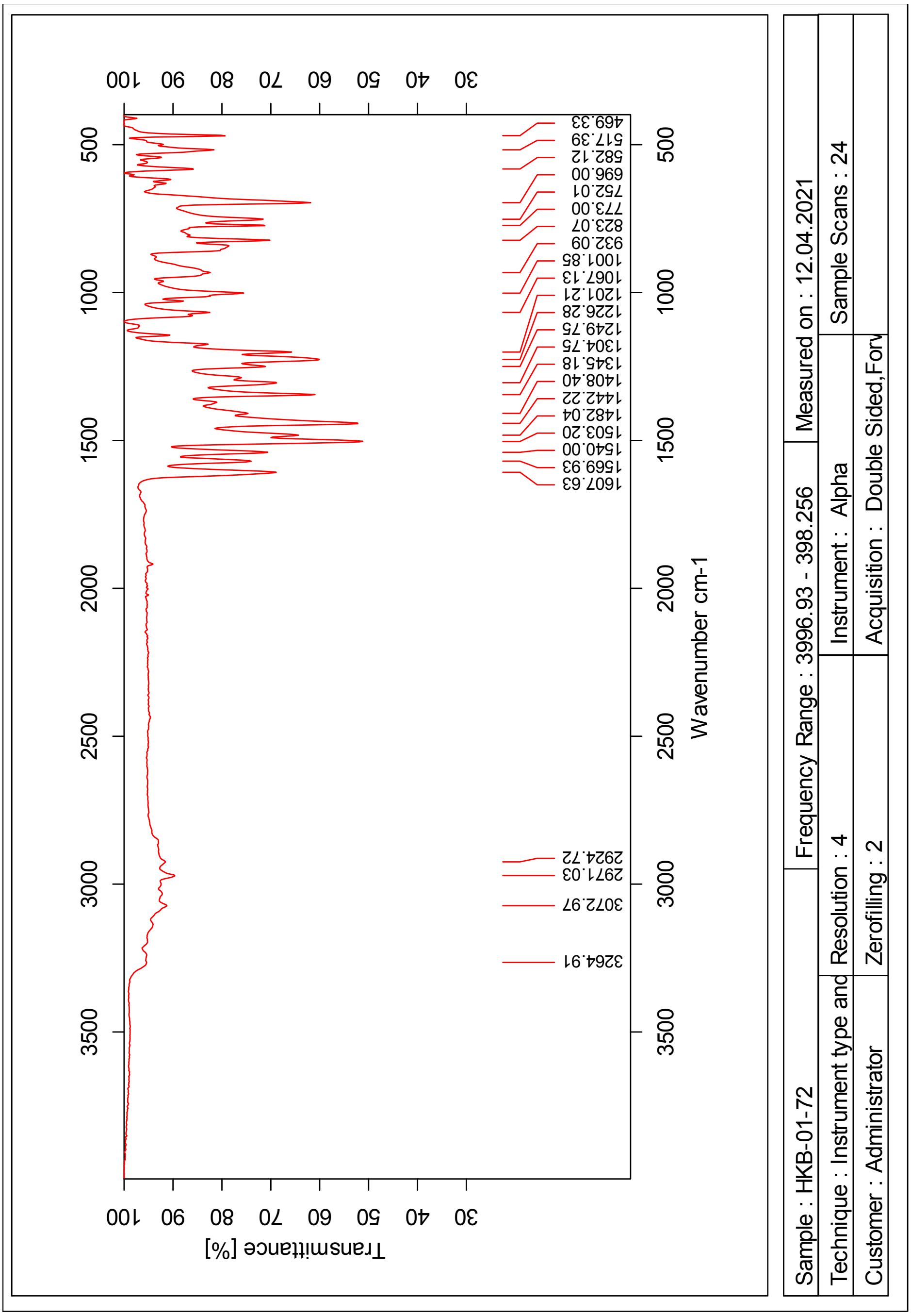

Figure 110: IR-spectrum of compound **(*S*)-9**

Elemental Composition Report

Page 1

Single Mass Analysis

Tolerance = 5.0 PPM / DBE: min = -10.0, max = 50.0
Element prediction: Off
Number of isotope peaks used for i-FIT = 6

Monoisotopic Mass, Even Electron Ions
2919 formula(e) evaluated with 8 results within limits (all results (up to 1000) for each mass)
Elements Used:
C: 0-100 H: 0-100 N: 0-6 O: 0-6 S: 0-1 Br: 0-2 I: 0-2

2021-204 96 (0.909) AM2 (Ar,35000.0,0.00,0.00); Cm (96:112)
1: TOF MS ES+

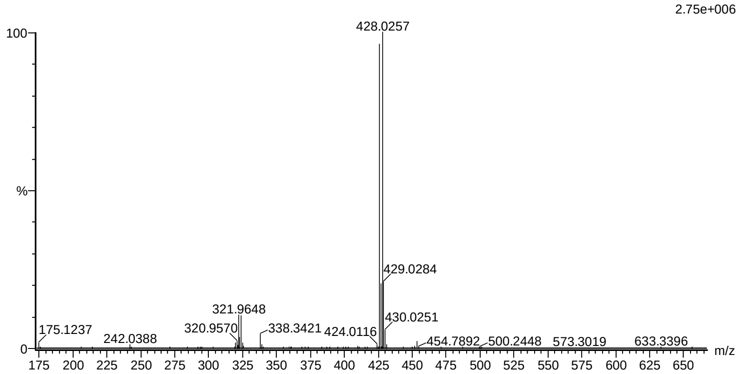

Mass	Calc. Mass	mDa	PPM	DBE	i-FIT	Norm	Conf(%)	Formula
Minimum:				-10.0				
Maximum:		5.0	5.0	50.0				
426.0278	426.0276	0.2	0.5	13.5	2276.8	0.000	100.00	C20 H17 N3 O S Br
	426.0287	-0.9	-2.1	-6.5	2293.7	16.900	0.00	C7 H30 N3 O2 S Br I
	426.0273	0.5	1.2	-6.5	2301.4	24.502	0.00	C7 H30 N3 O5 S Br2
	426.0279	-0.1	-0.2	2.5	2302.8	25.997	0.00	C15 H26 N O3 Br2
	426.0293	-1.5	-3.5	2.5	2303.0	26.113	0.00	C15 H26 N Br I
	426.0297	-1.9	-4.5	20.5	2310.6	33.714	0.00	C21 H8 N5 O4 S
	426.0274	0.4	0.9	5.5	2316.1	39.265	0.00	C11 H17 N5 O5 I
	426.0263	1.5	3.5	25.5	2316.7	39.804	0.00	C24 H4 N5 O4

Figure 111: MS specter of compound ***(S)*-9**

.1.16 Spectroscopic data for Compound (*rac*)-10

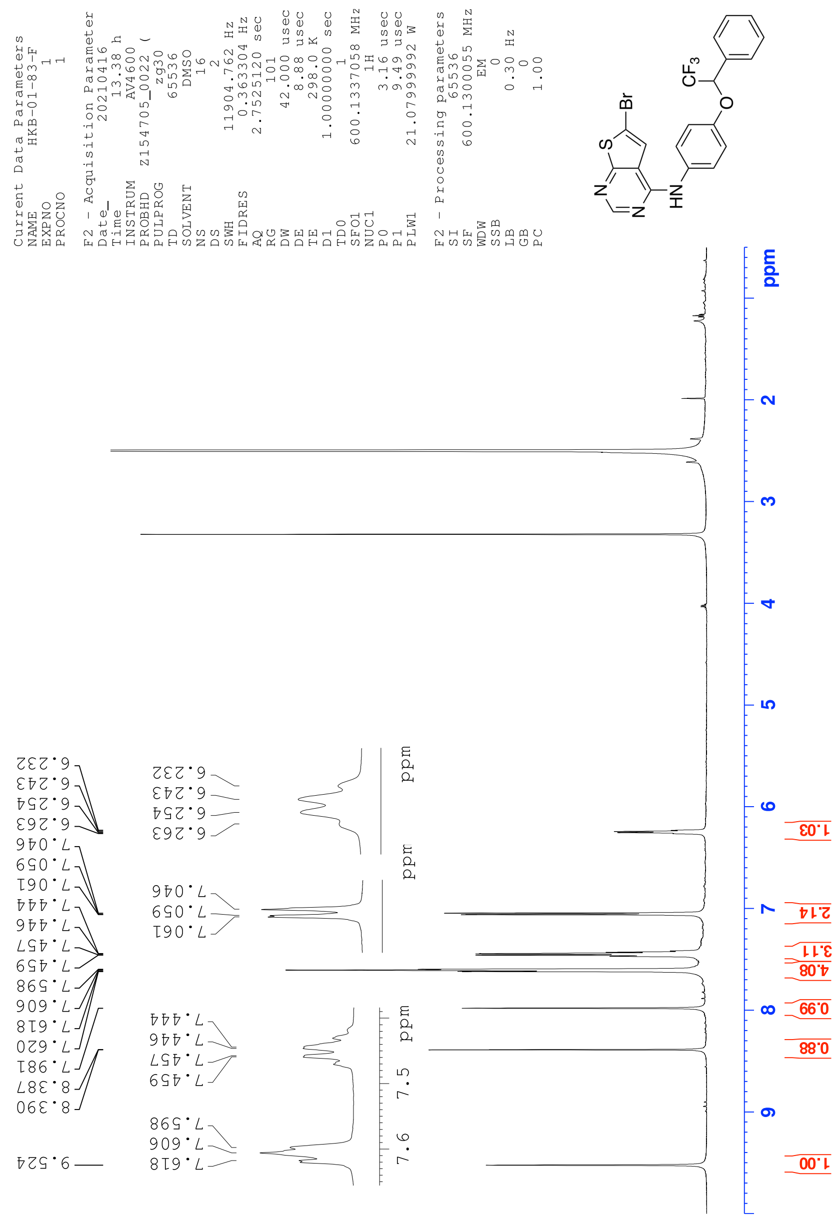

Figure 112: [1]H-NMR specter of compound **(*rac*)-10**

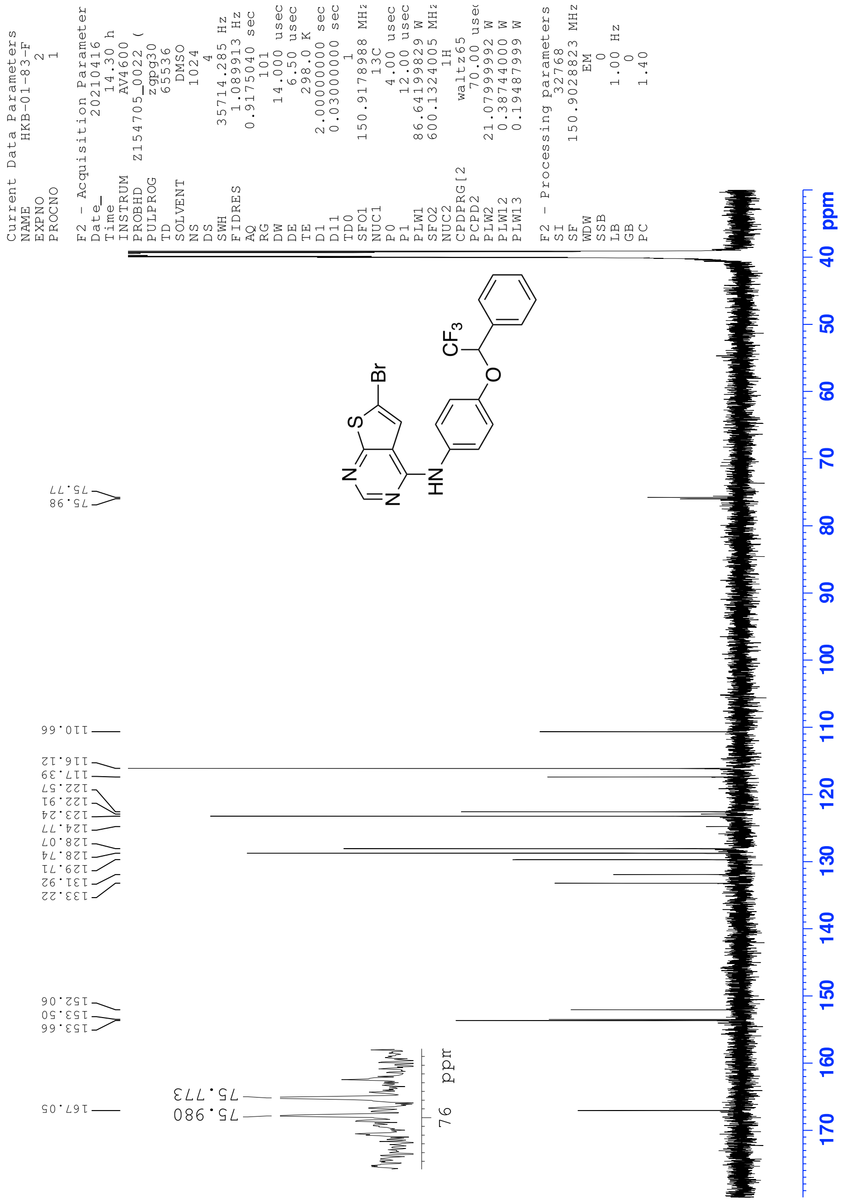

Figure 113: ^{13}C-NMR specter of compound **(*rac*)-10**

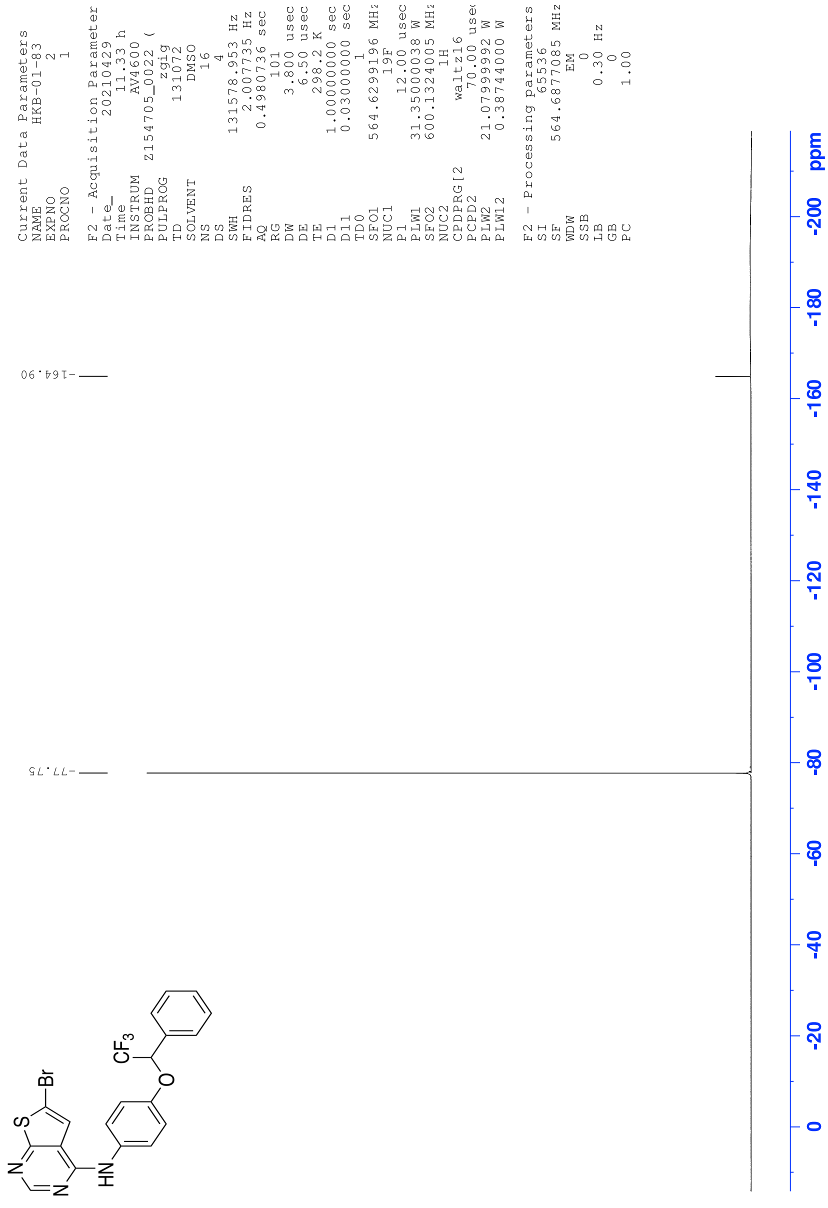

Figure 114: [19]F-NMR specter of compound ***(rac)*-10**

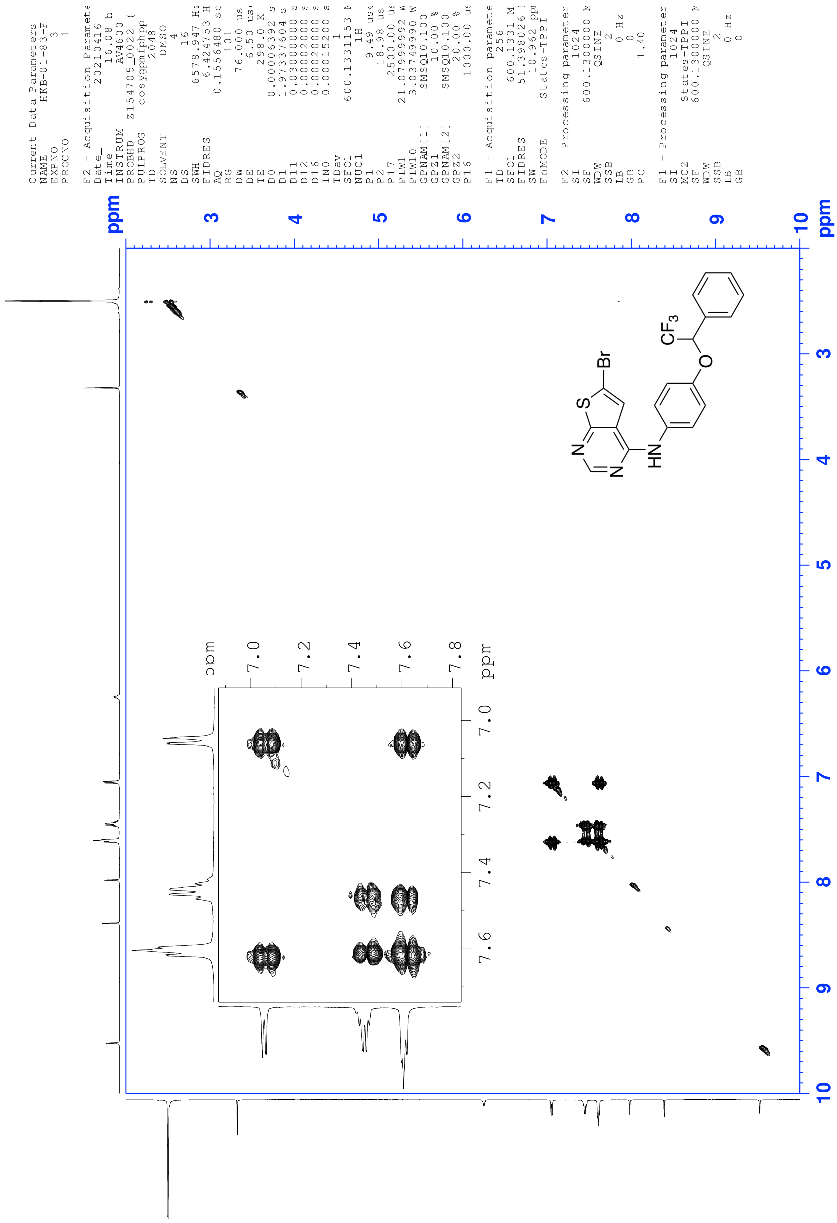

Figure 115: COSY specter of compound ***(rac)*-10**

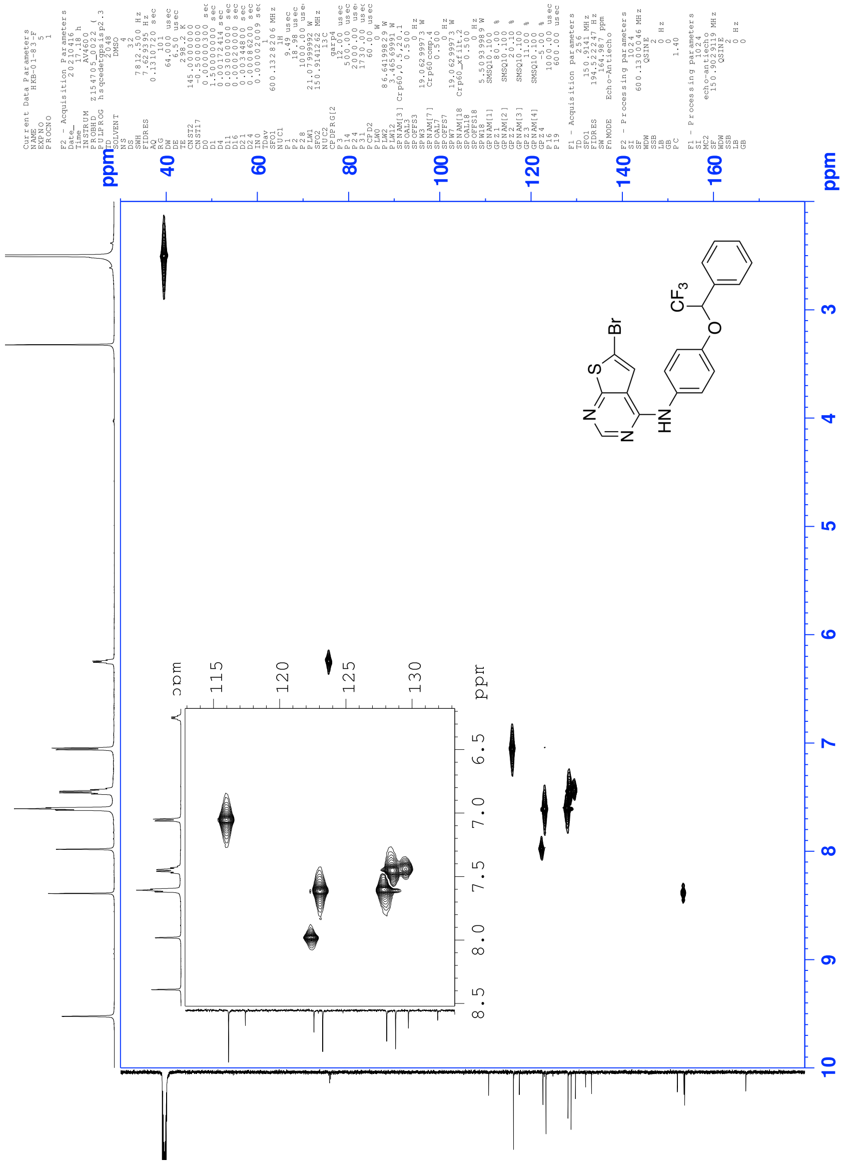

Figure 116: HSQC specter of compound ***(rac)*-10**

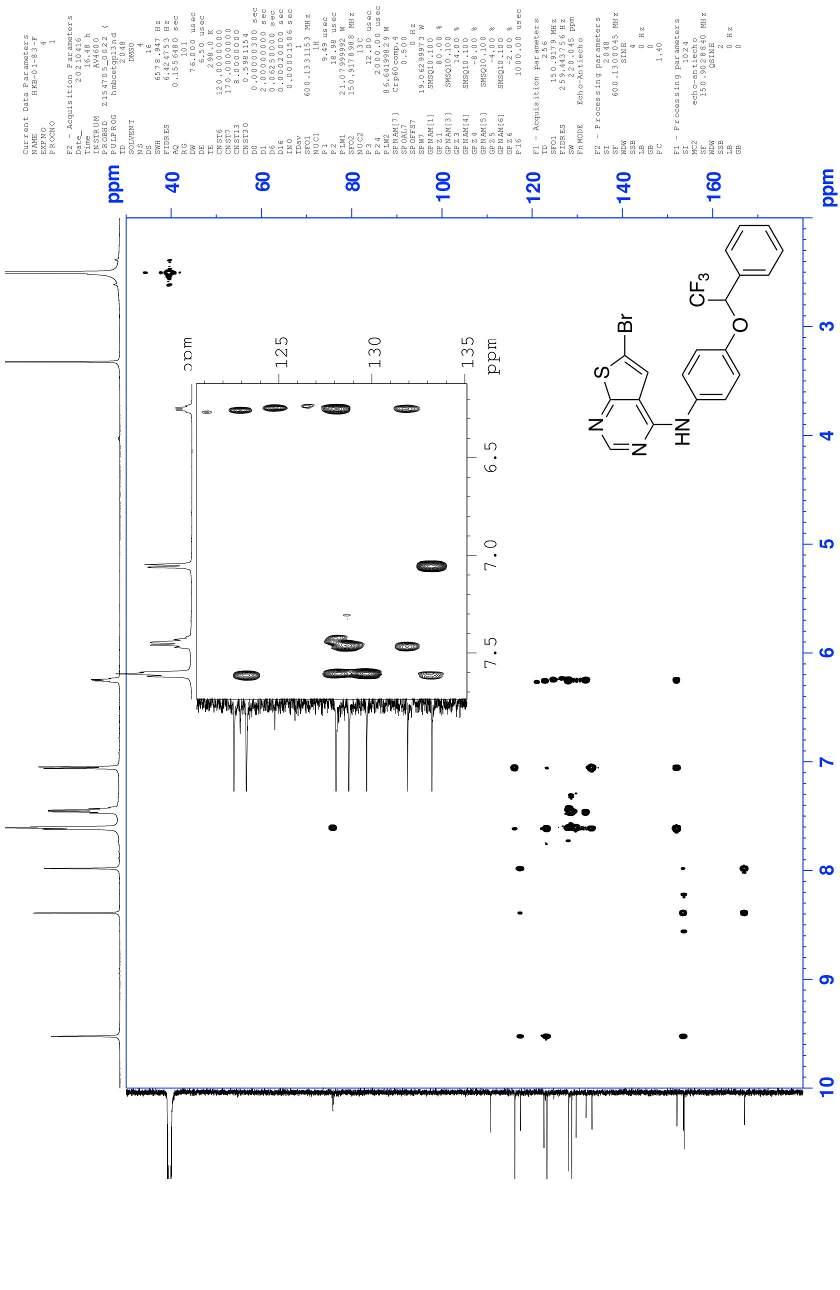

Figure 117: HMBC specter of compound **(*rac*)-10**

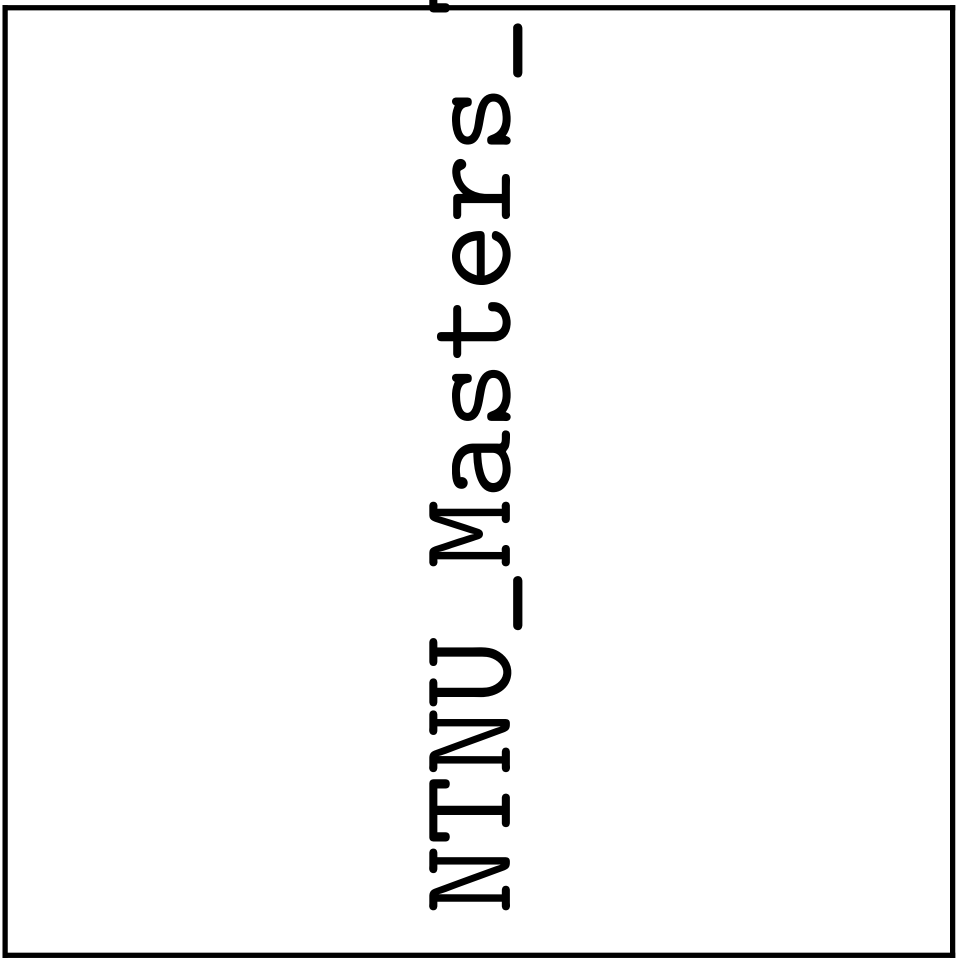

Figure 118: IR-spectrum of compound **(*rac*)-10**

Elemental Composition Report

Page 1

Single Mass Analysis

Tolerance = 5.0 PPM / DBE: min = -10.0, max = 50.0
Element prediction: Off
Number of isotope peaks used for i-FIT = 6

Monoisotopic Mass, Even Electron Ions
9888 formula(e) evaluated with 36 results within limits (all results (up to 1000) for each mass)
Elements Used:
C: 0-100 H: 0-100 N: 0-6 O: 0-6 S: 0-1 Br: 0-1 I: 0-2 F: 0-3

2021-208 98 (0.927) AM2 (Ar,35000.0,0.00,0.00); Cm (98:109)
1: TOF MS ES+

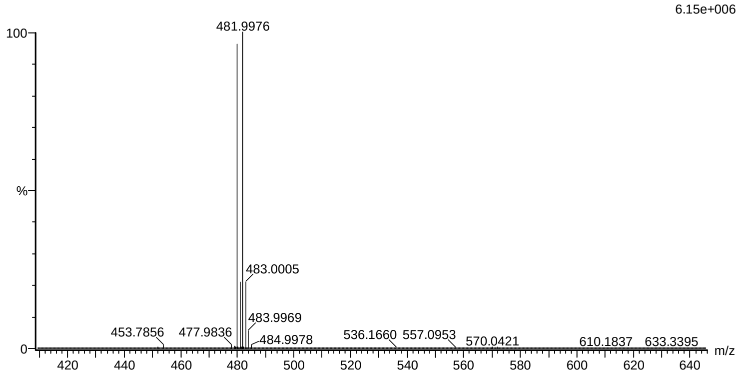

Mass	Calc. Mass	mDa	PPM	DBE	i-FIT	Norm	Conf(%)	Formula
Minimum:				-10.0				
Maximum:		5.0	5.0	50.0				
479.9995	479.9993	0.2	0.4	13.5	2237.0	0.051	95.04	C20 H14 N3 O S Br F3
	479.9989	0.6	1.3	8.5	2240.6	3.644	2.61	C14 H16 N5 O6 S Br F
	479.9977	1.8	3.8	12.5	2240.7	3.819	2.20	C17 H15 N5 O5 S Br
	479.9982	1.3	2.7	17.5	2243.7	6.731	0.12	C23 H13 N3 S Br F2
	479.9981	1.4	2.9	1.5	2245.1	8.160	0.03	C13 H25 N3 S Br I F
	480.0017	-2.2	-4.6	16.5	2247.1	10.168	0.00	C22 H15 N3 O3 S Br
	479.9993	0.2	0.4	-2.5	2248.8	11.919	0.00	C10 H26 N3 O S Br I F2
	480.0004	-0.9	-1.9	-6.5	2251.9	14.938	0.00	C7 H27 N3 O2 S Br I F3
	479.9988	0.7	1.5	-7.5	2253.3	16.350	0.00	C4 H28 N5 O6 S Br I
	480.0007	-1.2	-2.5	13.5	2254.7	17.751	0.00	C19 H13 N3 O5 Br F2
	479.9995	0.0	0.0	17.5	2256.3	19.368	0.00	C22 H12 N3 O4 Br F
	480.0018	-2.3	-4.8	9.5	2256.4	19.469	0.00	C16 H14 N3 O6 Br F3

Figure 119: MS specter of compound **(*rac*)-10**

.1.17 Spectroscopic data for Compound (*R*)-10

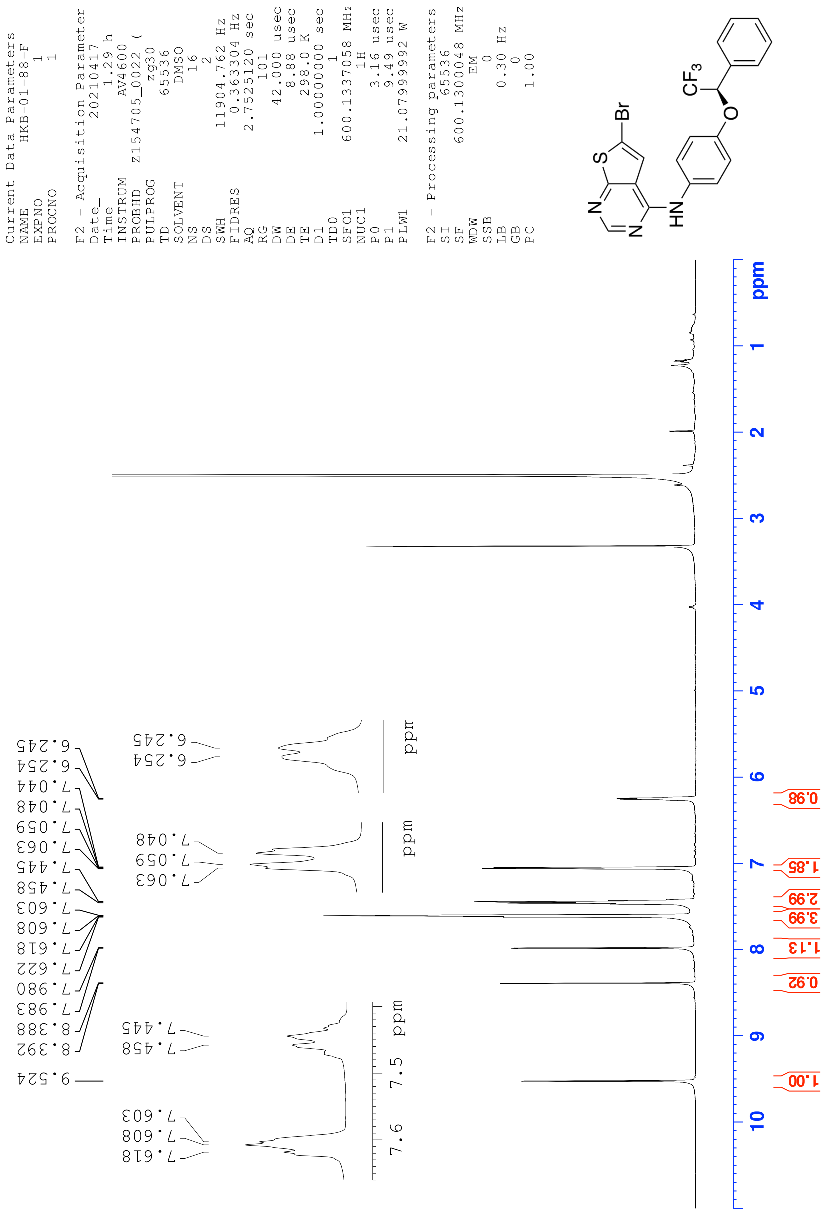

Figure 120: ^{1}H-NMR specter of compound **(*R*)-10**

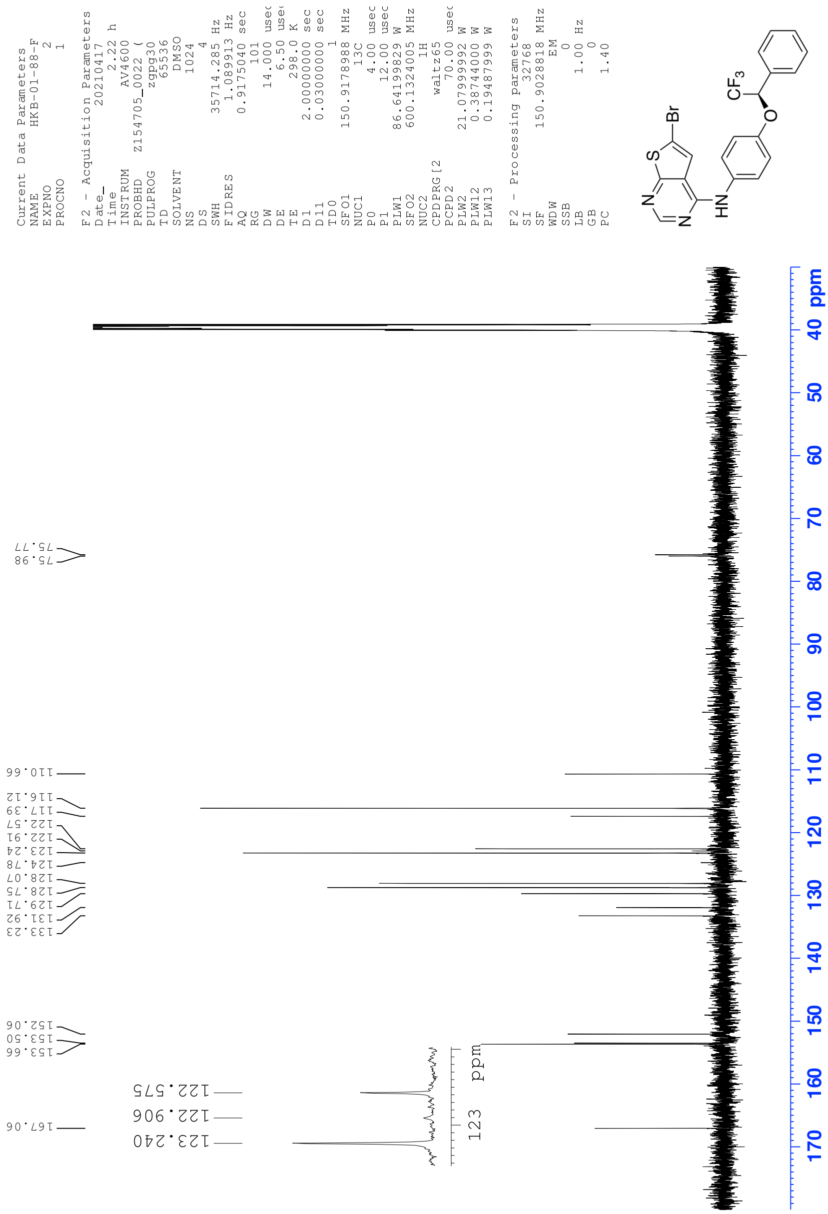

Figure 121: ^{13}C-NMR specter of compound ***(R)*-10**

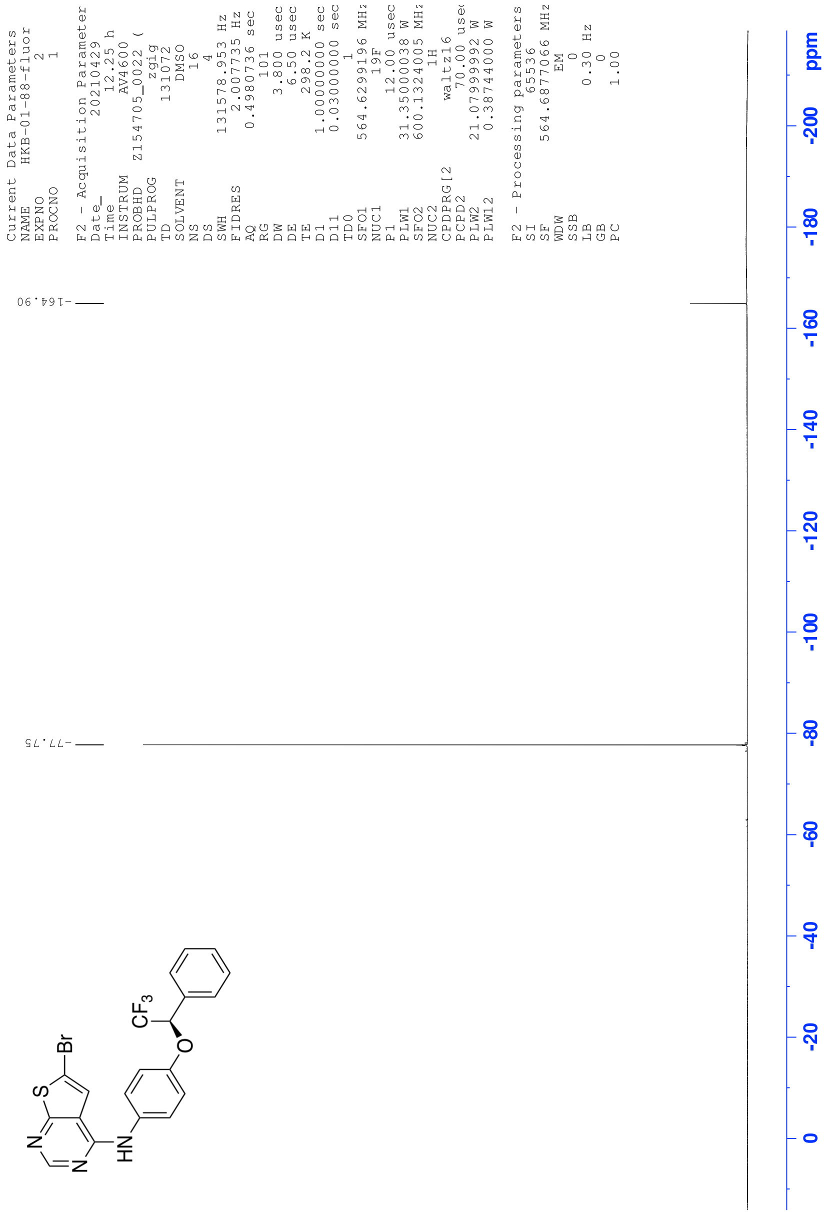

Figure 122: ^{19}F-NMR specter of compound **(*R*)-10**

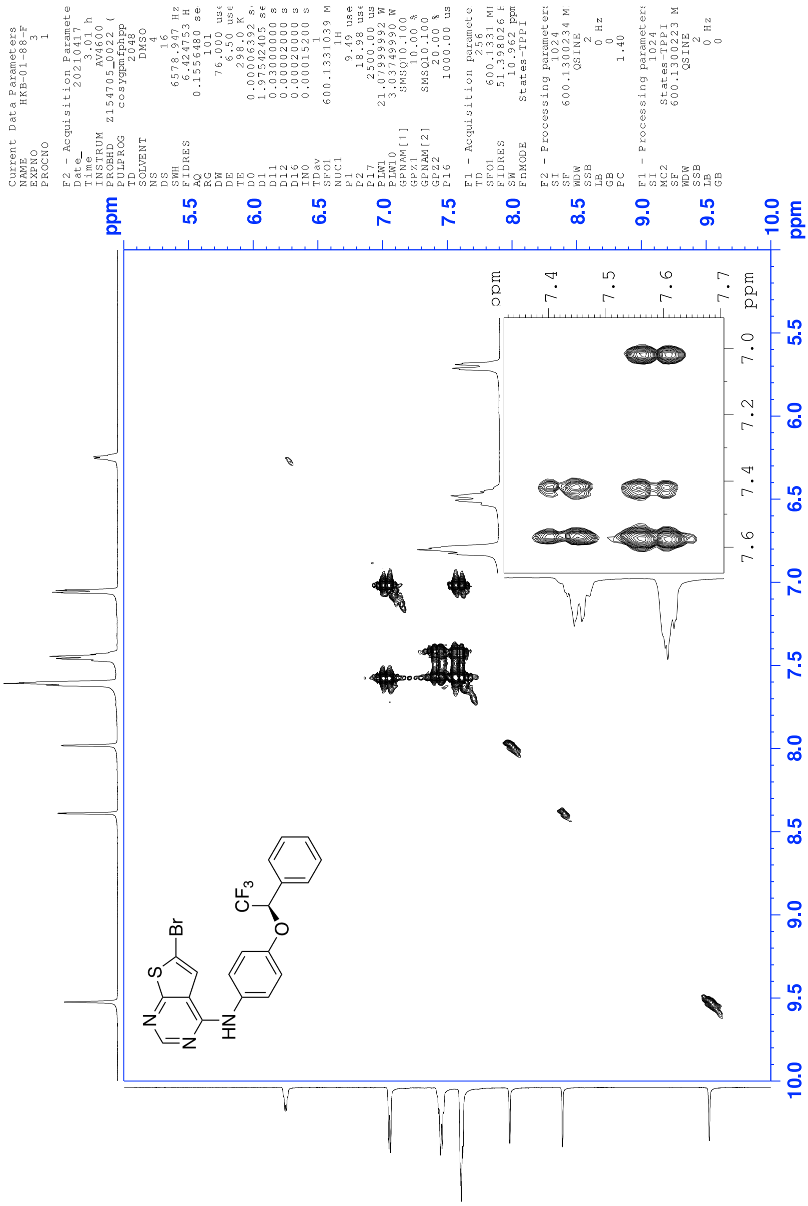

Figure 123: COSY specter of compound **(*R*)-10**

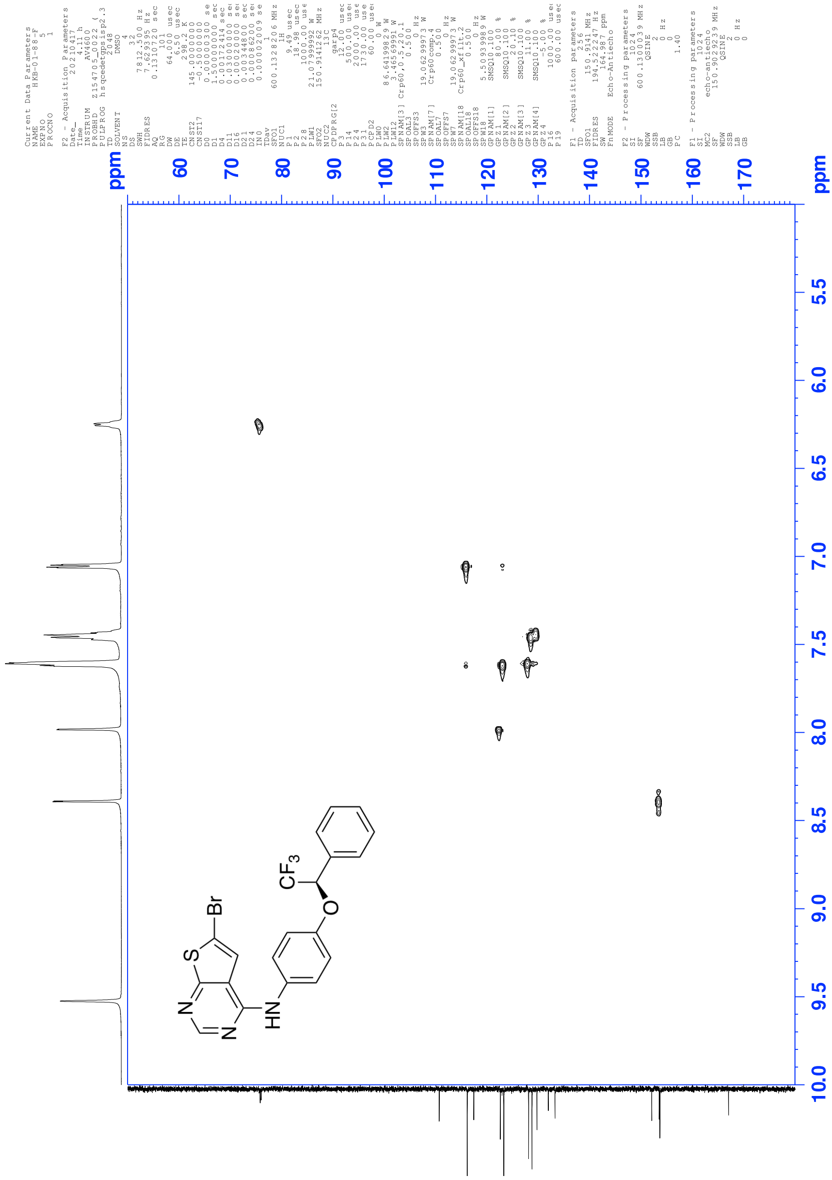

Figure 124: HSQC specter of compound **(*R*)-10**

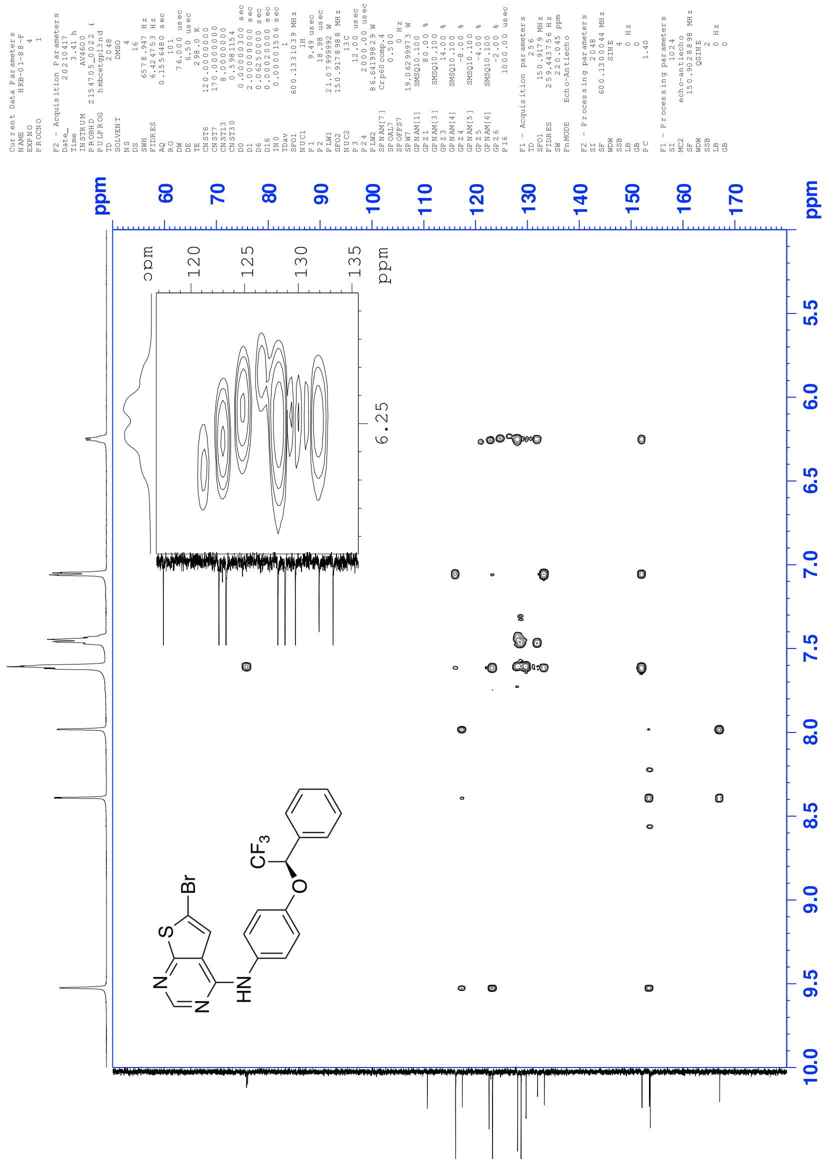

Figure 125: HMBC specter of compound ***(R)*-10**

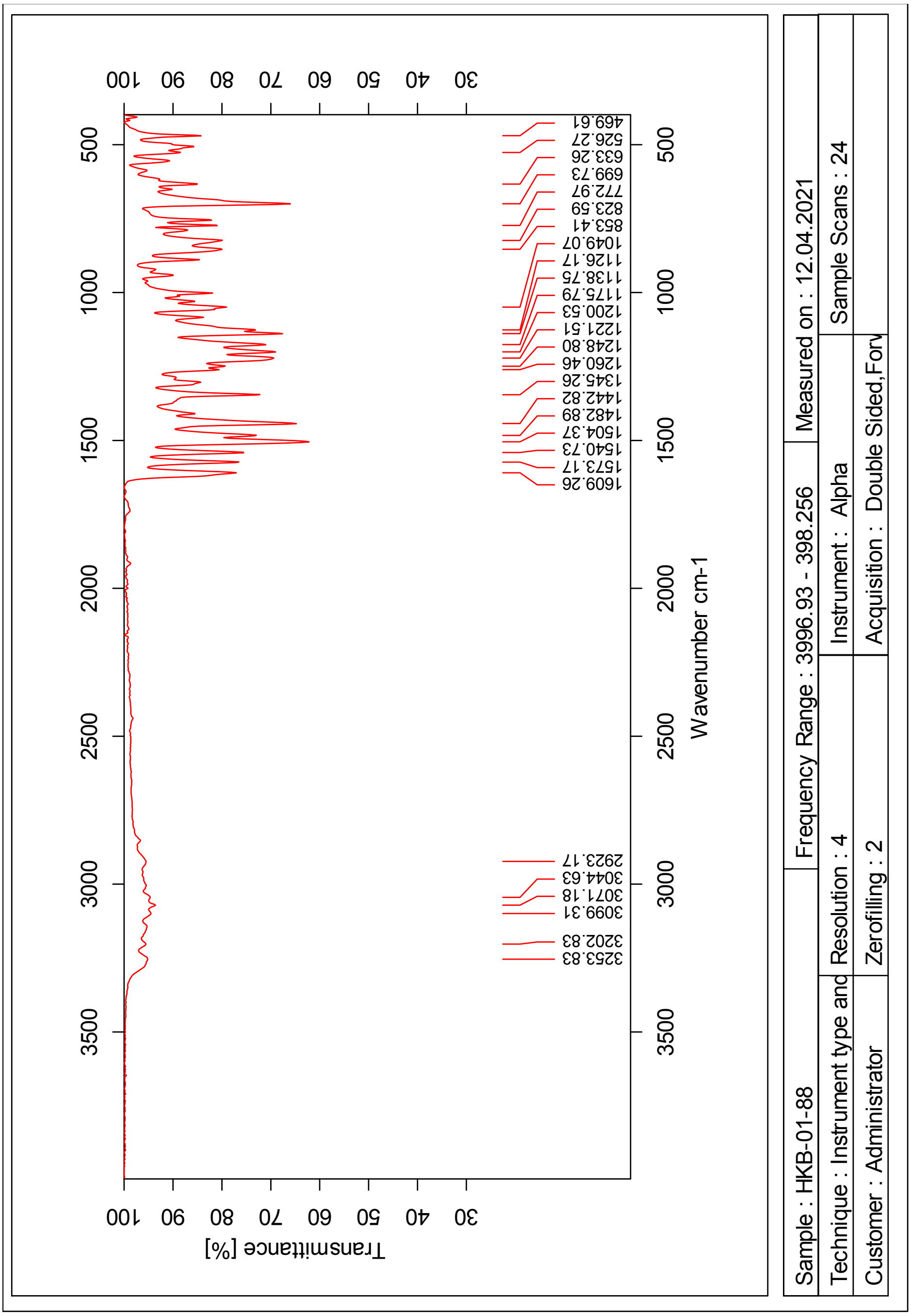

Figure 126: IR-spectrum of compound **(*R*)-10**

Elemental Composition Report

Page 1

Single Mass Analysis

Tolerance = 2.0 PPM / DBE: min = -10.0, max = 50.0
Element prediction: Off
Number of isotope peaks used for i-FIT = 6

Monoisotopic Mass, Even Electron Ions
9184 formula(e) evaluated with 18 results within limits (all results (up to 1000) for each mass)
Elements Used:
C: 0-100 H: 0-100 N: 0-5 O: 0-12 F: 0-3 S: 0-1 Br: 0-2

2021-282 99 (0.935) AM2 (Ar,35000.0,0.00,0.00); Cm (99:101)
1: TOF MS ES+

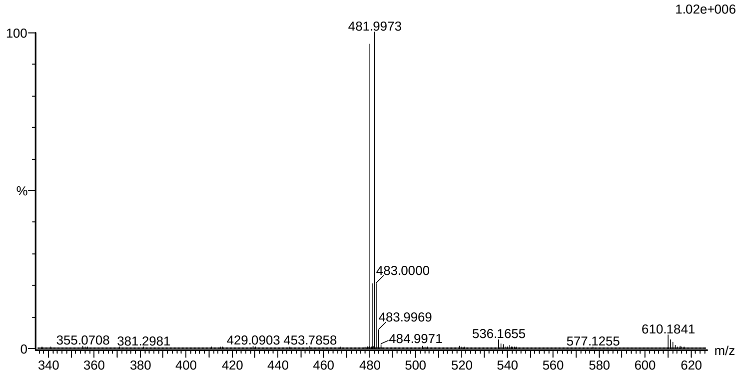

Minimum:				-10.0				
Maximum:		5.0	2.0	50.0				
Mass	Calc. Mass	mDa	PPM	DBE	i-FIT	Norm	Conf(%)	Formula
479.9993	479.9993	0.0	0.0	13.5	1834.2	0.049	95.23	C20 H14 N3 O F3 S Br
	479.9992	0.1	0.2	23.5	1871.1	37.031	0.00	C25 H6 N O10
	479.9992	0.1	0.2	-2.5	1857.5	23.397	0.00	C9 H25 N3 O8 F Br2
	479.9991	0.2	0.4	28.5	1865.4	31.276	0.00	C27 H3 N5 O2 F S
	479.9995	-0.2	-0.4	17.5	1853.1	18.981	0.00	C22 H12 N3 O4 F Br
	479.9990	0.3	0.6	19.5	1865.6	31.530	0.00	C23 H8 N O7 F2 S
	479.9996	-0.3	-0.6	9.5	1858.0	23.903	0.00	C21 H24 N S Br2
	479.9990	0.3	0.6	-6.5	1857.6	23.444	0.00	C7 H27 N3 O5 F3 S Br2
	479.9989	0.4	0.8	8.5	1837.2	3.052	4.73	C14 H16 N5 O6 F S Br
	479.9997	-0.4	-0.8	2.5	1858.5	24.387	0.00	C15 H23 N O3 F3 Br2
	479.9998	-0.5	-1.0	-4.5	1849.8	15.707	0.00	C7 H22 N O12 F3 S Br
	479.9987	0.6	1.3	-0.5	1846.9	12.806	0.00	C10 H21 N O11 F2 S Br
	480.0000	-0.7	-1.5	4.5	1842.0	7.873	0.04	C11 H17 N5 O7 F2 S Br

Figure 127: MS specter of compound **(*R*)-10**

.1.18 Spectroscopic data for Compound (*S*)-10

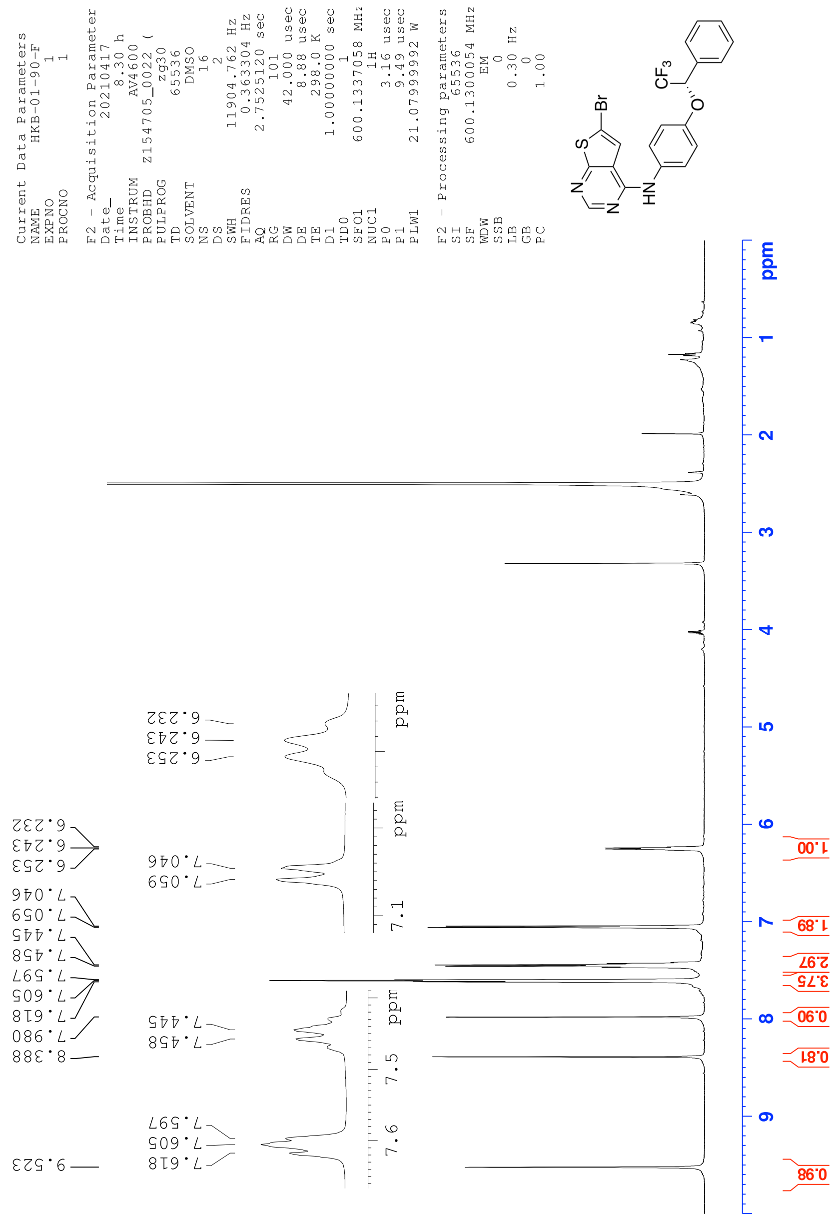

Figure 128: ^{1}H-NMR specter of compound **(*S*)-10**

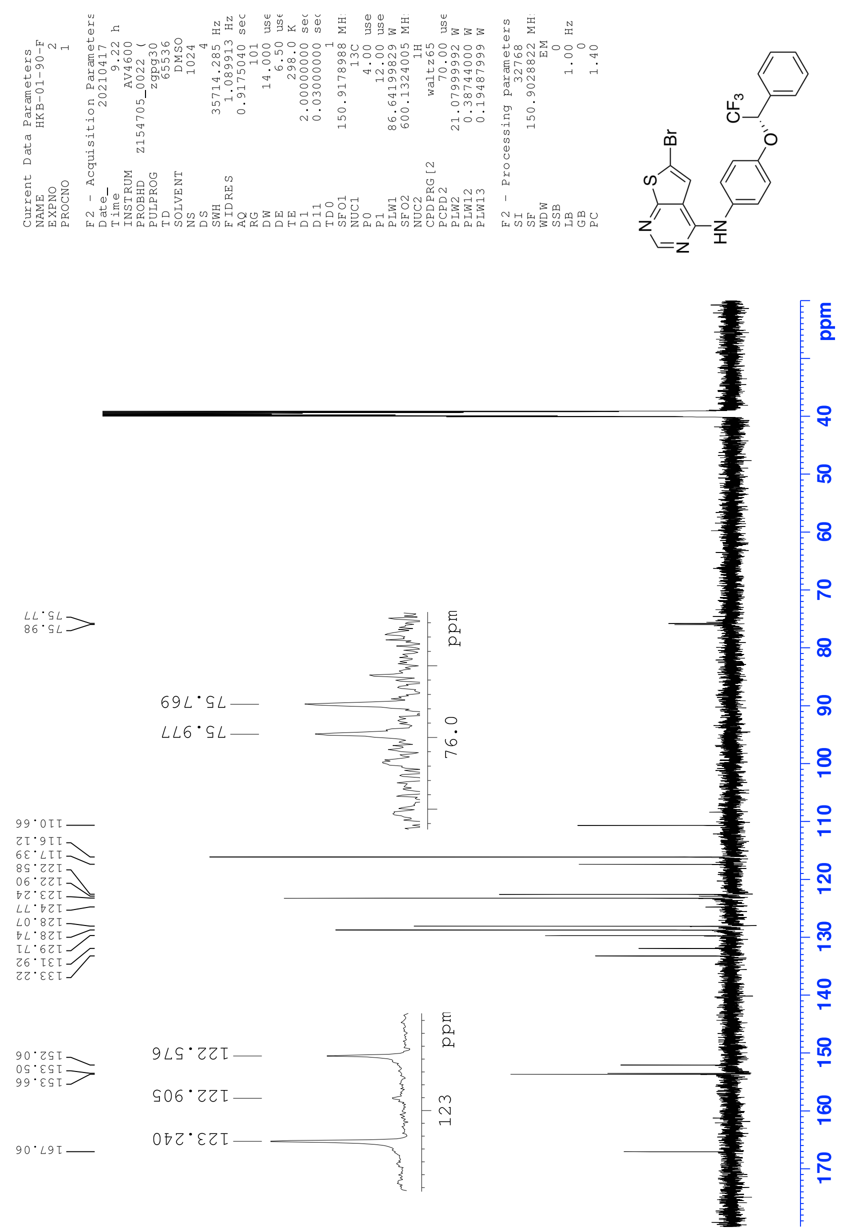

Figure 129: ^{13}C-NMR specter of compound ***(S)*-10**

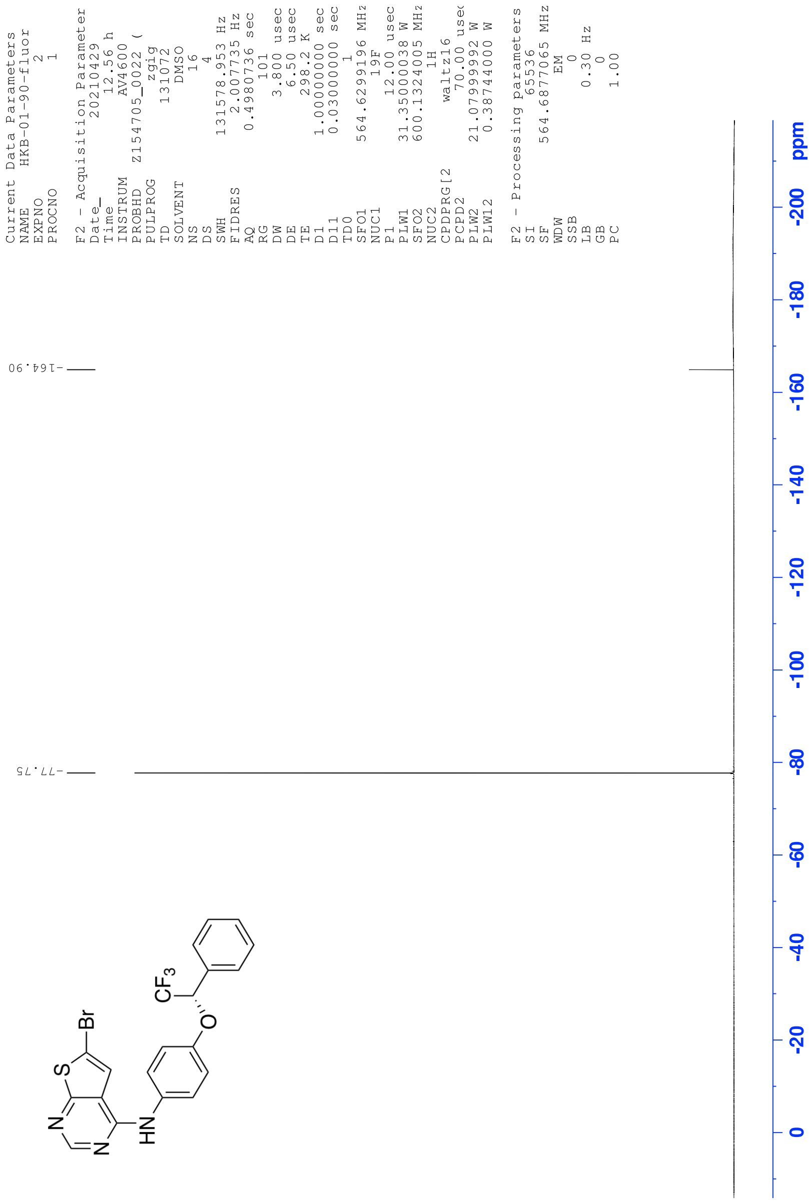

Figure 130: ^{19}F-NMR specter of compound ***(S)*-10**

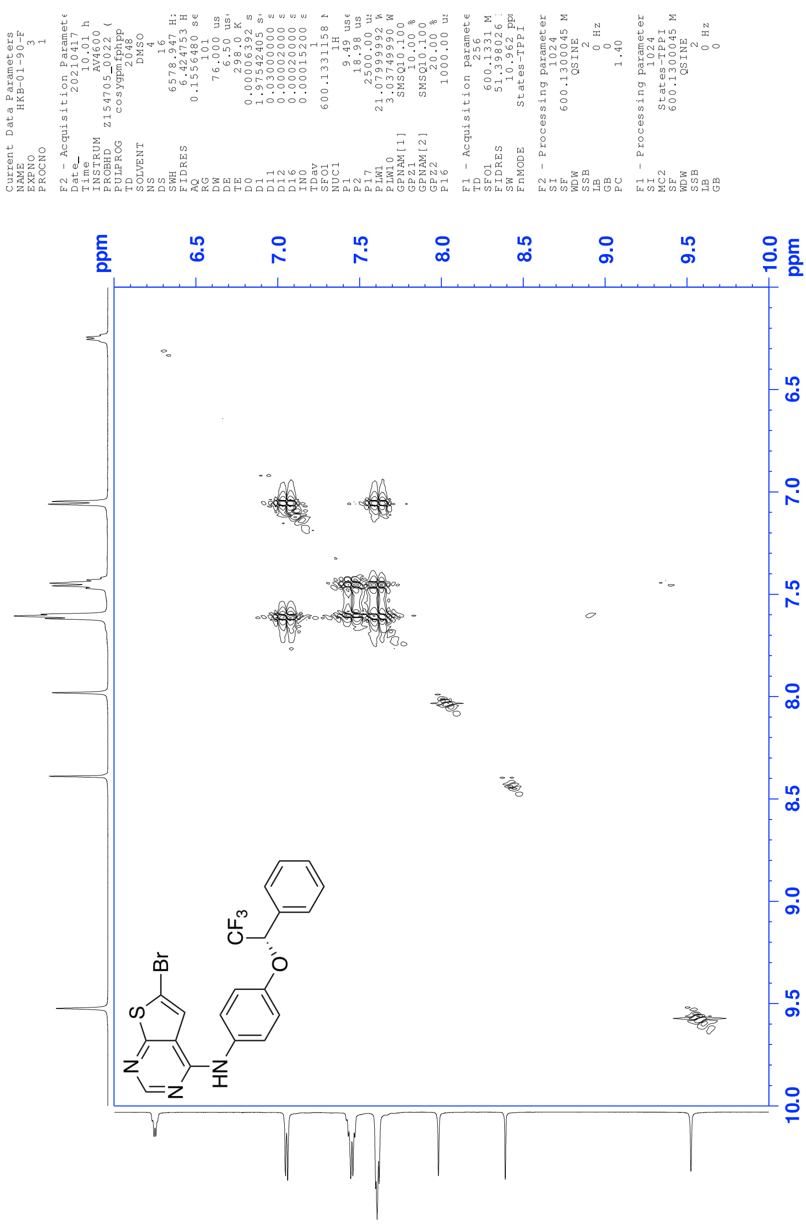

Figure 131: COSY specter of compound **(*S*)-10**

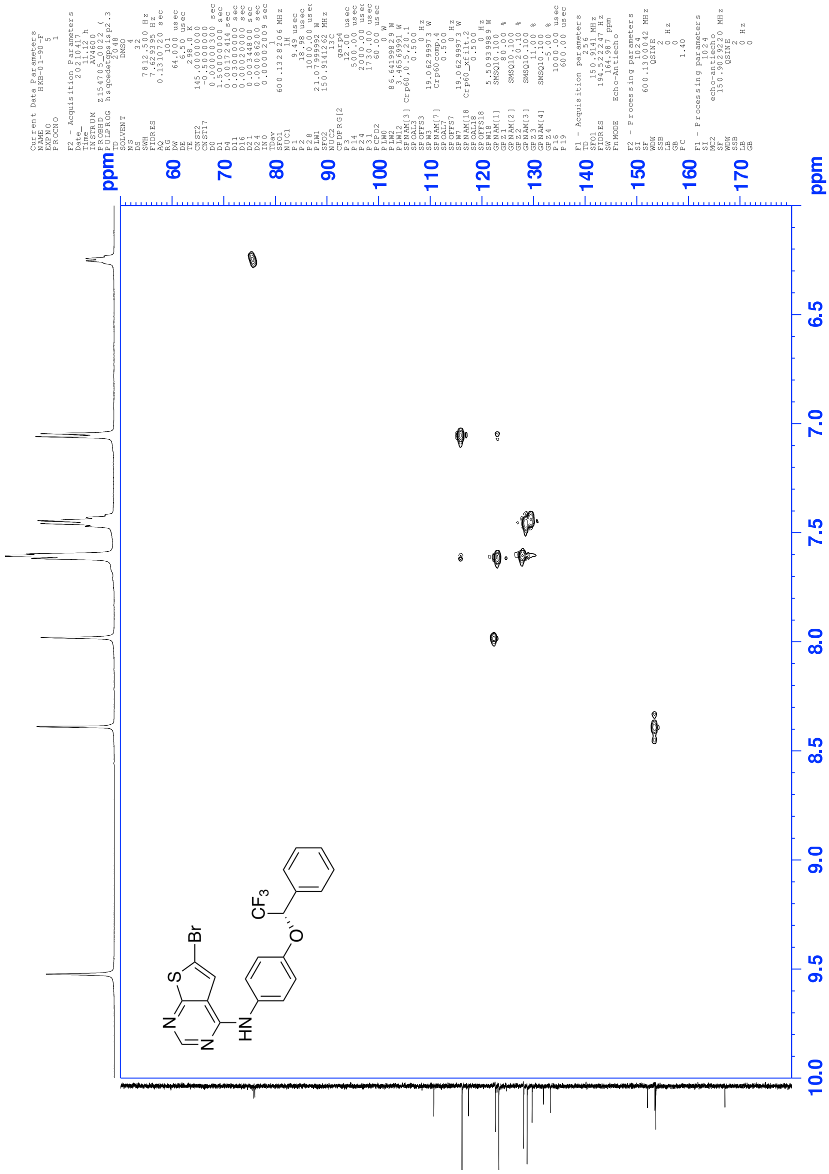

Figure 132: HSQC specter of compound **(*S*)-10**

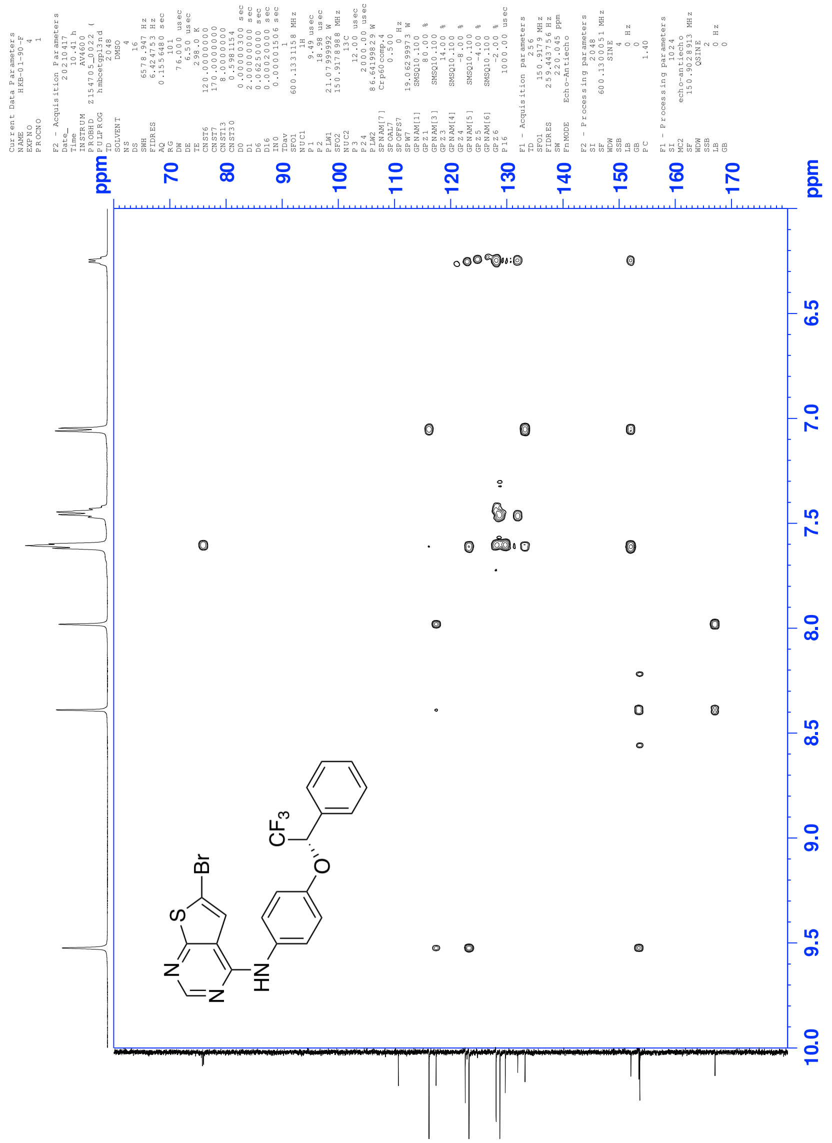

Figure 133: HMBC specter of compound **(*S*)-10**

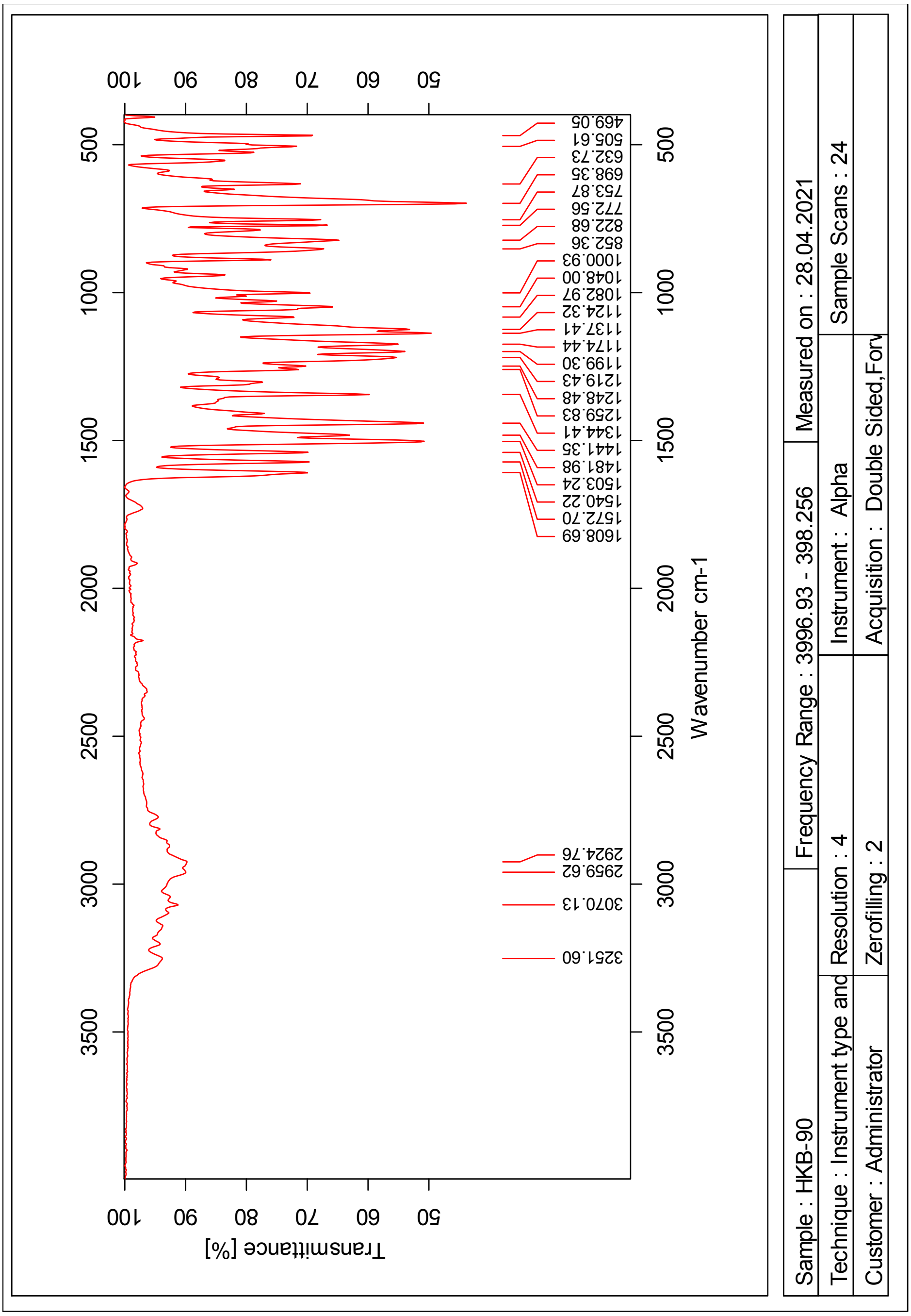

Figure 134: IR-spectrum of compound **(*S*)-10**

Elemental Composition Report **Page 1**

Single Mass Analysis
Tolerance = 2.0 PPM / DBE: min = -10.0, max = 50.0
Element prediction: Off
Number of isotope peaks used for i-FIT = 6

Monoisotopic Mass, Even Electron Ions
9184 formula(e) evaluated with 18 results within limits (all results (up to 1000) for each mass)
Elements Used:
C: 0-100 H: 0-100 N: 0-5 O: 0-12 F: 0-3 S: 0-1 Br: 0-2

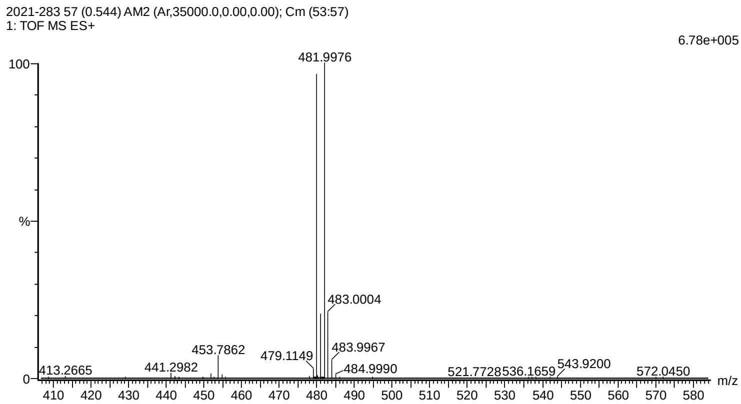

		mDa	PPM	DBE				
Minimum:				-10.0				
Maximum:		5.0	2.0	50.0				
Mass	Calc. Mass	mDa	PPM	DBE	i-FIT	Norm	Conf(%)	Formula
479.9995	479.9993	0.2	0.4	13.5	1726.2	0.600	54.88	C20 H14 N3 O F3 S Br
	479.9989	0.6	1.3	8.5	1726.5	0.897	40.80	C14 H16 N5 O6 F S Br
	480.0000	-0.5	-1.0	4.5	1728.7	3.172	4.19	C11 H17 N5 O7 F2 S Br
	479.9987	0.8	1.7	-0.5	1732.3	6.790	0.11	C10 H21 N O11 F2 S Br
	479.9998	-0.3	-0.6	-4.5	1734.3	8.732	0.02	C7 H22 N O12 F3 S Br
	479.9995	0.0	0.0	17.5	1743.6	18.043	0.00	C22 H12 N3 O4 F Br
	480.0002	-0.7	-1.5	8.5	1743.7	18.105	0.00	C13 H15 N5 O10 Br
	479.9992	0.3	0.6	-2.5	1745.4	19.802	0.00	C9 H25 N3 O8 F Br2
	480.0004	-0.9	-1.9	-6.5	1745.5	19.961	0.00	C6 H26 N3 O9 F2 Br2
	479.9996	-0.1	-0.2	9.5	1746.2	20.685	0.00	C21 H24 N S Br2
	479.9997	-0.2	-0.4	2.5	1746.3	20.730	0.00	C15 H23 N O3 F3 Br2
	479.9990	0.5	1.0	-6.5	1748.0	22.419	0.00	C7 H27 N3 O5 F3 S Br2
	479.9991	0.4	0.8	28.5	1756.0	30.416	0.00	C27 H3 N5 O2 F

Figure 135: MS specter of compound **(*S*)-10**

.1.19 Spectroscopic data for Compound 11

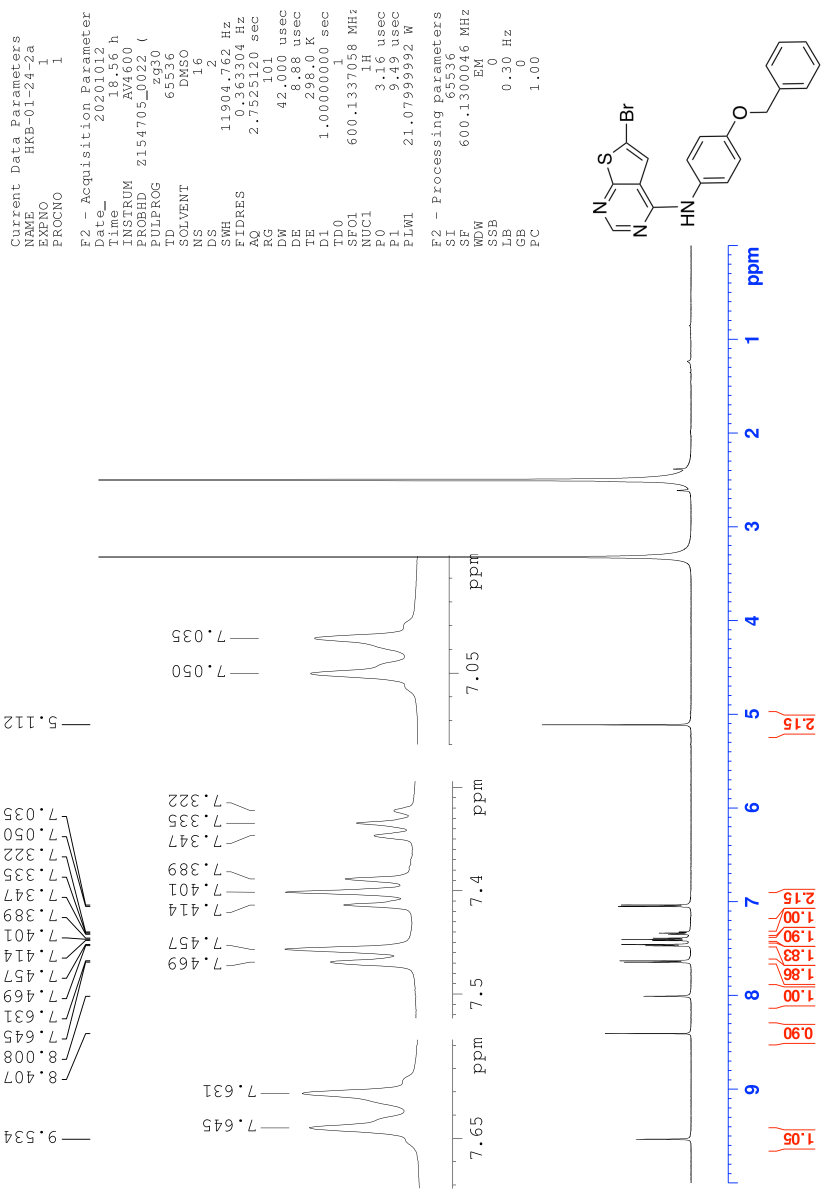

Figure 136: ^{1}H-NMR specter of compound **11**

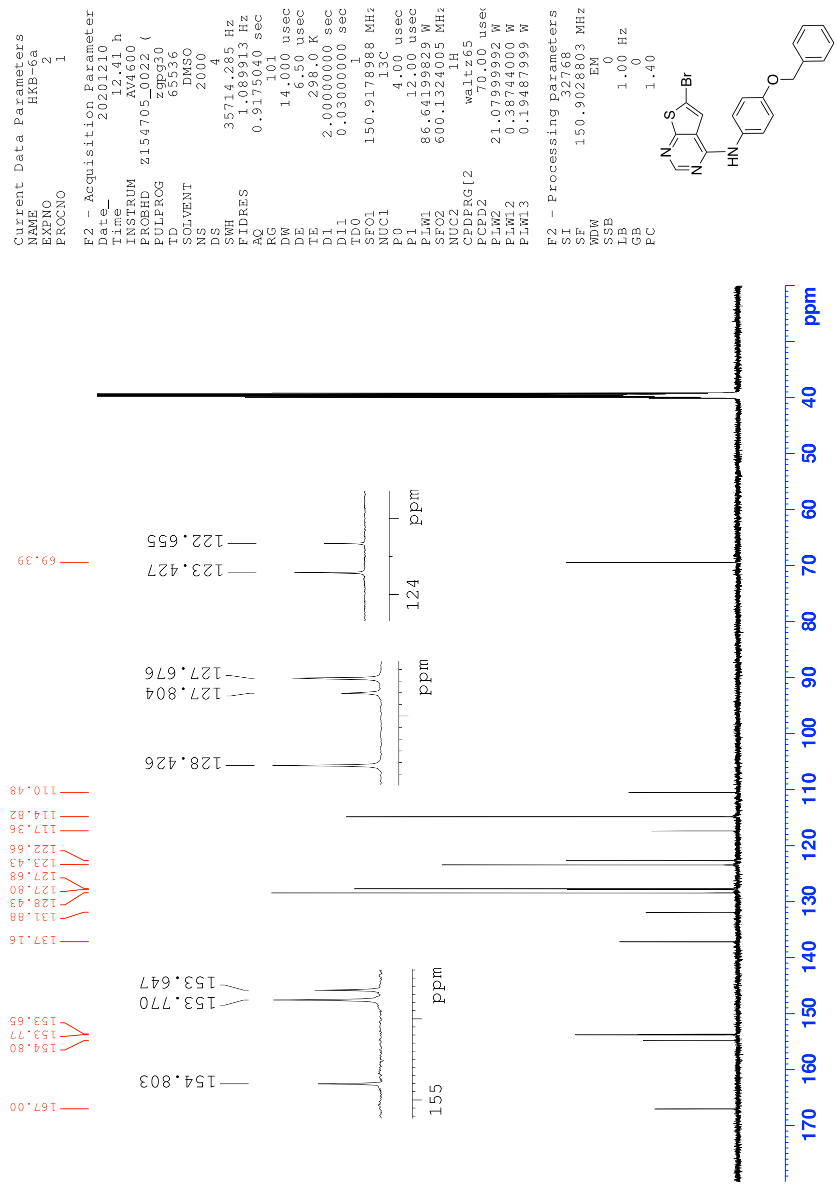

Figure 137: ^{13}C-NMR specter of compound **11**

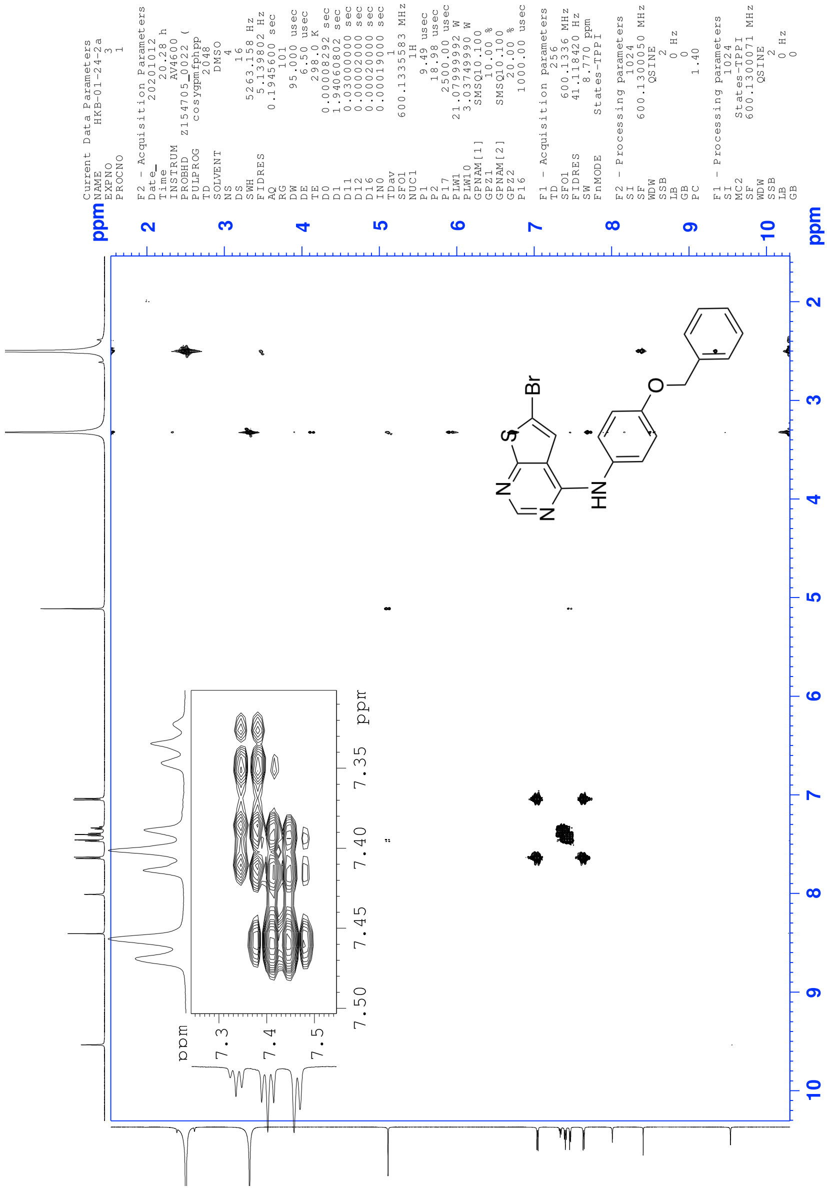

Figure 138: COSY specter of compound **11**

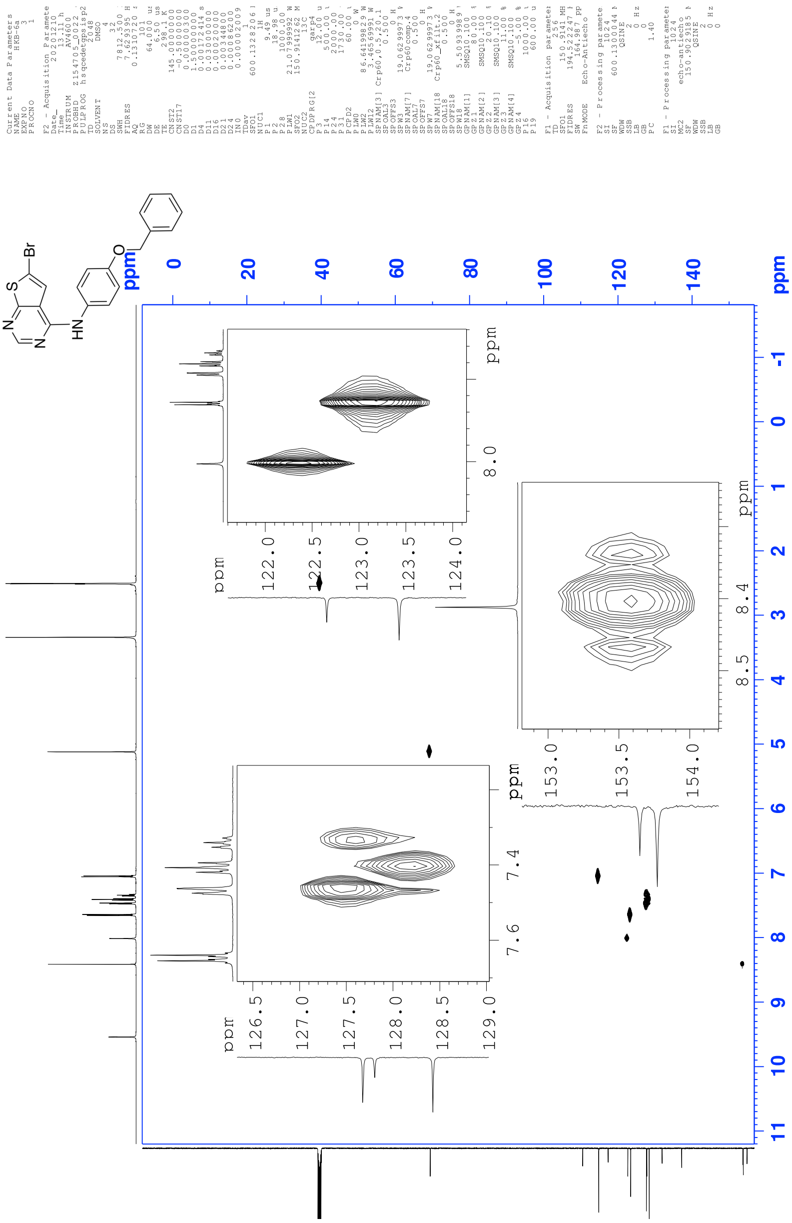

Figure 139: HSQC specter of compound **11**

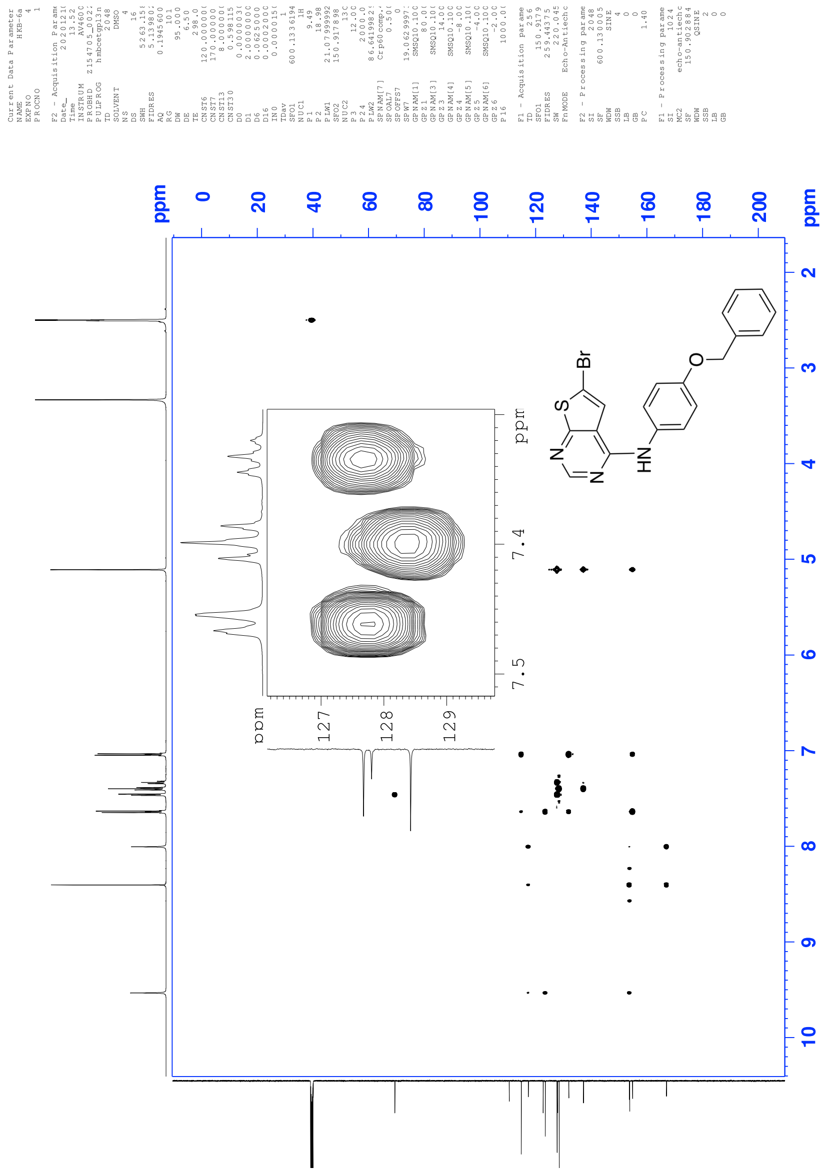

Figure 140: HMBC specter of compound **11**

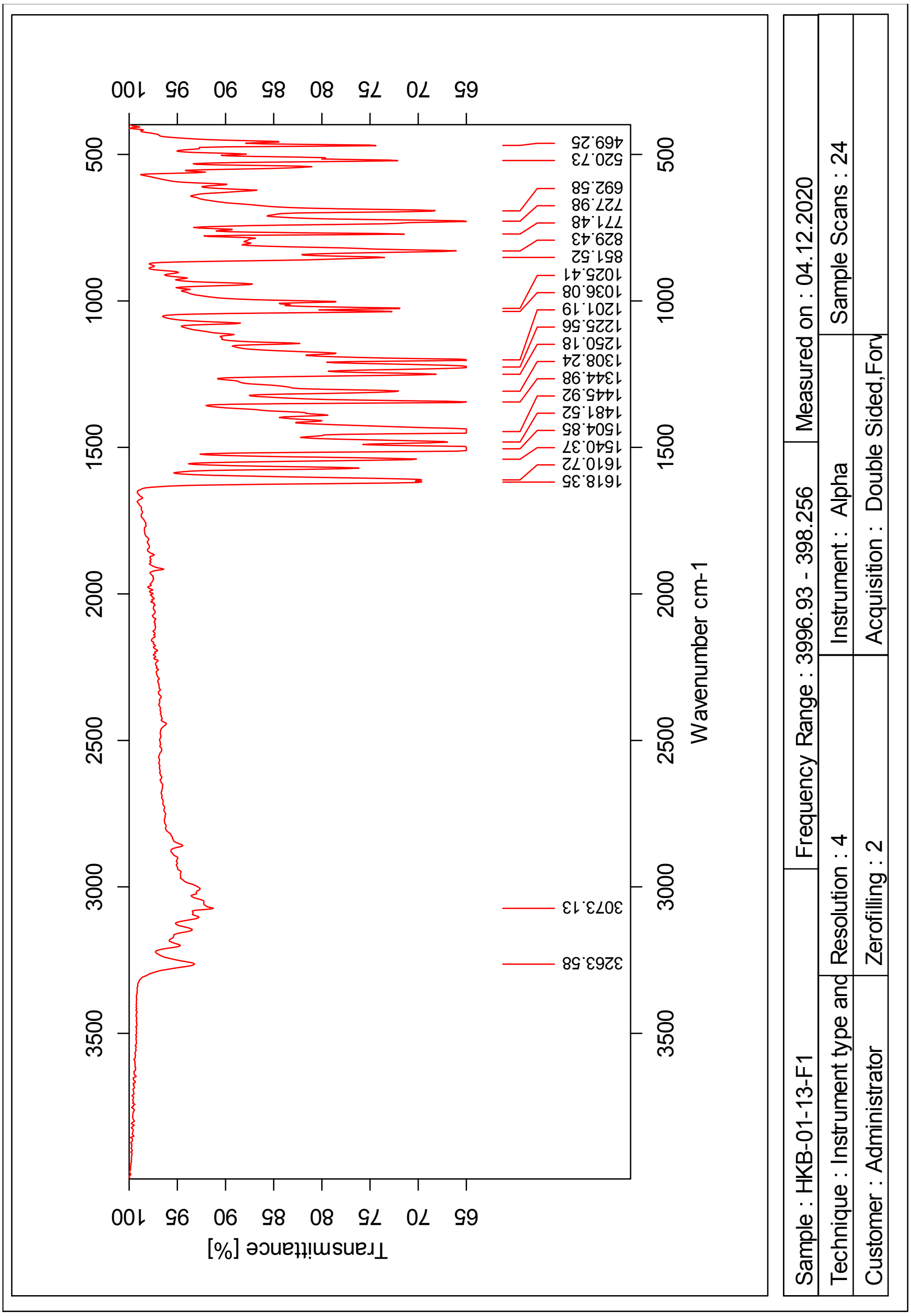

Figure 141: IR-spectrum of compound **11**

Elemental Composition Report **Page 1**

Single Mass Analysis
Tolerance = 1.0 PPM / DBE: min = -50.0, max = 100.0
Element prediction: Off
Number of isotope peaks used for i-FIT = 6

Monoisotopic Mass, Even Electron Ions
7985 formula(e) evaluated with 4 results within limits (all results (up to 1000) for each mass)
Elements Used:
C: 0-100 H: 0-100 N: 0-10 O: 0-10 Na: 0-1 S: 0-1 Br: 0-1

2020_437 59 (0.569) AM2 (Ar,35000.0,0.00,0.00); Cm (43:60)
1: TOF MS ES+

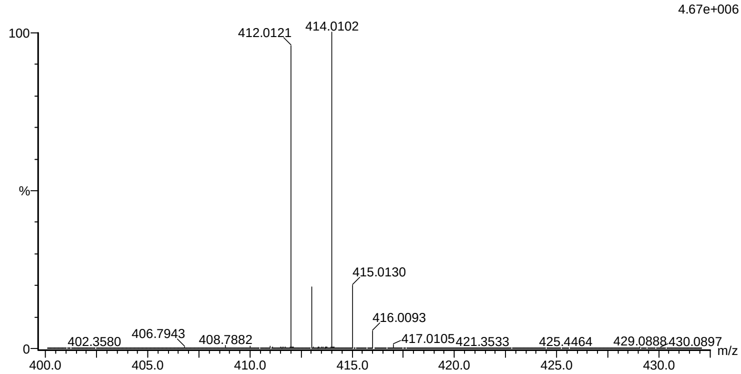

Minimum:				-50.0				
Maximum:		5.0	1.0	100.0				
Mass	Calc. Mass	mDa	PPM	DBE	i-FIT	Norm	Conf(%)	Formula
412.0121	412.0119	0.2	0.5	13.5	2590.4	0.000	100.00	C19 H15 N3 O S Br
	412.0117	0.4	1.0	10.5	2613.2	22.839	0.00	C11 H11 N9 O4 Br
	412.0120	0.1	0.2	6.5	2613.6	23.194	0.00	C13 H16 N3 O6 Na Br
	412.0123	-0.2	-0.5	26.5	2631.3	40.928	0.00	C26 H3 N3 O2 Na

Figure 142: MS specter of compound **11**

.1.20 Spectroscopic data for Compound 12

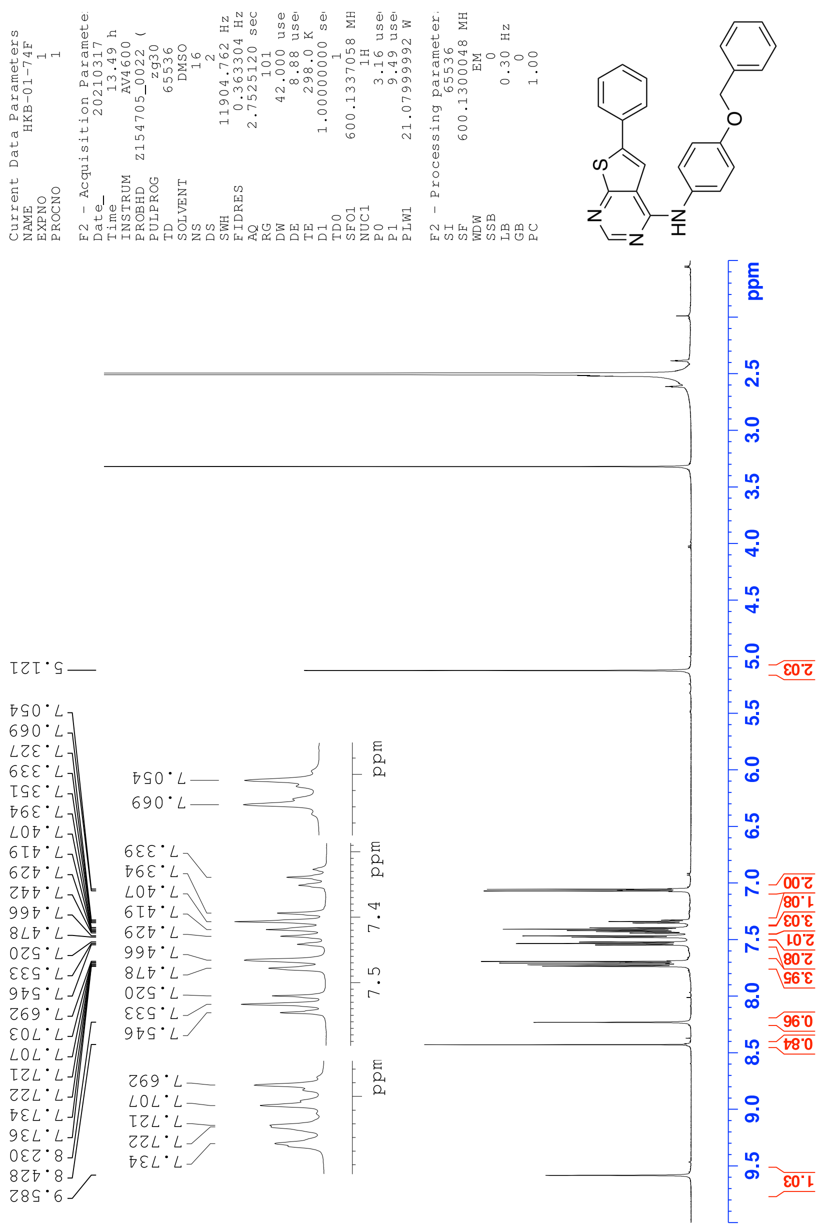

Figure 143: ^{1}H-NMR specter of compound **12**

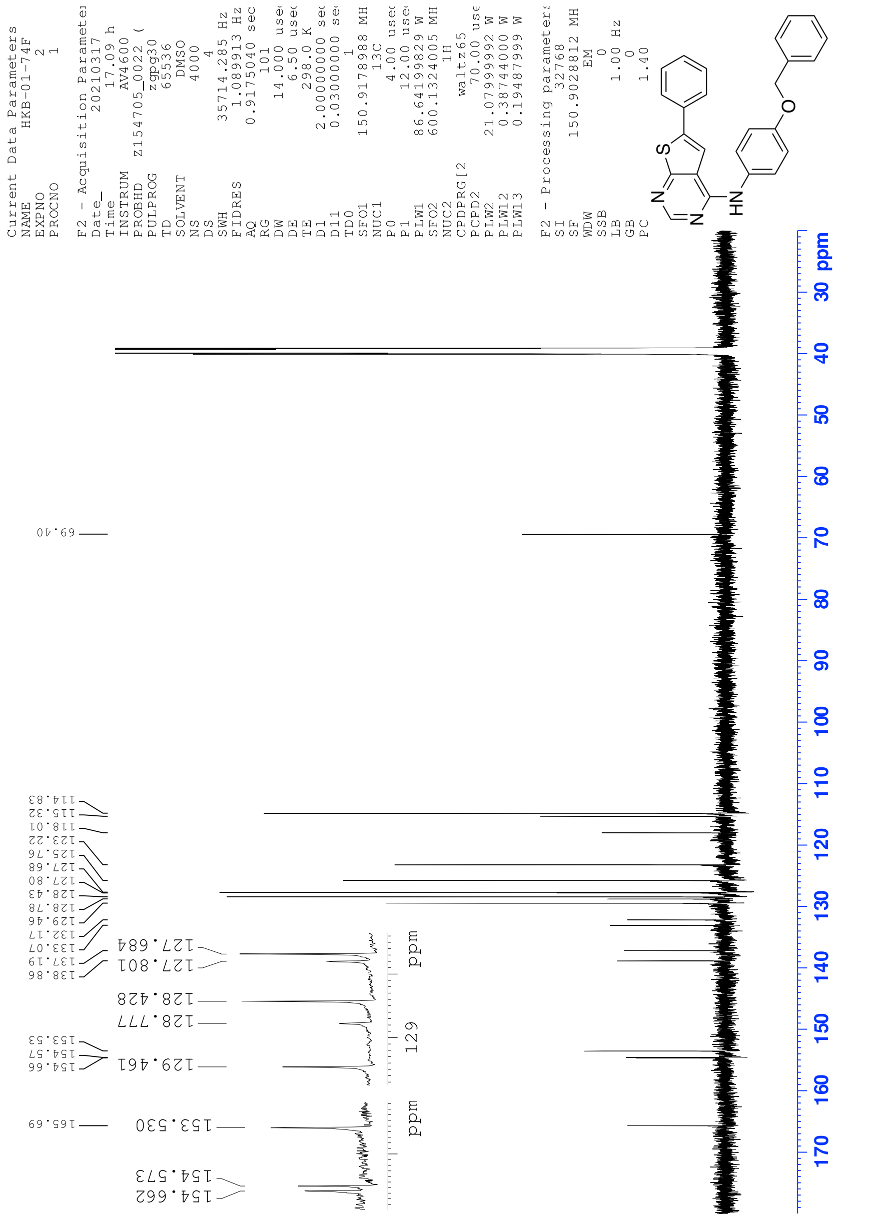

Figure 144: ^{13}C-NMR specter of compound **12**

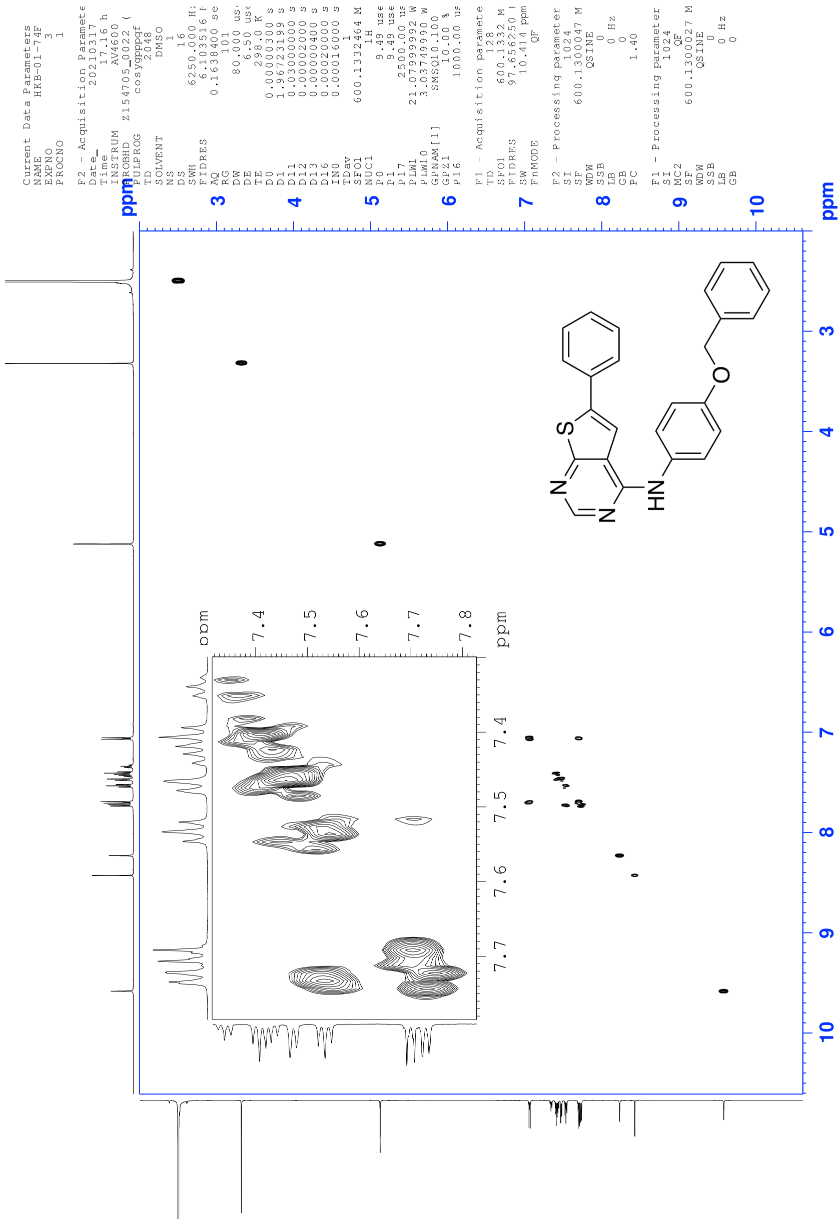

Figure 145: COSY specter of compound **12**

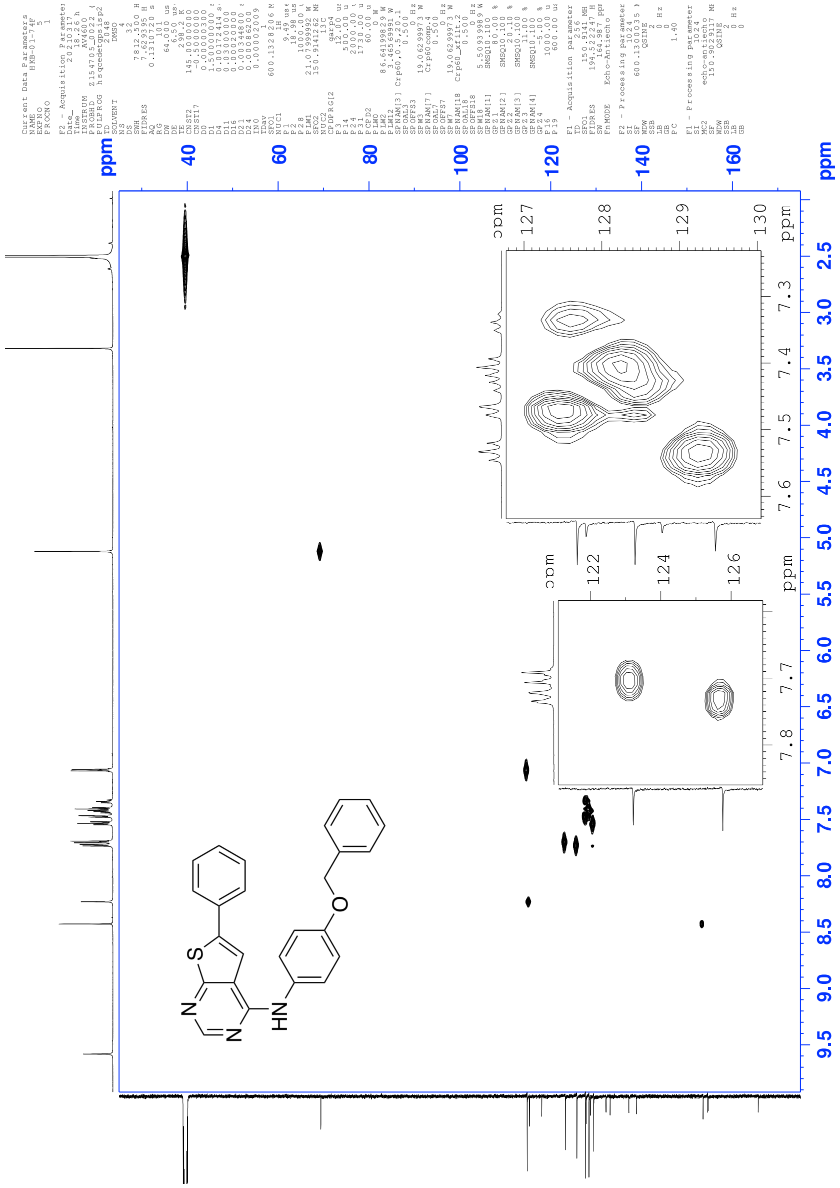

Figure 146: HSQC specter of compound **12**

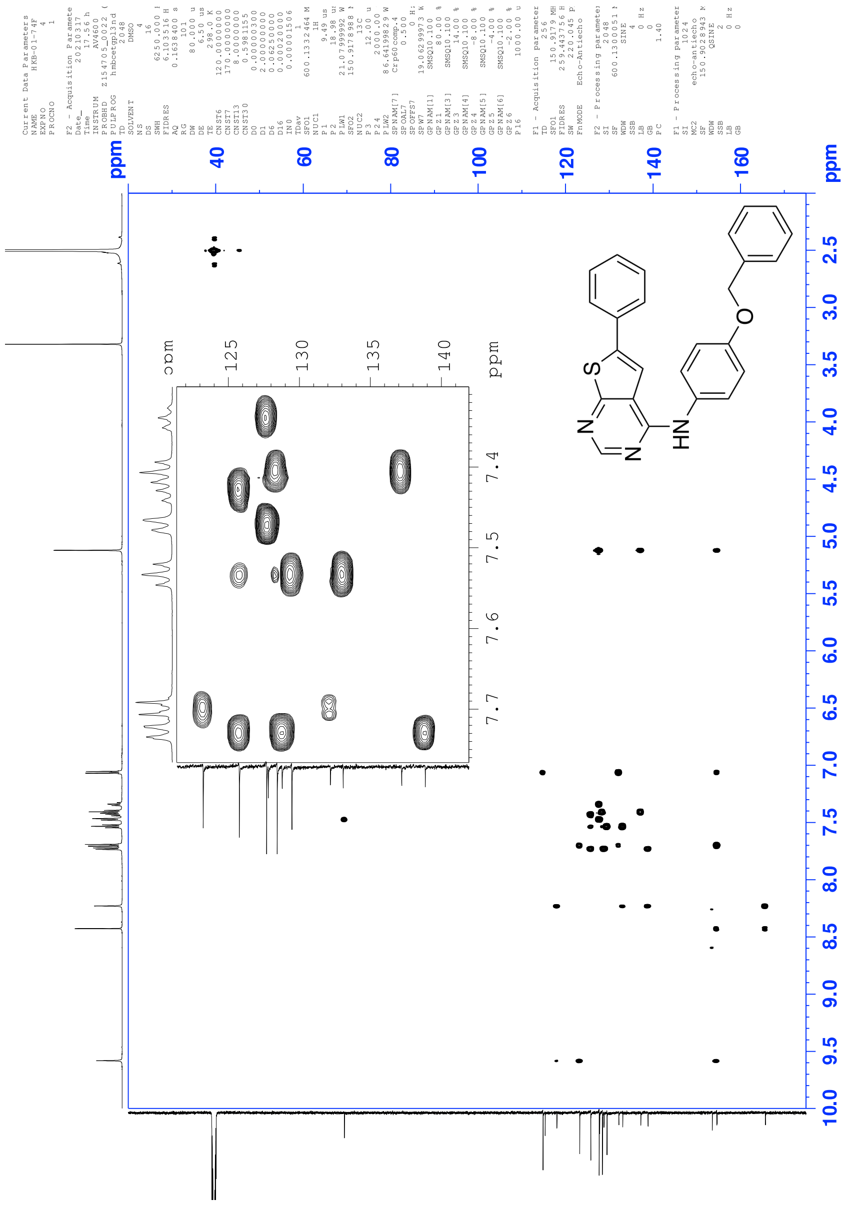

Figure 147: HMBC specter of compound **12**

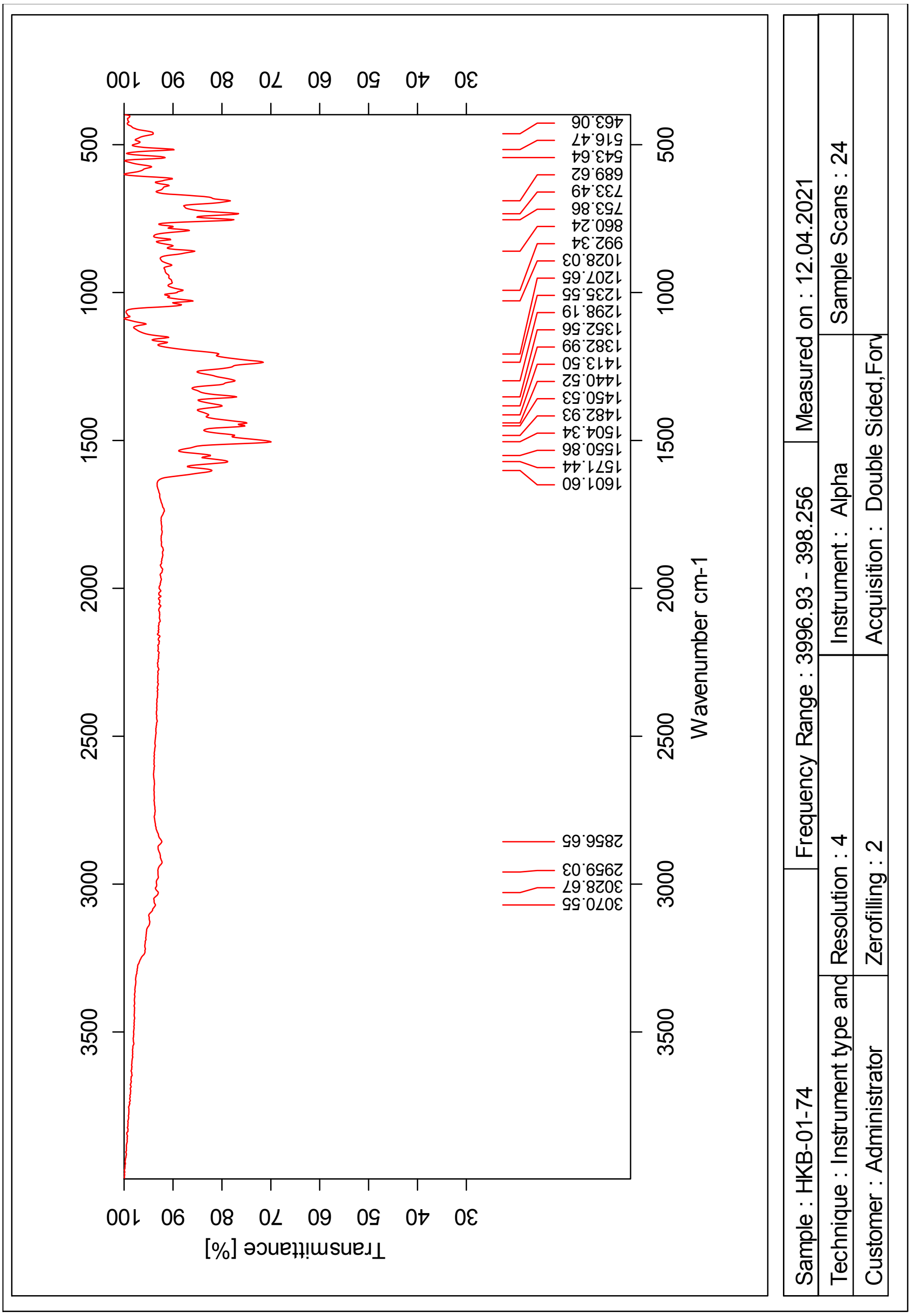

Figure 148: IR-spectrum of compound **12**

Elemental Composition Report **Page 1**

Single Mass Analysis
Tolerance = 5.0 PPM / DBE: min = -10.0, max = 50.0
Element prediction: Off
Number of isotope peaks used for i-FIT = 6

Monoisotopic Mass, Even Electron Ions
1270 formula(e) evaluated with 3 results within limits (all results (up to 1000) for each mass)
Elements Used:
C: 0-100 H: 0-100 N: 0-6 O: 0-6 S: 0-1 I: 0-2

2021-205 117 (1.109) AM2 (Ar,35000.0,0.00,0.00); Cm (110:122)
1: TOF MS ES+

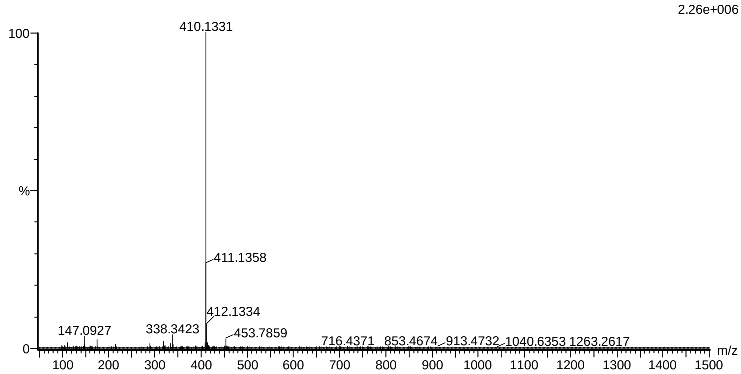

Mass	Calc. Mass	mDa	PPM	DBE	i-FIT	Norm	Conf(%)	Formula
Minimum:				-10.0				
Maximum:		5.0	5.0	50.0				
410.1331	410.1327	0.4	1.0	17.5	2136.4	0.000	99.98	C25 H20 N3 O S
	410.1338	-0.7	-1.7	-2.5	2145.0	8.614	0.02	C12 H33 N3 O2 S I
	410.1345	-1.4	-3.4	6.5	2155.1	18.656	0.00	C20 H29 N I

Figure 149: MS specter of compound **12**

.1.21 Spectroscopic data for Compound 13

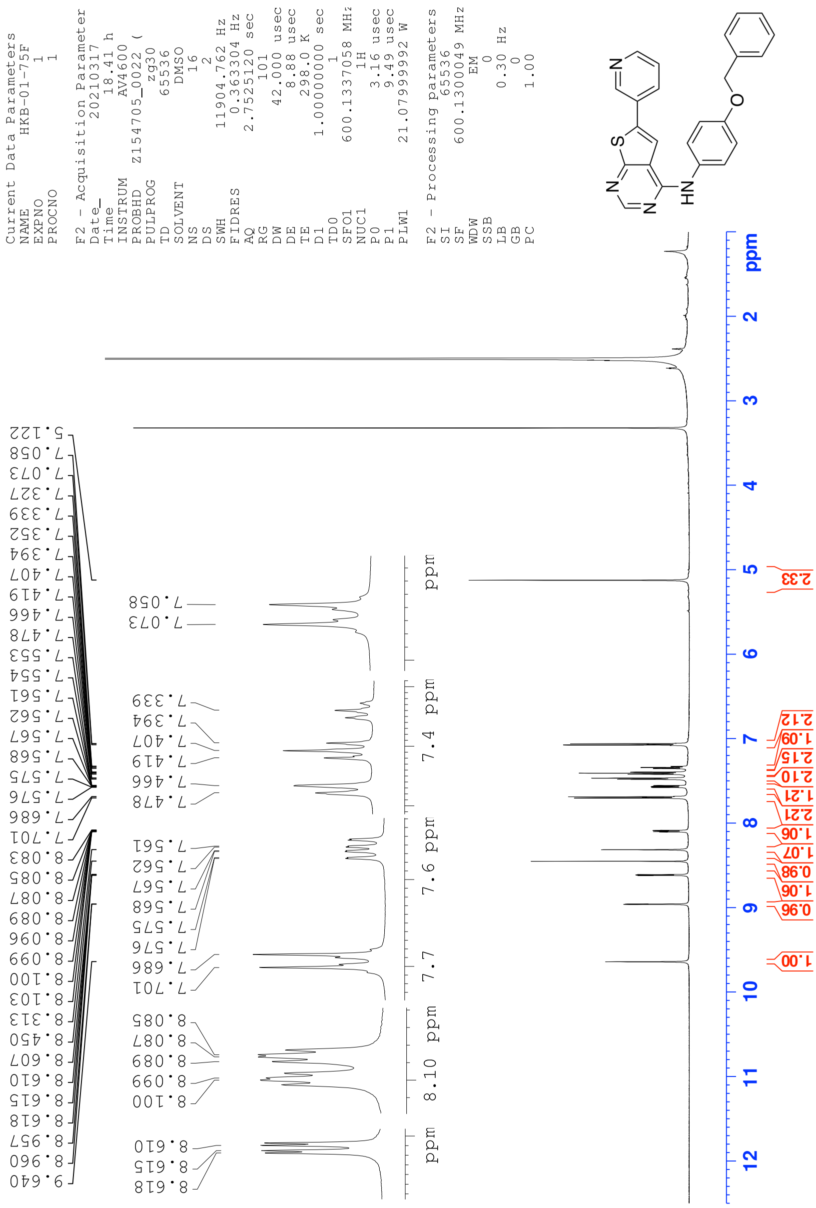

Figure 150: ^{1}H-NMR specter of compound **13**

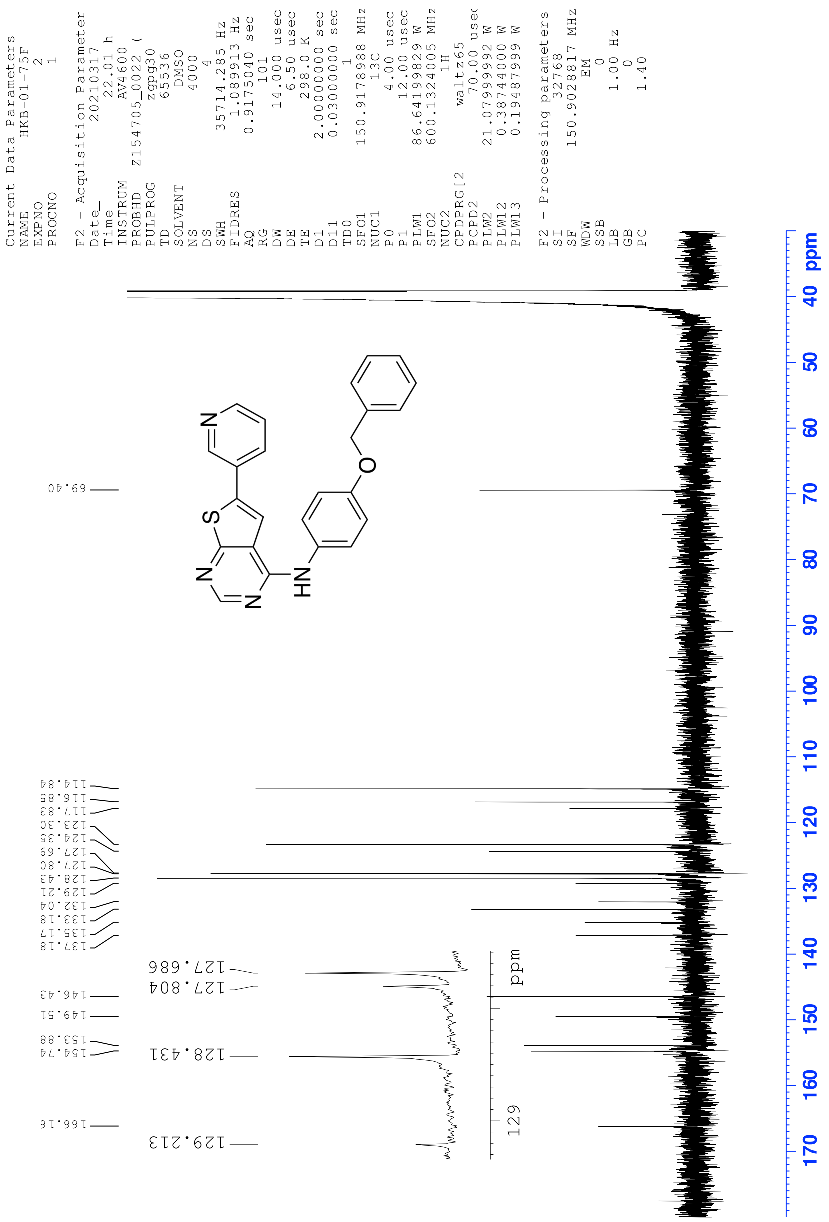

Figure 151: ^{13}C-NMR specter of compound **13**

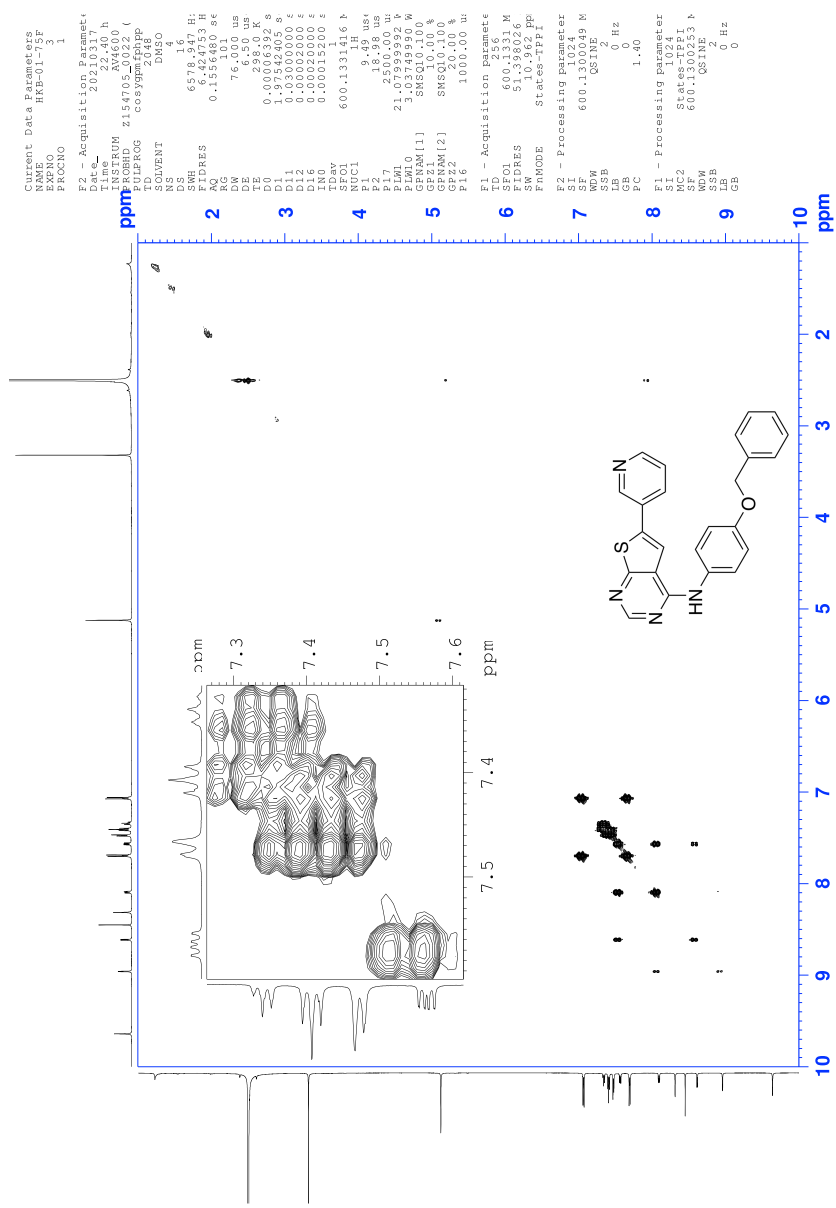

Figure 152: COSY specter of compound **13**

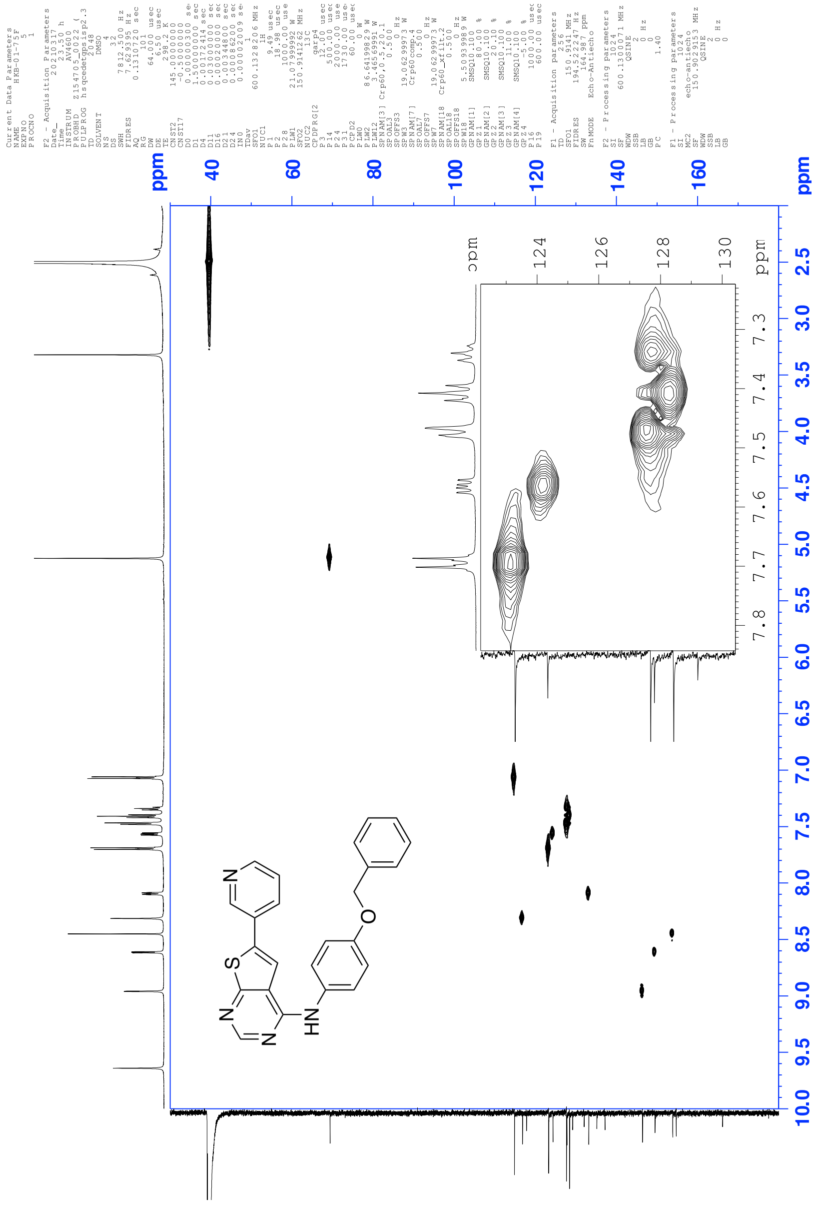

Figure 153: HSQC specter of compound **13**

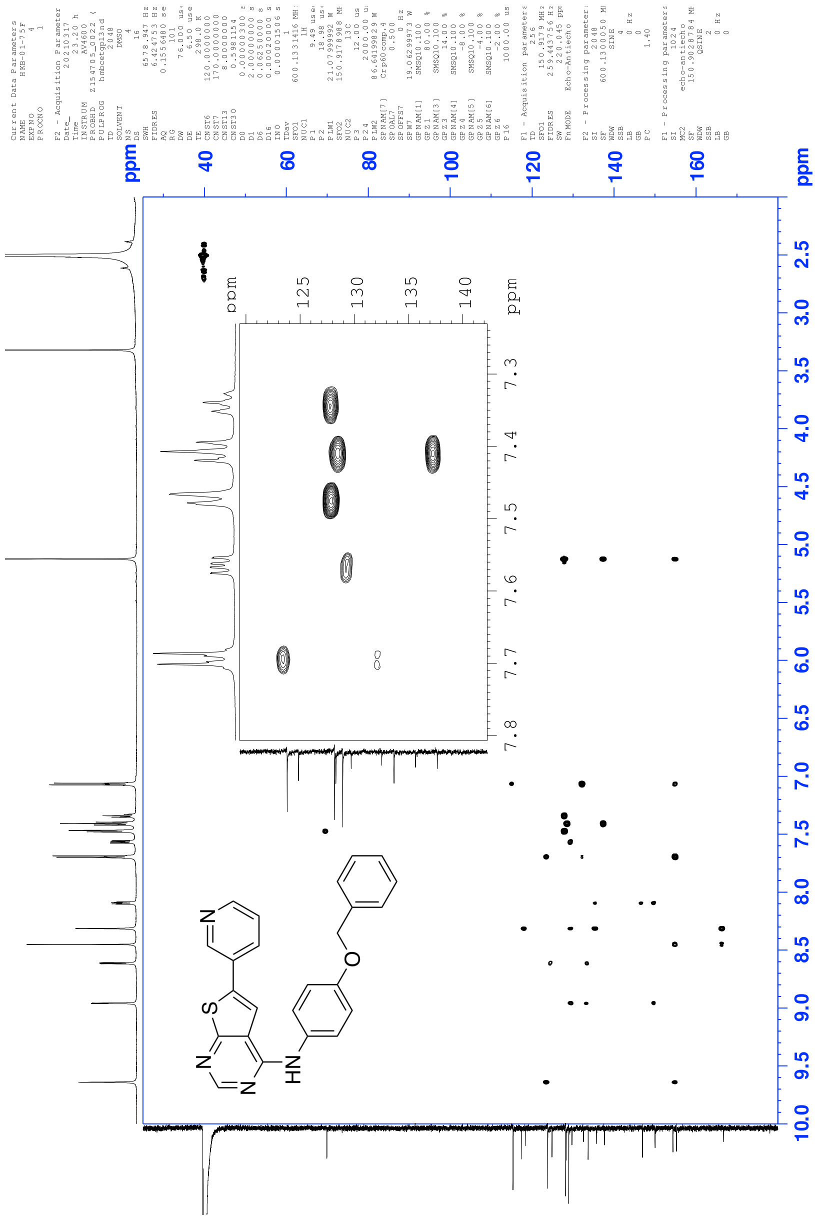

Figure 154: HMBC specter of compound **13**

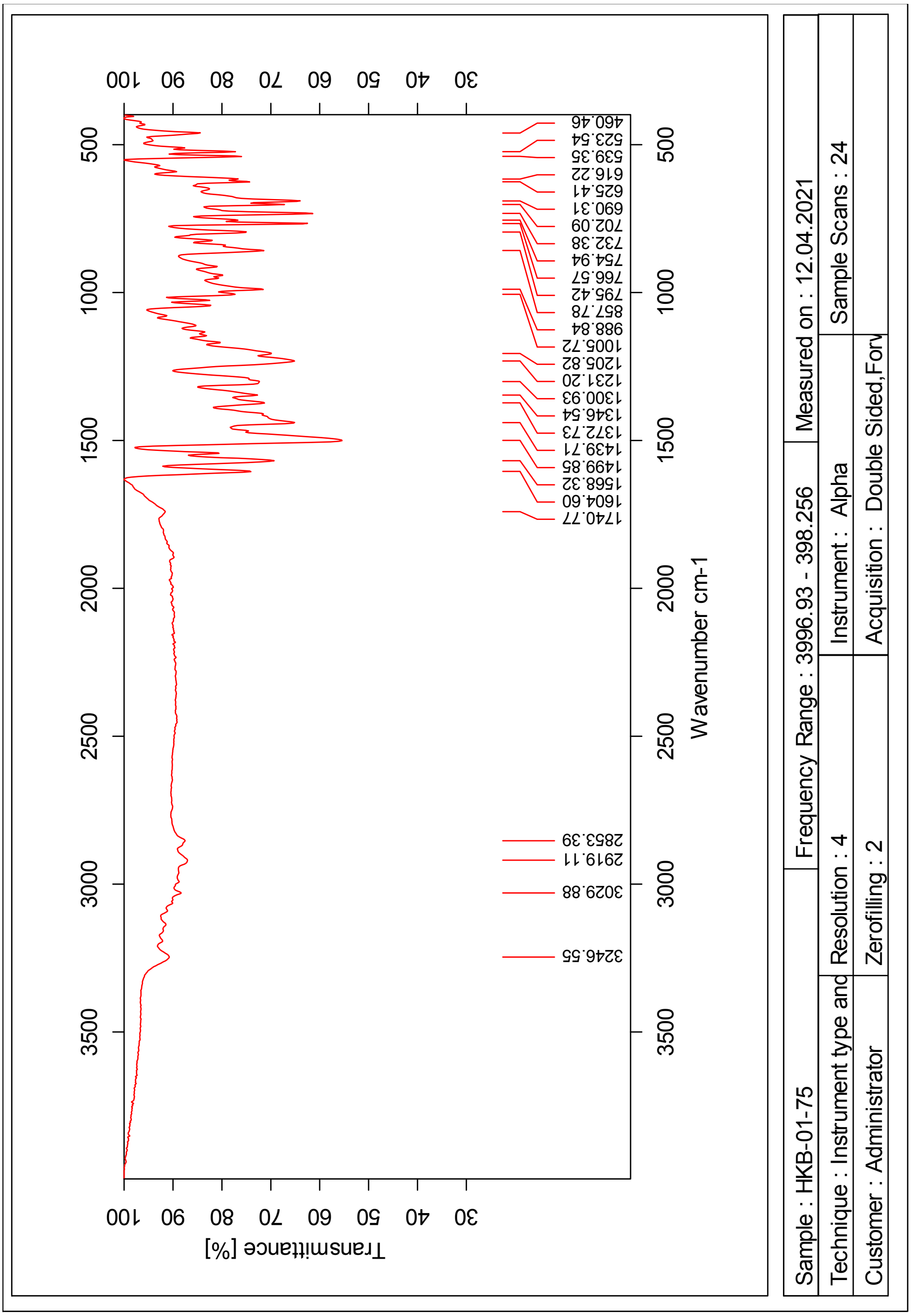

Figure 155: IR-spectrum of compound **13**

Elemental Composition Report **Page 1**

Single Mass Analysis
Tolerance = 2.0 PPM / DBE: min = -10.0, max = 50.0
Element prediction: Off
Number of isotope peaks used for i-FIT = 6

Monoisotopic Mass, Even Electron Ions
1284 formula(e) evaluated with 3 results within limits (all results (up to 1000) for each mass)
Elements Used:
C: 0-100 H: 0-100 N: 0-6 O: 0-6 S: 0-1 I: 0-2

2021-206 82 (0.778) AM2 (Ar,35000.0,0.00,0.00); Cm (82:93)
1: TOF MS ES+

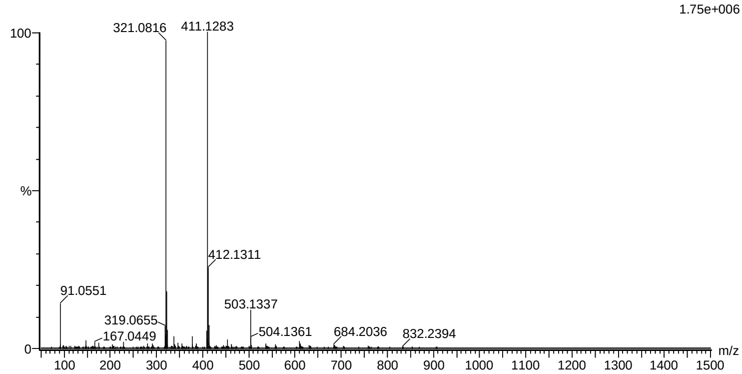

Minimum:				-10.0				
Maximum:		5.0	2.0	50.0				
Mass	Calc. Mass	mDa	PPM	DBE	i-FIT	Norm	Conf(%)	Formula
411.1283	411.1280	0.3	0.7	17.5	2046.9	0.001	99.90	C24 H19 N4 O S
	411.1277	0.6	1.5	-7.5	2056.5	9.599	0.01	C10 H36 O6 S I
	411.1291	-0.8	-1.9	-2.5	2053.9	7.032	0.09	C11 H32 N4 O2 S I

Figure 156: MS specter of compound **13**

.1.22 Spectroscopic data for Compound 14

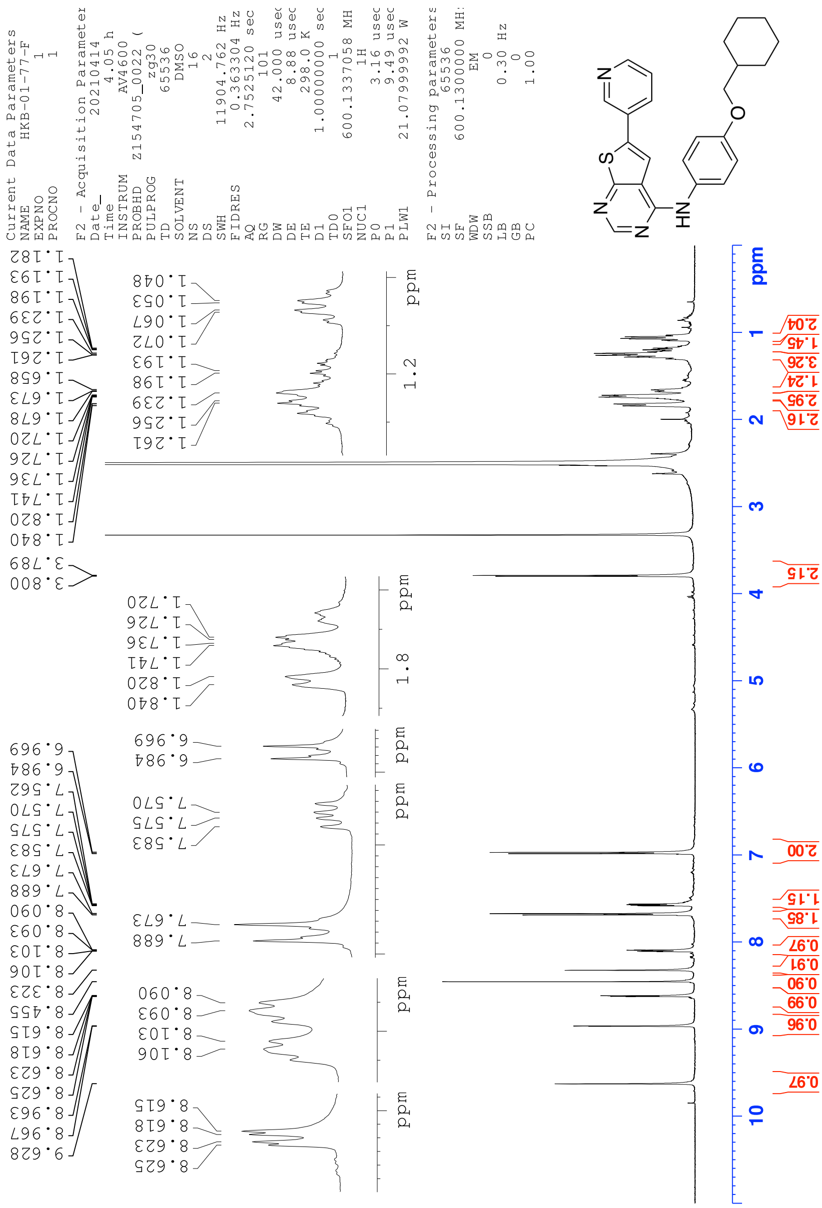

Figure 157: ^{1}H-NMR specter of compound **14**

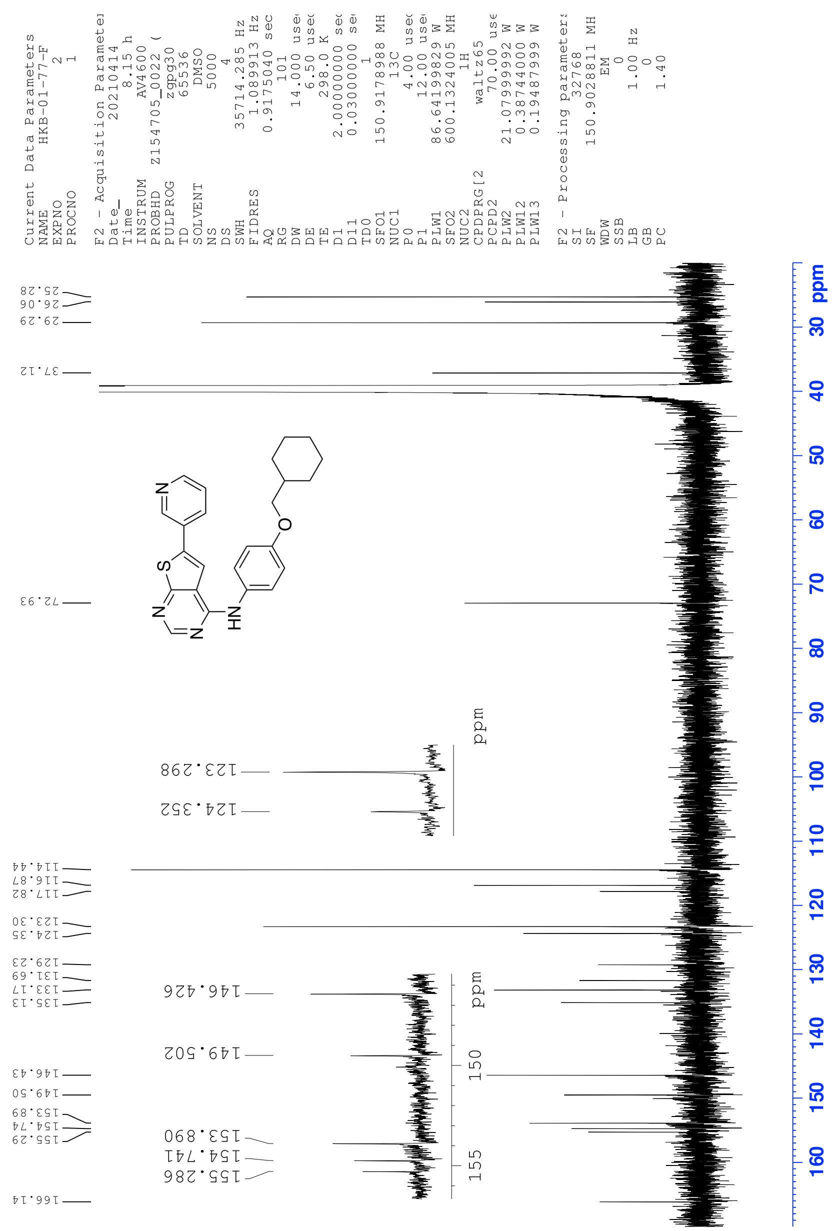

Figure 158: ^{13}C-NMR specter of compound **14**

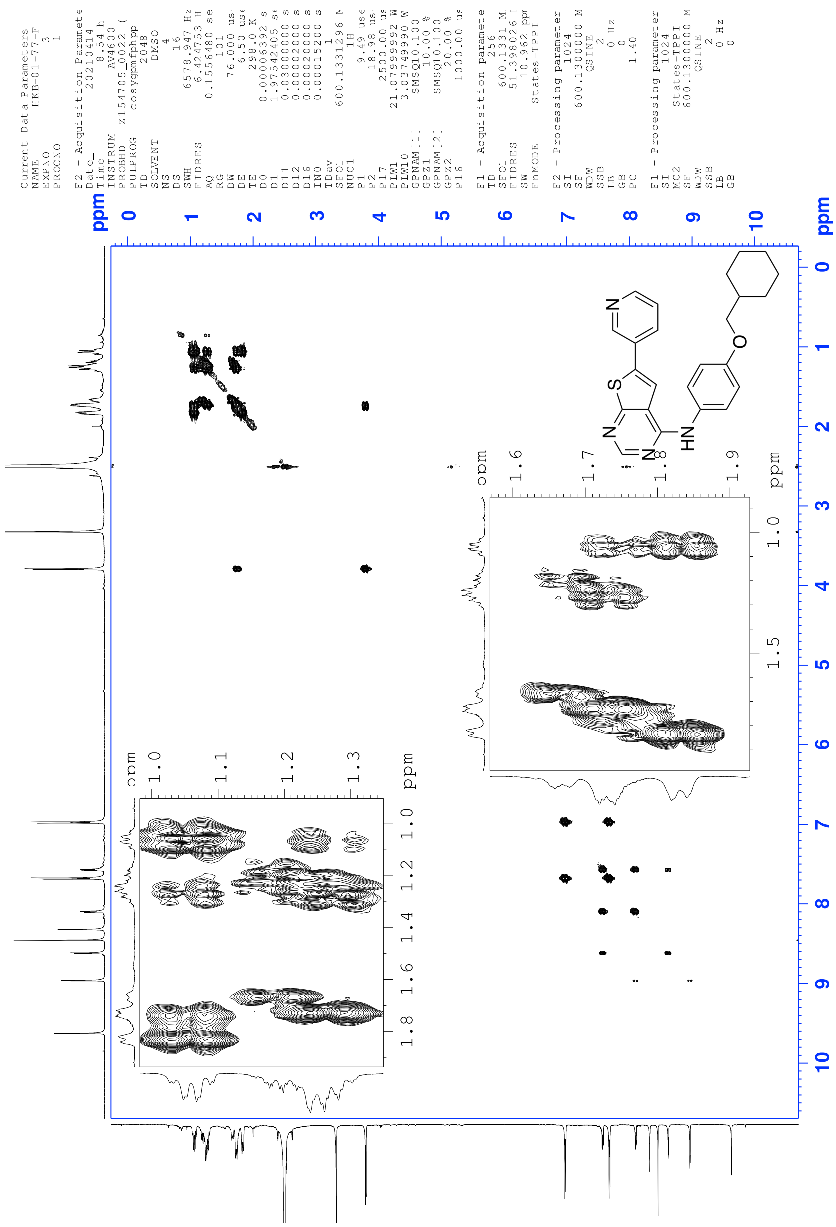

Figure 159: COSY specter of compound **14**

Figure 160: HSQC specter of compound **14**

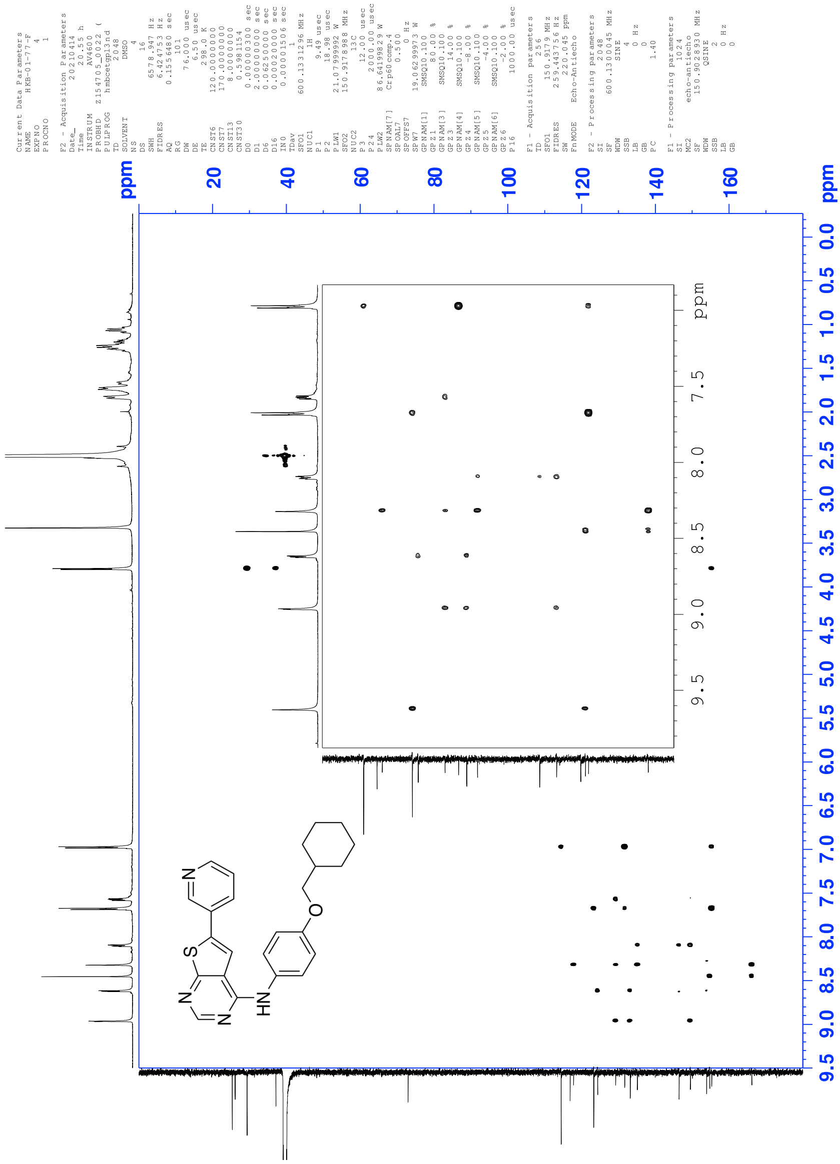

Figure 161: HMBC specter of compound **14**

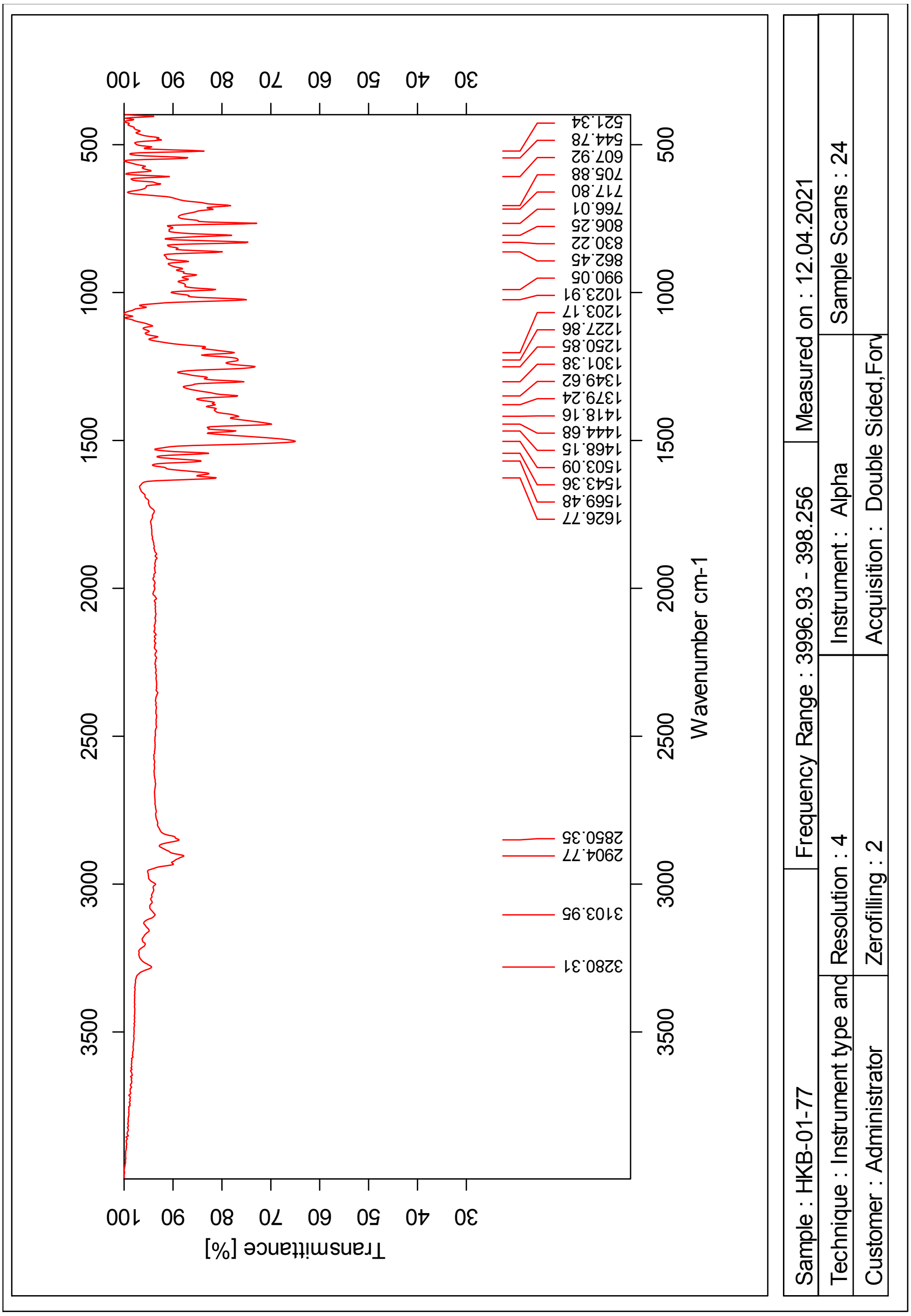

Figure 162: IR-spectrum of compound **14**

Elemental Composition Report **Page 1**

Single Mass Analysis
Tolerance = 2.0 PPM / DBE: min = -10.0, max = 50.0
Element prediction: Off
Number of isotope peaks used for i-FIT = 6

Monoisotopic Mass, Even Electron Ions
1303 formula(e) evaluated with 2 results within limits (all results (up to 1000) for each mass)
Elements Used:
C: 0-100 H: 0-100 N: 0-6 O: 0-6 S: 0-1 I: 0-2

2021-207 70 (0.666) AM2 (Ar,35000.0,0.00,0.00); Cm (65:75)
1: TOF MS ES+

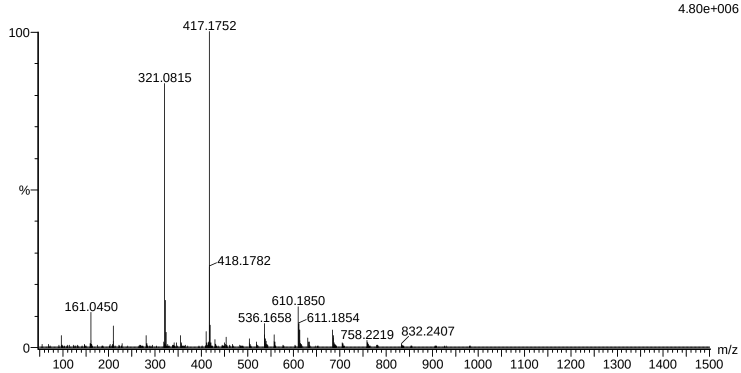

Minimum:				-10.0				
Maximum:		5.0	2.0	50.0				
Mass	Calc. Mass	mDa	PPM	DBE	i-FIT	Norm	Conf(%)	Formula
417.1752	417.1749	0.3	0.7	14.5	2282.4	0.000	99.96	C24 H25 N4 O S
	417.1760	-0.8	-1.9	-5.5	2290.2	7.830	0.04	C11 H38 N4 O2 S I

Figure 163: MS specter of compound **14**

.1.23 Spectroscopic data for Compound (*rac*)-15

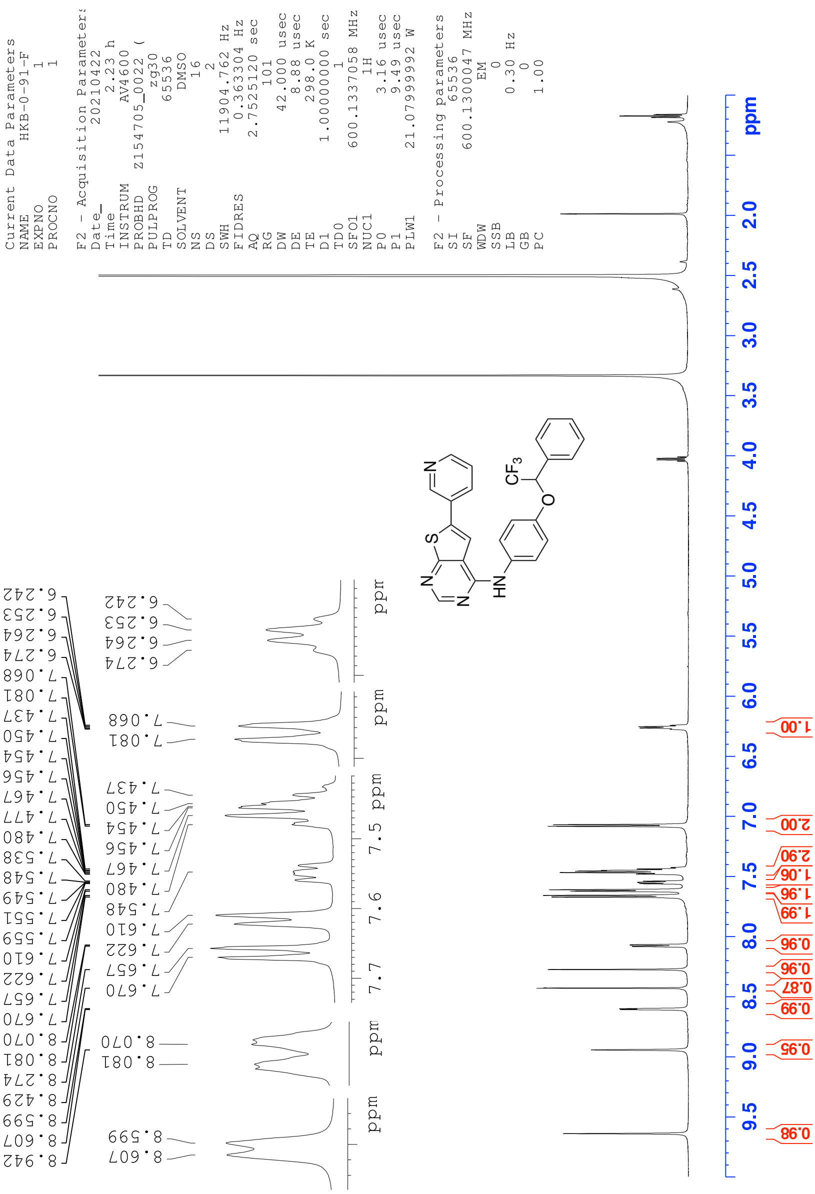

Figure 164: ^{1}H-NMR specter of compound **(*rac*)-15**

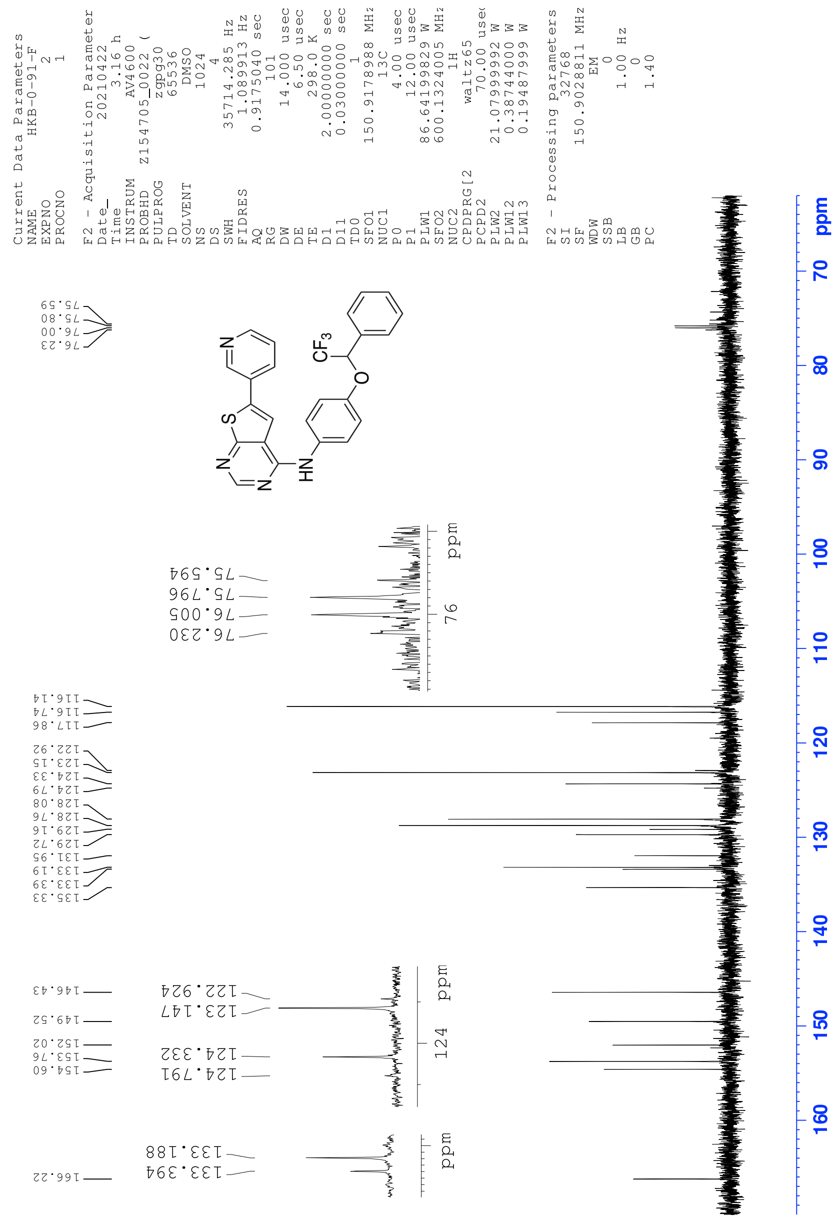

Figure 165: ^{13}C-NMR specter of compound ***(rac)*-15**

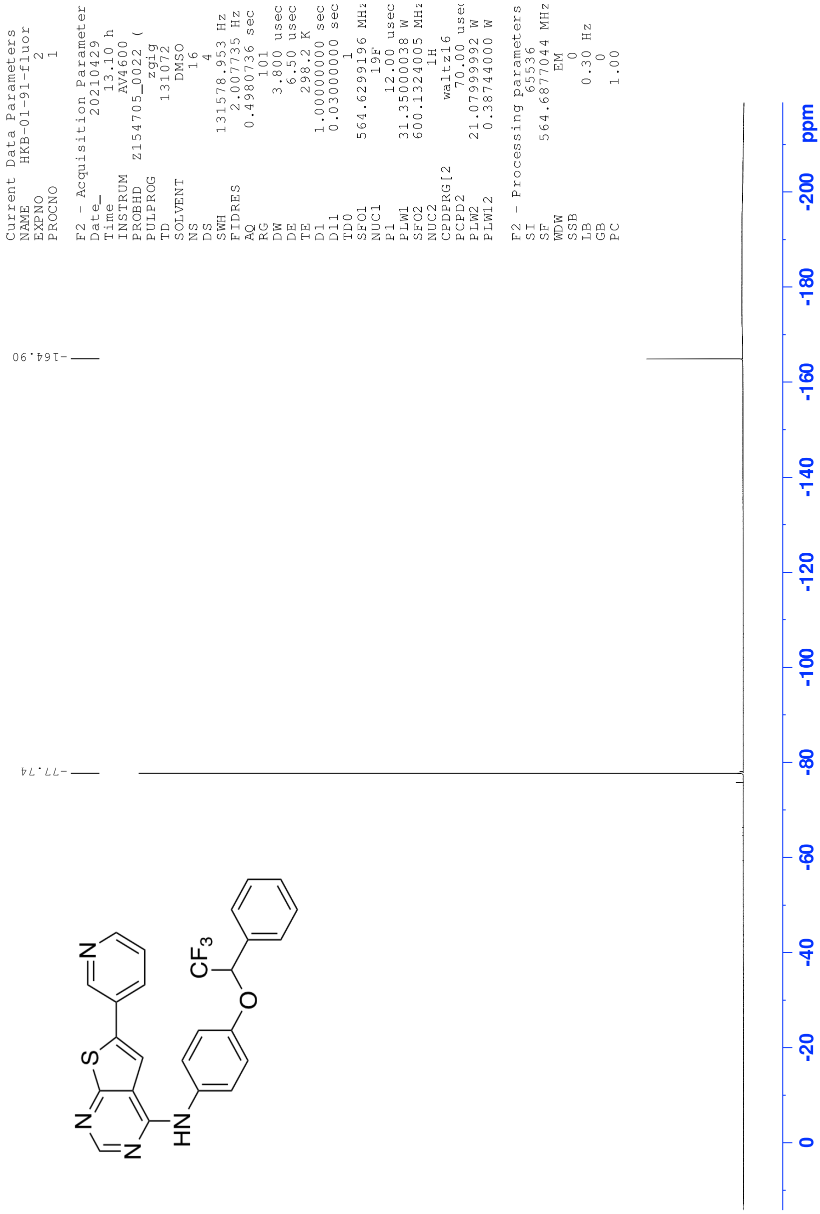

Figure 166: ^{19}F-NMR specter of compound **(*rac*)-15**

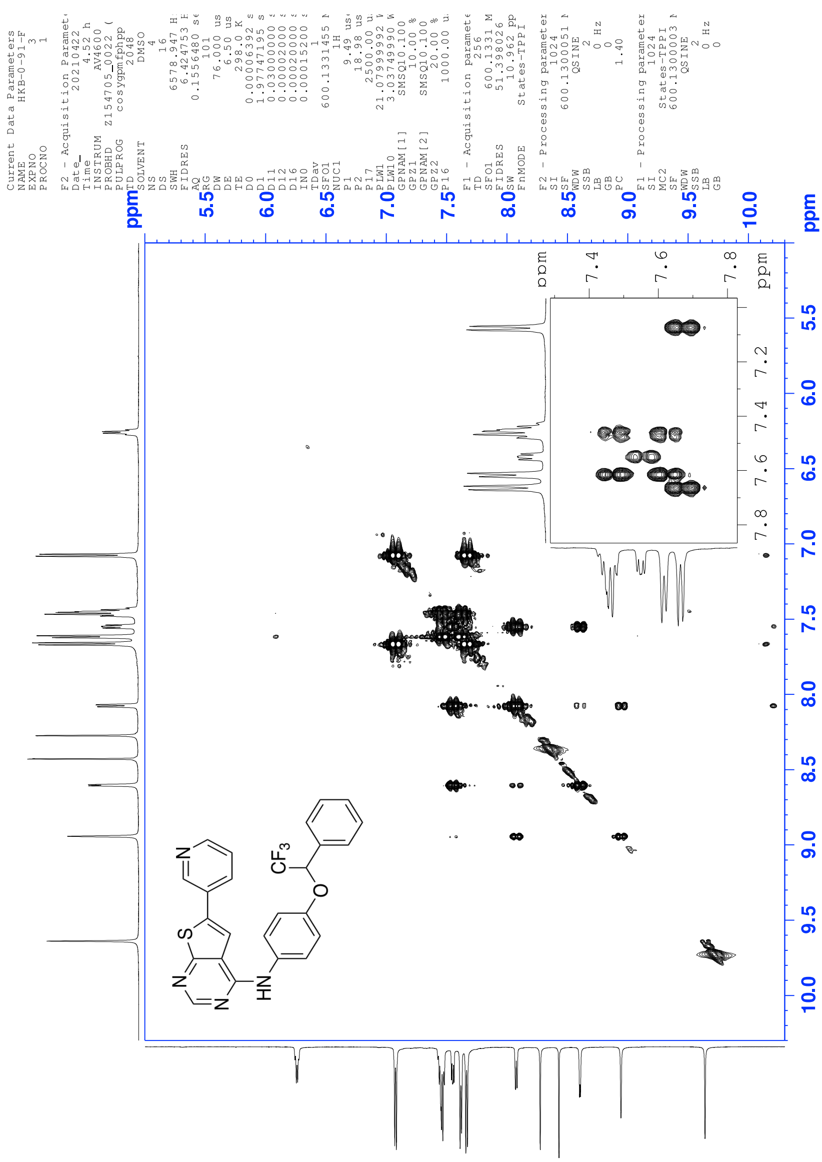

Figure 167: COSY specter of compound ***(rac)*-15**

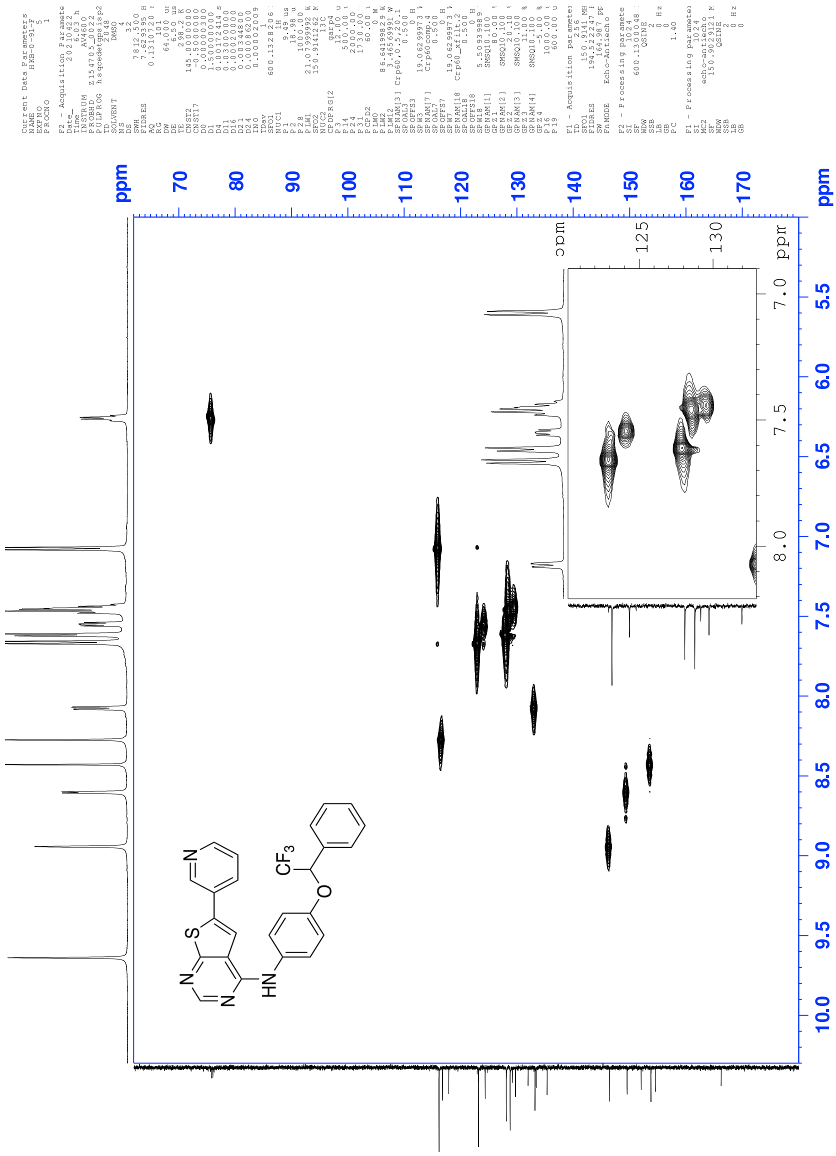

Figure 168: HSQC specter of compound ***(rac)*-15**

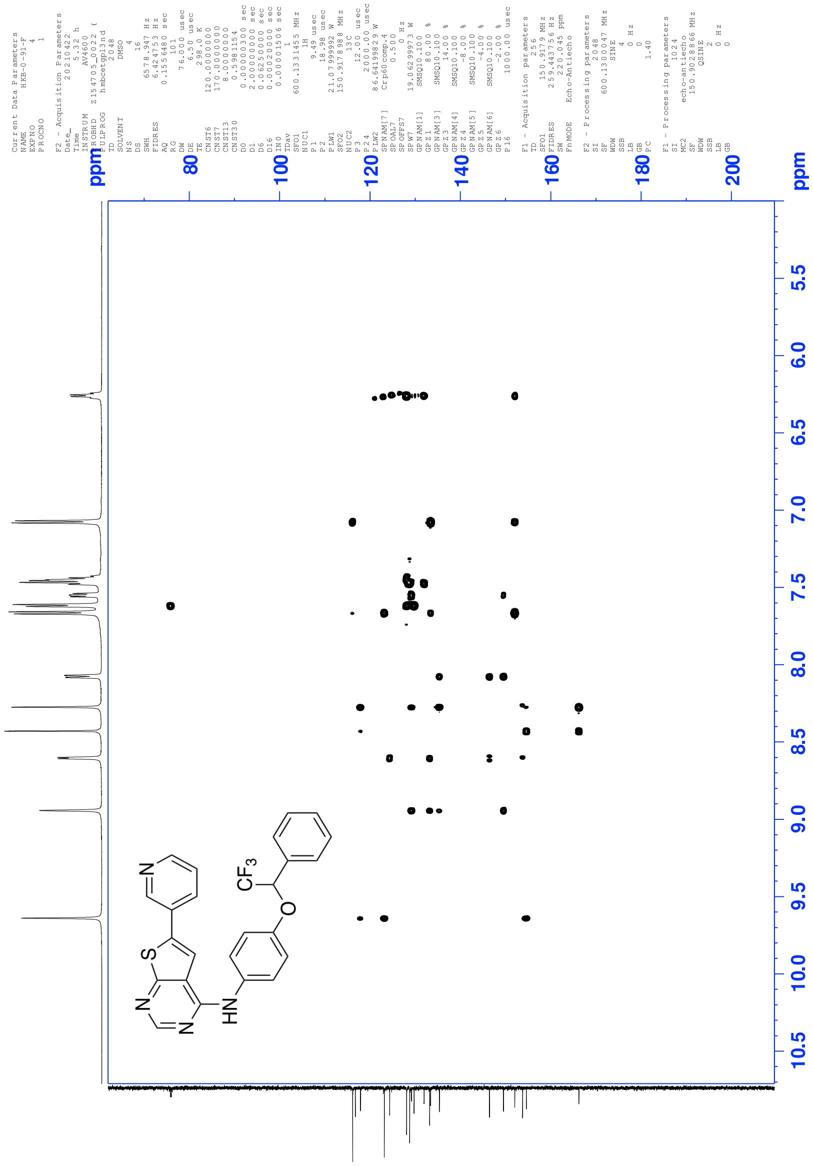

Figure 169: HMBC specter of compound ***(rac)*-15**

Figure 170: IR-spectrum of compound **(*rac*)-15**

Elemental Composition Report **Page 1**

Single Mass Analysis
Tolerance = 2.0 PPM / DBE: min = -10.0, max = 50.0
Element prediction: Off
Number of isotope peaks used for i-FIT = 6

Monoisotopic Mass, Even Electron Ions
9140 formula(e) evaluated with 14 results within limits (all results (up to 1000) for each mass)
Elements Used:
C: 0-100 H: 0-100 N: 0-5 O: 0-12 F: 0-3 S: 0-1 Br: 0-2

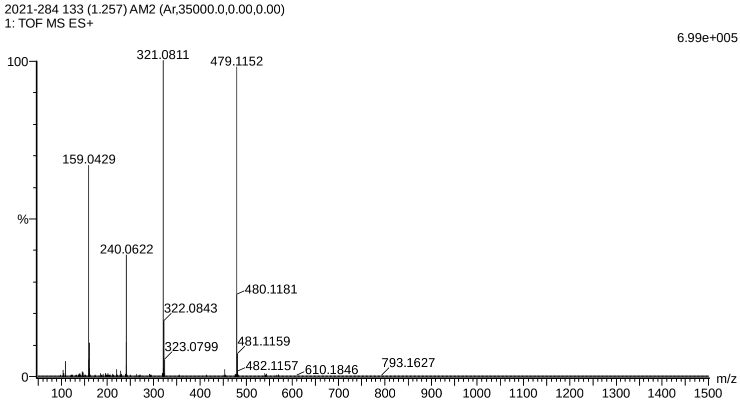

Minimum:				-10.0				
Maximum:		5.0	2.0	50.0				

Mass	Calc. Mass	mDa	PPM	DBE	i-FIT	Norm	Conf(%)	Formula
479.1152	479.1153	-0.1	-0.2	17.5	1620.8	0.019	98.15	C25 H18 N4 O F3 S
	479.1151	0.1	0.2	-2.5	1642.2	21.393	0.00	C12 H31 N4 O5 F3 S Br
	479.1153	-0.1	-0.2	1.5	1639.1	18.302	0.00	C14 H29 N4 O8 F Br
	479.1154	-0.2	-0.4	-6.5	1644.2	23.346	0.00	C13 H41 N2 O4 S Br2
	479.1154	-0.2	-0.4	12.5	1627.2	6.428	0.16	C23 H21 O9 F2
	479.1156	-0.4	-0.8	21.5	1629.0	8.148	0.03	C27 H16 N4 O4 F
	479.1147	0.5	1.0	3.5	1625.0	4.207	1.49	C15 H25 N2 O11 F2 S
	479.1157	-0.5	-1.0	6.5	1639.5	18.678	0.00	C20 H27 N2 O3 F3 Br
	479.1157	-0.5	-1.0	13.5	1641.9	21.083	0.00	C26 H28 N2 S Br
	479.1146	0.6	1.3	10.5	1639.5	18.718	0.00	C23 H26 N2 O2 F2 Br
	479.1159	-0.7	-1.5	-0.5	1627.2	6.392	0.17	C12 H26 N2 O12 F3 S
	479.1144	0.8	1.7	25.5	1630.2	9.421	0.01	C30 H15 N4 O3
	479.1160	-0.8	-1.7	2.5	1643.8	22.989	0.00	C21 H37 O2 Br2
	479.1143	0.9	1.9	-9.5	1644.2	23.411	0.00	C10 H39 N2 O6 F2 Br2

Figure 171: MS specter of compound **(*rac*)-15**

.1.24 Spectroscopic data for Compound (*S*)-15

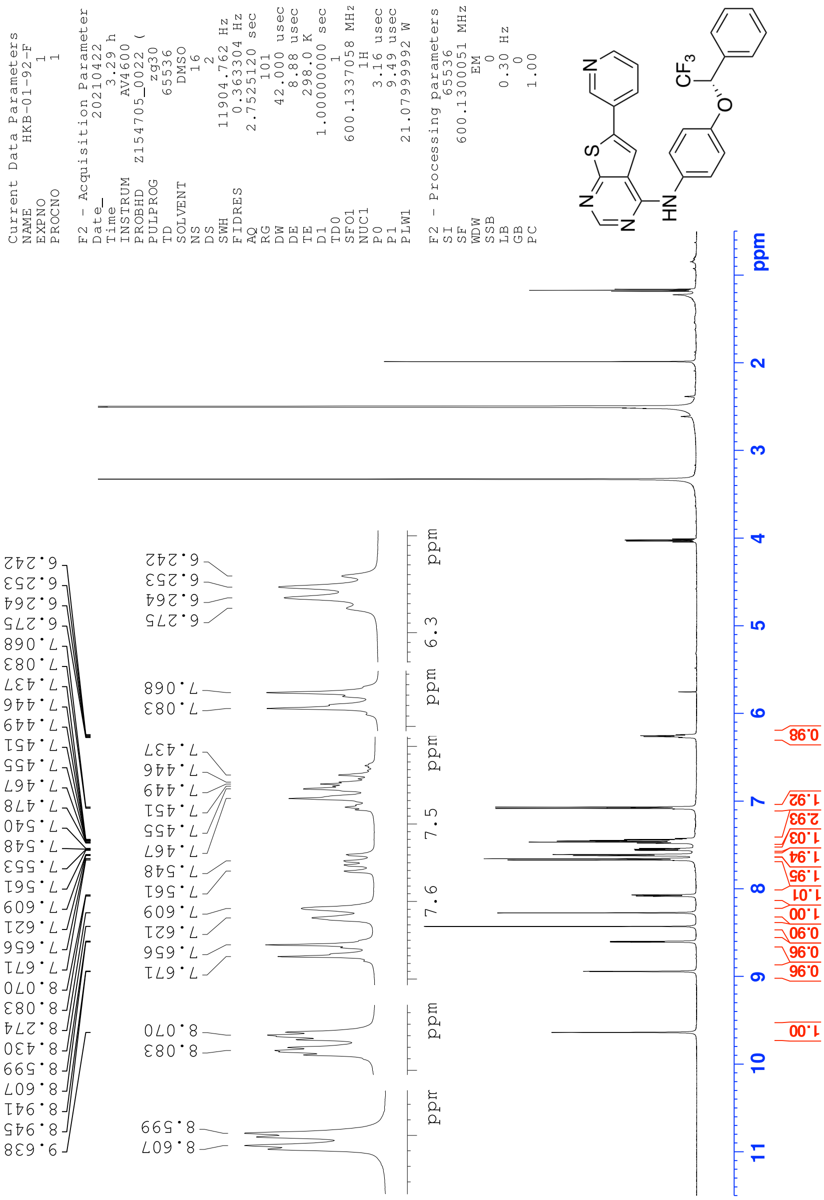

Figure 172: ^{1}H-NMR specter of compound **(*S*)-15**

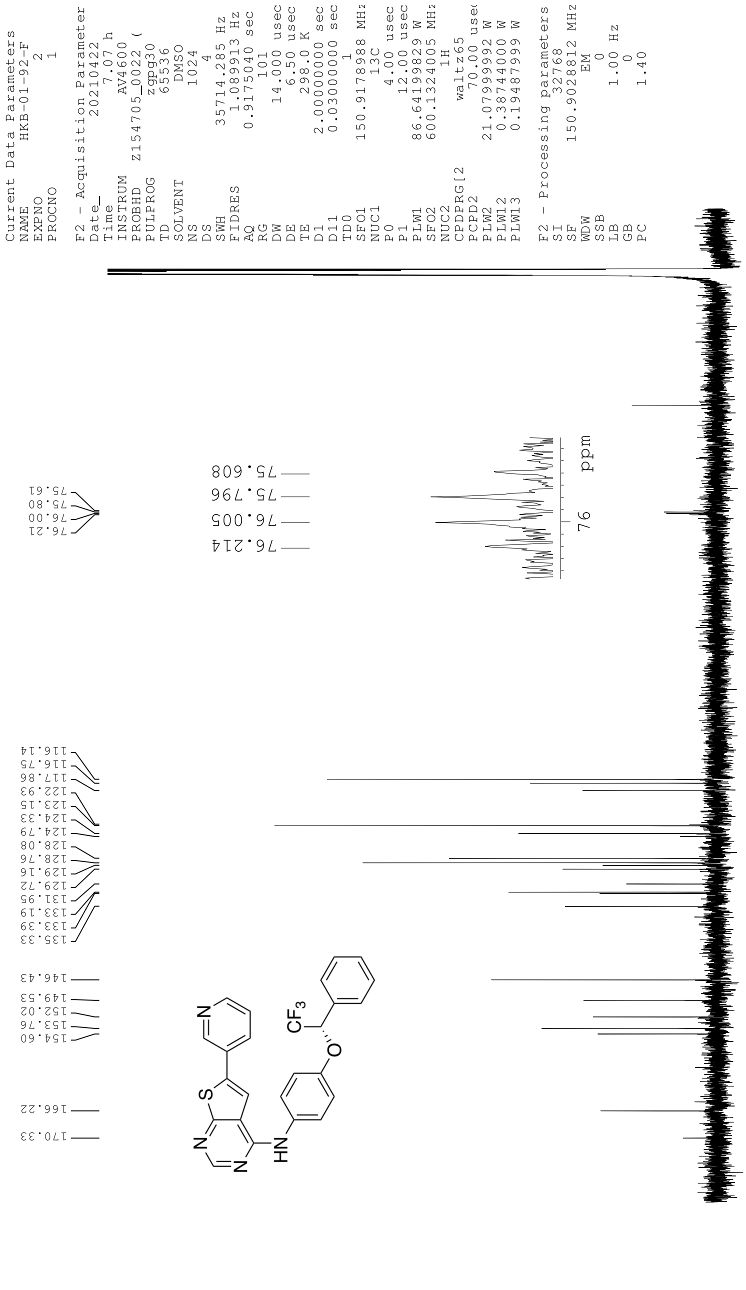

Figure 173: ^{13}C-NMR specter of compound **(*S*)-15**

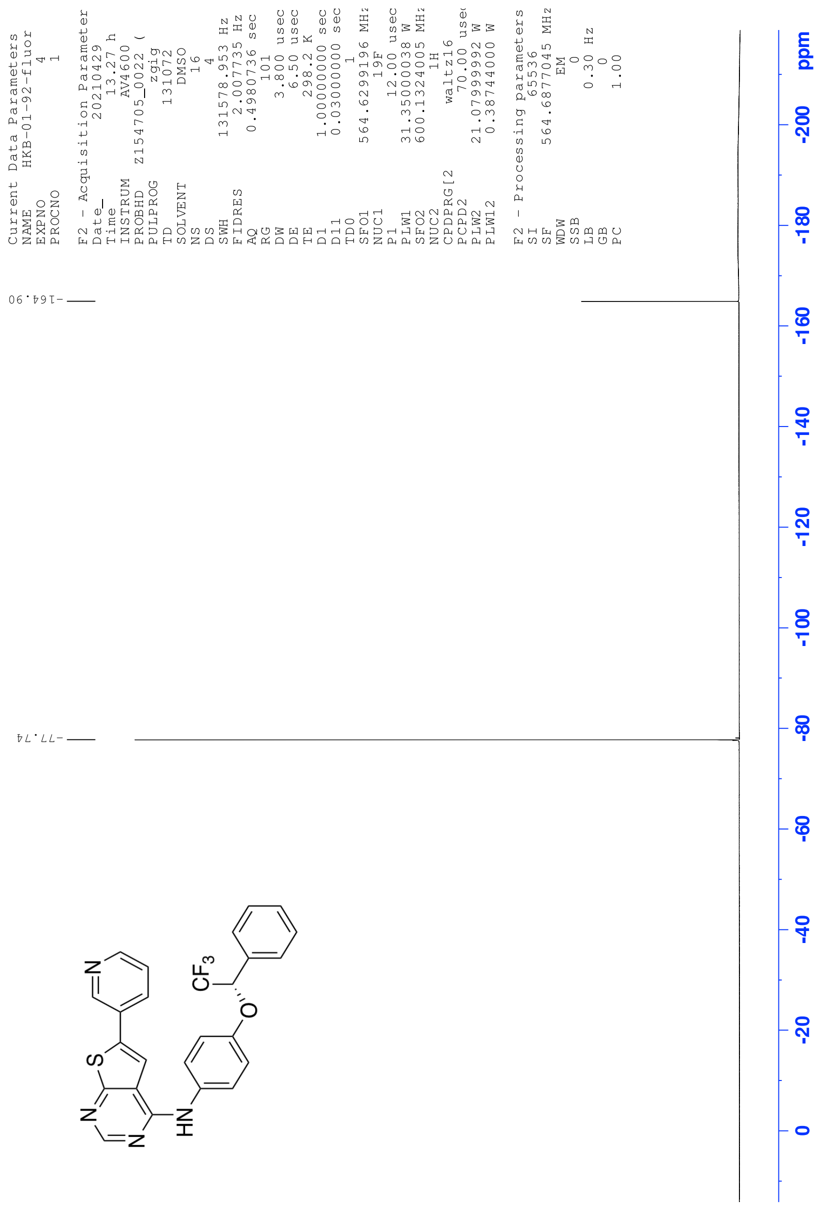

Figure 174: ^{19}F-NMR specter of compound ***(S)*-15**

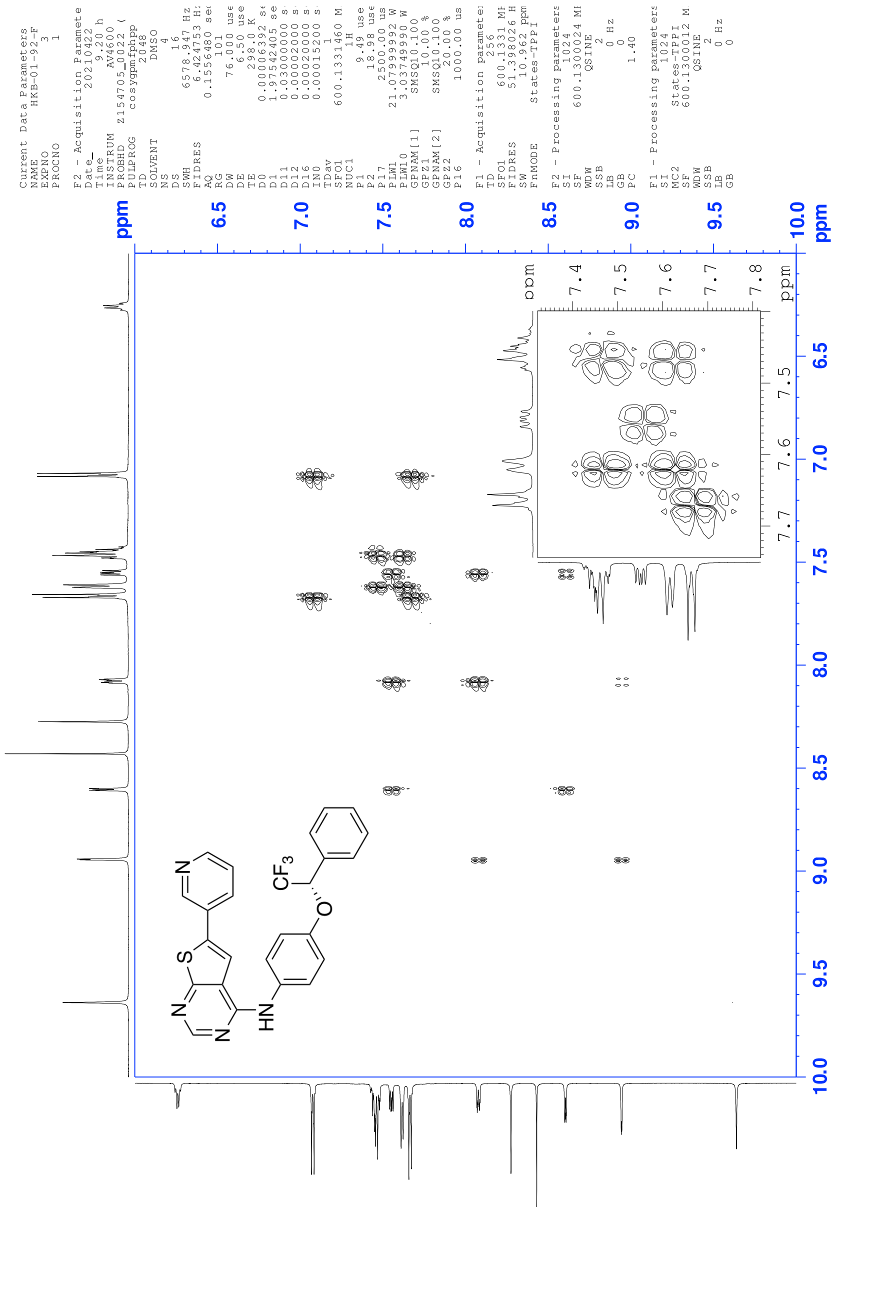

Figure 175: COSY specter of compound **(*S*)-15**

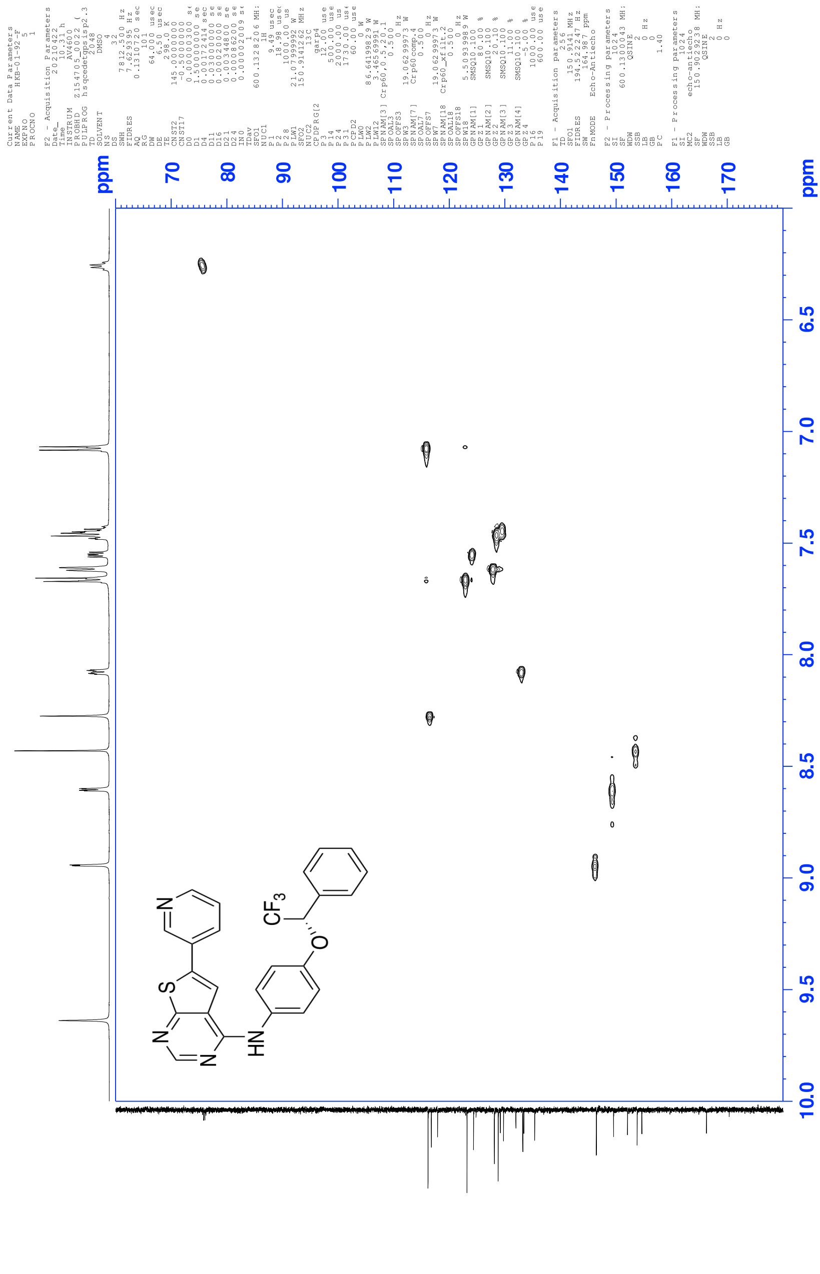

Figure 176: HSQC specter of compound **(*S*)-15**

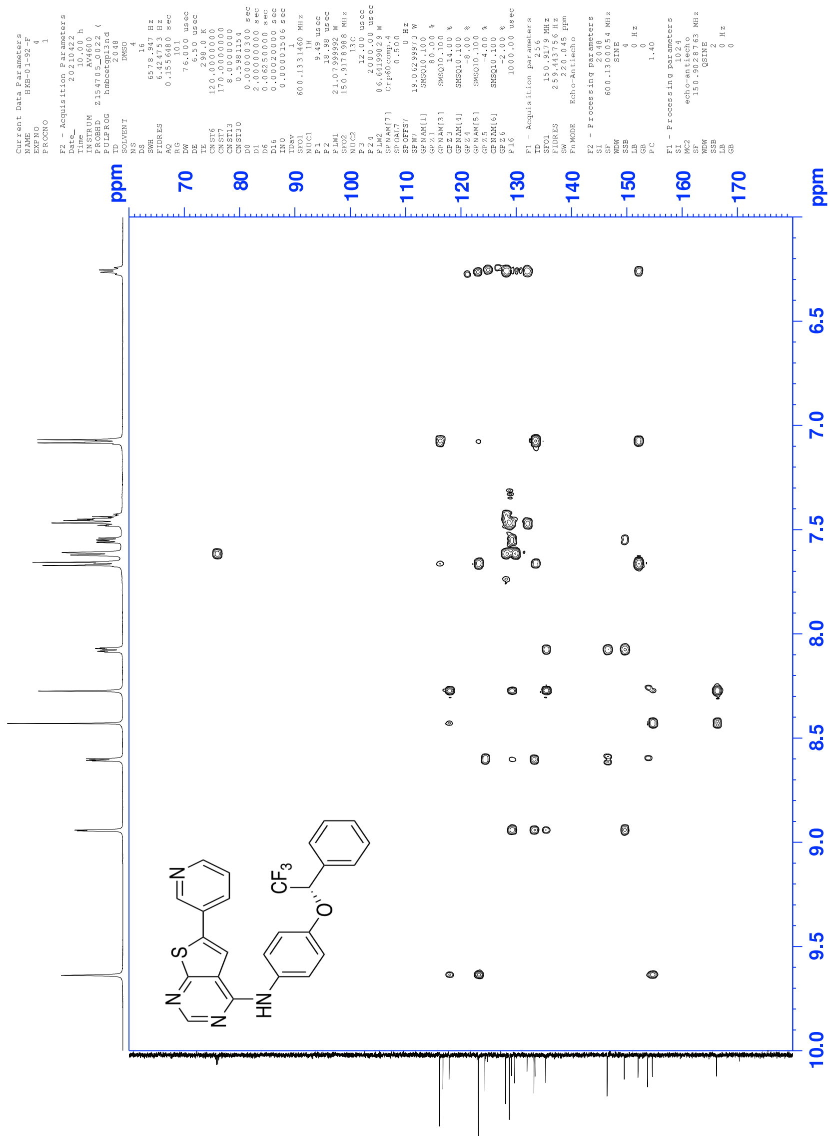

Figure 177: HMBC specter of compound **(*S*)-15**

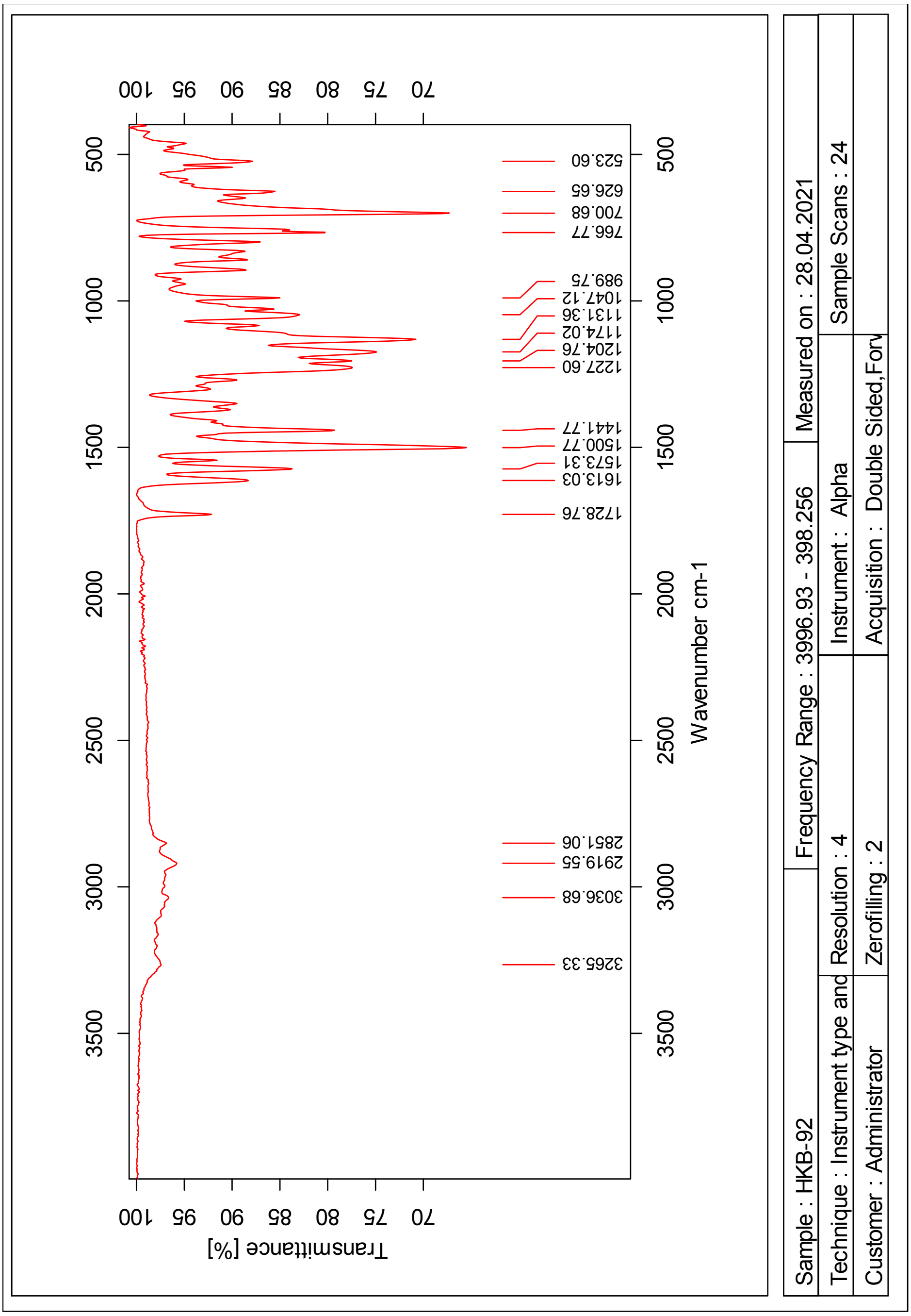

Figure 178: IR-spectrum of compound **(*S*)-15**

Elemental Composition Report

Page 1

Single Mass Analysis

Tolerance = 2.0 PPM / DBE: min = -10.0, max = 50.0
Element prediction: Off
Number of isotope peaks used for i-FIT = 6

Monoisotopic Mass, Even Electron Ions
9140 formula(e) evaluated with 14 results within limits (all results (up to 1000) for each mass)
Elements Used:
C: 0-100 H: 0-100 N: 0-5 O: 0-12 F: 0-3 S: 0-1 Br: 0-2

2021-285rerun 72 (0.683) AM2 (Ar,35000.0,0.00,0.00); Cm (68:72)
1: TOF MS ES+

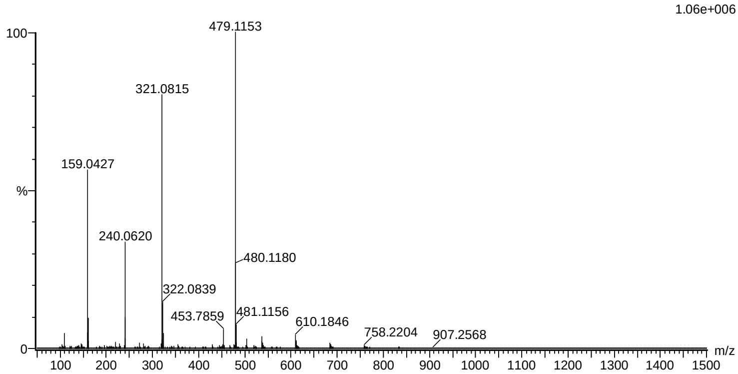

Minimum:				-10.0				
Maximum:		5.0	2.0	50.0				

Mass	Calc. Mass	mDa	PPM	DBE	i-FIT	Norm	Conf(%)	Formula
479.1153	479.1153	0.0	0.0	17.5	1895.5	0.116	89.01	C25 H18 N4 O F3 S
	479.1153	0.0	0.0	1.5	1913.5	18.130	0.00	C14 H29 N4 O8 F Br
	479.1154	-0.1	-0.2	12.5	1898.1	2.707	6.67	C23 H21 O9 F2
	479.1154	-0.1	-0.2	-6.5	1918.0	22.588	0.00	C13 H41 N2 O4 S Br2
	479.1151	0.2	0.4	-2.5	1915.7	20.334	0.00	C12 H31 N4 O5 F3 S Br
	479.1156	-0.3	-0.6	21.5	1899.1	3.654	2.59	C27 H16 N4 O4 F
	479.1157	-0.4	-0.8	6.5	1912.8	17.421	0.00	C20 H27 N2 O3 F3 Br
	479.1157	-0.4	-0.8	13.5	1914.9	19.464	0.00	C26 H28 N2 S Br
	479.1147	0.6	1.3	3.5	1900.6	5.174	0.57	C15 H25 N2 O11 F2 S
	479.1159	-0.6	-1.3	-0.5	1902.7	7.319	0.07	C12 H26 N2 O12 F3 S
	479.1160	-0.7	-1.5	2.5	1918.0	22.621	0.00	C21 H37 O2 Br2
	479.1146	0.7	1.5	10.5	1912.8	17.378	0.00	C23 H26 N2 O2 F2 Br
	479.1144	0.9	1.9	25.5	1899.9	4.512	1.10	C30 H15 N4 O3
	479.1162	-0.9	-1.9	-4.5	1915.9	20.481	0.00	C13 H36 O11 S Br

Figure 179: MS specter of compound **(*S*)-15**

.2 Chromatogram

.2.1 Chromatogram of Compounds (*R*)- and (*S*)-9

```
Data File C:\CHEM32\1\DATA\HAAKON\CHIRALMIX000001.D
Sample Name: HKB7172mix
    =====================================================================
    Acq. Operator   : Haakon
    Acq. Instrument : Instrument 1                   Location :   -
    Injection Date  : 3/15/2021 11:27:20 AM
    Acq. Method     : C:\CHEM32\1\METHODS\HAAKON\CHIRAL_SEP.M
    Last changed    : 3/15/2021 11:16:04 AM by Kristoffer
                      (modified after loading)
    Analysis Method : C:\CHEM32\1\METHODS\CECILIE\YIN_SYRE.M
    Last changed    : 4/21/2021 10:24:05 AM by Mari Rødseth
                      (modified after loading)
    Sample Info     : OD, Isocratic, Hexane:Propanol [90:10], 1 mL/min, 10 µL
                      .

    =====================================================================
```

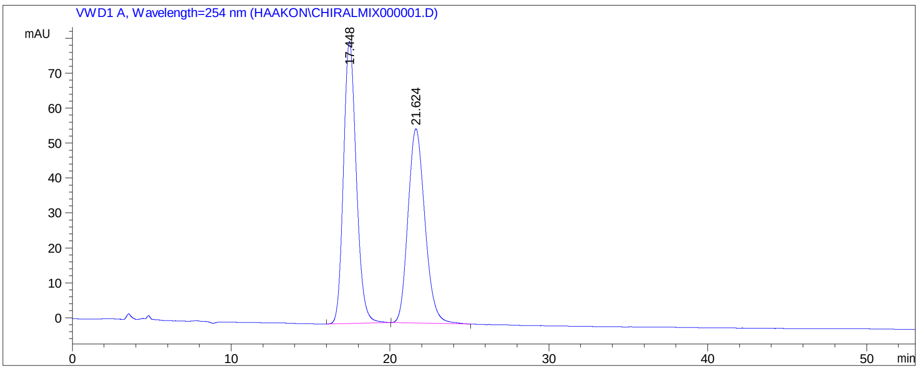


```
    =====================================================================
                             Area Percent Report
    =====================================================================

    Sorted By             :      Signal
    Multiplier:                   :      1.0000
    Dilution:                     :      1.0000
    Use Multiplier & Dilution Factor with ISTDs


    Signal 1: VWD1 A, Wavelength=254 nm

    Peak RetTime Type  Width     Area      Height     Area
      #   [min]        [min]  mAU   *s   [mAU   ]      %
    ----|-------|----|-------|----------|----------|--------|
       1  17.448 BB    0.8583 4539.93555   80.74996  52.4601
       2  21.624 BB    1.0676 4114.13525   55.57125  47.5399

    Totals :                  8654.07080  136.32121


    =====================================================================
                             *** End of Report ***

Instrument 1 4/21/2021 10:24:10 AM Mari Rødseth                          Page    1 of 1
```


Figure 180: Chromatogram from chiral HPLC from mix of compound **(*R*)-9** and **(*S*)-9**

```
Data File C:\CHEM32\1\DATA\HAAKON\HKB-01-71000001.D
Sample Name: HKB-01-71

    =====================================================================
    Acq. Operator   : Haakon
    Acq. Instrument : Instrument 1                    Location :   -
    Injection Date  : 3/15/2021 12:32:00 PM
    Acq. Method     : C:\CHEM32\1\METHODS\HAAKON\CHIRAL_SEP.M
    Last changed    : 3/15/2021 12:20:28 PM by Haakon
                      (modified after loading)
    Analysis Method : C:\CHEM32\1\DATA\ANNA TENNFJORD\F3S3_STD.D\DA.M (ESMOLOLKLORHYDRIN.M)
    Last changed    : 4/25/2021 12:14:39 PM by Mari Rødseth
                      (modified after loading)
    Method Info     : Separation of (R)- and (S)-chlorohydrin.

    Sample Info     : OD, Isocratic, Hexane:Propanol [90:10], 1 mL/min, 10 µL
                      .

    Additional Info : Peak(s) manually integrated
```

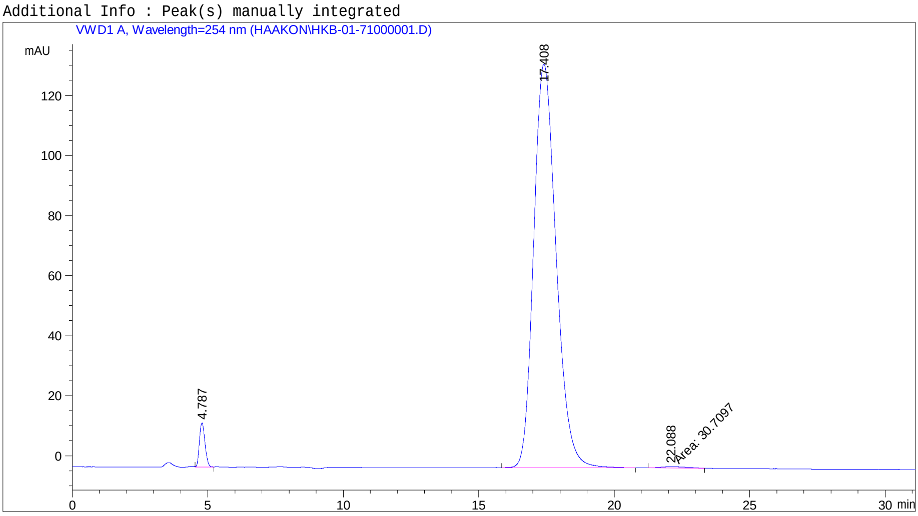


```
    =====================================================================
                             Area Percent Report
    =====================================================================

    Sorted By             :      Signal
    Multiplier:                   :      1.0000
    Dilution:                     :      1.0000
    Use Multiplier & Dilution Factor with ISTDs


    Signal 1: VWD1 A, Wavelength=254 nm
```

Instrument 1 4/26/2021 11:11:28 AM Mari Rødseth   Page   1 of 2

Figure 181: Chromatogram from chiral HPLC of compound **(*R*)-9**

```
Data File C:\CHEM32\1\DATA\HAAKON\HKB-01-72000002.D
Sample Name: HKB-01-72

    =====================================================================
    Acq. Operator   : Haakon
    Acq. Instrument : Instrument 1                   Location :   -
    Injection Date  : 3/15/2021 1:14:01 PM
    Acq. Method     : C:\CHEM32\1\METHODS\HAAKON\CHIRAL_SEP.M
    Last changed    : 3/15/2021 1:03:04 PM by Haakon
                      (modified after loading)
    Analysis Method : C:\CHEM32\1\DATA\ANNA TENNFJORD\F3S3_STD.D\DA.M (ESMOLOLKLORHYDRIN.M)
    Last changed    : 4/25/2021 12:14:39 PM by Mari Rødseth
                      (modified after loading)
    Method Info     : Separation of (R)- and (S)-chlorohydrin.

    Sample Info     : OD, Isocratic, Hexane:Propanol [90:10], 1 mL/min, 10 µL
                      .

    Additional Info : Peak(s) manually integrated
```

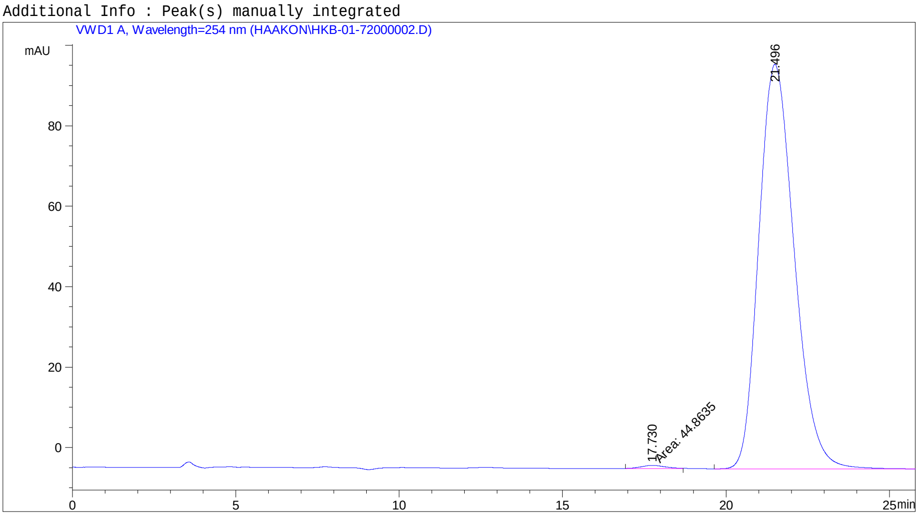


```
    =====================================================================
                             Area Percent Report
    =====================================================================

    Sorted By             :      Signal
    Multiplier:                   :      1.0000
    Dilution:                     :      1.0000
    Use Multiplier & Dilution Factor with ISTDs


    Signal 1: VWD1 A, Wavelength=254 nm
```

Instrument 1 4/26/2021 11:11:06 AM Mari Rødseth   Page   1 of 2

Figure 182: Chromatogram from chiral HPLC of compound ***(S)*-9**

.2.2 Chromatogram of Compounds (*rac*)-, (*R*)- and (*S*)-10

```
Data File C:\CHEM32\1\DATA\HAAKON\HKB-83.D
Sample Name: HKB-83-chiralmix
    =====================================================================
    Acq. Operator   : Haakon Bye
    Acq. Instrument : Instrument 1                    Location :   -
    Injection Date  : 4/21/2021 9:56:56 AM
    Acq. Method     : C:\CHEM32\1\METHODS\HAAKON\CHIRAL_SEP.M
    Last changed    : 4/21/2021 9:56:38 AM by Haakon Bye
                      (modified after loading)
    Analysis Method : C:\CHEM32\1\DATA\ANNA TENNFJORD\S4F2_70HEX.D\DA.M (CARTEOLOL.M)
    Last changed    : 6/1/2021 4:11:13 PM by Kristoffer
                      (modified after loading)
    Method Info     : Separation of carteolol enantiomers.

    Sample Info     : Isocratic n-Hexane:i-PrOH (90:10), flow 1.0 mL/min, 10
                      uL injection. Chiral mix

    =====================================================================
```

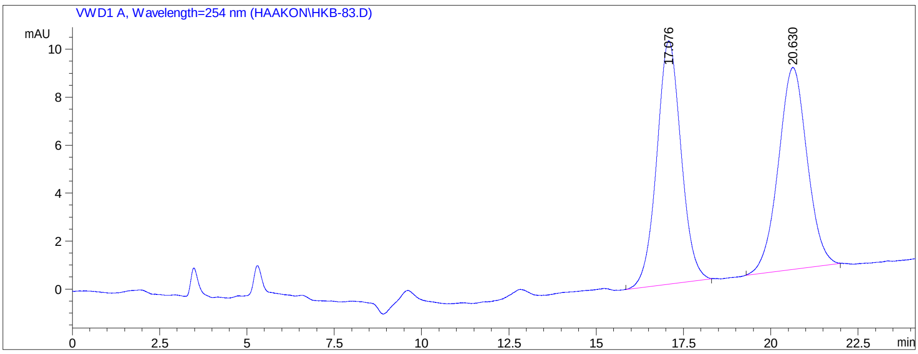


```
    =====================================================================
                             Area Percent Report
    =====================================================================

    Sorted By             :      Signal
    Multiplier:                   :      1.0000
    Dilution:                     :      1.0000
    Do not use Multiplier & Dilution Factor with ISTDs


    Signal 1: VWD1 A, Wavelength=254 nm

    Peak RetTime Type  Width     Area      Height     Area
      #   [min]        [min]  mAU   *s   [mAU   ]       %
    ----|-------|----|-------|----------|----------|--------|
       1  17.076 BB    0.5677  490.81873   10.15111  50.4334
       2  20.630 BB    0.6748  482.38358    8.42601  49.5666

    Totals :                   973.20230   18.57712


    =====================================================================

Instrument 1 6/1/2021 4:11:16 PM Kristoffer                           Page    1 of 1
```

Figure 183: Chromatogram from chiral HPLC of compound **(*rac*)-10**, rasemic mixture of compounds **(*R*)-10** and **(*S*)-10**.

Data File C:\CHEM32\1\DATA\HAAKON\HKB-88.D
Sample Name: HKB-88

```
=====================================================================
Acq. Operator   : Haakon Bye
Acq. Instrument : Instrument 1                  Location :   -
Injection Date  : 4/21/2021 10:28:46 AM
Acq. Method     : C:\CHEM32\1\METHODS\HAAKON\CHIRAL_SEP.M
Last changed    : 4/21/2021 10:21:29 AM by Haakon Bye
                  (modified after loading)
Analysis Method : C:\CHEM32\1\DATA\ANNA TENNFJORD\F3S3_STD.D\DA.M (ESMOLOLKLORHYDRIN.M)
Last changed    : 4/25/2021 12:14:39 PM by Mari Rødseth
                  (modified after loading)
Method Info     : Separation of (R)- and (S)-chlorohydrin.

Sample Info     : Isocratic n-Hexane:i-PrOH (90:10), flow 1.0 mL/min, 10
                  uL injection. HKB-88


Additional Info : Peak(s) manually integrated
```

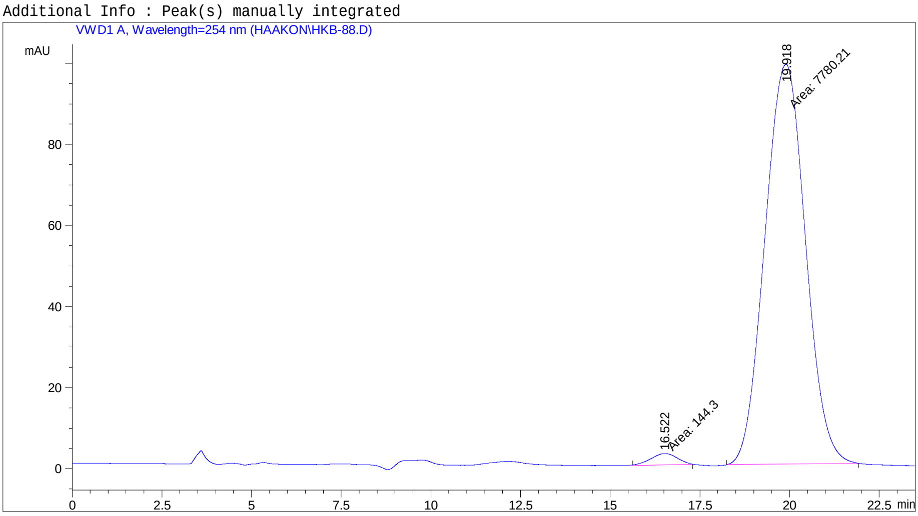


```
=====================================================================
                         Area Percent Report
=====================================================================

Sorted By             :      Signal
Multiplier:                   :      1.0000
Dilution:                     :      1.0000
Use Multiplier & Dilution Factor with ISTDs


Signal 1: VWD1 A, Wavelength=254 nm
```

Instrument 1 4/26/2021 11:09:13 AM Mari Rødseth   Page   1 of 2

Figure 184: Chromatogram from chiral HPLC of compound ***(R)*-10**

```
Data File C:\CHEM32\1\DATA\HAAKON\HKB-90.D
Sample Name: HKB-

    =====================================================================
    Acq. Operator   : Haakon Bye
    Acq. Instrument : Instrument 1                    Location :   -
    Injection Date  : 4/21/2021 11:06:04 AM
    Acq. Method     : C:\CHEM32\1\METHODS\HAAKON\CHIRAL_SEP.M
    Last changed    : 4/21/2021 10:52:36 AM by Haakon Bye
                      (modified after loading)
    Analysis Method : C:\CHEM32\1\DATA\ANNA TENNFJORD\F3S3_STD.D\DA.M (ESMOLOLKLORHYDRIN.M)
    Last changed    : 4/25/2021 12:14:39 PM by Mari Rødseth
                      (modified after loading)
    Method Info     : Separation of (R)- and (S)-chlorohydrin.

    Sample Info     : Isocratic n-Hexane:i-PrOH (90:10), flow 1.0 mL/min, 10
                      uL injection. HKB90


    Additional Info : Peak(s) manually integrated
```

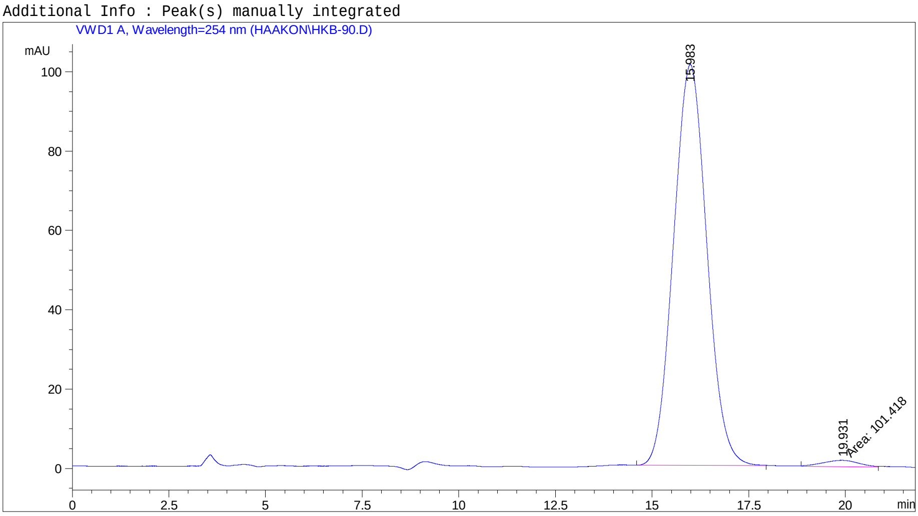


```
    =====================================================================
                             Area Percent Report
    =====================================================================

    Sorted By             :      Signal
    Multiplier:                   :      1.0000
    Dilution:                     :      1.0000
    Use Multiplier & Dilution Factor with ISTDs


    Signal 1: VWD1 A, Wavelength=254 nm



Instrument 1 4/26/2021 11:10:19 AM Mari Rødseth                    Page    1 of 2
```

Figure 185: Chromatogram from chiral HPLC of compound **(*S*)-10**

.2.3 Chromatogram of Compounds (*rac*)-15 and (*S*)-15

Data File C:\CHEM32\1\DATA\HAAKON\HKB-91-OD4.D
Sample Name: HKB-91

===

Acq. Operator : Haakon Bye
Acq. Instrument : Instrument 1 Location : -
Injection Date : 4/27/2021 10:29:12 AM
Acq. Method : C:\CHEM32\1\METHODS\HAAKON\CHIRAL_SEP.M
Last changed : 4/27/2021 10:26:27 AM by Haakon Bye
(modified after loading)
Analysis Method : C:\CHEM32\1\DATA\ANNA TENNFJORD\F3S3_STD.D\DA.M (ESMOLOLKLORHYDRIN.M)
Last changed : 4/25/2021 12:14:39 PM by Mari Rødseth
(modified after loading)
Method Info : Separation of (R)- and (S)-chlorohydrin.

Sample Info : Isocratic n-Hexane:EtOH (0.1% TFA) (95:5), flow 1.0 mL/
min, 10 uL injection.

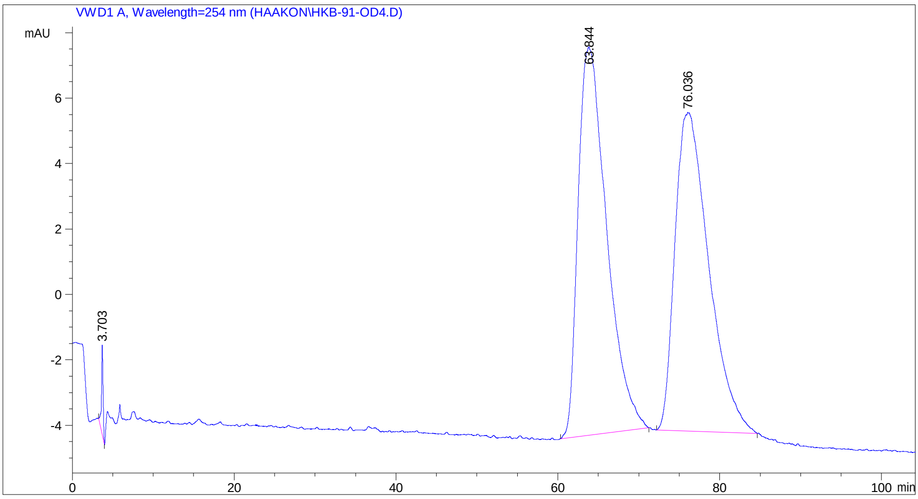

===

Area Percent Report

===

Sorted By : Signal
Multiplier: : 1.0000
Dilution: : 1.0000
Use Multiplier & Dilution Factor with ISTDs

Signal 1: VWD1 A, Wavelength=254 nm

Peak #	RetTime [min]	Type	Width [min]	Area mAU *s	Height [mAU]	Area %
1	3.703	BB	0.1985	37.97871	2.73288	0.6568
2	63.844	BB	2.8833	2914.55884	11.87127	50.4069

Instrument 1 4/27/2021 1:53:43 PM Mari Rødseth Page 1 of 2

Figure 186: Chromatogram from chiral HPLC of racemate compound **(*rac*)-15**

```
Data File C:\CHEM32\1\DATA\HAAKON\HKB-92.D
Sample Name: HKB-92

    =====================================================================
    Acq. Operator   : Haakon Bye
    Acq. Instrument : Instrument 1                    Location :   -
    Injection Date  : 4/27/2021 12:17:37 PM
    Acq. Method     : C:\CHEM32\1\METHODS\HAAKON\CHIRAL_SEP.M
    Last changed    : 4/27/2021 12:13:12 PM by Haakon Bye
                      (modified after loading)
    Analysis Method : C:\CHEM32\1\DATA\ANNA TENNFJORD\F3S3_STD.D\DA.M (ESMOLOLKLORHYDRIN.M)
    Last changed    : 4/25/2021 12:14:39 PM by Mari Rødseth
                      (modified after loading)
    Method Info     : Separation of (R)- and (S)-chlorohydrin.

    Sample Info     : Isocratic n-Hexane:EtOH (0.1% TFA) (95:5), flow 1.0 mL/
                      min, 10 uL injection.


    Additional Info : Peak(s) manually integrated
```

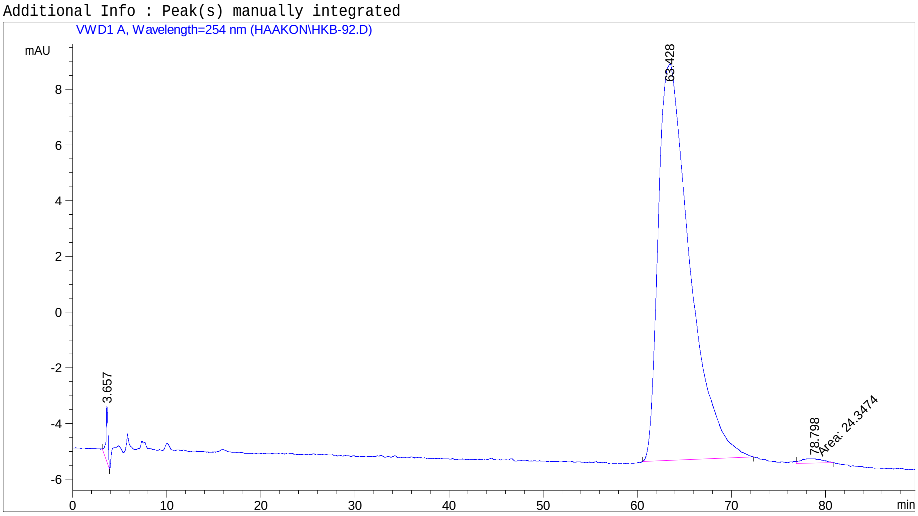


```
    =====================================================================
                             Area Percent Report
    =====================================================================

    Sorted By             :      Signal
    Multiplier:                   :      1.0000
    Dilution:                     :      1.0000
    Use Multiplier & Dilution Factor with ISTDs


    Signal 1: VWD1 A, Wavelength=254 nm
```

Instrument 1 4/27/2021 1:49:25 PM Mari Rødseth   Page   1 of 2

Figure 187: Chromatogram from chiral HPLC of compound **(*S*)-15**

Haakon Kristvik Bye

Synthesis of 4-Amine Substituted Thieno[2,3-*d*]pyrimidines for Breast Cancer and HER2 Activity Testing

NTNU
Norwegian University of
Science and Technology